



Ysgoloriaethau Sgiliau Economi Gwybodaeth  
Knowledge Economy Skills Scholarships



# Prifysgol Abertawe Swansea University

Use of Organic Solvent Nanofiltration (OSN) membranes for Counter-Current Chromatography (CCC) solvent recovery

Matthew James Walters MRes BEng (hons)

Submitted to Swansea University in fulfilment of the requirements  
for the Degree of Doctor of Philosophy

Swansea University

2020

*For Mila*

## Abstract

---

Solvent resistant membranes are a relatively new technology which has the potential to expand the possible utilities of membranes for process industries. Little is known in terms of generic characterisation and basic physical properties of the membranes, and the aim of this work is to explore and characterise such membranes in a systematic way and apply them in an industrial application. After characterisation of the Organic Solvent Nanofiltration (OSN) membranes are complete; solvent and solute properties, such as solubility, polarity and viscosity, are measured and compared to the rejection and permeate flux data of two charged dyes in alcohols of increasing molecular weight in an attempt to ascertain the dictating factors which govern separation in OSN membranes. Following on from this, Polyethersulfone (PES) membranes were fabricated and crosslinked using different materials and methods, with performance and FTIR data analysed to measure the effectiveness of the crosslinking for rejection of solutes in solvent systems. Finally, a process material from Counter-Current Chromatography (CCC) containing a mixture of solvents and a pesticide ( $\text{MW} = 350 \text{ g.mol}^{-1}$ ) is screened using OSN and aqueous-system nanofiltration membranes using dead-end filtration, to determine the optimum membrane for solute concentration. Following this, two bovine gelatin ( $\text{MW} = 100,000 \text{ g.mol}^{-1}$ ) in solvent mixtures are concentrated in a crossflow system for use before and after CCC to determine the viability of OSN as a counter-part to CCC.

Initially, characterisation of solvent resistant membranes are completed by testing the performance of very tight (OSN) membranes with volatile and neutral solutes in aprotic solvents. The Duramem 150 and 200 membranes were tested using salt, volatiles and polyethylene glycols in both water and solvents using dead – end filtration cells. The rejection was >90% of solutes with MW 150 and 200 respectively in some solvents, but not in others, which indicate that the solubility of the solute in the solvent and the degree of swelling in the membrane play a role in the rejection performance of the membrane.

A new application for the measurement of membrane surface zeta potential of positively charged membranes using the Laser Doppler Effect through the Malvern Zetasizer has been developed, by using positively charged particles in the place of negatively charged particles. This allows for the analysis of both negatively and positively charged membranes using the same system. This methodology was also tested using solvent systems, however, this proved to be challenging and little meaningful data was obtained.

Following on from zeta potential measurements, other physical properties of OSN membranes, solute and solvent properties were analysed to determine which properties (such as system viscosity, solubility of solute in solvent, membrane swelling etc) govern permeate flux and rejection two charged dyes of identical MW (Orange II and Safranin O) using Duramem 500 membrane. By comparing the performance data of the membrane against each alcohol solution, the permeate flux shows the best correlation with the viscosity of the solution suggesting that this is the governing properties of the system with respect to permeate flux, while the rejection of the solutes in each solution show good correlation with the solubility of the dye in

## Abstract

each alcohol, as well as the polarity of the dye and alcohol, suggesting that the degree of hydrogen bonding occurring in the system is the chief factor with regards to the rejection of the solute in OSN systems.

PES membranes have been shown to robust physical properties and have been used to filtration of hazardous chemicals, and as such PES membranes were fabricated to examine the viability of this material for solvent filtration systems. Previous studies using volatiles for modification of polysulfone membranes have shown to modify the physical properties of the membranes, thus this was attempted with polyethersulfone to observe if similar results would occur. The rejection of the solute remained at a relatively constant level while the permeate flux significantly increased with the addition of volatile alcohols to the dope mixture. Following on from this, different materials and methods of crosslinking were used in an attempt to lower the MWCO of the PES membranes. The crosslinking agents used were PEG 200 and Hexane Diamine, these were applied onto the membrane through “post” casting modification (submersion in crosslinking bath), Simultaneous Phase Inversion and Crosslinking (SIM) modification and flux modification. The use of PEG 200 as a crosslinking agent, applied through the flux method appears to give the highest degree of crosslinking.


Two pesticides from different cuts of Counter-Current Chromatography (CCC) were subjected to nanofiltration using different membranes, before and after chemical saturation to mimic aging. The GE DK membrane had the highest rejection of the range that was tested, while the HL membrane had the highest permeate flux rate. The solvents before and after filtration were measured to find that there was little change in solvent composition after filtration. In a cross – flow system, bovine gelatin (MW 100,000 g.mol<sup>-1</sup>) was dissolved in similar solvent compositions to that of the pesticides and concentrated using a 25 kDa MWCO membrane. There is total rejection of the solute, with a change in the solvent composition, namely ethyl acetate and hexane, depending on the composition of the initial feed solvent mixture.

Declaration

## Declaration

---

This work has not previously been accepted in substance for any degree and is not being concurrently submitted in candidature for any degree.

Signed..  .....

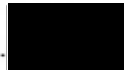
Date.. 25/3/20 .....

This thesis is the result of my own investigations, except where otherwise stated. Other sources are acknowledged by footnotes giving explicit references. A bibliography is appended.

Signed..  .....

Date.. 25/3/20 .....

I hereby give consent for my thesis, if accepted, to be available for photocopying and for inter-library loan, and for the title and summary to be made available to outside organisations.

Signed..  .....

Date.. 25/3/20 .....

## Acknowledgements

---

I would like to thank the KESS 2 project and the ESF for funding this project and the opportunities that it has led to.

I would like to thank Swansea University, particularly the staff of CWATER, for allowing me a place to conduct my research and the allowing me to use their equipment. I would also like to thank ESRI for giving me an office space to work out of.

I would like to thank the staff of Bioextractions Wales for giving me a project and I hope that any outcomes that I found will be useful for you going forward.

Would like to thank my supervisors Darren and Paul for the all the help and advice that they have given me, I would not have been able to complete this thesis without your guidance.

A big thanks to my colleagues at ESRI for not only their support, but for the friendships that I have made there. Thank you to Dr Tom Ainscough for his help and advice, your friendship has been invaluable.

Thank you to my family for their love and support, who kept me focused and driven. Especially to Ken, who saw the start but isn't around to see the end of this degree. Your advice has been invaluable, you are constantly in our thoughts.

Thank you to my long-suffering partner Lynsey, who continues to push me to better myself and has always been some to talk to. We have a wonderful family together and I wouldn't change it for the world.

## Publications

---

Nanofiltration membranes and processes: A review of research trends over the past decade, *2017*, Journal of Water Process Engineering, Volume 19, Pages 164-171

Fabrication of PES/PVP Water Filtration Membranes Using Cyrene®, a Safer Bio-Based Polar Aprotic Solvent, *2019*, Advances in Polymer Technology

Use of laser Doppler electrophoresis and electro-osmotic flow mapping for the zeta potential measurement of positively charged membrane surfaces (under review), *2020*, Journal of Membrane Science

## Table of Contents

## Table of Contents

Abstract.....	i
Declaration.....	iv
Acknowledgements .....	v
Publications.....	vi
Table of Contents.....	vii
List of Figures .....	xii
List of Tables .....	xv
1. Introduction .....	1
2. Background and Literature Review.....	5
2.1 Organic Solvent Nanofiltration (OSN) .....	5
2.2 Polymeric Membrane Materials and Types .....	6
2.3 Commercial OSN Membranes.....	7
2.4 Membrane Modification .....	9
2.4.1 Crosslinking bath.....	10
2.4.2 Flux method .....	10
2.4.3 SIM modification.....	10
2.5 Membrane Parameters and Performance .....	11
2.5.1 Pressure .....	11
2.5.2 Temperature .....	13
2.5.3 Charge .....	14
2.5.4 Concentration .....	16
2.5.5 Concentration Polarisation and Fouling.....	16
2.5.6 Preconditioning.....	18
2.6 Membrane Equipment and Set-up.....	19
2.6.1 Lab-scale Equipment.....	19
2.6.2 Pilot and Industrial Scale Equipment .....	20
2.7 Polyether sulfone (PES) Membranes for Solvent Systems .....	21
2.8 Membrane Characterisation .....	22
2.8.1 Molecular Weight Cut-Off (MWCO).....	22
2.8.2 Fourier Transform Infra-Red (FTIR) Spectroscopy .....	22
2.8.3 Surface Charge .....	23
2.9 Current OSN Research.....	24
2.9.1 Andrew Livingston <i>et al.</i> .....	24
2.9.2 Van der Bruggen <i>et al.</i> .....	26
2.9.3 Vankelecom <i>et al.</i> .....	27



## Table of Contents

3. Materials and Methods.....	29
3.1 Chemicals .....	29
3.2 Membranes .....	31
3.2.1 PTFE Membrane Modification .....	32
3.3 Equipment design .....	32
3.3.1 Dead-end Filtration .....	32
3.3.2 Cross-flow filtration .....	33
3.4 Experimental Method .....	34
3.4.1 Dead-end Filtration .....	34
3.4.2 Crossflow filtration.....	35
3.4.3 Tangential Streaming Potential (TSP) Measurements .....	35
3.4.4 Laser Doppler Electrophoresis (LDE) Measurements .....	36
3.5 Data Analysis .....	37
3.5.1 Solvent Recovery Data Analysis .....	37
3.5.2 Solvent Recovery Experimental Parameters.....	37
3.5.3 Solute Rejection analysis.....	37
3.5.4 Gas Chromatography / Mass Spectrometry (GCMS) Analysis .....	38
3.5.5 High Performance Liquid Chromatography (HPLC) Analysis.....	40
3.6 Membrane fabrication and modification .....	40
3.6.1 Membrane Preparation .....	40
3.6.2 Membrane Casting.....	41
3.6.3 Surface Modification .....	41
3.6.4 SIM Modification.....	41
3.6.5 Flux Modification .....	41
4. Characterisation of the Duramem OSN membranes .....	42
4.1 Introduction .....	42
4.2 Experimental Procedure .....	43
4.2.1 Salt rejections.....	43
4.2.2 1000 PPM rejection.....	43
4.2.3 Zeta Potential Measurements.....	43
4.3 Salt Rejection of Duramem 150 .....	44
4.3.1 NaCl Rejection and Flux .....	44
4.3.2 Na <sub>2</sub> SO <sub>4</sub> Rejection and Flux .....	45
4.3.3 MgCl <sub>2</sub> Rejection and Flux .....	46
4.4 Flux and rejections in aprotic solvents of Duramem 150.....	47
4.4.1 Methanol – water permeability .....	47

## Table of Contents

4.4.2	Rejection of volatiles and neutral compounds .....	48
4.4.3	Effect of temperature on PEG rejection.....	53
4.5	Salt rejection of Duramem 200 .....	54
4.5.1	NaCl rejection.....	54
4.5.2	Na <sub>2</sub> SO <sub>4</sub> rejection.....	55
4.5.3	MgCl <sub>2</sub> rejection .....	56
4.6	Flux and rejections in aprotic solvents using of Duramem 200 .....	57
4.6.1	Rejection of volatile and neutral solutes .....	57
4.6.2	Effect of temperature on PEG rejection.....	64
4.7	Zeta potential of Duramem 200 Membrane.....	66
4.7.1	TSP measurements.....	66
4.8	Conclusions .....	66
5.	Electrokinetic characterisation of OSN membranes.....	68
5.1	Introduction .....	68
5.2	Experimental procedures .....	69
5.3	Experimental results .....	69
5.3.1	Zeta Potential measurements of PTFE membrane .....	69
5.3.2	Zeta Potential measurements of APTES-modified PTFE membrane.....	72
5.3.3	TSP measurements of Duramem 200 in methanol-water systems .....	75
5.3.4	Zetasizer Measurements on Duramem 200.....	77
5.4	Conclusions .....	78
6.	Investigation into of the separation mechanisms of OSN membranes .....	80
6.1	Introduction .....	80
6.2	Experimental procedure .....	80
6.2.1	Dye rejection .....	80
6.2.2	Zeta potential.....	81
6.3	Methanol – Water Solutions .....	81
6.3.1	Rejection and flux of charged dyes in methanol – water solutions.....	81
6.3.2	The role of viscosity of methanol – water solutions in membrane performance .....	83
6.3.3	The role of Zeta Potential on membrane performance.....	85
6.3.4	The role of surface tension on membrane performance.....	87
6.4	Single solvent systems .....	88
6.4.1	Rejection and flux of charged dyes in alcohols.....	88
6.4.2	The role of solvent solubility on membrane performance .....	90
6.4.3	The role of solvent polarity on membrane performance .....	92
6.4.4	The role of solvent molar volume on membrane performance .....	94

## Table of Contents

6.4.5	The role of solvent solvation energy on membrane performance .....	95
6.4.6	The role of solvent viscosity and its effect on membrane performance .....	96
6.4.7	The role of membrane swelling and its effect on membrane performance .....	97
6.4.8	The role of solvation and its effect on solute size and membrane performance .....	99
6.4.9	Dimensionless correlations of data.....	101
6.5	Conclusions .....	104
7.	Modification of polyethersulfone (PES) membranes for improved OSN performance.....	105
7.1	Introduction .....	105
7.2	Experimental Methods.....	106
7.2.1	Dye Rejection .....	106
7.2.2	Zeta Potential.....	106
7.2.3	Fourier Transform Infra-Red Spectroscopy (FTIR) .....	106
7.3	Results.....	107
7.3.1	Additive Modification .....	107
7.3.2	Surface Modification .....	111
7.3.3	Zeta Potential.....	113
7.3.4	FTIR.....	114
7.3.5	Comparison of modification methods .....	115
7.4	Conclusions .....	118
8.	Application of OSN for Counter Current Chromatography Solvent Recycling .....	119
8.1	Introduction.....	119
8.1.1	Proposed uses of filtration with CCC .....	120
8.2	Experimental Procedure.....	120
8.2.1	Membrane screening by dead-end filtration.....	120
8.2.2	Solvent Recycling using OSN .....	121
8.2.3	Crossflow ultrafiltration .....	122
8.3	Results .....	123
8.3.1	Membrane Screening by dead-end filtration.....	123
8.3.2	Ultrafiltration of collagen.....	126
8.3.3	Solvent exchange during filtration .....	127
8.4	Conclusions.....	129
9.	Conclusions .....	130
	Characterisation of the Duramem OSN membranes .....	130
	Electrokinetic characterisation of OSN membranes.....	130
	Investigation into of the separation mechanisms of OSN membranes .....	131
	Modification of polyethersulfone (PES) membranes for improved OSN performance.....	131

## Table of Contents

Application of OSN for Counter Current Chromatography Solvent Recycling.....	132
10. Future Work .....	133
11. References.....	134
12. Appendix .....	144
12.1 Calibrations .....	144
12.2 Studies on Duramem series by other authors .....	148
Duramem 150 .....	148
Duramem 200 .....	149
Duramem 300 .....	151
Duramem 500 .....	153
Duramem 700 .....	154
Duramem 900 .....	154
12.3 Prospective publications .....	155
12.3.1 Use of Laser – Doppler Electrophoresis (LDE) measurements for zeta potential measurements in positively charged membranes.....	<b>Error! Bookmark not defined.</b>
12.3.2 Predictive computational modelling of Organic Solvent Nanofiltration (OSN) membranes in alcohols: a systematic study .....	155
12.3.3 Comparative study of membrane crosslinking methods on Polyethersulfone (PES) membranes for Organic Solvent Nanofiltration (OSN) .....	155

## List of Figures

---

Figure 1.1 Number of publications related to OSN published per year since 2007 (Oatley-Radcliffe, et al., 2017) .....	2
Figure 2.1 Rejection as a factor of modified Peclet number .....	13
Figure 2.2 Chemical Structure of 3 Dyes of Identical Molecular Weights .....	15
Figure 2.3 Concentration profile of (a) permeating and (b) retained component at steady state conditions where C is the concentration of the solvent (w) or species i in the in the bulk (b), permeate (p) or membrane boundary layer (m) and N is the flux of the solvent (w) and species i respectively (Bhattacharya & Hwang, 1997).....	17
Figure 2.4 basic schematic for a crossflow membrane rig.....	20
Figure 2.5 Cross section of spiral wound polymeric membrane .....	21
Figure 3.1 Diagram of dead-end filtration set up .....	33
Figure 3.2 P&ID of crossflow UF system .....	34
Figure 3.3 Picture of UF crossflow system .....	34
Figure 4.1 Rejection of NaCl at different concentrations over a range of pressures .....	44
Figure 4.2 Rejection of Na <sub>2</sub> SO <sub>4</sub> at different concentrations over a range of pressures.....	45
Figure 4.3 Rejection of MgCl <sub>2</sub> at different concentrations over a range of pressures.....	46
Figure 4.4 Effect of increasing water concentration and viscosity on permeability of Duramem 150 .....	47
Figure 4.5 Rejection of 1000 PPM toluene in different solvents at applied pressures .....	48
Figure 4.6 Rejection of 1000 PPM trichloroethylene in different solvents at applied pressures.....	49
Figure 4.7 Rejection of 1000 PPM triethylene glycol (PEG 150) in different solvents at applied pressures .....	50
Figure 4.8 Rejection of 1000 PPM tetraethylene glycol (PEG 200) in different solvent and mixtures over a range of pressures .....	50
Figure 4.9 Rejection of 1000 PPM dodecane in different solvent and mixtures over a range of pressures .....	51
Figure 4.10 Rejection of solutes based on molecular weight using Duramem 150 membrane at 40 bar ...	52
Figure 4.11 Rejections of solutes based on Van der Waals radius using Duramem 150 membrane at 40 bar .....	52
Figure 4.12 Effect of temperature on the membrane flux and rejection of PEG 150 using methanol as a solvent using the Duramem 150 membrane at 30 bar applied pressure .....	53
Figure 4.13 Permeate flux and viscosity of methanol using the Duramem 150 membrane as a function of temperature at 30 bar applied pressure .....	54
Figure 4.14 Rejection of NaCl by Duramem 200 at applied pressures over a range of NaCl concentrations .....	55
Figure 4.15 Rejection of Na <sub>2</sub> SO <sub>4</sub> by Duramem 200 at applied pressures over a range of Na <sub>2</sub> SO <sub>4</sub> concentrations .....	56
Figure 4.16 Rejection of MgCl <sub>2</sub> by Duramem 200 at applied pressures over a range of MgCl <sub>2</sub> concentrations .....	57
Figure 4.17 Rejection of 1000 PPM toluene using the Duramem 200 membrane in different solvents and applied pressures.....	58
Figure 4.18 Rejection of 1000 PPM trichloroethylene by Duramem 200 in different solvents and applied pressures.....	59
Figure 4.19 Rejection of 1000 PPM dodecane by Duramem 200 in different solvents and applied pressures .....	59
Figure 4.20 Rejection of 1000 PPM triethylene glycol (PEG 150) by Duramem 200 in different solvents and applied pressures.....	60
Figure 4.21 Rejection of 1000 PPM tetraethylene glycol (PEG 200) by Duramem 200 in different solvents and applied pressures.....	61

## List of Figures

Figure 4.22 Rejection of solutes using the Duramem 200 membrane at 40 bar applied pressure as a function of molecular weight.....	62
Figure 4.23 Rejection of solutes using the Duramem 200 membrane at 40 bar applied pressures as a function of Van der Waals radius .....	62
Figure 4.24 Rejection of solutes as a function of Van der Waals solute radius in methanol using the Duramem 200 membrane at applied pressures .....	63
Figure 4.25 Rejection of solutes as a function of Van der Waals solute radius in ethanol using the Duramem 200 membrane at applied pressures .....	63
Figure 4.26 Rejection of solutes as a function of Van der Waals solute radius in acetonitrile using the Duramem 200 membrane at applied pressures .....	64
Figure 4.27 PEG Rejection in methanol at 30 bar applied pressure using the Duramem 200 membrane at different temperatures.....	65
Figure 4.28 Viscosity of Methanol and PEG 200 as a function of temperature.....	65
Figure 4.29 Zeta potential of Duramem 200 at various NaCl concentrations in ultra-pure water .....	66
Figure 5.1 Zeta Potential of unmodified PTFE membrane using TSP and LDE methods .....	69
Figure 5.2 (A) Phase graph of carboxylate beads with unmodified PTFE with applied voltage (B) Particle mobility at each measurement displacement/height .....	71
Figure 5.3 (A) Phase diagram of Amidine beads on unmodified PTFE at the applied voltage (B) Particle mobility at each membrane displacement/height .....	72
Figure 5.4 Zeta Potential measurement of APTES-modified PTFE membrane using TSP and LDE methods	73
Figure 5.5 (A) Phase diagram of carboxylate beads on APTES-modified PTFE at the applied voltage (B) Particle mobility at each membrane displacement/height .....	74
Figure 5.6 (A) Phase diagram on Amidine beads on APTES-modified PTFE at the applied voltage (B) Particle mobility at each membrane displacement/height .....	75
Figure 5.7 Zeta potential of Duramem 200 membrane using 1mmol/L NaCl in different methanol - water systems .....	76
Figure 5.8 Extrapolated $pK_w$ as a function on methanol in water-methanol-NaCl tertiary systems .....	77
Figure 5.9 Zeta potential of Duramen 200 in 1mmol/L NaCl (aq) by TSP and LDE measurements .....	78
Figure 6.1 Rejection of 100 PPM Safranin O and Orange II using the Duramem 500 membrane as a function of methanol content in solution .....	82
Figure 6.2 Flux of 100 PPM Safranin O and Orange II using the Duramem 500 membrane as a function of methanol content in solution .....	82
Figure 6.3 Rejection of Safranin O and Orange II as a function of solution viscosity .....	84
Figure 6.4 Permeate flux of Safranin O and Orange II as a function of solution viscosity .....	84
Figure 6.5 Duramem 500 surface zeta potential in 1mmol/L NaCl at neutral pH .....	85
Figure 6.6 Rejection of 100 PPM Safranin O and Orange II as a function of Zeta Potential .....	86
Figure 6.7 100 PPM Safranin O and Orange II permeate flux as a function of ZP .....	86
Figure 6.8 Rejection of Safranin O and Orange II as a function of solution surface tension .....	87
Figure 6.9 Permeate flux of Safranin O and Orange II as a function of surface tension.....	88
Figure 6.10 Rejection of Safranin O and Orange II in alcohols of increasing carbons .....	89
Figure 6.11 Permeate flux of Safranin O and Orange II in alcohols and pure alcohols of increasing carbons .....	89
Figure 6.12 Comparison of clean solvent fluxes using the Duramem 500 membrane.....	90
Figure 6.13 Rejection and permeate flux of 100 PPM charged dyes as a function of solvent solubility.....	92
Figure 6.14 100 PPM charged dye flux and rejection as a function of solvent polarity .....	93
Figure 6.15 Solvent Solubility as a function of solvent polarity.....	94
Figure 6.16 100 PPM charged dye flux and rejection as a function of solvent molar volume .....	95
Figure 6.17 100 PPM charged dye flux and rejection as a function of solvent solvation energy .....	96
Figure 6.18 100 PPM charged dye flux and rejections as a function of solvent viscosity.....	97

## List of Figures

Figure 6.19 100 PPM charged dye rejection and permeate flux as a function of free volume fraction.....	98
Figure 6.20 Safranin O rejection as a function of solute solvation radius .....	100
Figure 6.21 Safranin O rejection as a function of the maximum solvation radius.....	100
Figure 6.22 Dye rejection and permeate flux as a function of Reynolds number of the experimental system.....	102
Figure 6.23 Dye rejection and permeate flux as a function of Schmidt number of the experimental system .....	103
Figure 6.24 Dye rejection and permeate flux as a function of Sherwood number of the experimental system.....	103
Figure 7.1 Effect of methanol as an additive on membrane performance .....	107
Figure 7.2 Effect of ethanol as an additive on membrane performance.....	108
Figure 7.3 Effect of isopropanol as an additive on membrane performance .....	109
Figure 7.4 Effect of n-butanol as an additive on membrane performance .....	110
Figure 7.5 Flux and rejection of RB in IPA as a function of HDA percentage .....	111
Figure 7.6 Flux and rejection of RB in IPA as a function of PEG 200 percentage.....	112
Figure 7.7 Zeta potential of modified and unmodified PES membrane as a function of pH using 10 wt% crosslinking agents.....	113
Figure 7.8 FTIR of PES membranes using HDA as a crosslinker at increasing weight percentages .....	114
Figure 7.9 FTIR of PES membranes crosslinked using PEG 200 at increasing weight percentages .....	115
Figure 7.10 Comparison of flux and rejection of PES membranes using different methods of crosslinking using 10 wt% PEG 200 and 5wt% HDA .....	116
Figure 7.11 Comparison of FTIR results of the 3 different crosslinking methods tested using 5 wt% HDA as the crosslinking agent .....	117
Figure 7.12 Comparison of modification methods of PES membranes using PEG 200 as a crosslinking agent .....	117
Figure 8.1 Basic schematic of how a Counter Current Chromatography (CCC) device operates .....	119
Figure 8.2 Rejection of Early and Late Minors in several membranes before and after 4 week saturation .....	124
Figure 8.3 Specific Flux of Early and Late Minors in several membranes before and after 4 week saturation .....	125
Figure 8.4 Water Specific Flux of several membranes before and after Early and Late Minors concentration and 4 week saturation.....	125
Figure 8.5 Flux of collagen solutions before and after CCC concentration.....	127

## List of Tables

---

Table 1-1 list of commercial providers of OSN membranes .....	3
Table 2-1 Summary of solute rejection in aqueous and non-aqueous solvents (Zhao & Yuan, 2006) .....	5
Table 2-2 Known system properties that effect a membrane performance (Darvishmanesh, et al., 2010) ..	6
Table 2-3 Summary of commercially available membranes available for purchase at the time of writing ...	8
Table 2-4 Permeability values of solvents by O-PASS membranes as published by Yuan, <i>et al</i> (2018) .....	27
Table 3-1 Names, CAS numbers, manufacturers of all chemicals and solids used.....	31
Table 3-2 Table of Specifications of GC Column .....	38
Table 3-3 GC/MS parameters for analysis of volatiles.....	39
Table 3-4 GC/MS parameters for analysis of PEGs .....	39
Table 3-5 Headspace GC/MS parameters for solvent analysis.....	40
Table 3-6 HPLC method for analysis of Spinosad samples .....	40
Table 4-1 molecular weight and Van der Waals radius of solutes used in study .....	51
Table 5-1 Properties of charged beads used in LDE experiments .....	70
Table 5-2 Zetasizer results of Duramem 200 in methanol - water solutions (3-1) using positive particles and 10mMol NaCl .....	78
Table 6-1 Viscosity of Methanol - Water Solutions (Mikhail & Kimel, 1961).....	83
Table 6-2 Surface tension of methanol - water solutions (Vazquez, et al., 1995) .....	87
Table 6-3 Hansen Solubility Parameters of Safranin O and Alcohols .....	91
Table 6-4 Hansen Solubility Parameters of Orange II and Alcohols.....	91
Table 6-5 Polarity of solvents studied (Reichardt & Welton, 2010) .....	92
Table 6-6 Solvent molar volume from Marvin Sketch program .....	94
Table 6-7 Solvation energy of solvents provided by Marvin Sketch.....	96
Table 6-8 Solvent viscosity at experiment temperature.....	97
Table 6-9 Swelling properties of Duramem 500 in alcohols .....	98
Table 6-10 Solvent and solute atomic radii calculated by MarvinSketch program .....	99
Table 6-11 Dimensionless correlations of dye rejections in alcohol.....	101
Table 8-1 Properties of membranes used in CCC recycling screening experiments.....	121
Table 8-2 Data from dead-end concentration of early minors in several membranes .....	123
Table 8-3 Data from dead-end concentration of late minors in several membranes .....	124
Table 8-4 Gelatin concentrations in Pre CCC and Posts CCC ultrafiltrations .....	127
Table 8-5 Solvent analysis of Late Minors before and after filtration using the Duramem 200 .....	128
Table 8-6 Solvent percentages in feed, permeate and retentate of pre-CCC concentration .....	128
Table 8-7 Solvent percentages in feed, permeate and retentate of post-CCC concentration .....	129



## 1. Introduction

---

The use of membranes as a non-thermal solid-liquid separation method has long been established for aqueous applications and in modern times used extensively for wastewater treatment and reverse osmosis processes (Cao, et al., 2020). However, until recently, the demand for a non-thermal separation method for organic solvent systems has yet to be satisfied within the field of membrane separations. In a world where energy usage, emissions and running costs are becoming just as important as the need for a product, there has been a steady increase in the demand for low energy separation systems which are applicable for organic solvents (Oatley-Radcliffe, et al., 2017). Over the past decade, there has been an increasing amount commercialisation of organic solvent nanofiltration (OSN) membranes becoming available on the global market, which may satiate the need for a low-cost solvent filtration. OSN is a pressure driven technique which uses a membrane to separate an incoming feed stream into two separate streams known as the permeate (solvents and solute which pass through the membrane) and the retentate (solvents and solutes which are unable to pass through the membrane). The separation technique is based mainly on steric factors with OSN membranes designed to operate between the ranges of 200 – 1000 g/mol. The success of OSN has meant that the technology has been implemented into a range of industries including: pharmaceutical (Darvishmanesh, et al., 2011), petrochemicals (Adi, et al., 2016) and fine chemicals (Priske, et al., 2016). The use of this application has found great success in laboratory scale operations with the technology slowly being implemented into larger scale operations. The hinderance with this technology is being able to model systems, of which there has been a large amount of research conducted and with much more still needed to be able to model solvent systems with a great accuracy (Goebel, et al., 2018). This is often hindered by a need for multicomponent systems, which is often required by industry, where chemical interactions between the solvents greatly increases the amount of computing needed to model separations accurately for design, optimisation and scale up. The complex microhydrodynamics and interfacial events, coupled with largely unknown solute – solute, solute – solvent and solute – solvent – membrane interactions, make for a challenging situation. Moreover, most industrial applications use a wide range or mixture of solvents where even the basic fundamental physical properties are unknown. Despite this, OSN is routinely mentioned as offering benefits of improved energy and mass efficiency, high process flexibility and capability of processing temperature sensitive material, when compare to other unit traditional operations. This is evident in the increasing amount of research being published around the topic (Figure 1.1)

## Introduction

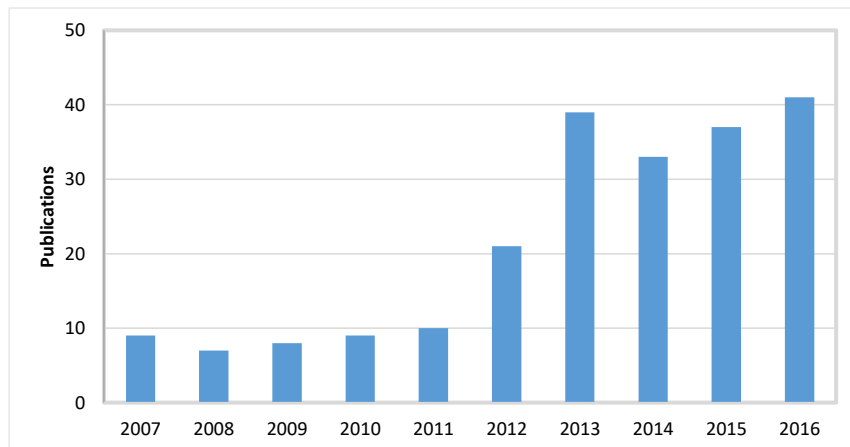


**Figure 1.1 Number of publications related to OSN published per year since 2007 (Oatley-Radcliffe, et al., 2017)**

Amongst all the research published on OSN membranes, there is a large portion of published data for an industrial process or mixture, e.g. recovery of a molecule of note (Martínez, et al., 2013), characterisation of membrane using a multi-solvent system (Schmidt, et al., 2013); while these pieces of research provide information about compatibility and performance of a membrane for a given process, there is very little research conducting a systematic study of a range of solvents, whereby the performance of the membrane gradually changes with the changing properties of the solvent (Davey, et al., 2017). This lack of comprehensive systematic studies is likely contributing to lack of comprehensive models derived of OSN systems, where now there is largely models for specific systems for a given membrane.

The increased growth in knowledge of OSN systems is down to two factors: a) more materials are being identified as solvent stable, thus leading to more publications highlighting the fact; b) solvent stable materials for OSN membranes are becoming more economical which allows research groups to acquire more materials/membranes which consequently leads to more research being published. Very few publications from industry have been published, meaning that the degree to which OSN is employed in an industrial setting is unknown so it is difficult to tell if the technology is being used in pharmaceutical or oil industries.

With so little research being available compared to publications researching aqueous membranes, there is a large scope for research to be completed on solvent resistant membranes, from characterisation to modelling. Initial attempts at OSN were in conducted by Sourirajan (1964) but progress has been hindered due to a lack of commercialisation due to the difficulty in fabricating and modelling these systems (Burgal, et al., 2015). To date, there are a handful of commercial OSN membrane manufacturers which are:

## Introduction

Manufacturer	Name	Material
Evonik MET	Duramem	Modified polyimide
	Puramem	Silicon coated PAN
SolSep BV	NF Series	PDMS
Koch	SelRO NF	Composite
	SPIRAPRO NF	Polyamide
MICRODYN-NADIR	NADIR	PES, PESH/PSUH, PC, PVDF

Table 1-1 list of commercial providers of OSN membranes

Each of these manufacturers has a range of products with a range of MWCO that are suitable in a range of solvents that would ordinarily swell or damage other polymeric membranes.

What is common between the performance of OSN membranes, is that the rejection of solutes and permeate flux are derived from the same calculations as traditional membranes where:

$$R_i = 1 - \frac{C_{ip}}{C_{if}} \times 100\%$$

Where:  $R_i$  is the rejection of solute  $i$ ,

$C_{ip}$  is the concentration of solute  $i$  in the permeate

$C_{if}$  is the concentration of solute  $i$  in the feed

And:

$$J = \frac{V_p}{At}$$

Where:  $J$  is the permeate flux through the membrane ( $L/m^2h$ )

$V_p$  is the volume of permeate passed through the membrane

$A$  is the area of the membrane

$t$  is the amount of time passed for the measurement

The specific flux of the membrane can be calculated by dividing the flux equation by the operating pressure of the membrane, hence:

$$J_s = \frac{V_p}{AtP}$$

The specific flux is typically given in metric as  $L/m^2hbar$

## Introduction

A parameter typically provided by membrane manufacturers to describe the performance of a membrane is the Molecular Weight Cut-Off (MWCO). The MWCO is defined as the molecular weight for which 90% of a given solute is rejected by the membrane (See-Toh, et al., 2008) and for commercial manufacturers, this data is often supplied so that the customer can deduce which membrane better suits their needs (Lenntech, 2018). In practice, the MWCO varies on the solvent – solute system and the method used for determining the MWCO can vary (MET, 2018) (Li, et al., 2009). A good example of this, is provided by Davey, *et al* (2017). Using polystyrene oligomers in toluene the MWCO of Duramem 150 and 200 are 150 and 200 g/mol respectively, however, by changing the solute slightly to polypropylene glycols, the MWCO changes to 250 and 400 respectively in methanol and acetone. In addition, the MWCO is typically given as a curve with a significant increase in molecular weight is required to achieve 100% rejection (See-Toh, et al., 2008).

## 2. Background and Literature Review

### 2.1 Organic Solvent Nanofiltration (OSN)

NF membrane operation is similar for both aqueous and solvent systems, with the polymeric membranes used for OSN having interactions with the solvent, resulting in compaction, solvation and differential swelling of the membrane. The rejection and permeation rate of the membrane is also affected by the solvent – solute environment that the membrane is subjected to (Silva, et al., 2008). While polymeric membranes designed for aqueous processes can be used for OSN, their performance decreases in the presence of solvents (8) (Rezzadori, et al., 2015). *Marchetti* (2013) found a decrease in salt rejection with increasing Acetonitrile (ACN) in ACN/Water mixtures across a range of pore sizes. The hydrophilicity (and conversely, hydrophobicity) of the membrane is significant to the solvent permeate flux and rejection properties. Zhao and Yuan (2006) studied methanol, acetone and water systems with both hydrophilic MPF-44 membrane and a hydrophobic MPF-50 membrane, the data is found in Table 2-1. The data shows that methanol and acetone flux is higher for the MPF-50 membrane and water flux is higher in the MPF-44 membrane. This behaviour is expected due to the hydrophobic and hydrophilic nature of the membranes respectively. The rejection of daidzin also changes with the hydrophilic and hydrophobic nature of the membrane, with the rejection of daidzin being higher in water with the hydrophilic MPF-44 membrane when compared to the hydrophobic MPF-50. Similarly, the rejection of daidzin is larger in methanol and acetone when the hydrophobic MPF-50 membrane is used compared to the hydrophilic MPF-44 membrane.

Membrane	Flux (L/m <sup>2</sup> h)			Daidzin Rejection (%)		
	Water	Methanol	Acetone	Water	Methanol	Acetone
<b>MPF-50</b>	6.6	42	267	34.4	82.7	72
<b>MPF-44</b>	27	7.4	0.89	88.6	71.9	56.1

Table 2-1 Summary of solute rejection in aqueous and non-aqueous solvents (Zhao & Yuan, 2006)

Variations in rejection for given solutes have been observed using the same membrane in a range of organic solvents, confirming that the solvent has a significant effect on the membrane performance (Rundquist, et al., 2012) (Ormerod, et al., 2013) (Sereewatthanawut, et al., 2011). Suggested reasons for this change in membrane performance include:

- Solve-membrane interactions resulting in membrane swelling or pores opening. These interactions result in a change in solute rejection (Ormerod, et al., 2013).

## Background and Literature Review

- Solvent-solute interactions resulting in increased effective molecule size and alterations in the molecule shape (Darvishmanesh, et al., 2010).

The type of solvent and solvent properties has been shown to impact the permeate flux through the membrane. The polarity of the solvent and subsequently the surface tension of the solvent are believed to be major factors in the permeate flux of the membrane. Darvishmanesh, *et al* (2010) suggest that there are 16 different parameters involved in the membrane performance of a particular OSN system, which are defined in **Error! Reference source not found.:**

<b>Solvent Properties</b>
1. Polarity of the solvent
2. Solvent surface tension
3. Viscosity of the solvent
4. Solvent molar volume (size)
<b>Solute properties</b>
5. Solute molar volume (size) in solvent
6. Solute molecular weight
7. Solute geometrical shape
8. Solute solubility in solvent
9. Solute charge
<b>Membrane Properties</b>
10. Pore size and pore size distribution
11. Surface charge of the membrane
12. Degree of crosslinking of the polymeric membrane
<b>Process properties</b>
13. Feed concentration
14. Applied pressure and osmotic pressure
15. Feed temperature
16. Module type and characteristics

**Table 2-2 Known system properties that effect a membrane performance (Darvishmanesh, et al., 2010)**

While these factors that apply to operational parameters, there are many more factors that influence OSN separation, such as fabrication conditions, of which there are many. Thus, the complexity and extent to which one or more of these factors impacts on subsequent process is largely unknown.

## 2.2 Polymeric Membrane Materials and Types

The earliest polymeric membranes to be used for in industry were cellulose acetate (CA) due to their high-water permeability and high salt rejection. CA membranes, however, were found to not be suitable for chemical filtration as CA was found not to be chemically or mechanically stable in the presence of solvents, and have been phased out for more robust polymers such as poly ether ether ketone (PEEK), polyimide

## Background and Literature Review

(PI), polyamide (PA) and polydimethylsiloxane (PDMS) to name a few (Lim, et al., 2017) (Nunes & Peinemann, 2006). Based on the membrane fabrication material, and thus, the structure of the membrane (whether the membrane is porous or nonporous) determines the separation mechanism used (Livingston, et al., 2006). Nonporous/dense membranes are made up of tightly packed polymer chains, where the solvent and solutes pass through the membrane along a solution-diffusion mechanism. Transport is made possible through the free-volume elements that appear and disappear at approximately the same time-scale as the transport of permeate through the membrane, and the selectivity of the membrane is determined by the solubility and diffusivity of the solute, with the overall resistance to mass transfer is proportional to the membrane thickness. For a mechanically stable membrane, there is a minimum thickness required, however, increased membrane thickness leads to a decline in permeate flux in nonporous membranes (Mulder, 2012) (Nunes & Peinemann, 2006) (Baker, 2012) (Baker, 2012).

Porous membranes are similarly comprised of packed polymer chains; however, the structure contains clearly defined pores, which are fixed in space. Porous membranes can be divided into symmetric and asymmetric structures, with symmetric membranes having a repetitive uniform structure and asymmetric differing in both structure and material in different parts of the membrane (Nunes & Peinemann, 2006). Asymmetric membranes are commonly composed of a thin dense top layer, performing the separation while minimising the resistance to solvent flux. The top layer is further attached to a porous support layer, helping the membrane to maintain sufficient mechanical strength. This is highly desirable for all membrane application, and asymmetric structures are utilised in commercially available membranes (Baker, 2012).

Asymmetric membranes can be further classified into two types; integrally skinned asymmetric (ISA) membranes and thin film composite (TFC) membrane. ISA's are composed of the same material throughout and separation is achieved through a thin, denser top layer (Yuan, et al., 2017). TFC's are made via dip-coating or interfacial polymerisation, differing from ISA membranes in that the support and top-layer can be of different chemical composition. TFC's offer benefits of having optimized individual layers dependant on selectivity and permeability, as well as high chemical, mechanical and thermal resistance. As a caveat to this, TFC's are more sensitive to mechanical failure due to differential swelling or chemical incompatibility between the layers of the TFC (Vankelecom, et al., 2004).

### 2.3 Commercial OSN Membranes

There are a range of commercially available OSN membranes for purchase on the open market, that have applications in a range of solvents. The pore size of these membranes ranges from a MF scale 0.1  $\mu\text{m}$  to a near RO size of 150 Da. A summary of available suppliers and their products are given in Table 2-3 along with some material characteristics. This list is restricted to NF membranes:

# Background and Literature Review

Manufacturer	Product	MWCO (g/mol)	Material	Membrane Type	Source
Evonik MET	Duramem™ 150	150	Polyimide	ISA	(MET, 2018)
	Duramem™ 200	200	Polyimide	ISA	
	Duramem™ 300	300	Polyimide	ISA	
	Duramem™ 500	500	Polyimide	ISA	
	Duramem™ 700	700	Polyimide	ISA	
	Duramem™ 900	900	Polyimide	ISA	
	Puramem™	280	Polyimide	TFC (silicon-coated PAN)	
	Puramem™ S	600	Polyimide	TFC (silicon-coated PAN)	
SolSep BV	NF010206	300	PDMS	ISA	(Székely, et al., 2011)
	NF010306	≈400	PDMS	ISA	(Syed, et al., 2017) (Ormerod, et al., 2013)
	NF090101	350	PDMS	ISA	(Bastin, et al., 2017)
	NF090801	350	PDMS	ISA	(Bastin, et al., 2017)
	NF030306	500	PDMS	ISA	(Ormerod, et al., 2013)
	NF080105	500	PDMS	ISA	(Bastin, et al., 2017)
	NF030705	500	PDMS	ISA	(Bastin, et al., 2017) (Ormerod, et al., 2013)
	NF070706	250	PDMS	ISA	(Bastin, et al., 2017)
Koch	SeIRO™ MPF-34	200	PDMS	ISA	(Koch, 2018)
	SeIRO™ MPF-36	1000	PDMS	ISA	
	SeIRO™ MPS-34	200	Poly Sulfone	Proprietary	
	SPIRAPRO™	200	Polyamide	TFC	

**Table 2-3 Summary of commercially available membranes available for purchase at the time of writing**

Evonik MET has a range of OSN membranes available, with a wide range of MWCO's available, made from solvent stable P84 Lenzig polyimide and PAN. P84 Lenzig has shown to be stable in a range of solvents including; alcohols, esters, aromatics and ethers, and PAN has been shown to be solvent stable [ref]. The Duramem™ range is made from P84 Lenzig and has a range of MWCO in correspondence to the number associated with it e.g. Duramem 150 has a MWCO of 150 g/mol, Duramem 500 has a MWCO of 500 g/mol. The Puramem™ series has only 2 products available, the Puramem and Puramem S, with a MWCO of 280 and 500 g.mol<sup>-1</sup> respectively. The Puramem™ series are stable in non-polar solvents such as alkanes and MEK (MET, 2018).

The Duramem™ series are integrally skinned asymmetric membranes and are formed using immersion precipitation which is a phase inversion technique [ref]. This technique converts the liquid polymer solution into a solid state in a controlled transformation, then immersing the cast polymer into a non-solvent bath.



## Background and Literature Review

Immersion precipitation results in an integrally skinned asymmetric membrane which has a dense top layer. This type of membrane is treated with a cross-linker to allow for a lower MWCO and are treated with a conditioning agent to improve flexibility and stability during transport. The Duramem™ series are stable up to 60°C and 50 bar pressure and are available commercially as a flat sheet membrane or as a spiral wound module.

The Puramem™ also developed by Evonik MET are silicon coated TFC's which are also stable up to 60 bar pressure and 50°C and are designed for use in non-polar solvents. The Puramem™ series are thin-film composite membranes, coating a silicon-based chemical onto polyimide. This membrane series has 2 products, the Puramem and the Puramem S which have MWCO of 280 and 500 g/mol respectively.

Borsig GmbH have two membranes for OSN use, the GMT-oNF 1 and 2 respectively. The GMT-oNF 1 and 2 MWCO is highly dependent of the solvent system (Schmidt, et al., 2014) (Székely, et al., 2011). This membrane is comprised of a silicon polymer-based composite with a non-porous top layer and a micro-porous base layer.

Koch membranes have a range of OSN membranes. The current generation of OSN membranes available from Koch are the SPIRAPRO NF and SELRO NF series. The SelRO series includes the MPF-36 (1000 Da) (Conidi, et al., 2017), MPF-34 (200 Da) (Arkell, et al., 2013), MPS-34 (200 Da) (Santos, et al., 2016) (Garcia-Ivars, et al., 2017).

Solsep has a large range of NF membranes available at a range of MWCO and chemical resistances. The membranes available include; NF 090101 and 090801 (500 Da), NF 080105 (500-1000 Da dependant on the solvent), NF 030705 (1000 Da), 070706 (250 Da) (Bastin, et al., 2017).

## 2.4 Membrane Modification

There are several types of membrane modification techniques used in literature which can be broken down into two main types: post-synthesis modification (POST modification) and simultaneous crosslinking and coagulation (SIM modification). Post modification can also be broken down by the methods used: submersion in crosslinking bath for an allotted amount of time (Hermans, et al., 2015) (Vanherck, et al., 2010); Drip/dry method, similar to submersion but membrane is removed periodically and dried in an oven to removed solvent before being re-submerged or placed into another crosslinking solution (typically used for fabrication of TFCs) (Wei, et al., 2008) (Wang, et al., 2011); and flux method, where the crosslinking solution is permeated through the membrane (Reddy, et al., 2003). SIM modification involves dissolving the crosslinking agent in the solvent exchange bath, so that when the cast dope solution is placed inside the solvent exchange bath the crosslinking agent helps form narrower pores (Hermans, et al., 2015) (Vanherck, et al., 2010). While there are other methods of post synthesis modification membranes such as

plasma treatment (Volkova, et al., 2015) and ozone treatment (Pan, et al., 2012), they will not be covered as they are beyond the scope of this thesis.

### 2.4.1 Crosslinking bath

Surface modification of a membrane by immersion in a crosslinking bath is regarded as the most common form of membrane modification. The process involves submerging the membrane in a solvent bath which includes a certain percentage of the crosslinking agent for an allotted amount of time to allow the crosslinker to attach to the surface of the membrane (Vanherck, et al., 2013). Vanherck, *et al* (2010), studied the stability, permeability and rejection properties of polyimide (PI) membranes crosslinked with various diamines of different lengths at different crosslinking agent concentrations and crosslinking times, amongst other things. Crosslinking with hexane diamine consistently rejected RB in IPA of >90% regardless of the dope solution solvent and co-solvent.

### 2.4.2 Flux method

Modification of the membrane by fluxing the crosslinking agent through the membrane helps to ensure that all the pores are exposed to the agent, and that all the membrane surface that would normally be used for separation is crosslinked to some degree. Reddy, *et al* (2003), modified PES membranes in a dead end cell by initially permeating poly(sodium 4-styrenesulfonate) (PSS) as the crosslinking agent, but does not go into detail as to concentrations, only giving the membrane reference. The authors show consistent increases in rejection of both PEG-6000 and 35000 after flux modification with PSS for all of the membranes tested, with all except one (PES-85) having >99% rejection of PEG-35000.

### 2.4.3 SIM modification

Simultaneous solvent polymerisation and crosslinking is becoming a more attractive option for membrane modification as the method removes the additional step of placing the membrane into the crosslinking bath after the solvent exchange has occurred. Hermans, *et al* (2015) tested phase inversion and TFC membranes crosslinked using SIM method with different types of diamines. Both types of membranes show increases in dye rejection in ethanol with decreases in membrane permeability, interestingly, the permeability of TFC membranes was worse than that of phase inversion prepared membranes with increased rejection.

## 2.5 Membrane Parameters and Performance

NF separations are influenced by a range of factors, which makes modelling NF systems difficult, which is further complicated by the solvent chemistry happening in tandem in OSN system. The selectivity of the membrane is believed to be primarily influenced by steric factors, additional parameters such as pressure, temperature, charge and concentration have been observed to influence the selectivity of the membrane, and thus can be adjusted as to fine tune the separation of the system. Furthermore, factors such as concentration polarisation and membrane preconditioning should be considered when designing the system. For OSN, the interaction between the chemical solvent, solute and the membrane also effect the selectivity of the membrane, which can lead to significant changes to the performance of a given membrane during operation using different solvents (Schmidt, et al., 2014).

### 2.5.1 Pressure

Pressure is the main driving force in NF systems, with operational pressures carried out between 5 – 60 bar. However, there is a distinction between the applied and effective pressure, with the effective pressure being defined as the difference between the applied and the osmotic pressure. Effective pressure can be calculated according to:

$$\Delta P_{effective} = \Delta P_{applied} - \Delta \Pi$$

**Error! Reference source not found.** Where  $\Delta P$  is the pressure difference and  $\Delta \Pi$  is the osmotic pressure difference.

The osmotic pressure is caused by a difference in solute concentration on either side of the membrane. For a dilute system the osmotic pressure is assumed to be negligible, making the applied pressure equal to the effective pressure. However, for more concentrated systems the osmotic pressure should be included in all calculations. For low concentrations (<0.1 M) the osmotic pressure can be calculated using the Van't Hoff equation:

$$\Delta \Pi = i R_{gas} T \Delta C_i$$

Where  $i$  is the Van't Hoff coefficient (1 for non-electrolytes),  $R_{gas}$  is the ideal gas constant,  $T$  is the temperature and  $C$  is the concentration of species  $i$ . For higher concentrations the Van't Hoff equation is not valid and the osmotic pressure must be evaluated experimentally (Mulder, 1996).

As a general observation, increasing the applied pressure of the membrane system increases the performance of the membrane, in terms of flux and solute rejection, for both aqueous and non-aqueous systems. A linear increase in flux was observed by Chau, *et al* (2018) where a custom-made membrane exhibits increased flux in various solvents including; methanol, heptane, DMSO over a range of 10-25 bar.

## Background and Literature Review

During high pressure operation, polymeric membranes are believed to become compacted, resulting in a less permeable membrane structure. Increased compaction will result in a gradual levelling of the flux towards a plateau value. Depending on the compaction occurring in a given solvent, the plateau is reached at different pressures and the flux increase can appear linear or non-linear depending on the pressure interval studied (Chau, et al., 2018), (Conidi, et al., 2017), (Zhang, et al., 2017). The theory of membrane compaction is supported by an observed decrease in flux during the initial stages of membrane operation. Compaction is believed to be partially reversible, which is supported by the observation that when a polymeric membrane is allowed to rest (no applied pressure) before starting a second filtration, the pure solvent flux is generally found to be higher during the initial stage of the second filtration compared to the final flux observed during the first filtration (Whu, et al., 2000).

The rejection of a solute also increases with increasing pressure. Whu, *et al* (2000), found that the rejection of Brilliant Blue increased from  $\approx 54\%$  at 10 bar to  $\approx 95\%$  at 30 bar using a MPF-60 membrane. Similarly, the rejection of Safranin O increased from  $\approx 45\%$  at 15 bar to  $\approx 85\%$  at 30 bar. A similar trend was found by Chau *et al* (2018) where the rejection of Brilliant Blue was  $\approx 97.2\%$  at 15 bar and  $\approx 100\%$  at 30 bar and the rejection of Safranin O was  $\approx 94.3\%$  at 15 bar and  $\approx 96.4\%$  at 30 bar for a custom membrane made at a thickness of  $1.67 \mu\text{m}$ . The increase in rejection with increasing pressure is believed to also be a result of membrane compaction resulting in a decreased size of pores or free-volume elements. A high solute rejection is often desired for increased product yield, thus varying the solute rejection with pressure could provide a way to optimise membrane performance. The increase in rejection with increasing pressure can be derived by:

$$R = 1 - \frac{C_p}{C_f} = 1 - \frac{k_c \Phi}{1 - [1 - k_c \Phi] \exp(-Pe)}$$

$$Pe = \frac{k_c}{k_d} \frac{rp^2}{8\eta D_{\infty}} \Delta P$$

Therefore, as  $\Delta P$  increases,  $Pe$  increases, thus:

$$(1 - k_c \Phi) \exp(-Pe) \rightarrow 0$$

And

$$R = 1 - k_c \Phi \quad \text{limiting rejection}$$

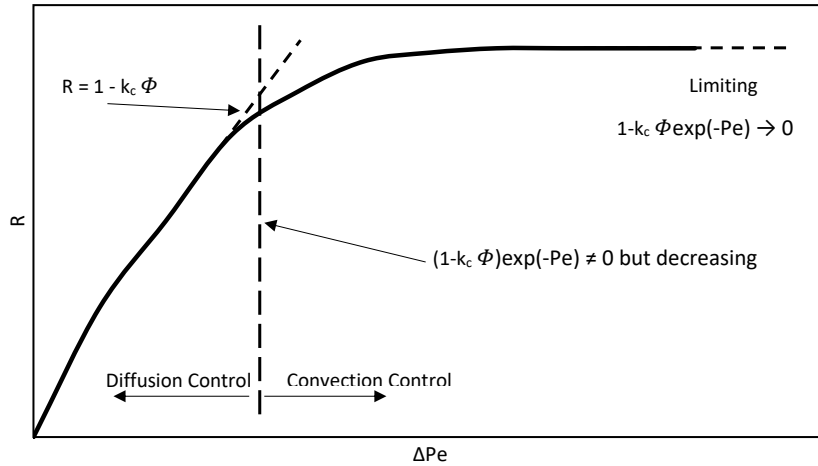


**Figure 2.1 Rejection as a factor of modified Peclet number**

$k_c$  and  $\Phi$  are both functions of the solute radius and pore radius only. In porous membranes, this behaviour is essentially the result of diffusion control converting to convection control as the pressure increases. Compaction reduces the pore size and thus impacts both  $k_c$  and  $\Phi$ .

### 2.5.2 Temperature

Zedel *et al.*, (2016) observed an increase in the permeate flux of 1-dodecene using a oNF-1 membrane from Borsig. At a range of transmembrane pressures, the flux is consistently faster due to the increased temperature (at 20 bar, flux at 10°C is  $\approx 18$ , 20°C is  $\approx 25$  and at 45°C flux is  $\approx 38$  L/m<sup>2</sup>h). Subsequently, the authors also found that the rejection (retention) of Marlipol 24/70 decreased with increasing temperature (decrease of  $\approx 15\%$  with a temperature increase of  $\approx 30$ K). Similarly, Burgal, *et al.*, (2017) had similar findings using DMF on custom made PEEK and PBI membranes. The authors found that the MWCO of both PEEK and PBI membrane increased significantly when the temperature was increased from 30°C to 140°C, along with an increase of solvent permeability in PEEK membranes, but a decrease in permeability when using PBI membranes (with a large margin of error). PEEK membrane MWCO increases from 90% of 300 g.mol<sup>-1</sup> to 1100 g/mol at temperatures 30 to 140°C respectively. For PBI membranes, the MWCO increases from 90% rejection at 400 to 900 g/mol at 30 to 140°C respectively. The decrease in solvent permeability for PBI membrane with increasing temperature is likely attributed to thermal damage to the membrane as PBI isn't as thermally stable when compared to PEEK. The author also reported that the commercially available Duramem 300 had a decrease in solvent permeability at increased temperature and also failed at 140°C, however the MWCO did increase to 600 g/mol from 30 to 85°C.

## Background and Literature Review

The flux dependency of membranes with temperature is usually the result of changes to the solvent viscosity. Viscosity is temperature dependant according all derived models including Reynolds (1886) (Eq 1) or the Arrhenius model for first order fluids (Eq 2):

$$\mu(T) = \mu_0 \exp(-bT) \quad \text{Eq 1}$$

$$\mu(T) = \mu_0 \exp\left(\frac{E}{RT}\right) \quad \text{Eq 2}$$

Where:  $\mu_0$  and  $b$  are coefficients,

$T$  is temperature

$E$  is the activation energy

$R$  is the universal gas constant

Thus, as the temperature increases, viscosity will decrease and according to the general membrane equation, the flux must increase:

$$J = \frac{\Delta P}{\mu R_m}$$

While the temperature is not directly involved in the rejection of a given solute, it does affect diffusion which is involved in the rejection of a solute as determined by the Stokes – Einstein equation:

$$D = \frac{k_B T}{6\pi\eta r}$$

Where:  $D$  is the diffusion coefficient

$k_B$  is Boltzmann's constant

$T$  is absolute temperature

$\eta$  is the dynamic viscosity

$R$  is the radius of the spherical particle

As the temperature increases and the viscosity decreases, depending on the solvent being used, the diffusion coefficient can increase significantly resulting on a change in rejection properties of a membrane.

### 2.5.3 Charge

For NF operation in aqueous systems, electrostatic interactions and the charge of solute molecules are widely considered to be an important influence on the rejection properties of the membrane (Donnan, 1995) (Wang, et al., 2014) (Bowen, et al., 2004). For applications in organic solvents, charge effects are generally assumed to be of less importance due to the uncharged nature of solvents (no dissociation of hydrogen). However, Yang, *et al* (2001) observed differences in rejection for 3 dyes of identical MW (350

## Background and Literature Review

g/mol) in methanol; Orange II, Safranin O and Solvent Blue 35. The differences in rejection may be due to charge effects, however there are additional factors that could be of importance.

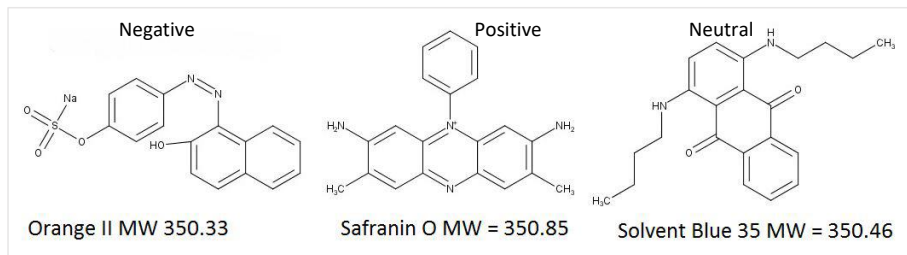


**Figure 2.2 Chemical Structure of 3 Dyes of Identical Molecular Weights**

Yao *et al.*, (2016) found comparable results while attempting to develop a positively charged membrane. The authors found that, in methanol, the positively charged Safranin O had a higher rejection than the disperse red (MW 314 g/mol) and methyl orange (MW 327.3 g/mol) dyes, with the methyl orange being rejected the least and is negatively charged in nature. While the authors emphasise that the rejection is due to the surface charge of the membrane, the rejection of the dyes may also be due to the size and shape of the chosen dyes also.

Charge effects on membrane rejection can be explained by looking at the interactions between solute and the membrane. For any given membrane system, solutes are driven towards the permeate side in an attempt to minimise the concentration and reduce the osmotic pressure of the solution. Most polymeric membranes carry a slight charge (known as zeta potential (ZP)) which is a result from the polymer side-chains. When charged molecules encounter a charged membrane, co-ions are repelled resulting in a higher rejection of these solutes. To maintain overall charge neutrality in the system, an equal number of counter-ions must be retained by the membrane resulting in a high rejection for all charged solutes. The retained solutes will strive to minimise the system charge effect and solutes will become arranged with the counter-ions forming an electrical double-layer at the interface between the membrane and the feed solution. If the ion concentration is sufficiently high (> 0.1 M) the double-layer will achieve full coverage, resulting in the counter-ions completely screening the membrane charge, rendering rejection to be dependent primarily on steric factors. For a lower ion concentration, the counter-ions present are not sufficient to balance the full membrane charge, and only a partial screening effect will be achieved. For a charged solute-membrane system the rejection is concentration dependent, with the rejection increasing for a decrease in concentration (Donnan, 1995) (Bowen, et al., 2004).

#### 2.5.4 Concentration

There have been many publications that have observed the solute concentration has affected solute rejection and permeate flux. Generally, with increasing solute concentration the permeate flux through the membrane decreases. The decrease in permeate flux is a result of increased osmotic pressure, lowering the driving force in the system. However, the solute concentration used for testing have generally been low and hence the osmotic pressure is not sufficient to account for the significant changes in flux observed. The more likely scenario is that decreasing flux is due to a combination of factors, including; increased osmotic pressure, concentration polarisation and pore blocking (Whu, *et al.*, 2000) (Peeva, *et al.*, 2004) (Ryzhkov & Minakov, 2016) (Shaaban, *et al.*, 2016).

An example of solute concentration affecting the membrane rejection has been observed by Whu, *et al* (2000). The authors observed an increase of solute rejection from 67.6% to 93.5% of Safranin O and an increase from 94.8% to 99.7% for Brilliant Blue R when increasing the solute concentration from 0.01% to 1% (w/w) when using the MPF-44 membrane in methanol. Shaaban, *et al* (2016) observed an increase in the rejection of RB dye from 82.3% to 89.7% when increasing the solute concentration from  $\approx 12$  g/L to  $\approx 37.5$  g/L of dye, with the permeate flux decreasing from 28 to 19 L/m<sup>2</sup>h respectively. However, the authors did report that rejection of salt (not specified) decreased from 89.3% to 86% at concentrations of 12 to 37.5 g/L respectively. The opposing trends in rejection for salt and dye suggests that more factors than concentration are effecting the rejection properties of the membrane. Peeva, *et al* (2004) found an opposing trend with the rejection of docosane for a change in concentration from 0.33M to 0.67M while using the Starmem™ 122 membrane during operation when using toluene. Furthermore, the same trend was observed in rejection of tetraoctylammonium bromide (TOABr), with the permeate flux also decreasing with increasing solute concentration.

#### 2.5.5 Concentration Polarisation and Fouling

During operation some solutes are retained by the membrane, causing accumulation and formation of a boundary layer with a higher concentration close to the membrane surface. This phenomenon is referred to as concentration polarisation and can have a significant effect on membrane performance, as the increased concentration acts as an additional resistance against solute and solvent mass-transfer. During membrane operation, solutes are brought to the boundary layer by convective transport and removed through diffusive flow back to the bulk solution (Figure 2.3). The convective and diffusive flows are assumed to be in equilibrium and the ratio of concentrations between the feed and the boundary layer ( $C_m$ ) can be calculated as a function of the flux ( $J$ ), the solute mass-transfer coefficient ( $k$ ) and the concentration in the bulk ( $C_b$ ) and the permeate ( $C_p$ ) as detailed by:



$$J = k \cdot \ln \left( \frac{C_m - C_p}{C_b - C_p} \right) \text{ where } k = \frac{D_i}{\delta}$$

where  $D$  is the diffusion coefficient of solute  $i$  and  $\delta$  is the boundary layer thickness (Schäfer, *et al.*, 2005).

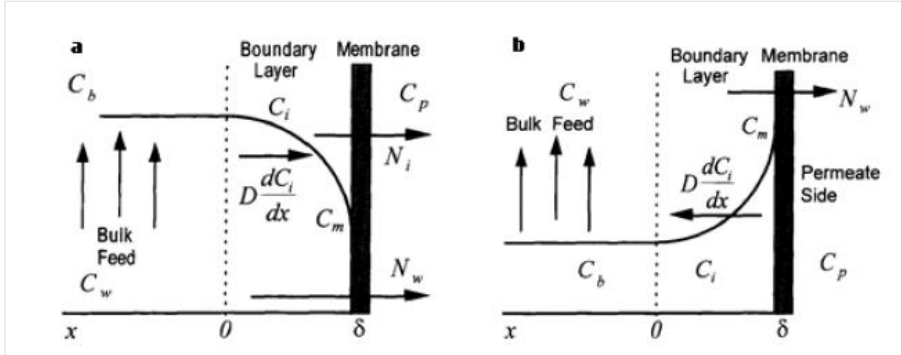


**Figure 2.3** Concentration profile of (a) permeating and (b) retained component at steady state conditions where  $C$  is the concentration of the solvent ( $w$ ) or species  $i$  in the bulk ( $b$ ), permeate ( $p$ ) or membrane boundary layer ( $m$ ) and  $N$  is the flux of the solvent ( $w$ ) and species  $i$  respectively (Bhattacharya & Hwang, 1997)

Severe concentration polarisation commonly results in a decreased flux, which is attributed to a significant increase in osmotic pressure resulting from the elevated concentration observed immediately adjacent to the membrane surface. Increased osmotic pressure further influences the separation performance, resulting in a decreased driving force for highly permeable components and an increased driving force for less permeable components (Bhattacharya & Hwang, 1997).

Concentration polarisation results from poor hydrodynamic conditions in the equipment used for filtration. The process is reversible and can be rectified by improving mass-transfer in the system through increased stirring, permeate pulsing, use of cross-flow operation and/or inclusion of baffles or spacers. If the concentration polarisation is not rectified, the build-up in solute concentration may cause precipitation and crystallisation on the membrane surface, potentially causing membrane damage (Schäfer, *et al.*, 2004).

Deposition of solids at the membrane surface or in pores is referred to as membrane fouling and can be the result of a number of mechanisms, including adsorption, gel layer formation, cake formation and pore blocking. Adsorption is an interaction between a membrane and a solute, resulting in a solid layer forming on the membrane surface. Adsorption is generally considered to be the first step in fouling and results in an alteration of the membrane's surface characteristics. Gel layer formation results from the precipitation and deposition of organic material on the membrane surface and is commonly a result of concentration polarisation causing the concentration of a specific solute to exceed the solubility limit. Cake formation and pore blocking refers to a build-up of solid particles on the membrane surface or inside the pores.

## Background and Literature Review

Where the solute radii are smaller than the pore, the solute can enter and deposit on the pore walls, gradually decreasing the pore radius until the pore is fully blocked. Where the solute radii are similar in size to the pore radius, immediate blockage can occur, while solute radii larger than the pore will result in cake formation on the membrane surface. Initially, pore blocking and cake formation is a result of membrane-solute interactions, but solute-solute interactions become increasingly more important as the solute layer is built-up (Koros, et al., 1996) (Bhattacharya & Hwang, 1997) (Peeva, et al., 2004) (Schäfer, et al., 2004).

To mitigate the effect of concentration polarisation in dead-end filtration, the cell is mechanically stirred with the stirrer itself being as close to the membrane as possible. Oatley-Radcliffe, *et al* (2015) determined a correlation that removes the solute permeating through the membrane as a factor in solute rejection. Traditionally, the rejection ( $R_{obs}$ ) is calculated as;

$$R_{obs} = 1 - \left( \frac{C_p}{C_f} \right)$$

Where  $C_f$  is the solute concentration in the feed and  $C_p$  is the concentration of the solute in the permeate. Oatley-Radcliffe, *et al* determined that the mass transfer coefficient ( $k$ ) is a function of the stirrer speed:

$$k = a\omega^n$$

Where  $a$  and  $n$  are constants of the dead-end cell, and  $\omega$  is the stirrer speed (rad/s). This leads to the correlation:

$$R_{real} = \frac{1}{\exp\left(\ln\left(\frac{1-R_{obs}}{R_{obs}}\right) - \frac{J_v}{k}\right)} + 1$$

Where  $J_v$  is the permeate flux (m/s). The rejection of a given solute will be given between a range 0 – 1 which is equivalent to 0 - 100%

### 2.5.6 Preconditioning

OSN data is dependent on the membrane-solvent-solute system used for testing, where varying membrane performance is commonly observed for the same membrane type during operation in different solvents. Additionally, inconsistent membrane performance has been observed during operation in the same solvent when comparing data reported by different authors for a given membrane type. Several authors have suggested that observed variations could be a result of varying protocols for washing and pre-conditioning prior to membrane operation (Zhao & Yuan, 2006) (Soltane, et al., 2016).

## Background and Literature Review

The majority of commercial membranes are supplied with a preservative that allows for safe transit and dry handling of the membrane (e.g. Duramem™, Dow NF Series, GE Nanofiltration range). In the case of Duramem™ series, the membrane discs should be soaked in the desired solvent prior to fitting, or by permeating the desired solvent through the membrane and the desired operating pressure, this serves to remove the protective chemicals from the membrane and to compact the membrane for steady state operations.

Following initial pressurisation, a reduction in flux is commonly observed. This is believed to be a result of membrane compaction occurring as polymer chains are rearranged under the applied pressure. After permeation of a sufficient amount of solvent, a steady-state is reached, and stable flux and rejection data can be obtained. The required time to reach steady-state is highly dependent on the solvent-membrane system used for operation and for each test sufficient pre-conditioning time to reach maximum membrane compaction must be allowed before samples are collected. Additionally, compaction effects are partially reversible, so if the system has been depressurised or altered (e.g. change of solvent), a new pre-conditioning is required before the membrane can be considered to operate at steady-state and reliable measurements can be made (Zhao & Yuan, 2006) (Yao, et al., 2016).

## 2.6 Membrane Equipment and Set-up

The feasibility of a separation system is typically assessed using lab-scale dead-end filtration using flat sheet membranes. Lab-scale studies in dead-end (or “frontal”) filtration cells require a low amount of material and solvent volume when compared to crossflow systems (50 - 300 mL compared to litres in crossflow systems). The smaller scale allows for more experiments to be conducted as well as (potentially) shorter experimentation times, along with a much faster cleaning regime for the membrane being tested. For larger scale operations, the use of flat sheet membranes becomes impractical so membranes are typically scaled up into modules of spiral wound flat sheets or tubular banks to facilitate handling, minimise equipment footprint and provide effective fluid management (Vandezande, et al., 2008).

### 2.6.1 Lab-scale Equipment

Lab scale equipment can be classed broadly into two categories;

- Dead – end Filtration
- Cross – flow Filtration

Both of these systems use flat sheet membrane but operate differently. Dead – end filtration uses a membrane disk which is held in place inside the cell using O-rings and the liquid is pushed through the pores (or diffuses in the case of RO membranes) by applying pressure using pressurised inert gas, typically

nitrogen (this system is known as a “gas pump”). The advantage of this system is that the cells are widely available (Sterlitech™, Amicon™, Membranology™) and are cheap in comparison to a full crossflow system, with the system pressure is easy to control through a regulator. The drawback from this system is the concentration polarisation and surface fouling as the solution has nowhere to go except through the membrane. To combat this, a magnetic stirrer is suspended above the membrane surface to disrupt the liquid, with previous literature giving a guideline for what stirrer speed should be used (Oatley-Radcliffe, et al., 2015). Furthermore, typically less than 10% of the solution inside is permeated during the experiment to minimise any concentration polarisation that may occur and to maintain a consistent feed concentration (section 3.4.1).

Cross – flow systems have the solution flow across the surface of the membrane. As such, the bulk liquid will pass through the membrane due to particle size and osmotic effects while the solutes will be retained by the same effects. Furthermore, the bulk solution scours the surface of the membrane which prevents the solute from passing through the membrane while minimising membrane fouling. The pressure is controlled using a centrifugal pump or having pumps in series, one to produce pressure while the second produces velocity, with the pressure can be tuned from a back-pressure regulator after the membrane. The advantages of small scale crossflow systems are that they are representative of how the membrane would perform if scaled up to an industrial scale system, and that multiple membranes can be tested at the same time (Holda & Vankelecom, 2014). The disadvantage of these systems is the initial cost, particularly if high pressures for NF and RO are required.

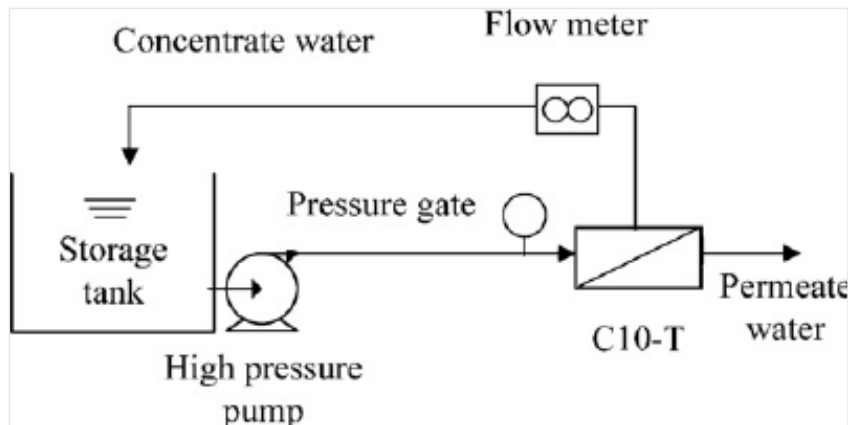


Figure 2.4 basic schematic for a crossflow membrane rig

## 2.6.2 Pilot and Industrial Scale Equipment

For larger operations, there is an increased product demand which then leads to an increase in membrane area and an increase in the number of membrane modules being used. Depending on the type of membrane used, the area for filtration can be increased by 1 or 2 methods. For robust membranes (ceramic, tubular or spiral wound), the area cannot be increased so more membrane(s) or modules are added to the system. For polymeric membranes, multiple spiral wound membranes are used, which significantly increase the membrane area while minimising the physical footprint of the membrane module. In industry, membrane systems are typically run in a single pass with more feed solution being added as needed, to allow for faster throughput and to minimise any concentration polarisation that may occur.

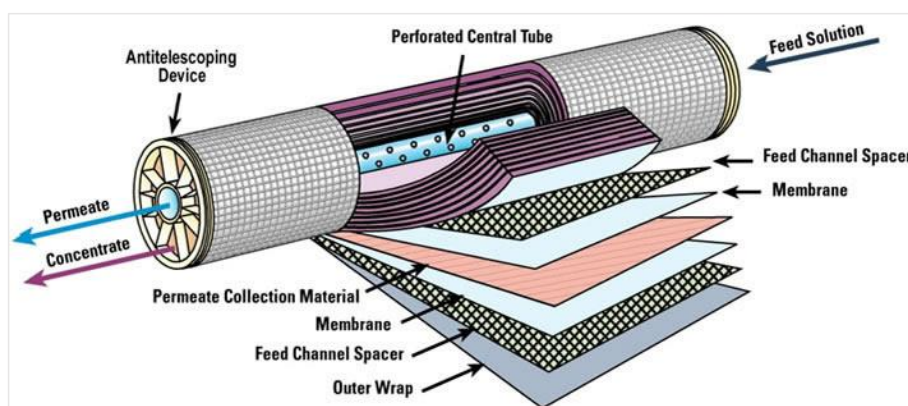


Figure 2.5 Cross section of spiral wound polymeric membrane

## 2.7 Polyether sulfone (PES) Membranes for Solvent Systems

One of the many issues of OSN is having a polymer that is chemically resistant but will also perform consistently in harsh chemicals (Sterlitech, 2018). PES membranes can be manufactured for a range of UF sizes. Several commercial suppliers provide UF membranes up to 500,000 Da, but only one supplier, Microdyn Nadir™, supplies NF membranes of 500 and 1000 Da. PES membranes have shown to work consistently in the presence of harsh chemicals, such as hydrogen peroxide, (Tsehay, et al., 2018), suitable for use in acidic conditions (Ernst, et al., 2000) (Yun, et al., 2018) and have been used in the filtration of uranium (Torkabad, et al., 2018) (Torkabad, et al., 2017) and heavy metals (Zhu, et al., 2014) (Wei, et al., 2018).

While PES membranes have been advertised as chemically resistant, they're used more frequently in wastewater applications for NF. Some examples of PES membranes being used for OSN applications are: PES shown to be a viable option for filtration in solvent filtration such as THF and DMF at room and high temperatures (140°C) (Pulido, et al., 2018). Rezzadori, et al (2015) found that PES membranes of 400 MWCO from Microdyn Nadir™ (NP030) had performed similarly in alcohols (methanol to butan-1-ol) and

## Background and Literature Review

hexane, with very little change in surface energy or water contact angle post filtration. Vieira, *et al* (2018) examined the use of commercial NF membranes for concentration of plant matter with the feed being an ethanol/water blend (70/30). The authors found that the 400 and 1000 MWCO PES membranes had higher flux rates than the other polymer types tested but with the 1000 MWCO having the lowest rejection and the 400 MWCO having comparable rejection to 200 MWCO membranes.

Satyawali, *et al* (2017) screened NP030 and other OSN membranes for concentrating plant extract in heptane, isopropanol and acetone. While the authors didn't publish the data obtained using NP030, there is clear indication that PES membranes can be used in solvent systems.

## 2.8 Membrane Characterisation

### 2.8.1 Molecular Weight Cut-Off (MWCO)

For large pore ultrafiltration and microfiltration membranes, pore sizes can be measured using visualisations techniques such as Scanning Electron Microscopy (SEM), however, the near atomic scale dimensions of NF and small pore UF membranes makes visualisation techniques very difficult with correct best practice and technologies. While there are some visualisation methods that can be used for analysis at this scale e.g. Atomic Force Microscopy (AFM), they are very expensive and require specialised techniques and experience to be able to obtain clear results. Therefore the use of neutral solutes of different sizes are commonly used to determine the pore size or MWCO of the membrane by measuring the rejection of the solutes. Some examples of solutes used are styrene oligomers (Burgal, *et al.*, 2015), polypropylene glycols (PPGs) (Davey, *et al.*, 2017) and polyethylene glycols (PEGs) (Rohani, *et al.*, 2011). Inside each bottle of a 'standard', there is typically a narrow range of solutes with an overlap into the next size of 'standard' (Davey, *et al.*, 2017). Furthermore, the shape of the molecule has an impact, so typically long straight chains are used as branched molecules are more easily rejected (Zheng, *et al.*, 2008) (Zheng, *et al.*, 2009).

### 2.8.2 Fourier Transform Infra-Red (FTIR) Spectroscopy

FTIR is a widely used technique to investigate the chemical functionality of surfaces. Similar to other infrared spectroscopy techniques, FTIR probes the frequency of molecular bonds. This is due to infra-red (IR) frequencies (approximately 10<sup>12</sup> – 10<sup>14</sup> Hz) overlap with molecular vibration frequencies. If the frequency of IR radiation is identical to that of a particular molecular vibration, then this can cause the vibration to move to a higher energy state.

The majority of FTIR instruments fall into one of four categories: transmission, attenuated total reflectance (ATR), diffuse reflectance spectroscopy (DRIFTS) and specular reflectance/reflection-absorption (Griffiths

& Haseth, 2007) (Smith, 2011). The oldest and simplest technique is transmission, where an IR beam is passed through the sample and the transmission energy is detected and used to produce the resultant spectrum. ATR-FTIR is more useful to examining surface samples rather than bulk materials and is therefore of great interest for studying membrane surfaces, but an add-on is typically required to be attached to the FTIR instrument. FTIR instruments typically operate in the middle of the IR range, with wavenumbers of approximately  $666 - 4000\text{cm}^{-1}$ . In this region, the transition energies for many functional groups' vibrational states are found. As a result, the presence of specific absorption bands can be used to identify the presence of the corresponding functional groups. The vibration of whole molecules produces complex absorption patterns at high frequencies, which is often specific to that chemical and hence is of great utility in identifying particular molecules.

### 2.8.3 Surface Charge

Membranes typically carry a charge in aqueous solution, whether polymeric or ceramic, with the state and magnitude of the charge being dependant on the membrane surface chemistry, environmental pH and ionic concentration. Feed solutions are typically complex mixtures containing a wide variety of charge carrying substances including surfactants, macromolecules, ions, polyelectrolytes etc. Interactions between these species and the membrane surface can significantly alter the surface charge of the membrane (Ernst, et al., 2000). Due to the charge interactions between the membrane surface and charged solutes and particulates, the charge of the membrane surface plays a significant role in the mediating the separation properties of the membrane, the nature and extent of fouling and concentration polarisation.

Actual membrane surface potential is very difficult to measure directly. Estimation of the zeta ( $\zeta$ ) potential at the shear, or slip, plane is more accessible, leading to this measurement being used more extensively when studying the electrical potential of membranes. There are a number of electro kinetic methods available. The primary methods of interest studying phenomenon are electrophoresis, electro-osmosis, sedimentation potential and streaming potential. When a fluid containing charged ionic species is allowed through a charged membrane, capillary, plug or diaphragm due to a pressure gradient then the potential difference measured at zero current is the streaming potential (Singh, et al., 2005). The streaming potential is dependent upon a number of solution properties including the  $\zeta$ -potential, solution viscosity, ionic diffusivities and dielectric constants. For measurements the streaming potential can be generated in two ways. The electrolyte solution can be forced through a porous material, such as membrane pores, to measure the transverse streaming potential. Here the electrical double layer in the pores is being measured with errors arising if an overlap in the double layer from the opposite sides of the pores occurs. Secondly, the electrolyte can be forced through a narrow channel formed by the membrane being sandwiched

between two plates, with the flow across the surface of the membrane, allowing measurement of the tangential streaming potential.

## 2.9 Current OSN Research

There are three main groups researching OSN at the time of writing which are; Andrew Livingston's group, Bart Van der Bruggen's group and Ivo Vankelecom's group, that is without independent researchers (Davey et al) and research conducted in China. To that end, a summary of recent research conducted by the three groups given will be reviewed below.

### 2.9.1 Andrew Livingston *et al*

Andrew Livingston is a professor at Imperial College London and was a director of Membrane Extraction Technology (MET) producing the Starmem® series of OSN membranes before producing the Duramem® and Puramem® series of membranes before there merged with Evonik to become Evonik MET. The Livingston group publishes work on a range of membrane applications and fabrications.

The latest research from the group concerns the fabrication of poly(piperazine trimesamide) TFC OSN membranes (Butler, et al., 2019). The authors investigated how different solvents used in the solvent phase of fabrication affect the membrane performance. The use of hexane in the solvent phase has a large variation on 0.1% TMC (w/v) fabricated membranes; but show much more consistent results when hexane is used with 0.3% TMC (w/v), yielding a membrane which has 90 – 95% rejection of Disperse Red (mw = 314 g/mol) in methanol. When nitrobenzene is used in the solvent phase along with 0.1% TMC (w/v), the rejection of Disperse Red decreases with increasing MIL-101 concentration while the permeance of the dye increases.

The group has also studied the effectiveness of roll to roll dip coating of three different polymers onto a PAN and crosslinked Ultem 100 support membranes (Cook, et al., 2018). The authors found that this method of coating and choice of polymers can have an active layer thickness between 100 to 800 nm depending on the concentration of the coating chemical to be used. The first coating used, designated PIM-1, had similar rejection patterns for both solvents used (heptane and toluene) and for both support membranes, with the MWCO being  $\approx 700$  g/mol. The permeate flow is largest when toluene is the solvent for both support membranes, but with significantly fast flow when PAN is the support compared to ultem 100 (12.5 L/m<sup>2</sup>hbar compared to 7 L/m<sup>2</sup>hbar respectfully). Further testing by expanding the range of solvents tested (methanol, acetonitrile and acetone) on PIM-1 on an ultem 100 support membrane found that the membrane's performance in methanol is significantly worse than the others tested, with the rejection not rising above 20% of any of the polystyrene particles tested (with acetonitrile and acetone having similar MWCO patterns to heptane and toluene). Acetone had the largest permeate flux with 11 L/m<sup>2</sup>hbar over the course of 3 days of testing.



## Background and Literature Review

Testing of the other two coatings, designated PIM – 7 and 8, found that PIM – 7 has the largest MWCO of the three coatings with 90% rejection occurring around  $\approx 550$  g/mol when toluene is the solvent, while PIM -8 had the lowest of the three with a MWCO of  $\approx 1000$  g/mol. While PIM – 7 had the lowest solvent permeability of 4 L/m<sup>2</sup>hbar, PIM – 1 had a faster solvent permeate flow rate compared to PIM – 8 despite the smaller MWCO (11 L/m<sup>2</sup>hbar compared to 6 L/m<sup>2</sup>hbar respectively).

Also in 2018, the Livingston group collaborated with Korean researchers to study thermal rearranging of polymers in support membranes to facilitate OSN and pressure retarded osmosis (Kim, et al., 2018). Initial testing of thermally rearranged nanofibrous membranes (TR-NRM) show very high pure solvent permeabilities in all solvents tested with very little observed damage to the membrane, however, these membrane have yet to be crosslinked hence the large permeabilities. TR-NRMs are then crosslinked with polydopamine (PDA) and are then referred to as TR-PDA. Following this step, the membrane is further crosslinked using MPD and TMC to form thin-film composite membranes. The fabricated TFC's are testing used polystyrene oligomers in DMF and dyes respectively, yielding a MWCO 600 g/mol, Chrysodine G rejection of 6Methyl Orange rejection of 87% and a rejection of brilliant blue of 95%. Testing the membranes at elevated temperatures (60 and 90°C) showed that while the permeate flowrate increased with temperature (9 and 11 L/m<sup>2</sup>hbar respectively) the MWCO did not change when tested with polystyrenes. The authors also found that after testing with DMF, the permeate flux increases when THF and methanol are permeated through the membrane, but no rejection data is given.

The Livingston group has also been researching new ways of modifying PEEK, PAN, Ultem 100 and PBI membranes for OSN use, notably using Plasma Enhanced Chemical Vapour Deposition (PECVD) (Mitev, et al., 2018). The membranes were coated using pentane, HMDSO and toluene, where for all solvents, the membrane thickness increases with longer submersion to the PECVD process. The PECVD enhanced PEEK membranes show MWCO of range of 300 – 500 g/mol in 3 out of 4 samples, with a permeability range of 2.1 to 15 L/m<sup>2</sup>hba when heptane is used in the PECVD chamber compared a MWCO of 600 g/mol in unmodified PEEK with a permeability of 0.6 L/m<sup>2</sup>hbar. PECVD significantly increases the MWCO of Ultem and PAN supports when HMDSO is the crosslinking agent, increasing the MWCO of Ultem  $\approx 550$  g/mol and PAN with a MWCO of 400 g/mol while decreasing the permeability of Ultem from 111 L/m<sup>2</sup>hbar to 9.6 L/m<sup>2</sup>hbar. The modification of PAN by PECVD appears to give varying results depending on the crosslinking agent, use of HMDSO gives MWCO <500 g/mol with permeability values ranging between 3.7 – 9.2 L/m<sup>2</sup>hbar. Using ethylene as part of PECVD drastically decreases the permeability (0.2 L/m<sup>2</sup>hbar) and the MWCO is > 1400 g/mol.

### 2.9.2 Van der Bruggen *et al*

Bart Van der Bruggen is a professor at KU Leuven who specialises in all areas of membrane research, from membrane development to membrane applications to process modelling. Of late, the research conducted by Van der Bruggen has been varied but this summary will only concern research on OSN topics.

In 2018, a study was conducted on Hansen Solubility Parameters (HSP) of ceramic membranes and attempting to use them to model solute rejection based on these properties (Saiz, et al., 2018). The authors found that the pure solvent permeate flux rate of an unmodified ceramic membrane is largely dependent on having a large hydrogen bonding parameter compared to the polarity and diffusion parameters. Modifying the membrane with Benzyl finds that the permeate flux still increases with decreasing diffusion parameters but the polarity parameter also now plays some role in the permeate flux however, the permeate flux still appears to be solvent dependent. The rejection properties of PEG 600 by a ceramic membrane changes drastically depending on the solvent used as the rejection is 55% in acetone and -5% in toluene, with the rejection of polystyrene dropping from 85% in acetone to 55% in toluene also. The authors conclude that while HSP measurements can be useful for predicting pure solvent flux, this method is not as effective for solute rejections as the HSP does not take into account the solute – solvent – membrane interactions.

Also in 2018, a study was completed on using oxidized poly (arylene sulphide sulfone) (O-PASS) as a polymer for OSN applications (Yuan, et al., 2018). The O-PASS shows much higher degree of chemical resistance when compared to PASS in  $\text{CHCl}_3$ , NMP and  $\text{H}_2\text{SO}_4$  as PASS is severely deformed in  $\text{CHCl}_3$  and is completely dissolved in the other two solvents. Conditioning the membrane in a solvent before water permeation and Rose Bengal rejection experiments increases both the permeability of the membrane and yields higher rejection of the dye also, when also compared to PASS membrane, as the water permeability of PASS is 65  $\text{L/m}^2\text{hbar}$ , 78  $\text{L/m}^2\text{hbar}$  in O-PASS. The permeability of O-PASS increases to 92  $\text{L/m}^2\text{hbar}$  after submersion in  $\text{CHCl}_3$  for 72 hours. The permeability further increased to 112  $\text{L/m}^2\text{hbar}$  after submersion in NMP, and the permeability was 90  $\text{L/m}^2\text{hbar}$  after submersion in 98%  $\text{H}_2\text{SO}_4$ . The rejection of Rose Bengal was 38% in PASS membrane, compared to 41% in O-PASS. Treatment of O-PASS membrane in  $\text{CHCl}_3$  yield a Rose Bengal rejection of 45 – 50%, compared to a rejection of 64% after treatment in NMP and  $\text{H}_2\text{SO}_4$  respectively. Pure solvent studies on several solvents shown in table dkfm, show that THF has the largest permeability of 5.98  $\text{L/m}^2\text{hbar}$  followed closely by methanol with a permeability value of 5.88  $\text{L/m}^2\text{hbar}$ . The solvent with the lowest permeability is IPA with a value of 0.79  $\text{L/m}^2\text{hbar}$ . Rejection studies of dyes were carried out using DMF as the solvent which shows MWCO 350 g/mol based on 90% rejection of methyl orange and 99% rejection of the other dyes tested. the authors concluded that O-PASS can be used as a polymer suitable for OSN applications due to its simplicity to create and high chemical resistance.

## Background and Literature Review

Solvent	Permeability (L/m <sup>2</sup> hbar)
N-heptane	2.36
Methanol	5.88
THF	5.97
Toluene	2.64
DMF	2.67
NMP	0.97
IPA	0.79

**Table 2-4 Permeability values of solvents by O-PASS membranes as published by Yuan, *et al* (2018)**

More recently, a study into the use of Kevlar for use in OSN applications has been completed (Yuan, *et al.*, 2019). Three concentrations of Kevlar nanofibrous membranes were fabricated of 1wt%, 1.5 wt% 2 wt%, each of these batches were then characterised by the membrane thickness (200 µm, 100 µm, 60 µm and 20µm (for 2 wt% only)). The permeation of ethanol decreases with increasing membrane thickness, decreasing from 5.5 L/m<sup>2</sup>hbar at 1% Kevlar compared to 3 L/m<sup>2</sup>hbar at 2% concentration. The rejection of Rose Bengal only increases slightly with the increase of membrane thickness, increasing from 90% at 1% to 98% at 2% Kevlar. The thickness of the membrane also effects the permeation rate of ethanol, increasing from 3 L/m<sup>2</sup>hbar at 200 µm to 35 L/m<sup>2</sup>hbar at 20 µm. The rejection of Rose Bengal decreases with decreasing membrane thickness decreasing from 98% at 200 µm to 65% at 20 µm. The authors conclude that Kevlar is a suitable polymer for OSN applications, especially as the polymer can be fabricated from greener solvents.

### 2.9.3 Vankelecom *et al*

Ivo Vankelecom is a professor in KU Leuven and heads a team of researchers studying OSN as well as other membrane applications e.g. gas separation and membrane bioreactors, but this summary will only be considering works on OSN applications. In 2017, research was conducted on crosslinking polyimide UF membranes to assess the suitability for OSN applications (Mariën & Vankelecom, 2017). Polyimide membranes were fabricated and crosslinked using Hexane Di-Amine. Initial testing was carried out by submersing membrane coupons in solvents for 30 hours before being Rose Bengal in ethanol rejection experiments were carried out. No treatment of the membrane showed high permeance (85 L/m<sup>2</sup>hbar) with very little rejection (5%). Pre-treatment with hexane had the highest ethanol permeability with a value of 55 L/m<sup>2</sup>hbar with a rejection of 30%, while pre-treatment with DMF yielded the lowest ethanol permeability of <5 L/m<sup>2</sup>hbar, while the rejection of Rose Bengal is at its highest with a rejection of 95%. The authors also found that by adjusting the NMP/THF ratio and/or the evaporation time, the rejection of methyl orange increases with little change to the permeance of ethanol. The authors found that this method of crosslinking yielded better rejection and permeance results than the commercially available

## Background and Literature Review

Duramem® 300 and 500 membranes (1.2 L/m<sup>2</sup>hbar and 95% compared to 0.4 L/m<sup>2</sup>hbar and 85% for Duramem 300 and 0.3 L/m<sup>2</sup>hbar and 90% for Duramem 500).

The research group has studied further application of post – fabrication of PVDF and Polysulfone membranes to make them suitable for OSN applications (Li, et al., 2019). PVDF suffers from a severe decrease in water permeance after being submerged in a solvent, decreasing from a normalised value of  $1.2 \cdot 10^{-12}$ m for untreated to a range of 0.2 to  $0.3 \cdot 10^{-12}$ m for all the other solvents tested, with the exception of methanol which resulted in a water permeance of  $0.05 \cdot 10^{-12}$ m. The permeance of acetonitrile is not changed as much as water permeance, with untreated membranes having a normalised acetonitrile permeance of  $58 \cdot 10^{-12}$ m, with the permeance of acetonitrile decreasing after submersion in water and acetonitrile to  $50 \cdot 10^{-12}$ m, with submersion in hexane yielding the highest acetonitrile permeance of  $64 \cdot 10^{-12}$ m. Polysulfone membranes also decrease in performance after submersion in solvents, decreasing from a normalised water permeance of  $1.7 \cdot 10^{-10}$ m to  $1.1 \cdot 10^{-10}$ m after submersion in acetonitrile,  $0.5 \cdot 10^{-10}$ m after submersion in hexane and negligible results after submersion in water and methanol. Acetonitrile permeance of untreated polysulfone membranes is  $7 \cdot 10^{-10}$ m and increases to  $8 \cdot 10^{-10}$ m after submersion in hexane, and decreases in all the other solvent submersions, with submersion in methanol again having the lowest permeance with a value of  $1.6 \cdot 10^{-10}$ m.

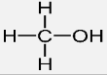
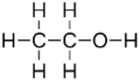
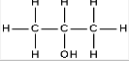
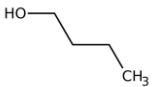
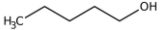
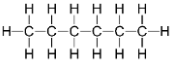
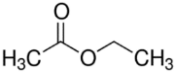
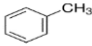
The group has also researched new methods of crosslinking membranes to make them suitable for solvent applications, such as UV crosslinking (Mooter, et al., 2019) (Mooter, et al., 2020). Tensile testing of the membranes indicate that UV curing of the membrane increases the tensile strength of the but decreases the extension of the membrane, therefore making them more robust. UV – LED curing of polysulfone membranes has lower permeance levels of water than uncured membranes (2.16 L/m<sup>2</sup>hbar and 0.33 L/m<sup>2</sup>hbar respectfully) while storing the membranes in aluminium foil has further decreased permance with a value of 0.22 L/m<sup>2</sup>hbar.

### 3. Materials and Methods

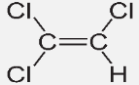
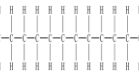
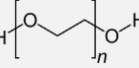
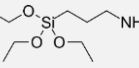
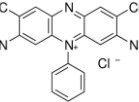
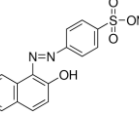
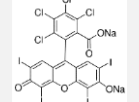
This chapter will focus on the materials used, detail the methodology for experimental procedure and include the design of any bespoke equipment used for experimentation.

#### 3.1 Chemicals

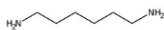
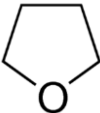
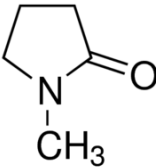
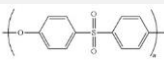
Herein contains the chemicals used for characterisation of membranes, or fabrication and modification of membrane as detailed throughout this thesis, found in Table 3-1. The organic solvents are used in solute rejection and permeate flux studies, salts and dyes are used as solutes for rejection studies. APTES, Hexane di-amine and PEG 200 are used for crosslinking membranes, while PES, NMP and THF are used for fabrication of membrane.

Material Name	CAS number	Grade	Brand	Supplier	Location	Structure
Methanol	67-56-1	99.8%+	Alfa Aesar	Fisher Scientific	Loughborough, UK	
Ethanol	64-17-5	99.9%+	Fisher Chemical	Fisher Scientific	Loughborough, UK	
Isopropanol	67-63-0	99.5%+	Honeywell	Fisher Scientific	Loughborough, UK	
N-butanol	71-36-3	99%	Acros Organics	Fisher Scientific	Loughborough, UK	
N-pentanol	71-41-0	99%	Acros Organics	Fisher Scientific	Loughborough, UK	
n-Hexane	92112-69-1	95%+	Fisher Chemical	Fisher Scientific	Loughborough, UK	
Ethyl Acetate	141-78-6	99.9%+	Fisher Chemical	Fisher Scientific	Loughborough, UK	
Toluene	108-88-3	99%+	Fisher Chemical	Fisher Scientific	Loughborough, UK	

# Materials and Methods

Trichloroethylene	79-01-6	99%+	ACROS Organics	Fisher Scientific	Loughborough, UK	
Dodecane	112-40-3	99%	ACROS Organics	Fisher Scientific	Loughborough, UK	
Polyethylene Glycol (PEG) 200	25322-68-3	MW 100 - 350	Alfa Aesar	Fisher Scientific	Loughborough, UK	
Nitrogen Gas (Oxygen Free)	7727-37-9	99.99% Pure	BOC	BOC	Port Talbot, UK	$\text{N}\equiv\text{N}$
Helium	7440-59-7	-	BOC	BOC	Port Talbot, UK	He
Sodium Chloride	7647-14-5	Pure	Fisher Chemical	Fisher Scientific	Loughborough, UK	$[\text{Na}]^+ [\text{Cl}]^-$
Sodium Hydroxide	1310-73-2	-	Fisher Chemical	Fisher Scientific	Loughborough, UK	$[\text{Na}]^+ [\text{OH}]^-$
Hydrochloric Acid	7647-01-0	32 wt%	Fisher Chemical	Fisher Scientific	Loughborough, UK	$[\text{H}]^+ [\text{Cl}]^-$
3-Aminopropyltriethoxysilane (APTES)	919-30-2	99%	ACROS Organics	Fisher Scientific	Loughborough, UK	
Ammonia (aq)	7664-41-7	-	Fisher Chemical	Fisher Scientific	Loughborough, UK	$[\text{NH}_4]^+ [\text{OH}]^-$
Safranin O	477-73-6	-	Sigma Aldrich	Sigma Aldrich	Gillingham, UK	
Orange II Sodium Salt	633-96-5	>85%	Sigma Aldrich	Sigma Aldrich	Gillingham, UK	
Rose Bengal	632-69-9	95%	Sigma Aldrich	Sigma Aldrich	Gillingham, UK	

## Materials and Methods

<b>Hexane diamine 1,6</b>	124-09-4	+99.5%	Acros Organics	Fisher Scientific	Loughborough, UK	
<b>Tetrahydrofuran</b>	109-99-9	>99.9	Sigma Aldrich	Sigma Aldrich	Gillingham, UK	
<b>N-Methyl-2-Pyrrolidone</b>	872-50-4	99.5%	Sigma Aldrich	Sigma Aldrich	Gillingham, UK	
<b>Polyethersulfone</b>	25667-42-9		Solvay	Solvay	Halifax, UK	

**Table 3-1 Names, CAS numbers, manufacturers of all chemicals and solids used**

Where water was required, ultra-pure reverse osmosis water was used from the Millipore (Watford, UK)

Elix 5® essential water purification systems.

### 3.2 Membranes

The Membranes primarily used for this thesis are the Duramem® (Evonik MET, Wembley, UK) 150, 200 and 500. The MWCO of these membranes are 150, 200 and 500 g/mol respectively, being determined by the rejection of styrene oligomers in acetone. These integrally skinned asymmetric (ISA) membranes are prepared via the phase inversion method using the P84® polyimide (MET, 2017). The membrane usage parameters are:

- MWCO - 150, 200 and 500 g/mol respectively
- Maximum Pressure - 60 barg (20 barg Duramem® 500)
- Maximum Temperature - 50°C
- pH - 7

The membranes are prepared for dead end filtration in the following manner:

- Membranes are cut into circles of 4.31 or 7.3 cm in diameter.
- The membrane disk is placed into either a Sterilitech dead end filtration cell or a Membranology HP350 dead end filtration cell.
- The filtration cell is filled with methanol and pressurised to 40 bar. Methanol is filtered such that 5.1mL of methanol is permeated for every 1cm<sup>2</sup> of membrane area to allow for compaction, for

## Materials and Methods

the use in the Membranology HP350 frontal filtration cell a 7.3cm diameter disc required 213 mL of solvent to be permeated through the membrane for compaction and cleaning.

- Once the sufficient amount of solvent had permeated through the membrane, the cell is emptied and fresh solvent is left inside the cell and sealed, as the membrane must not be allowed to dry out.

For surface charge experiments, a 0.2µm PTFE microfiltration membrane was acquired from Porex, UK.

### 3.2.1 PTFE Membrane Modification

APTES was coated onto the PTFE membrane via hydrolysis and condensation, using HCl and NH<sub>4</sub>OH as catalysts, in the same method as described by (Wang, et al., 2015). HCl (0.01 wt%) was added to a mixture composed of APTES, Ethanol and ultra-pure water (6:89:5) and stirred at 25°C until mixture was homogeneous. Following this, 2 wt% NH<sub>4</sub>OH was added into the mixture for condensation. The mixture was poured onto the membrane which is held in a mould. Condensation was achieved at 25°C after 12 hours. The PTFE membrane was then washed with distilled water and dried overnight.

## 3.3 Equipment design

### 3.3.1 Dead-end Filtration

For this thesis, 2 dead-end filtration cells have been used; one provided by Membranology and the other from Sterlitech. The Membranology cell has a volume hold up of 350 mL, has a membrane surface area of 41.92 cm<sup>2</sup> and uses a sweeping stirrer which hangs approximately 1 mm above the membrane to prevent cake build up. The Sterlitech dead-end filtration cell is narrower than the Membranology cell, with a volume hold up of 250 mL, a membrane surface area of 14.6 cm<sup>2</sup> and uses the manufacturer's stirrer. A full analysis of the cells and their properties has already been studied (Oatley-Radcliffe, et al., 2015).

Despite the Membranology cell having better mass transfer properties than the Sterlitech (Oatley-Radcliffe, et al., 2015), the Sterlitech was preferred over the Membranology cell for three principal reasons:

- Solvent cost
- Waste solvent disposal
- Stirrer life longevity

Both dead-end filtration cells operate in the same manner, as shown in Figure 3.1, by pressurising the dead-end filtration cell (4) with nitrogen provided from a cylinder (1). The cell passes through a 3-way valve (2) and a pressure gauge (3) and into the cell, where due to the increased pressure inside the cell, the liquid inside permeates through the membrane. The cell rests on top of a stirrer (5) where the liquid inside is



## Materials and Methods

mixed to prevent a cake layer from building up. The permeate is collected into a container which rest on a balance (6), where the data of collected mass is stored onto a computer (7) via a USB connection.

Once the experiment is completed, the gas cylinder valve is closed and the gas inside is released via the 3-way valve.

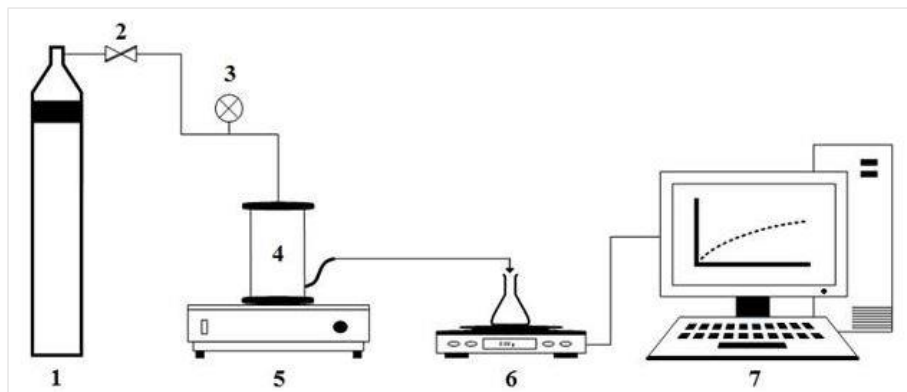


Figure 3.1 Diagram of dead-end filtration set up

For experiments that were conducted at elevated temperatures, the dead-end filtration cell was submerged into a water bath (rested on top of the stirrer unit), where the cell was left to warm up (with the contents inside) for 60 minutes. To prevent solvent from vaporising, the permeate line was clamped shut, and the cell was pressurised to 1-2 bar.

### 3.3.2 Cross-flow filtration

A custom made crossflow system was designed and built for this study. The rig is illustrated in Figure 3.2 and Figure 3.3. The components of the rig are an AEG AM71ZAA2 3 phase magnetically driven pump, with the magnetic pump head being supplied by Micropump (PN: L21279), the maximum flowrate of the pump is 1.32 m/s and the maximum operating pressure is 14 bar. All fittings, valves and pressure gauges used on the system were purchased from Swagelok (Bristol, UK) and the feed tank was purchased from Direct Water Tanks (Nottinghamshire, UK).

## Materials and Methods

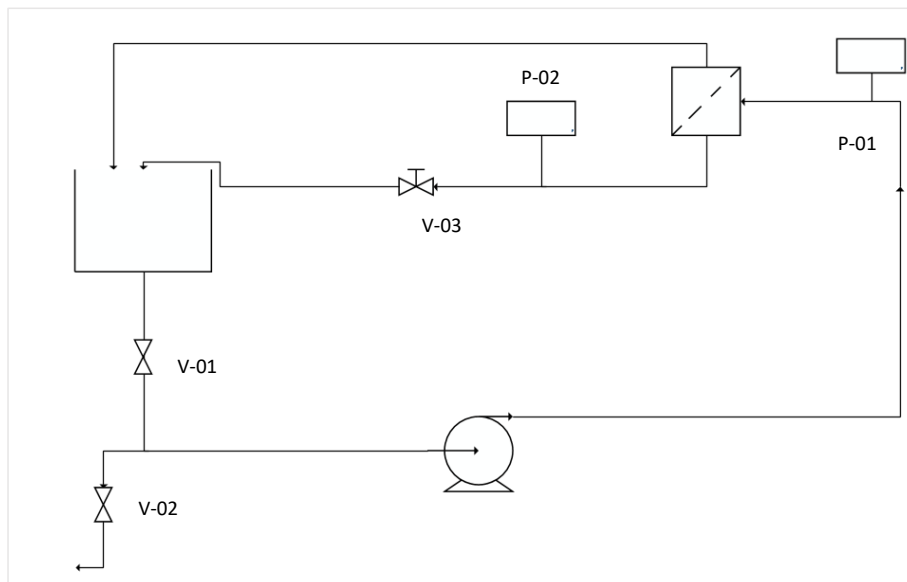


Figure 3.2 P&ID of crossflow UF system



Figure 3.3 Picture of UF crossflow system

### 3.4 Experimental Method

#### 3.4.1 Dead-end Filtration

Feedstock of the required solute and solvent was made by dissolving the desired solute ( $\pm 1\%$  of the target mass or volume (depending on solute)) into the solvent. The solute is measured by a balance for solid

## Materials and Methods

solutes while liquid solutes are measure through a micropipette. The mixture is then placed onto a heated stirrer plate and mixed for 15 minutes using a magnetic stirring bar until homogeneous.

For solute rejection experiments, 125 mL of the solute/solvent mixture was emptied into the desired filtration cell. The stirrer speed was set to the desired value and the cell pressurised to the desired value via the nitrogen cylinder. The filtration was allowed to permeate through 12 mL ( $\approx 10\%$ ) of the mixture before a sample was taken in a 2mL vial. Samples were stored in a refrigerator at 4.5°C, when necessary, before being analysed.

For sample concentration experiments, 100 mL of sample was emptied into the cell, with the stirrer and cell pressure being set to the desired values. 25mL of solution was permeated through the membrane before a sample was collected in a 2mL sample vial. Samples were stored in a refrigerator at 4.5°C, when necessary, before being analysed.

### 3.4.2 Crossflow filtration

The membrane is initially compressed in the crossflow rig (as be manufacturer's instructions) by permeating water through the membrane at 5 bar, setting the pump speed to 30 Hz, resulting in a cross-flow velocity of 0.5 m/s. Once compressed, the water is drained through V-02, and feed solution is added to the system (2 litres). Some residual water may remain in the system, however the residual amount remaining is expected to have little impact as the solutions used for experimentation contain 25% water. The pump is started to a frequency of 30 Hz and pressure is gradually built up by adjusting the control valve. The concentration experiment is run so that 20% of the original volume is permeated through the membrane. The sample is taken at the end of the experiment, then the system is drained though V-02 and disposed of into glass bottles. The system is then filled with water and flushed several times to remove all the solvent from the system.

### 3.4.3 Tangential Streaming Potential (TSP) Measurements

TSP measurements were carried out using the Electro kinetic analyser (EKA) (Anton Paar GmbH, Graz, Austria). Membranes were cut to fit the dimensions of the rectangular measurement cell attachment, (2 sheets, 12.5x5.5cm).

NaCl (Fisher Scientific Ltd, UK), was used as the electrolyte for this study, using a concentration of 1mM/L. The electrolyte was prepared using ultra-pure water and adjusted periodically using 0.1M HCl (Fisher Scientific Ltd, UK) and 0.1 NaOH (Fisher Scientific, UK) as required. For methanol – water systems, 1mM/L NaCl was dissolved in the mixture, and stirred until the NaCl is completely dissolved in the solution. Fresh solution was introduced to the system when swapping from an acidic to an alkali solution. Prior to introducing solutions for analysis, the system was washed with ultra-pure water to ensure that any prior

## Materials and Methods

solution was removed. Similarly, the electrolyte solution was introduced and rinsed through the unit to equilibrate the membrane sample.

A pressure gradient program of 0-700 mbar over 30-seconds was applied to generate the streaming current and was measured using a pair of AgCl electrodes. For individual pH points, 10 measurements were made using alternating flow directions to limit electrode polarisation. Background electrolyte pH and conductivity were monitored using a pH and conductivity probe. For aqueous solutions, a Fisherbrand pH electrode was used, for alcohol-water solutions a Jenway non-aqueous pH electrode was used. All experiments were carried out at room temperature ( $25^{\circ}\text{C} \pm 2^{\circ}\text{C}$ ).

### 3.4.4 Laser Doppler Electrophoresis (LDE) Measurements

Electrophoretic mobility and electro-osmotic measurements were carried out using a Zetasizer Nano ZS with the surface zeta potential accessory (Malvern, UK) and the method used is as described in literature (Thomas, et al., 2017).

Electrolyte solution was prepared in the same manner as section 3.4.3 but with the addition of 1 drop of  $0.5\text{ }\mu\text{m}$  negatively charged carboxylated polystyrene latex particles (Polysciences Inc., PA, USA) or  $0.5\text{ }\mu\text{m}$  positively charged amidine particles (Fisher Scientific Ltd., UK) into 200 mL of electrolyte solution.

Membranes were cut to fit the dimensions of the surface cell holder ( $3.5 \times 5\text{ mm}$ ) and the membrane was attached using epoxy (Araldite) resin. The membrane was washed with 5 mL of the electrolyte solution to remove any particulate debris before the being submerged into the cuvette. In between subsequent measurements, the surface cell was sonicated for 30 seconds in toluene (Fisher Scientific Ltd., UK) and was repeated as necessary until the toluene remained clear. The membrane is then washed with ethanol, water and is then dried using compressed air.

The Zetasizer was set to forward scatter with the attenuator in position 10. The count rate was adjusted to the optimal 250-500 kcps range and an effective applied voltage of 2V. The instrument was set to take four distance positions in  $125\text{ }\mu\text{m}$  steps, consisting of three measurements (each measurement consisted of 15 sub-runs with 60s interval) at each position for each pH data point. Furthermore, five measurements consisting of 100 sub-runs with a 60s interval in between measurements were used to measure the electro-osmotic mobility of the tracer particles. All measurements were carried out at  $25^{\circ}\text{C}$ .

### 3.5 Data Analysis

#### 3.5.1 Solvent Recovery Data Analysis

The total permeate sample was taken from the outlet tube of the filtration cell into a 2mL sample vial (Agilent technologies, UK). Samples were stored in a refrigerator at 5°C until analysed by GCMS (section 3.5.4) or HPLC (section 3.5.5).

#### 3.5.2 Solvent Recovery Experimental Parameters

The flux through the membrane can be calculated experimental by dividing the total mass collected over the membrane disk area multiplied over a period of time:

$$J_g = \frac{m}{A\Delta t}$$

Where:

$J_g$  = Membrane Flux (g/m<sup>2</sup>hr)

$m$  = Quantity of permeate collected

$A$  = Effective membrane Area (m<sup>2</sup>)

$t$  = time (hr)

Where applicable, the mass flux ( $J_m$ ) was converted into liquid flux ( $J_l$ ) by dividing the mass collected by the density of solvent in question at the experimentation temperature:

$$J_l = J_g / \rho_s$$

Where:

$J_l$  = Liquid flux (L/m<sup>2</sup>hr)

$\rho_s$  = Solvent density relative to water density at experimental temperature

#### 3.5.3 Solute Rejection analysis

The rejection of a solute in a membrane is commonly calculated by;

$$R_{i,obs} = 1 - \frac{C_{i,p}}{C_{i,f}}$$

Where:

$R_{obs}$  is the observed rejection of solute  $i$  (%)

$C_{i,p}$  is the concentration of solute  $i$  in the permeate (ppm)

$C_{i,f}$  is the concentration of solute  $i$  in the feed (ppm)

## Materials and Methods

This method of rejection calculation does not consider the concentration polarisation that occurs during dead-end filtration. To compensate for this, a new equation has been derived in literature and is shown in section 2.5.5 and is thus (Oatley-Radcliffe, et al., 2015);

$$R_{real} = \frac{1}{Exp\left(\ln\left[\frac{1-R_{I,obs}}{R_{I,obs}}\right] - \frac{Jv}{a\omega^n}\right) + 1}$$

Where

$R_{real}$  is the rejection of solute / at infinite speed

$J_v$  is the permeate flux through the membrane (m/s)

$a$  is a constant

$\omega$  is the stirrer speed (rad/s)

$n$  is a constant

### 3.5.4 Gas Chromatography / Mass Spectrometry (GCMS) Analysis

The GCMS system used for the analysis of this study is an Agilent Technologies system (Cheshire, UK) using a 6850 Gas Chromatography system, with a HP-1 Polysiloxane Column. The column specifications are as shown in Table 3-2.

<b>Length (m)</b>	30
<b>Diameter (mm)</b>	0.32
<b>Film (µm)</b>	0.25

**Table 3-2 Table of Specifications of GC Column**

The sample for analysis was injected into the GC via a G-4613A autosampler or a 7697A headspace sampler as required. The carrier Gas for the system is Helium. The Mass Spectrometer is an 5977A MSD.

#### 3.5.4.1 Volatiles Analysis

The parameters for GC/MS for analysis of volatiles in organic solvents are shown in Table 3-3.

<b>Injection Volume</b>	1µL
<b>Pre-injection Wash</b>	1 sample wash 1 Solvent A wash (hexane)
<b>Post-injection Wash</b>	2 Solvent A wash
<b>Inlet Pressure</b>	2.1 PSI
<b>Inlet Heater</b>	275°C
<b>Split Ratio</b>	50:1
<b>Column Pressure</b>	2.1 PSI
<b>Column gas Flow</b>	1.6 mL/min
<b>Oven Ramp</b>	Hold 40°C for 1 minute

## Materials and Methods

	Ramp 15°C/min to 150°C
<b>Detector Temperature</b>	280°C
<b>Mass Spectrometer</b>	150°C
	230°C
<b>Identifying Ions</b>	Dodecane – 57 m/z Toluene – 91 m/z Trichloroethylene – 130 m/z

**Table 3-3 GC/MS parameters for analysis of volatiles**

### 3.5.4.2 PEG Analysis

The parameters for GC/MS for analysis of PEGs in organic solvents are shown in Table 3-4.

<b>Injection Volume</b>	2µL
<b>Pre-injection Wash</b>	1 Solvent A Wash
<b>Post-injection Wash</b>	2 Solvent A wash 1 Solvent B was (methanol)
<b>Inlet Pressure</b>	6.5 PSI
<b>Inlet Heater</b>	275°C
<b>Split Ratio</b>	5:1
<b>Column Pressure</b>	6.5 PSI
<b>Column gas Flow</b>	1.6 mL/min
<b>Oven Ramp</b>	Hold 140°C for 10 minutes
<b>Detector Temperature</b>	280°C
<b>Mass Spectrometer</b>	150°C
	230°C
<b>Identifying Ions</b>	PEG 150 + 200 – 89 m/z

**Table 3-4 GC/MS parameters for analysis of PEGs**

### 3.5.4.3 Solvent Analysis

The parameters for GC/MS for analysis of organic solvent solutions are shown in Table 3-5.

<b>Headspace</b>	
<b>Oven Temperature</b>	55°C
<b>Loop Temperature</b>	70°C
<b>Transfer Line Temperature</b>	105°C
<b>Vial Equilibrium Time</b>	10 minutes
<b>Injection Duration</b>	0.3 minutes
<b>GC Cycle Time</b>	28 minutes
<b>Gas Chromatography</b>	
<b>Inlet Temperature</b>	150°C
<b>Inlet Pressure</b>	4.1 PSI
<b>Column Flow Profile</b>	Constant flow, split 175:1 (0.8 mL/min
<b>Oven Temperature Profile</b>	30°C hold for 5 minutes
<b>Detector Temperature</b>	250°C
<b>Mass Spectrometer</b>	
	150°C

## Materials and Methods

	230°C
<b>Identifying Ions</b>	Water – 18 m/z Methanol – 31 m/z Ethyl Acetate – 45 m/z Hexane – 57 m/z

**Table 3-5 Headspace GC/MS parameters for solvent analysis**

### 3.5.5 High Performance Liquid Chromatography (HPLC) Analysis

The HPLC system used in this study was provided by Perkin Elmer (Seer Green, UK) the system is comprised of: -

- Flexar Quaternary LC Platform
- Flexar PDA Plus Detector
- Flexar LC Autosampler
- Flexar Peltier Switching Oven

The column used for the analysis of Spinosad samples was the Brownlee C18 column dimensions 3x50 mm, packing 2.7µm.

The method for analysis of Spinosad samples is found in Table 3-6 :

<b>Solvent A</b>	Methanol
<b>Solvent B</b>	Acetonitrile
<b>Solvent C</b>	2% Ammonium Acetate (aq), 67% Water, 33% Acetonitrile
<b>Solvent profile</b>	Isocratic
<b>Solvent ratios</b>	45:45:10
<b>Solvent Flow rate</b>	1 mL/min
<b>Oven temperature</b>	30°C

**Table 3-6 HPLC method for analysis of Spinosad samples**

## 3.6 Membrane fabrication and modification

### 3.6.1 Membrane Preparation

NMP and alcohols (methanol, ethanol, isopropanol and n-butanol (when used)) are heated to 70°C whilst being stirred in a sealed glass beaker, 25% (w/w) PES is then added (MW 60000-62500) and stirred until all polymer has been dissolved. 1% (w/w) THF is then added dropwise into the dope solution while the solution is being cooled but still stirred. The dope solution is then resealed and left overnight to de-gas. The alcohols are added at percentages of 5, 10, 15 and 20 wt% respectively.



## Materials and Methods

### 3.6.2 Membrane Casting

The dope solution is cast onto a polyester non-woven backing layer CraneMat CU632 (Neenah Technical Materials, USA) using a RK Print K101 bench casting machine (RK Print, UK) at 3cm/s and a casting height of 250µm. While the temperature and humidity of the room could not be controlled, they were monitored (18-22°C and humidity of 45-66%). Once the dope solution has been cast, the polymer underwent solvent exchange via phase inversion in a water bath at 22°C (±2°C). The polymer was left in the water bath for 10 minutes before the water was changed and left for an additional 50 minutes before being placed into deionised water and left in a dark cupboard at room temperature.

### 3.6.3 Surface Modification

The cast membrane was left in 0.001 wt% NaOH for 1 hour before being removed and rinsed with deionised water. The membrane was then left in 2.5, 5, 7.5 or 10 wt% of crosslinking agent (either hexane diamine or PEG 200) in water for 24 hours. After 24 hours the membranes were rinsed with isopropanol and tested. The crosslinking agents used are hexane-1,6-diamine (HDA) and polyethylene glycol 200 (PEG 200).

### 3.6.4 SIM Modification

Polymer dope solution was cast in the same method as described in Section 3.6.2 but the crosslinking agent is dissolved into the solvent exchange bath at 10 wt.% PEG 200 or 5 wt.% HDA. The membrane is left in the solution for 30 minutes for coagulation to complete before the membrane is removed, dried and placed in storage until tested.

### 3.6.5 Flux Modification

Polymer dope solution was cast in the same method as described in Section 3.6.2 and activated by submerging the membrane in 0.01 wt.% NaOH<sub>(aq)</sub> for 1 hour. 10 wt% PEG 200 and 5 wt% HDA were permeated through the membrane respectively until 150 mL of the crosslinking solution was permeated. The polymer is then air dried and placed into storage.

## 4. Characterisation of the Duramem OSN membranes

---

### 4.1 Introduction

Most commercial nanofiltration membranes quote a MWCO, which for membranes designed for aqueous system, is usually very accurate. For OSN membranes the MWCO value must be taken as an advisory due to the complex chemistry happening at the surface and in the pores of OSN membranes. Changing the solvents used changes the surface properties of the membrane and induce swelling or constriction of the pores of the membrane, resulting in the performance capabilities of the membrane changing significantly (Kappert, et al., 2019) (Davey, et al., 2017). This change in membrane flux and rejection, coupled with OSN membranes being a relatively young topic, makes creating predictive models difficult despite some attempts from other authors (Marchetti & G.Livingston, 2015) (Schmidt, et al., 2014). To add further complication, some industrial processes have binary or tertiary mixtures of solvents in their process, where the membrane has a selectivity towards one of the solvents over the others depending on the polymer and/or crosslinking agents used (Rundquist, et al., 2012).

To characterise membranes, typically a neutral solute is used, normally a series of straight chain molecules such as polyethylene glycols, polypropylene glycol oligomers (Davey, et al., 2017) (Rohani, et al., 2011). These types of molecules can have their dimensions accurately calculated and thus a pore size can be accurately estimated from rejection data (Dohmen, et al., 2008). These types of experiments are easier to conduct in solvents due to solubility issues that arise when attempting to dissolve neutral organics into water, hence leading to a wider availability of solutes instead of exclusive use of PEGs for water systems. The use of solvents also allows for molecules of different shapes to be used for exclusion studies to examine how branching of a molecule effects the rejection properties of a membrane (Zheng, et al., 2008).

To this end, there are very few attempts to characterise OSN membranes below MWCO of 200, most likely due to the difficulty in finding molecules that can easily be identified through analytical techniques e.g. GC/MS and are neutral. Such molecules that can be used are longer chain solvents e.g. hexane, octanol, ethyl acetate etc, or through the use of volatiles that are not soluble in water e.g. toluene, trichloroethylene to name a few. Similarly, to the best of the authors knowledge, there are only a limited number of OSN membranes that have a MWCO of 200 or below and these are part of the Duramem series by Evonik MET.

Duramem membranes were first used in 2010 extraction of biological compounds from propolis, having previously being incarnated as Starmem membranes (Tylkowski, et al., 2010). They are one of a few different brands of OSN membranes available on the commercial market and are widely used for solvents dissolved in alcohols (Sereewatthanawut, et al., 2011), (Peshev, et al., 2011), with MWCO's ranging from 150 to 900 (Behnke & Ulbricht, 2015) (Davey, et al., 2017). These membranes are made from modified

## Characterisation of the Duramem OSN membranes

polyimide and offer good separation of solutes, with a summarised list of solvent/solute rejections provided in the appendix (section 12.2). The major issue that has been found in previous work and is also shown in this study is the low permeability of the membranes, particularly at low MWCOs (Mariën & Vankelecom, 2017). The aim of this characterisation study is to filter a range of solutes, both charged and neutral, to determine if the MWCO is affected by the different solvents permeating through the membrane and if possible, determine what is causing any changes in rejection.

Previous studies have determined that there are 16 factors involved in solute rejection by a membrane (Darvishmanesh, et al., 2010) and this study aims to see the Duramem 150 and 200 membranes perform with different solvents, how pressure effects performance of OSN membranes and how temperature will significantly effect on separations.

## 4.2 Experimental Procedure

### 4.2.1 Salt rejections

Details of dead-end filtration method can be found in section 3.4.1. The salt solutions used for experiments are NaCl, Na<sub>2</sub>SO<sub>4</sub> and MgCl<sub>2</sub> at concentrations of 0.001, 0.01 and 0.1 Mol/L, and the solvent ultra-pure water. For sample collection, the initial 5 mL of solution was discarded and the next 10 mL was collected for analysis by pH and conductivity meter.

### 4.2.2 1000 PPM rejection

Feeds Details of dead-end filtration method can be found in section 3.4.1. The solvents used for experiments are methanol, ethanol and acetonitrile and the solutes are toluene, trichloroethylene, dodecane and PEG 200 dissolved at concentrations of 1000PPM each for the feedstock.

### 4.2.3 Zeta Potential Measurements

The method for surface charge (or zeta potential measurements) can be found in section 3.4.3.

### 4.3 Salt Rejection of Duramem 150

#### 4.3.1 NaCl Rejection and Flux

The rejection of NaCl generally increases with increasing applied pressure, but the rejection decreases with increasing salt concentration, see Figure 4.1. at 0.001 mol/L, the rejection increases from 0.79 to 0.92 at over the pressure range 10 to 30 bar respectively. Similarly, for 0.01 mol/L, this was 0.62 and 0.79, and at 0.1 mol/L this was 0.54 and 0.8 respectively.

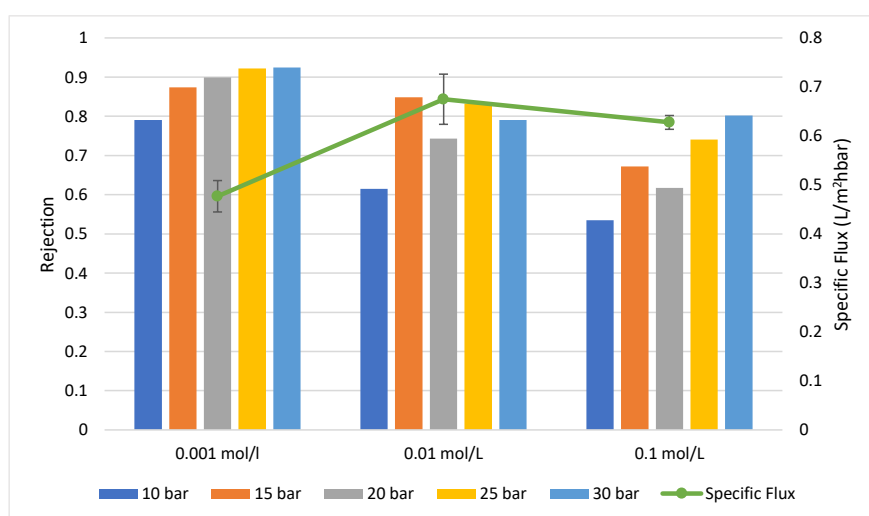


**Figure 4.1 Rejection of NaCl at different concentrations over a range of pressures**

The decrease in rejection with increasing salt concentration is due to a smaller pressure gradient being exerted onto the membrane due to an increased osmotic pressure of the increased salt concentration e.g. the rejection of the salt at a concentration of 0.001 mol/L with an applied pressure of 10 bar, needs an applied pressure of 30 bar for a salt concentration of 0.1 mol/L for the same level of rejection. This hypothesis is also supported by the specific flux increasing from 0.001 to 0.01 mol/L and plateauing at 0.1 mol/L (within experimental error).

Comparing other NF membrane salt rejection and permeate flux data, the Duramem 150 has significantly smaller specific flux in comparison but higher rejection of NaCl (Oatley, et al., 2012). The author shows a rejection of 0.001 mol/L NaCl 0.6 at 20 bar using NF99HF and NF270 membrane compared a rejection of 0.9 using the Duramem 150 membrane. Conversely, the NF99HF and NF270 membranes shows a permeate flux of 250 and 320 L/m²h at 20 bar respectively, compared to a permeate flux of 10.3 L/m²h when the Duramem 150 is used.

### 4.3.2 Na<sub>2</sub>SO<sub>4</sub> Rejection and Flux

The Duramem 150 membrane shows consistently high degree of rejection the Na<sub>2</sub>SO<sub>4</sub> salt at all pressures and concentrations, see Figure 4.2. However, the rejection of Na<sub>2</sub>SO<sub>4</sub> decreases slightly at 0.1 mol/L compared to 0.01 mol/L, where the rejection decreases from 0.98 to 0.95 at 10 bar respectively, 0.99 to 0.96 at 30 bar respectively.

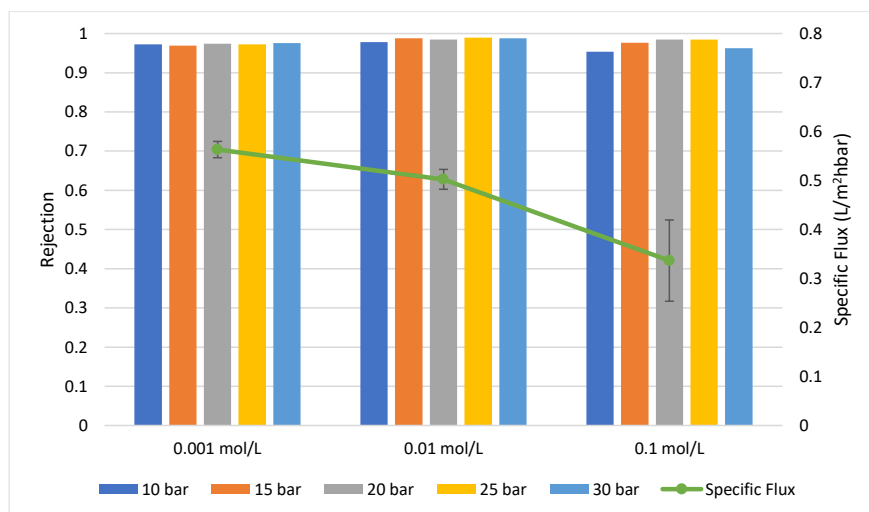


Figure 4.2 Rejection of Na<sub>2</sub>SO<sub>4</sub> at different concentrations over a range of pressures

The high degree of rejection may be due to the anions of SO<sub>4</sub><sup>2-</sup> being larger than Cl<sup>-</sup> when comparing the results in section 4.3.1, and are thus excluded due to size restrictions of the pores (effective hydrated radius of Cl<sup>-</sup> = 3.32Å and SO<sub>4</sub><sup>2-</sup> = 3.79Å (Nightingale, 1959)). Based on the higher rejection of Na<sub>2</sub>SO<sub>4</sub> compared NaCl, the hypothesis could be made that the Duramem 150 membrane has a negatively charged surface, which is to be determined by zeta potential measurements. The theory of size exclusion is supported by the significant reduction in specific flux of the membrane with increasing concentration, dropping from 0.55 to 0.34 L/m²hbar, however, this may also be due to concentration polarisation during the experiment, which may be causing the decrease in rejection at 0.1 mol/L compared to the other concentrations tested.

When comparing the results published by Oatley, *et al* (2012), the rejection of 0.001 mol/L Na<sub>2</sub>SO<sub>4</sub> is 0.9 at 20 bar applied pressure when both the NF99HF and the NF270 membranes are used with the rejection being 0.97 with the Duramem 150 membrane. The permeate flux of the Duramem 150 membrane is significantly slower than the NF270 and NF99HF at 11.26 L/m²h.

### 4.3.3 $\text{MgCl}_2$ Rejection and Flux

The rejection of  $\text{MgCl}_2$  increases with both pressure and concentration, see Figure 4.3, at 0.001 mol/L the rejection increases from 0.85 to 0.9 over the range of pressure from 10 to 30 bar respectfully. This is also the case for 0.01 mol/l where the rejection is 0.93 to 0.97, and at 0.1 mol/L the rejection is 0.9 to 0.97 respectively, with the specific flux decreasing from 0.53 to 0.451  $\text{L/m}^2\text{hbar}$  at 0.001 to 0.1 mol/l respectfully.

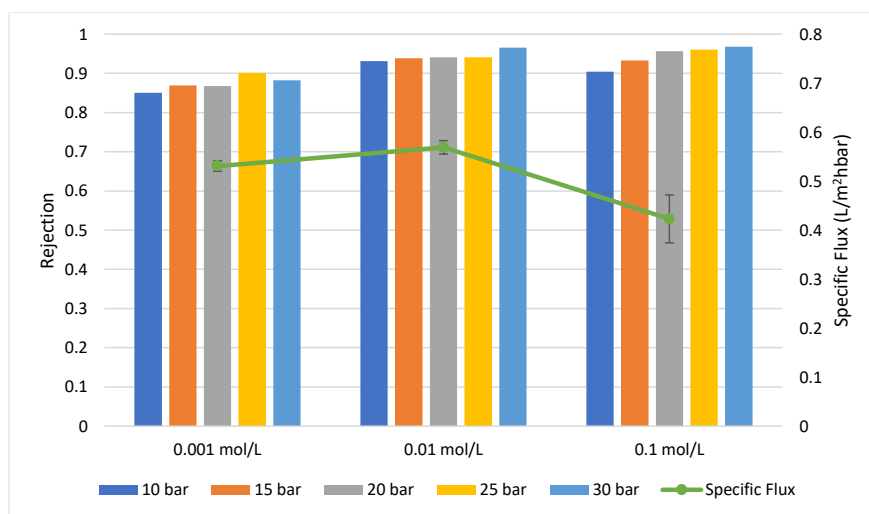


Figure 4.3 Rejection of  $\text{MgCl}_2$  at different concentrations over a range of pressures

Typically, NF membranes are characterised by rejection divalent salts (Lenntech, 2018) thus the degree of rejection of  $\text{MgCl}_2$  exhibited by the Duramem 150 membrane is to be expected. Usually, the performance of membranes decrease with increasing solute concentration, see Figure 4.1, which is shown with decreasing specific flux through the membrane as a result of concentration polarisation, but the rejection is increasing with increasing salt concentration. The increased rejection of  $\text{MgCl}_2$  may be due to size exclusion (hydrated radius of  $\text{Na}^+ = 3.58\text{\AA}$  and  $\text{Mg}^{2+} = 4.28\text{\AA}$  (Nightingale, 1959)), with the increased amount of anions present restricting the pores and increasing rejection.

#### 4.4 Flux and rejections in aprotic solvents of Duramem 150

##### 4.4.1 Methanol – water permeability

The specific flux of methanol-water through the Duramem 150 membrane is initially 0.52 L/m<sup>2</sup>hbar at 100% methanol, then decreases with increasing water content to 0.2 L/m<sup>2</sup>hbar at 75% methanol to 25% water and with the lowest flux rate occurring at 50% methanol to water at 0.19 L/m<sup>2</sup>hbar, see Figure 4.4. The specific flux then increases to 0.26 L/m<sup>2</sup>hbar at 25% methanol to water and further increases to 0.4 L/m<sup>2</sup>hbar at 100% water. When considering the viscosity of methanol-water systems over the same ratios, the viscosity is increasing linearly from 0.58 MPa.s at 100% methanol to 1.26 and 1.79 MPa.s at 75% and 50% methanol respectively. the viscosity then decreases slightly to 1.71 at 25% methanol to 75% water before decreasing again to 1 MPa.s with 100% water.

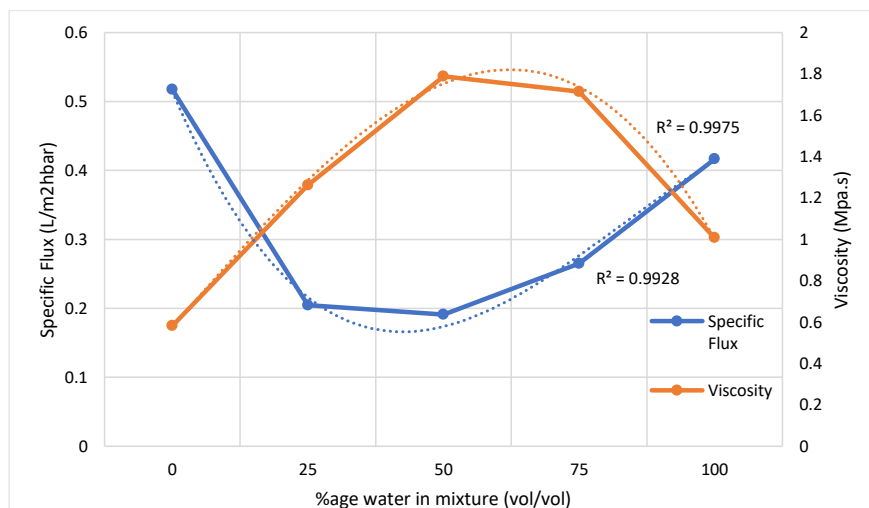


**Figure 4.4 Effect of increasing water concentration and viscosity on permeability of Duramem 150**

The trends for these two data sets appear to be proportional to each other, which can be explained by the basic membrane equation for pore flow through a membrane shown in equation 4.1. Based on this model, an argument can be made that if the permeate flux is inversely proportional to the viscosity, then the membrane has pores. Figure 4.4 shows that there is a direct correlation between the viscosity of the solvent and the specific flux of solvent on this membrane, suggesting that even as a near RO scale, there could be pores in the membrane that are too small to be picked up by current visual analytical methods.

$$J = \frac{a}{\mu} \quad 4.1$$

Where: J = membrane flux, a = constant,  $\mu$  = viscosity

#### 4.4.2 Rejection of volatiles and neutral compounds

The rejection of toluene remains fairly constant with increasing applied pressure, see Figure 4.5, where when methanol is the solvent the rejection is 0.31, 0.37 and 0.29 at pressures to 20, 30 and 40 bar respectively. When ethanol is the solvent, the rejection decreases with increasing pressure, decreasing from 0.96 at 20 bar to 0.74 at 40 bar. The rejection of toluene in acetonitrile is highest at 30 bar (0.64), with the rejections at 20 and 40 bar being comparable at 0.38 and 0.41 respectively. The specific flux when highest when acetonitrile is used at the solvent at 0.29 L/m<sup>2</sup>hbar and lowest at 0.03 L/m<sup>2</sup>hbar when ethanol is used, with a specific flux of methanol of 0.21 L/m<sup>2</sup>hbar.

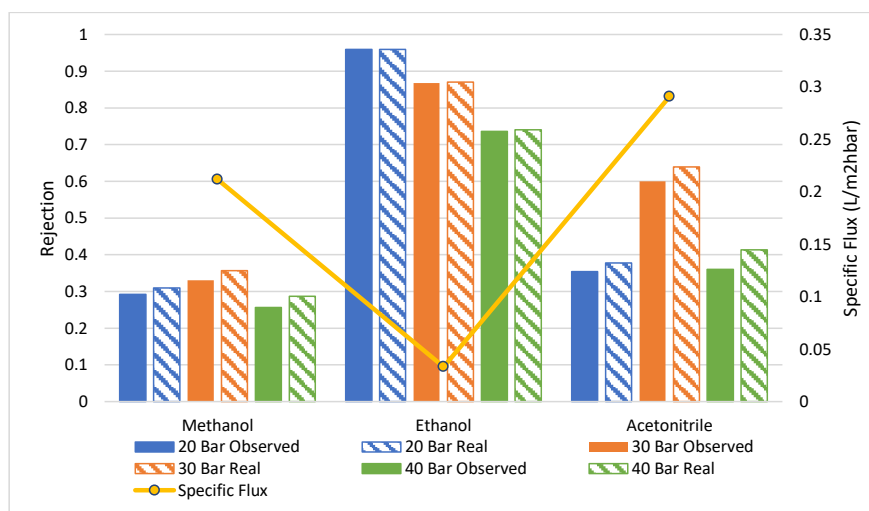


**Figure 4.5 Rejection of 1000 PPM toluene in different solvents at applied pressures**

When comparing toluene rejection in methanol and ethanol, the rejection of toluene is significantly less than what is exhibited in ethanol, likely due to the significantly smaller specific flux. The rejection of toluene is fairly constant at all applied pressures in methanol, suggesting that the rejection is independent of pressure. When considering ethanol, the increasing rejection with decreasing applied pressure suggests that the membrane has swollen and blocked the pores leading to the mass transfer being controlled by diffusion only. Variations in permeate flux in different solvents has also been observed in other studies (Darvishmanesh, et al., 2011), with the specific flux appearing to be effected by solvent properties as well as the operating pressure of the system (Darvishmanesh, et al., 2010). In acetonitrile, the comparable rejection at 20 and 40 bar suggests that at 40 bar, the operating pressure is forcing the solute through the membrane, with the pores being more open when compared to methanol and ethanol, as suggested by the higher specific flux. The decreasing rejection between 30 and 20 bar respectively suggests that the solute is being rejected by size exclusion. The variations in specific flux could be due to several factors,



including the polarity of the solvent, swelling of the membrane and the physical size in space of the solvent (Nightingale, 1959).

The rejection of trichloroethylene is the lowest of the solutes tested as this solute has the smallest size physically, see Figure 4.6 (molar volume is  $84.14 \text{ cm}^3$  with a MW of 131, compared toluene which has a molar volume of  $101.4 \text{ cm}^3$  and a MW of 92.) For methanol and acetonitrile, the rejection of trichloroethylene increases with increasing applied pressure, increase from 0.03 to 0.14 for methanol and 0.16 to 0.7 from 20 to 40 bar respectively. When ethanol is used, the rejection increases from 0.1 at 20 bar to 0.56 at 30 and 40 bar applied pressure.

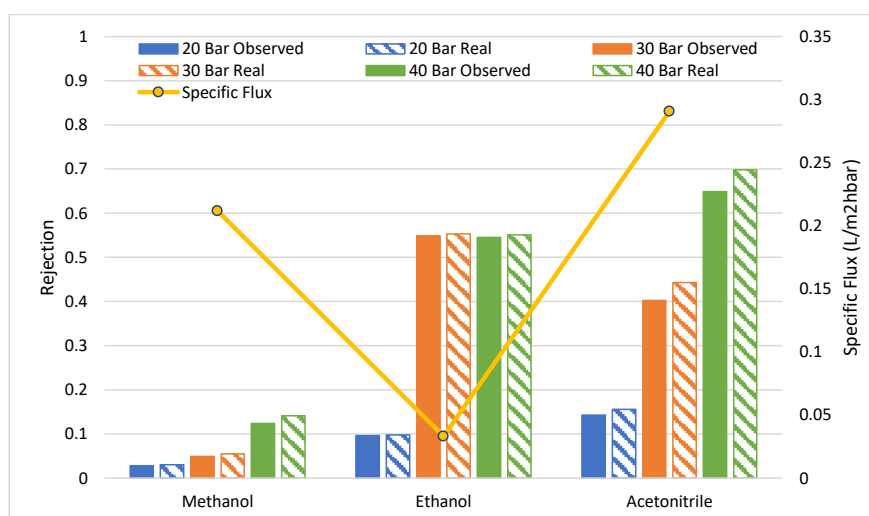


**Figure 4.6 Rejection of 1000 PPM trichloroethylene in different solvents at applied pressures**

The increasing rejection with increasing pressure in all solvents suggests that the solute is being rejected by size exclusion mechanics, with the only exception being the rejection of trichloroethylene in ethanol at 40 bar being the same as the rejection at 30 bar.

#### Characterisation of the Duramem OSN membranes

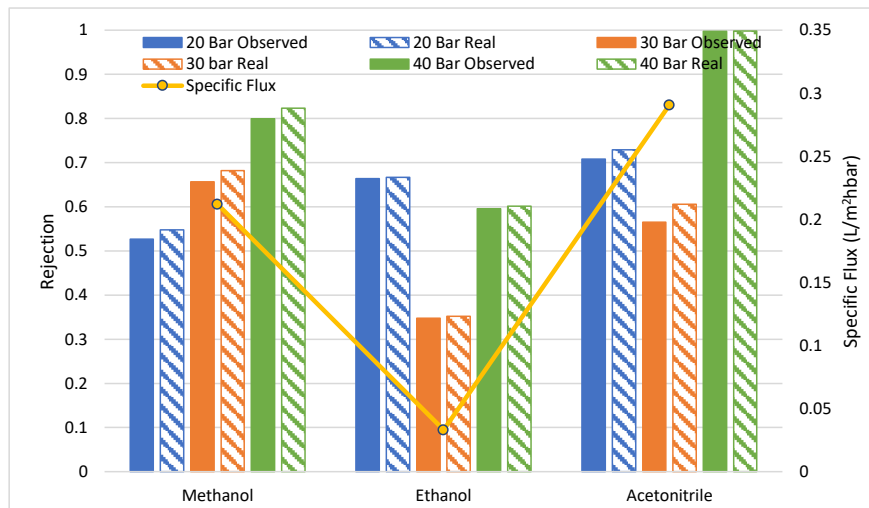


**Figure 4.7 Rejection of 1000 PPM triethylene glycol (PEG 150) in different solvents at applied pressures**

The rejection of triethylene glycol in methanol still appears to be governed by size exclusion, see Figure 4.7, as the rejection increases with increasing pressure (0.55 to 0.82 at 20 and 40 bar respectively). The rejection of PEG 150 in ethanol is highest at 20 bar (0.67) and lowest at 0.35 at 30 bar. Similarly, the rejection is also lowest at 30 bar when acetonitrile is the solvent at 0.6 and highest at 40 bar with a rejection of 0.99.

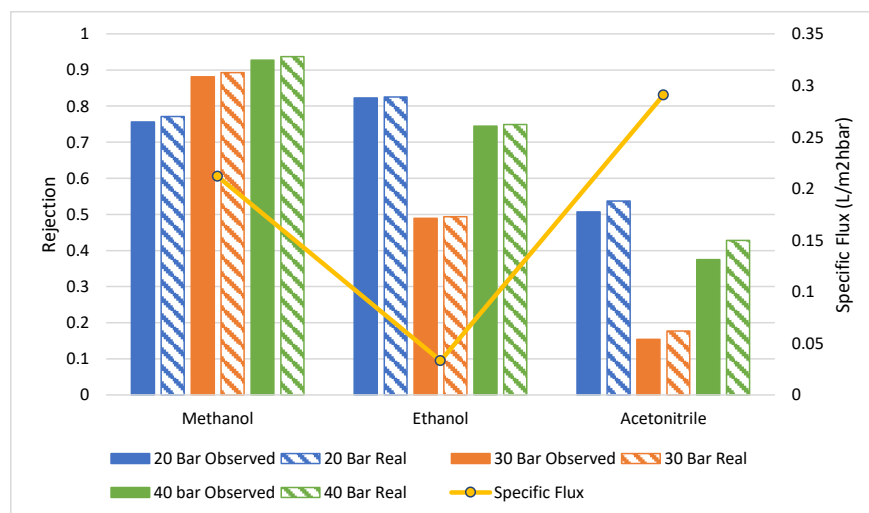


**Figure 4.8 Rejection of 1000 PPM tetraethylene glycol (PEG 200) in different solvent and mixtures over a range of pressures**

#### Characterisation of the Duramem OSN membranes

The rejection of PEG 200 follows a near identical trend that that of PEG 150, see Figure 4.8, with the rejection in methanol increasing with increasing applied pressure from 0.77 to 0.94 at 20 and 40 bar respectfully. In ethanol, the rejection at 30 bar is the lowest at 0.49 and highest at 20 bar at 0.82. The rejection in acetonitrile is also lowest at 30 bar at 0.18 and highest at 0.53 at 20 bar. As PEG 150 and 200 are the same shape with PEG 200 being an extra monomer attached to PEG 150 it is not surprising that the two solutes exhibit the same behaviour. The rejection of PEG 150 is higher than that of PEG 200 in acetonitrile, which suggests that there may be some chemistry occurring at the solute – solvent – surface level.

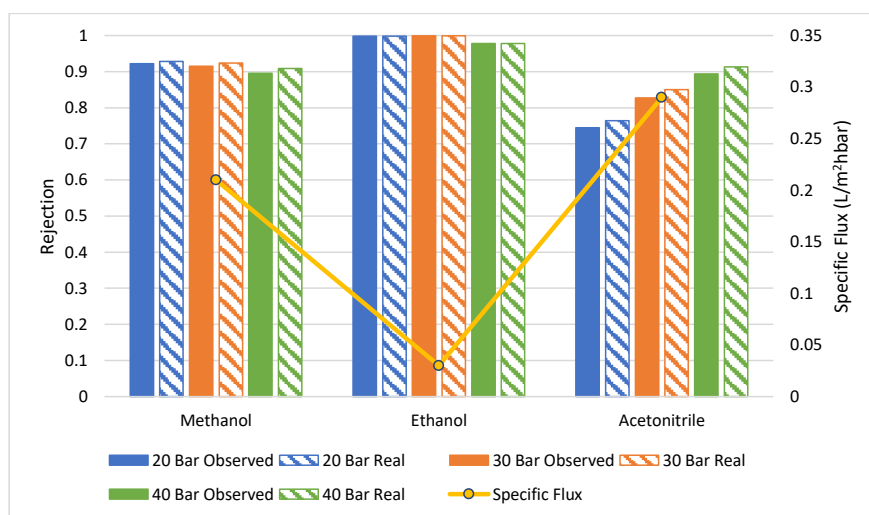


**Figure 4.9 Rejection of 1000 PPM dodecane in different solvent and mixtures over a range of pressures**

The rejection of dodecane in methanol is decreasing slightly with increasing pressure, decreasing from 0.93 to 0.91 and a pressure range of 20 to 40 bar respectfully, see Figure 4.9. There is near total rejection of dodecane in ethanol at 20 and 30 bar with a slight decrease at 40 bar (0.98). In acetonitrile, the rejection increases with increasing pressure, ranging from 0.76 to 0.91 at 20 to 40 bar respectfully.

Solute	Molecular weight	Van der Waal radius
	g/mol	Å
Toluene	92	8.81
Trichloroethylene	131	7.90
Triethylene glycol	150	10.80
Tetraethylene glycol	200	12.27
Dodecane	170	13.54

**Table 4-1 molecular weight and Van der Waals radius of solutes used in study**

# Characterisation of the Duramem OSN membranes

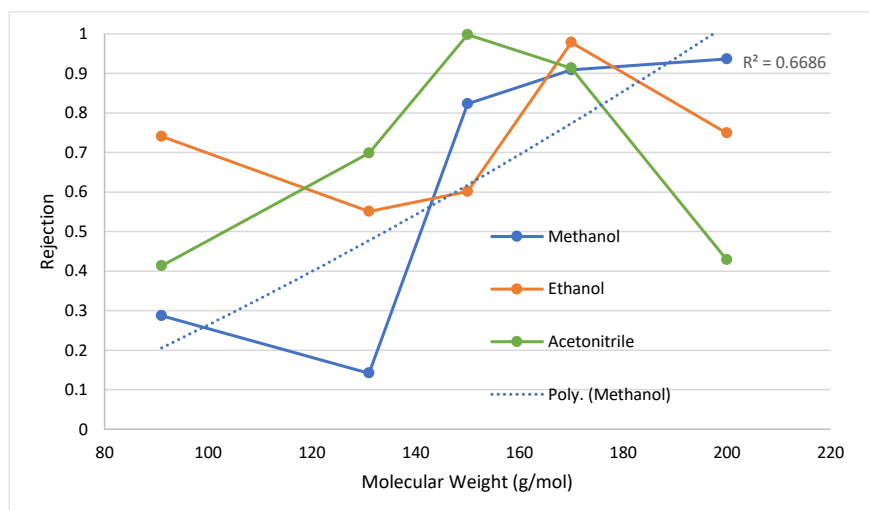


**Figure 4.10 Rejection of solutes based on molecular weight using Duramem 150 membrane at 40 bar**

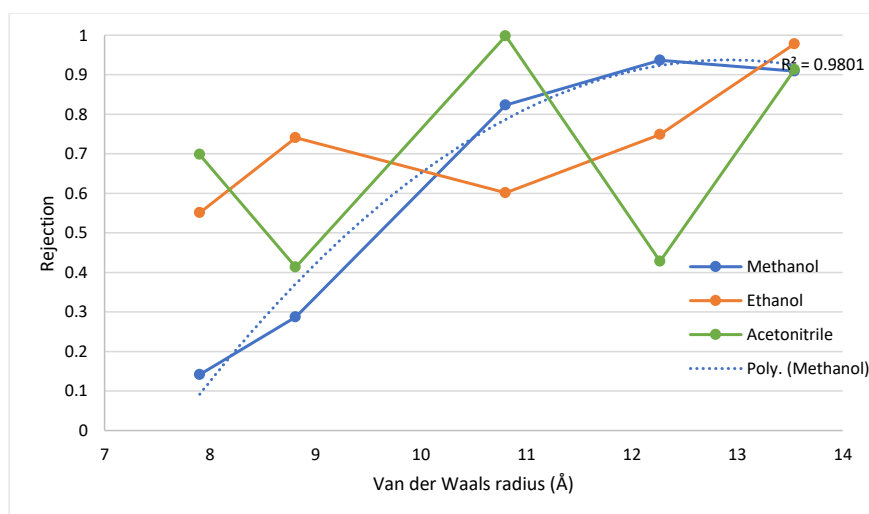


**Figure 4.11 Rejections of solutes based on Van der Waals radius using Duramem 150 membrane at 40 bar**

Previous studies have found that the shape and size of a molecule are larger factors in the rejection of solutes in OSN than the molecular weight, particularly for volatiles (Agenson & Urase, 2007) (Zheng, et al., 2008). That that end, Figure 4.10 shows the real rejection of solutes based on molecular weight at 40 bar and Figure 4.11 shows the real rejection of the same solutes at the same pressure based on their Van der Waals radius as opposed to their molecular weight. When considering Figure 4.10, there is no discernible

trend in the results for any of data sets while in Figure 4.11, there is a trend when considering the rejection of solutes when methanol is the solvent there is a clear trend of increasing rejection with increasing solute radius before plateauing when the rejection reaches 0.9. Agenson & Urase (2007) suggest the solute radius should be the basis for NF/RO membrane rejection profile as opposed to molecular weight and the data shown in Figure 4.10 and Figure 4.11 agrees with their suggestion. The Van der Waals radius was calculated using a program called Marvin sketch, where the Van der Waals Surface Volume is calculated from measuring the lengths along the x,y and z axis of the solute, with the radius back calculated from the calculated values. The changes in rejection profiles when different solvents are used can be attributed to solute – solvent – membrane interactions which require further study.

At the time of writing, only one similar characterisation study have been carried out on the Duramem 150 membrane by Davey, *et al* (2017) where the authors used polypropylene glycols (PPGs) to characterise several membranes in different solvents. The authors also found that the rejection behaviour of the membranes change in different solvent, which they attribute to membrane swelling, but no permeate flux was published. The PPGs used by the authors were 200 – 1200 g/mol, which led to very high rejection of the PPGs in methanol and acetone used on the Duramem 150 membrane.

#### 4.4.3 Effect of temperature on PEG rejection

The rejection of triethylene glycol increases from 81.01% to 90.24% at 25 and 40°C respectively, see Figure 4.12, with the permeate flux increasing from 14.18 to 26.17 L/m<sup>2</sup>h respectively. At 45°C the rejection decreases slightly to 87.73% while the permeate flux increases to 29 L/m<sup>2</sup>h.

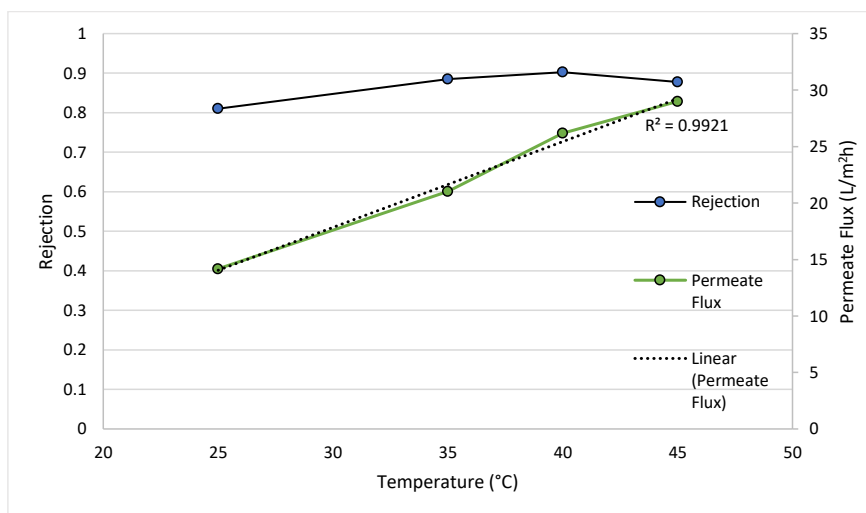


**Figure 4.12 Effect of temperature on the membrane flux and rejection of PEG 150 using methanol as a solvent using the Duramem 150 membrane at 30 bar applied pressure**

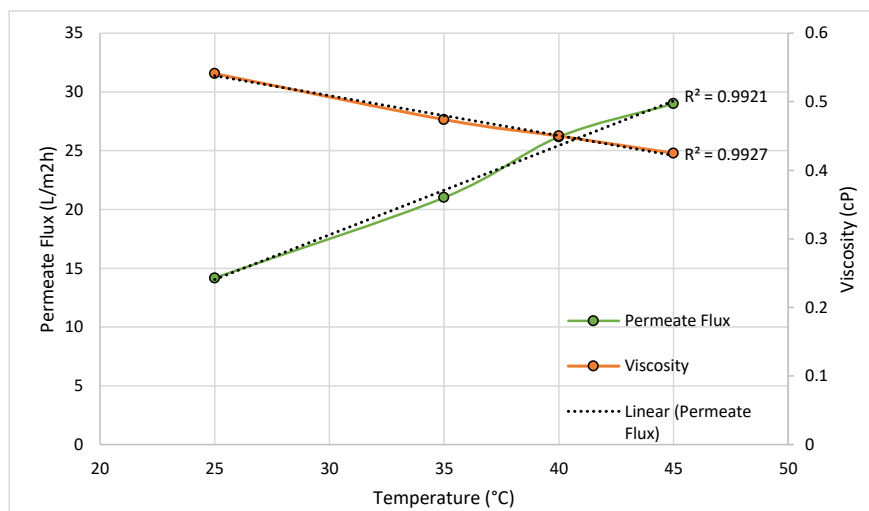


**Figure 4.13 Permeate flux and viscosity of methanol using the Duramem 150 membrane as a function of temperature at 30 bar applied pressure**

There is an argument that the little change in rejection between 35 and 45°C has plateaued (within experimental error) despite the increase in permeate flux, which lends to the theory that the separation mechanism for this membrane is diffusion. This is backed up by SEM images published by Martínez, *et al* (2013), where there appears to be no distinct pathway for solutes to pass through, but this is common for other NF membranes also (Sotto, et al., 2013) (Almazán, et al., 2015). This is contradictory to the data in Figure 4.4, thus a hypothesis can be made that there may be pores present in the membrane, but current visual equipment and techniques are not sophisticated enough to see them. However, the permeate flux appears to be directly proportional to the viscosity of the methanol, see Figure 4.13, thus the changes in permeate flux can most likely be attributed to the change in viscosity of methanol.

## 4.5 Salt rejection of Duramem 200

### 4.5.1 NaCl rejection

Similar to the Duramem 150 membrane, the Duramem 200 membrane shows increasing NaCl rejection with increasing applied pressure, with the rejection also decreasing with increasing salt concentration also, see Figure 4.14. The Duramem 200 shows a consistently high level of rejection at NaCl concentration of 0.001 mol/L ( $0.96 \pm 0.01$ ). When considering 0.01 mol/L, the rejection increases from 0.92 at 20 bar to 0.96 at 40 bar respectively. The rejection of NaCl also increases with pressure at 0.1 mol/L, increasing from 0.89 to 0.95 at pressure ranges of 20 to 40 bar respectively. The specific flux of the salt solutions are very similar with respect to 0.001 and 0.01 mol/L ( $1.12 \text{ L/m}^2\text{hbar}$ ) but decreases at 0.1 mol/L to  $1.03 \text{ L/m}^2\text{hbar}$ .

#### Characterisation of the Duramem OSN membranes

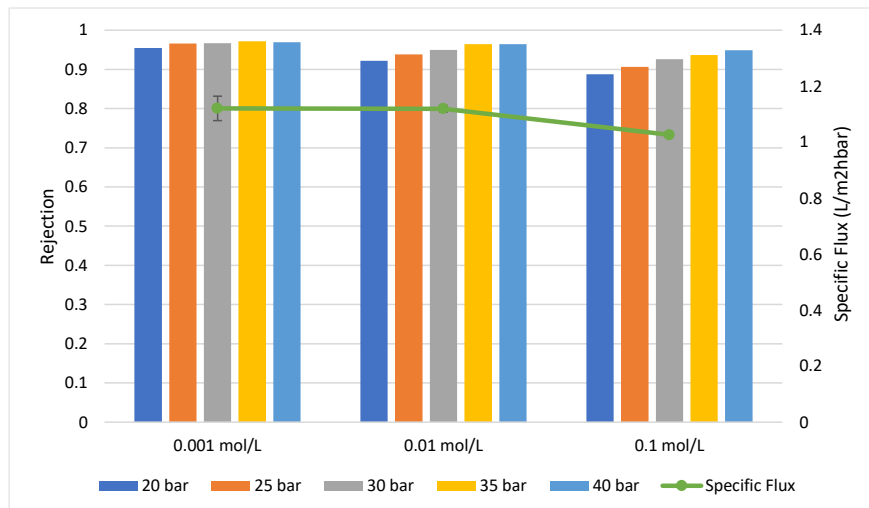


**Figure 4.14 Rejection of NaCl by Duramem 200 at applied pressures over a range of NaCl concentrations**

When comparing NaCl rejection using the Duramem 150 and 200 membranes respectively (Figure 4.1 and Figure 4.14), NaCl rejection between the two membranes are comparable at low concentrations, with the Duramem 150 showing a rejection of 0.92 at 30 bar and 0.001 mol/L and the Duramem 200 showing a rejection of 0.97 at the same applied pressure and concentration. There is a marked difference in rejection at 0.1 mol/L with the Duramem 150 showing a NaCl rejection of 0.8 at 30 bar and the Duramem 200 showing a rejection of 0.95 at the same applied pressure. There is also a noticeable difference in the permeate flux between the two membranes, with the Duramem 150 having a specific flux of 0.47 L/m²hbar and the Duramem 200 having a specific flux of 1.12 L/m²hbar for NaCl concentration of 0.001 mol/L. Similarly for 0.1 mol/L the specific flux is lower using the Duramem 150 membrane compared to the Duramem 200 (0.63 and 1 L/m²hbar respectively).

When comparing NaCl rejection data with that published by Oatley, *et al* (2012), the Duramem 200 membrane shows much better rejection of NaCl compared to both the NF270 and NF99HF membranes (rejections of 0.9 to 0.6 respectively). Similar to the Duramem 150 membrane, the permeate flux of the Duramem 200 membrane is significantly slower than the NF270 and NF99HF, with a permeate flux at 20 bar of 21.2 L/m²h.

#### 4.5.2 Na<sub>2</sub>SO<sub>4</sub> rejection

The Duramem 200 membrane shows excellent rejection of Na<sub>2</sub>SO<sub>4</sub> at all pressures and concentrations used, see Figure 4.15. The rejection at salt concentration of 0.001 mol/L is consistent at 0.96 at all applied pressures. The rejection of 0.01 mol/L salt concentration is 0.99 with the rejection of 0.1 mol/L being 0.98. The specific flux of the salt solution similar to the Duramem 150, thus the explanations for the rejection

#### Characterisation of the Duramem OSN membranes

and flux decline are also similar. The rejection of the salt generally remains constant at all applied pressures, with very little difference in rejection at each concentration also. The specific permeate flux declines significantly from 0.97 to 0.7 L/m<sup>2</sup>hbar at 0.001 to 0.1 Mol/L respectively.

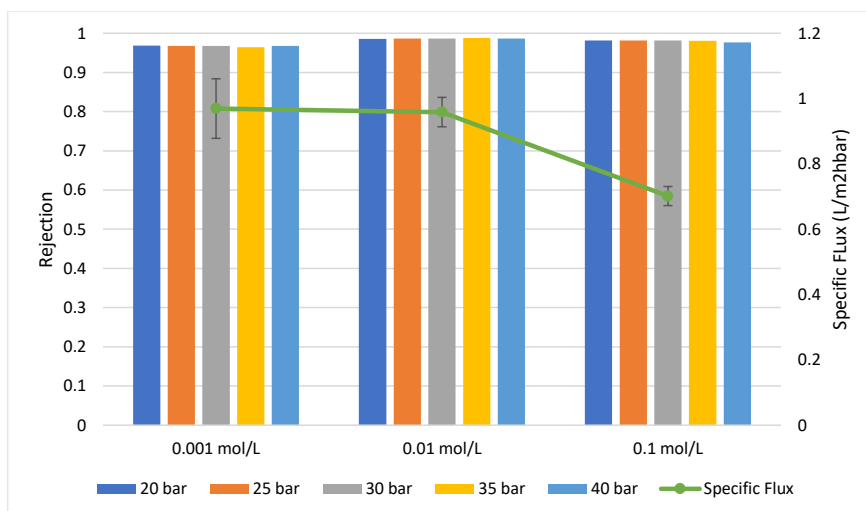


**Figure 4.15 Rejection of Na<sub>2</sub>SO<sub>4</sub> by Duramem 200 at applied pressures over a range of Na<sub>2</sub>SO<sub>4</sub> concentrations**

Comparing the rejection of Na<sub>2</sub>SO<sub>4</sub> between the Duramem 150 and 200 membranes, the two membranes exhibit comparable rejections at all concentrations tested, with the only difference between the two membranes being the permeate flux, with the specific flux of the Duramem 150 membrane at 0.001 and 0.01 mol/L being significantly slower than the specific flux of the Duramem 200 membrane (0.56 compared to 0.97 L/m<sup>2</sup>hbar respectively). When considering 0.1 mol/L, the specific flux of the Duramem 150 membrane is 0.34 compared to 0.7 L/m<sup>2</sup>hbar of the Duramem 200 membrane.

Comparing the Duramem 200 membrane rejection and permeate flux data to the data published by Oately, *et al* (2012), the Duramem 200 membrane shows better rejection of Na<sub>2</sub>SO<sub>4</sub> than the NF270 and NF99HF membranes, but has significantly lower permeate flux rate by comparison.

#### 4.5.3 MgCl<sub>2</sub> rejection

The Duramem 200 shows increasing rejection of MgCl<sub>2</sub> with increasing applied pressure, Figure 4.16, e.g. for 0.001 Mol/L the rejection increases from 90.7% to 95.76% at an applied pressure of 20 to 40 bar respectively. Interestingly, there is no real change in rejection with increasing salt concentration, for 20 bar the rejection is 90.7% and 92.61% for concentrations of 0.001 and 0.1 Mol/L respectively, and for 40 bar the rejection is 95.76% and 96.71% at concentrations of 0.001 and 0.1 Mol/L respectively. The specific flux



#### Characterisation of the Duramem OSN membranes

decreases drastically with increasing salt concentration, decreasing from 1.1 to 0.64 L/m<sup>2</sup>hbar at 0.001 to 0.1 Mol/L concentrations respectively.

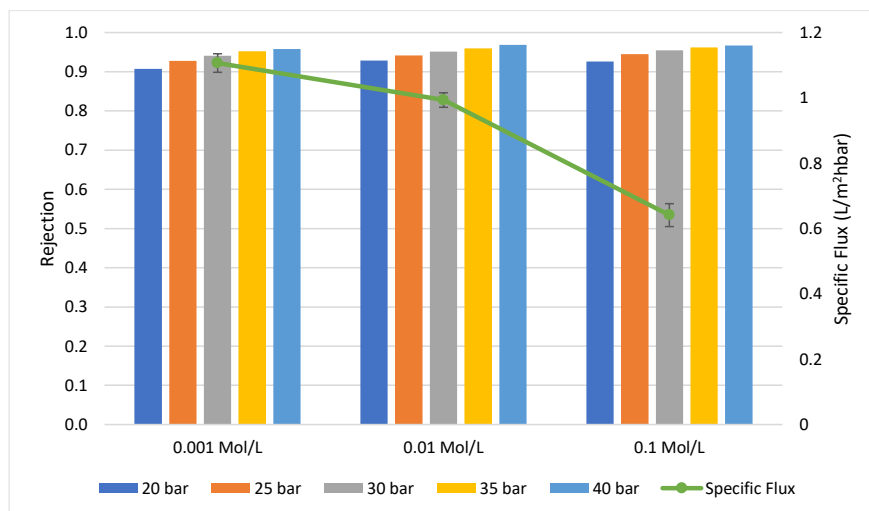


Figure 4.16 Rejection of MgCl<sub>2</sub> by Duramem 200 at applied pressures over a range of MgCl<sub>2</sub> concentrations

#### 4.6 Flux and rejections in aprotic solvents using of Duramem 200

##### 4.6.1 Rejection of volatile and neutral solutes

The rejection of toluene shows different patterns depending on the solvent used, see Figure 4.17. The rejection of toluene when using methanol as the solvent stays comparable at applied pressures of 20 and 30 bar (0.51 and 0.48 respectively) while the rejection increases to 0.67 at 40 bar. When ethanol is used as the solvent, the rejection increases with increasing pressure from 0.2 to 0.65 at pressure ranges of 20 to 40 bar respectively. The rejection of toluene in acetonitrile are comparable at 20 and 40 bar, with rejections of 0.66 and 0.68 respectively, with 30 bar showing the lowest rejection of 0.46. The specific flux also varies depending on the solvent used with the specific flux of methanol, ethanol and acetonitrile being 0.28, 0.04 and 0.16 L/m<sup>2</sup>hbar respectively.

#### Characterisation of the Duramem OSN membranes

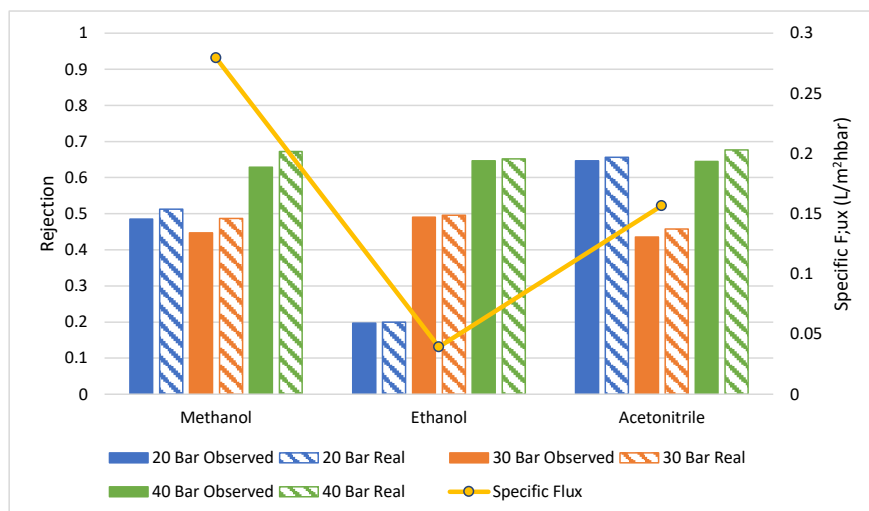


**Figure 4.17 Rejection of 1000 PPM toluene using the Duramem 200 membrane in different solvents and applied pressures**

The rejection pattern of trichloroethylene follows the same pattern as toluene for each of the solvents used but with lower rejection values due to the molecules smaller size, see Figure 4.17 and Figure 4.18 respectively. When methanol is used as the solvent, the rejection is at its lowest at 30 bar applied pressure at 0.25 and highest at 40 bar with a rejection of 0.48. When ethanol is used, the rejection increases with increasing pressure, increasing from 0.6 to 0.45 over pressures ranging from 20 to 40 bar applied pressures respectfully. When acetonitrile is used, 30 bar pressure has the lowest rejection (0.17) and highest at 40 bar (0.45).

#### Characterisation of the Duramem OSN membranes

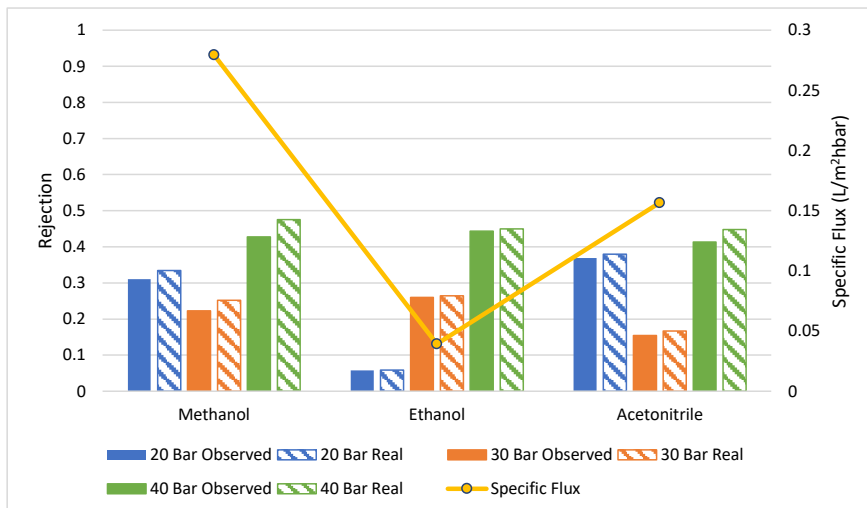


**Figure 4.18 Rejection of 1000 PPM trichloroethylene by Duramem 200 in different solvents and applied pressures**

Comparing the rejection of trichloroethylene using the Duramem 150 and 200 membranes (Figure 4.17 and Figure 4.18), the rejection profiles are very similar which is to be expected, with the Duramem 150 membrane having higher rejections than the Duramem 200 membrane in ethanol but not in methanol.

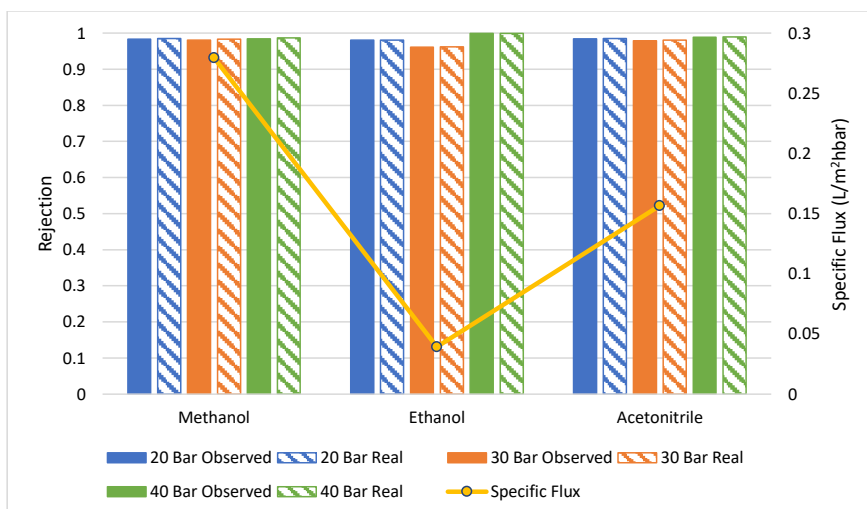


**Figure 4.19 Rejection of 1000 PPM dodecane by Duramem 200 in different solvents and applied pressures**

The rejection of dodecane is consistently high for solvents and pressure tested, see Figure 4.19. This is consistent with the rejection results of the Duramem 150 membrane, suggesting that the rejection of this

#### Characterisation of the Duramem OSN membranes

solute could simply be due to size exclusion, or whether physical or chemical properties of the solute / solvent may be affecting the rejection.

The rejection of triethylene glycol (PEG 150) in methanol is highest at 30 bar pressure with a rejection of 0.8 and lowest at 20 bar pressure with a solute rejection of 0.63, see Figure 4.20. There is a similar story with respect to acetonitrile, with the highest rejection at 30 bar pressure at 0.77 and lowest at 20 bar with a rejection of 0.64. The rejection of triethylene glycol increases with increasing pressure when ethanol is the solvent with the rejection increasing from 0.35 to 0.6 over pressures ranging from 20 to bar 40 respectfully.

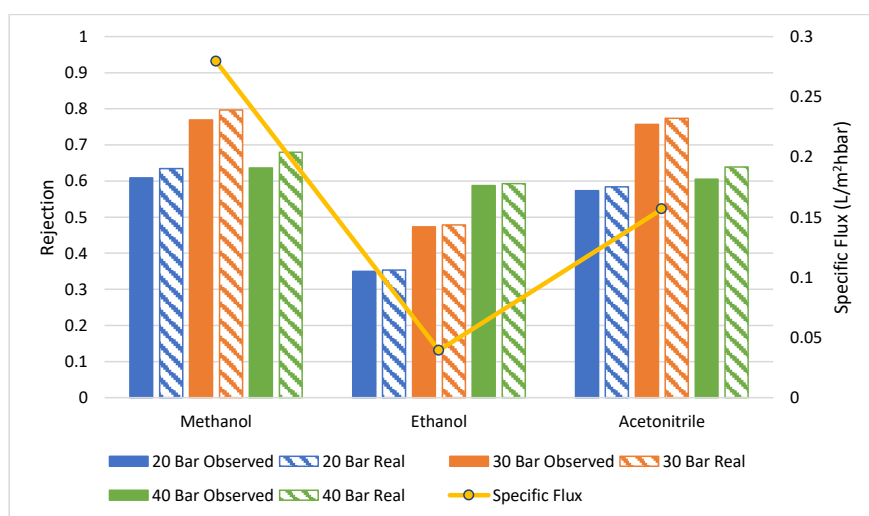


**Figure 4.20 Rejection of 1000 PPM triethylene glycol (PEG 150) by Duramem 200 in different solvents and applied pressures**

The rejection of triethylene glycol is higher when the Duramem 150 membrane is used, which is to be expected when the advertised MWCO is lower than the Duramem 200 membrane. The rejection at 30 bar is highest for triethylene glycol in methanol and acetonitrile, while the rejection is highest at 20 bar in methanol and acetonitrile when the Duramem 150 membrane is used, which may be due to swelling of the membrane.

# Characterisation of the Duramem OSN membranes

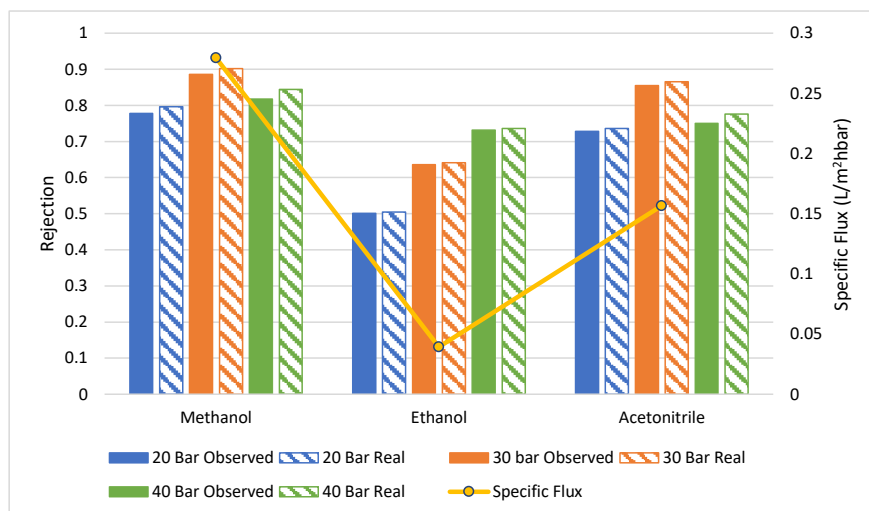


**Figure 4.21 Rejection of 1000 PPM tetraethylene glycol (PEG 200) by Duramem 200 in different solvents and applied pressures**

The rejection of tetraethylene glycol using the Duramem 200 follows the same pattern of rejection as the rejection of triethylene glycol, see Figure 4.21, which is to be expected as the latter solute is an extension of the former by one methyl group. The rejection of tetraethylene glycol is highest at 30 bar for methanol and acetonitrile, with a rejection of 0.9 and 0.86 respectively, with the lowest rejection at 20 bar with rejection values of 0.8 and 0.74 respectively. The rejection of tetraethylene glycol increases with increasing applied pressure when ethanol is the solvent, increasing from 0.5 to 0.74 and a range of 20 to 40 bar.

# Characterisation of the Duramem OSN membranes

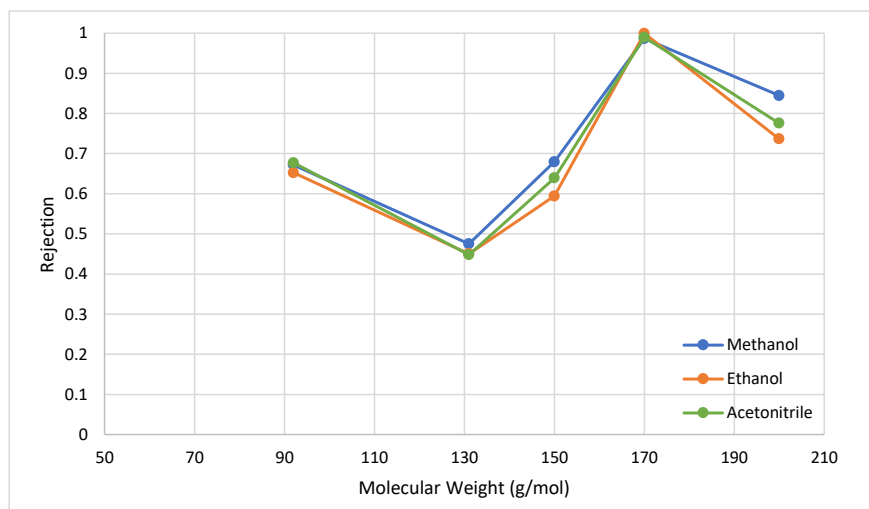


**Figure 4.22** Rejection of solutes using the Duramem 200 membrane at 40 bar applied pressure as a function of molecular weight

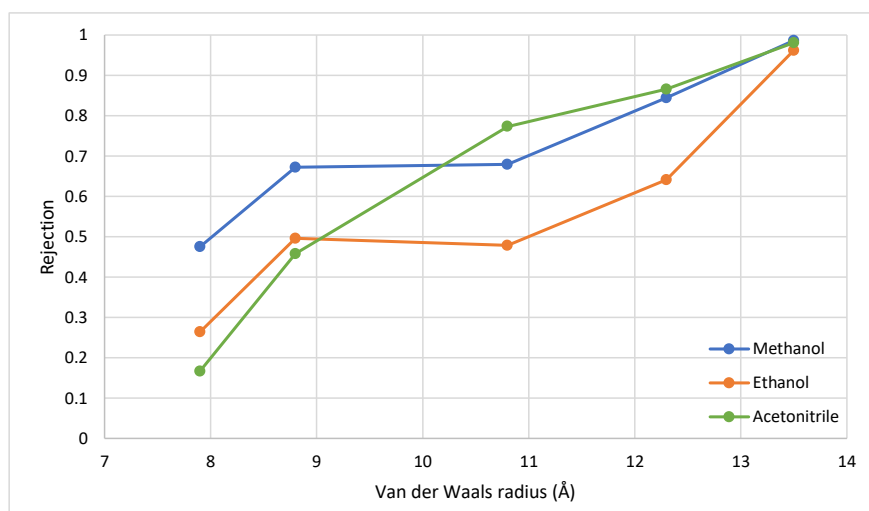


**Figure 4.23** Rejection of solutes using the Duramem 200 membrane at 40 bar applied pressures as a function of Van der Waals radius

Similar to the Duramem 150 membrane, plotting the MWCO of a membrane in solvent is not feasible, see Figure 4.22. The MWCO may be feasible for solutes of the same type e.g. PPGs, but for solutes that are different species, MWCO is not feasible (Davey, et al., 2017). Plotting the rejection against the radius of the solute shows that there is a correlation between rejection and Van der Waal's radius, see Figure 4.23.

# Characterisation of the Duramem OSN membranes

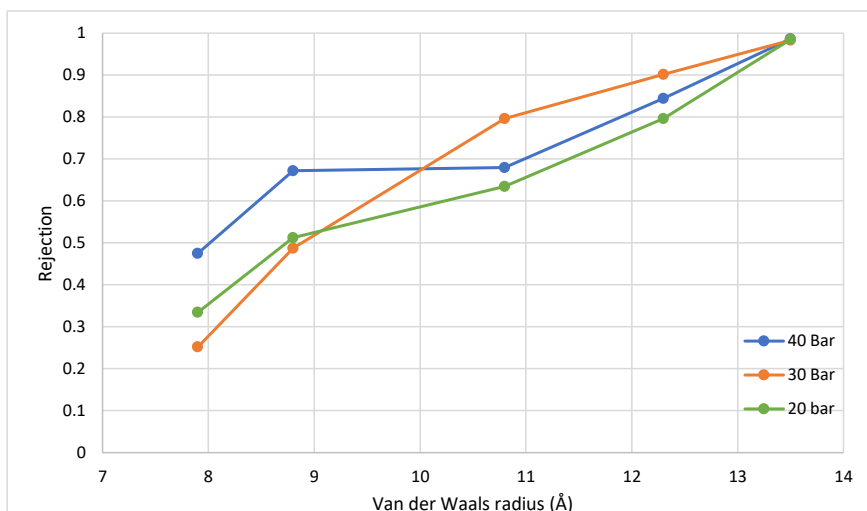


**Figure 4.24 Rejection of solutes as a function of Van der Waals solute radius in methanol using the Duramem 200 membrane at applied pressures**

Analysing the rejection of neutral and volatile solutes as a function of the calculated solute size, the rejection of solutes in methanol is increasing linearly with increasing solute radius at applied pressures of 20 and 40 bar, but the rejection increases polymerically with increasing solute radius at 30 bar.

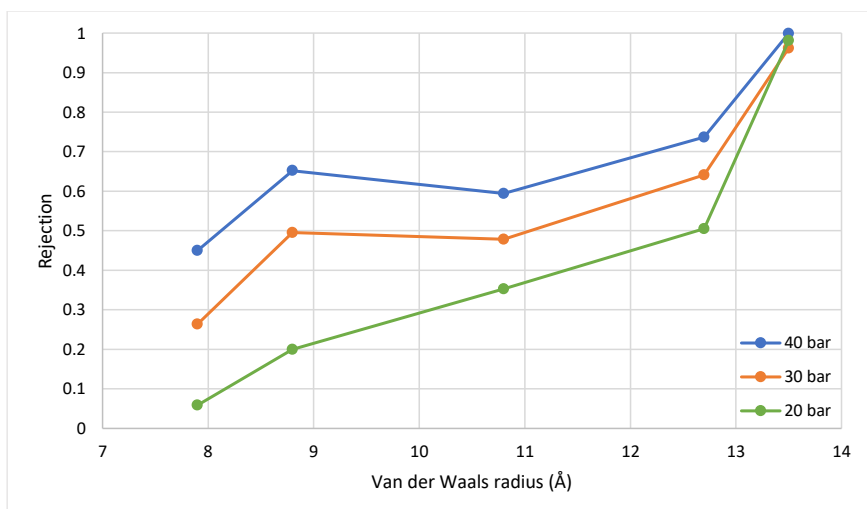


**Figure 4.25 Rejection of solutes as a function of Van der Waals solute radius in ethanol using the Duramem 200 membrane at applied pressures**

#### Characterisation of the Duramem OSN membranes

The rejection of solutes in ethanol increases with increasing pressure, but for 30 and 40 bar, the rejection appears to plateau between 8.5 and 11 Å and then increases again, see Figure 4.25. At 20 bar, the rejection increases linearly until 12.75 Å where the rejection jumps from 0.5 to 1.

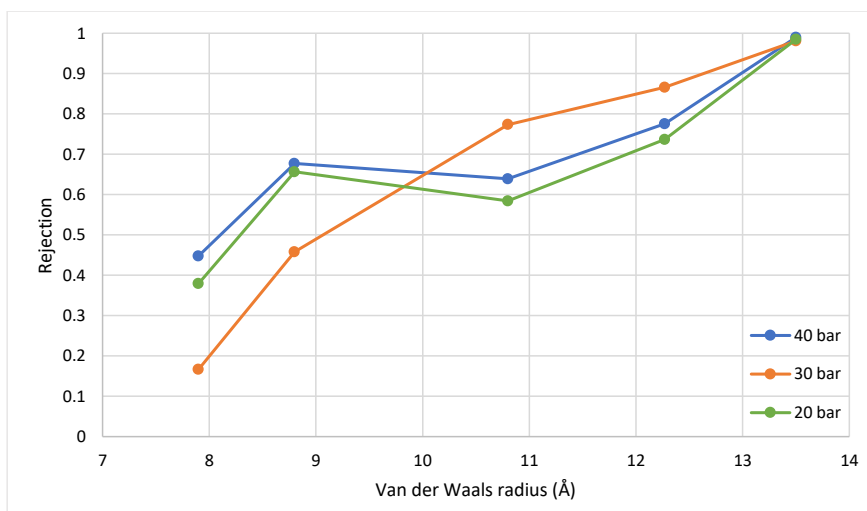


**Figure 4.26** Rejection of solutes as a function of Van der Waals solute radius in acetonitrile using the Duramem 200 membrane at applied pressures

The rejection of solutes at 20 and 40 bar have identical profiles, with 40 bar pressure showing higher rejection values for each solute than at 20 bar, see Figure 4.26. The rejection of solutes at 30 bar increases in a polynomial fashion in acetonitrile, which is similar to the rejection profile of solutes in methanol at 30 bar.

#### 4.6.2 Effect of temperature on PEG rejection

The permeate flux of the Duramem 200 membrane increases from 26.4 to 33.6 at a temperature range of 25 to 35°C but plateaus for 40 and 45°C with flux values of 31.3 and 33.25 respectively, see Figure 4.27. The rejection profiles of PEG 150 and 200 are identical but with the rejection PEG 200 being higher (e.g. at 35°C, the rejection of PEG 150 is 0.76 and the rejection of PEG 200 is 0.85).



# Characterisation of the Duramem OSN membranes

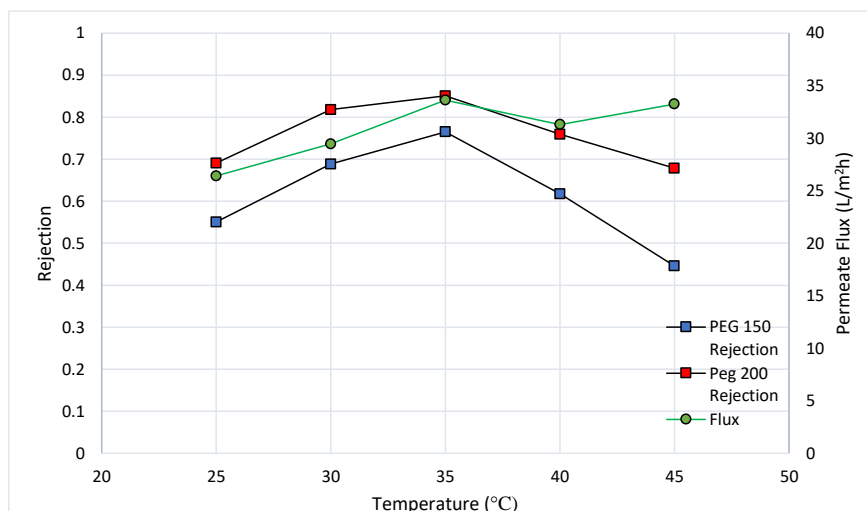


**Figure 4.27 PEG Rejection in methanol at 30 bar applied pressure using the Duramem 200 membrane at different temperatures**

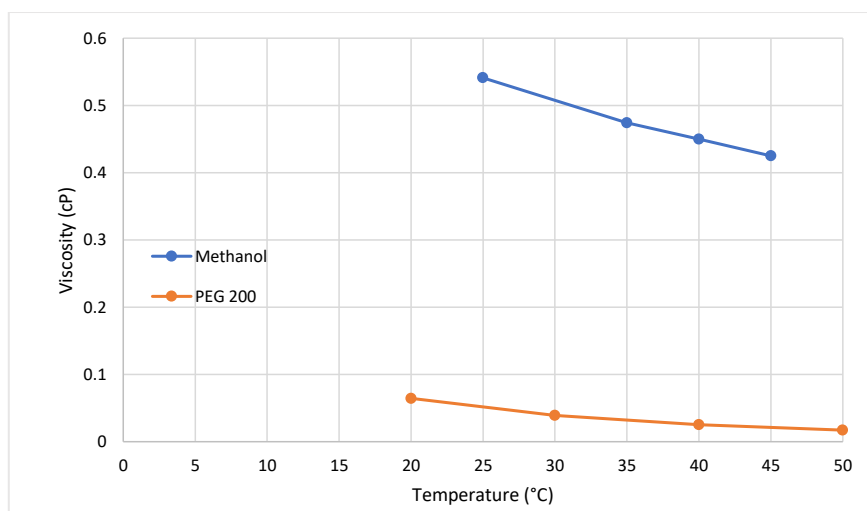


**Figure 4.28 Viscosity of Methanol and PEG 200 as a function of temperature**

The initial increase in flux and rejection may be due to the viscosity of methanol decreasing with increasing temperature the PEG 150 and 200 being, see Figure 4.28. The decrease in rejection and plateauing of the permeate flux may be due to thermal degradation of the surface of the membrane and resulting in a decrease in rejection properties of the membrane.

## 4.7 Zeta potential of Duramem 200 Membrane

### 4.7.1 TSP measurements

The surface charge of the Duramem 200 membrane at 0.001 mol/L is constant at -20mV at pH's 6 to 10, before increasing to -13mV at pH 4.6 and to 6.5mV at pH 3.5, see Figure 4.29. At NaCl concentration of 0.01 mol/L, the surface charge of the membrane is  $-26 \pm 3$  between a pH range of 5.1 to 8.35, before increasing to -8.16mV at pH 3.6. At NaCl concentration of 0.1 mol/L, the surface charge of the membrane is -39.61mV at pH 9, before decreasing to -61.73 mV at 7.7 pH and increasing linearly from -47.9 to -16.9mV at a pH range of 7 to 3.66.

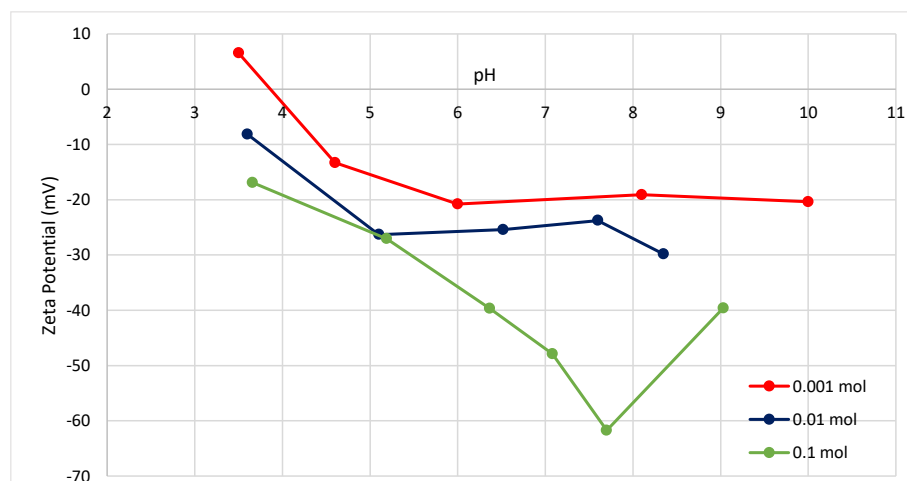


**Figure 4.29 Zeta potential of Duramem 200 at various NaCl concentrations in ultra-pure water**

The iso-electric point of the membrane at 0.001 mol/L is at pH 3.8, but the membrane did not show an iso-electric point at the other two concentrations tested. This may be due to  $\text{Cl}^-$  ions adsorption onto the membrane, which becomes more prominent when increasing the salt concentration from 0.01 to 0.1 mol/L, which is likely why the manufacturer suggests only operating this membrane at pH 7.

## 4.8 Conclusions

The Duramem 150 and 200 both reject salt solutions at a similar level to commercial aqueous membranes produced for this purpose, having a rejection >90% of all salts at high pressure. The permeate flux rate of the Duramem 150 is very slow due to the dense polymer layer that is needed to produce the level of rejection that the membrane is able to perform, with the Duramem 200 falling into the same bracket, albeit with lower rejection values of the same solutes and higher permeate flux rates (at 40 bar pressure and methanol is the solvent, the flux of the Duramem 150 is 8.2 L/m<sup>2</sup>h while its 10.25 L/m<sup>2</sup>h when the Duramem

200 is used) see Figure 4.5 and Figure 4.17. Comparing these membranes to other commercially available NF membranes e.g. NF270 and DK, the specific flux of the Duramem 150 and 200 membranes are significantly lower than other available on the market. The lower specific flux rates of the Duramem series are likely to the dense nature polymer compared to the thin film composites of the NF270 and DK amongst others.

The performance of an OSN membrane is heavily dependent on the solvent which is being used, see figures 4.5-9 and 4.17-21, which is also evident in other studies (Davey, et al., 2017). What is lacking at this moment in time are comprehensive studies into OSN membrane performance in a variety of solvents, monitoring the change in solvent properties and measuring them against the performance of the membrane being tested.

The change in permeate flux through the membrane at different viscosities, see Figure 4.4, suggests that there are pores even at the near RO scale which agrees with data published by other authors. To accurately measure the pores and MWCO of OSN membranes below 200 g/mol, solutes of different species should be examined, which has been examined in this study and by other authors (Zheng, et al., 2008) (Zheng, et al., 2009). Measuring the solute radius has shown to be successful in predicting the pore size of the membrane using solutes with molecular weights below 100 g/mol and are of different species (Agenson & Urase, 2007). The downside of this method is that additional computer software is needed as well as a GC-MS system. While the computer program will predict the pore size based on rejection, the program will not consider the properties of the solutes (e.g. solubility) when taking rejection into account.

The surface charge of the Duramem 200 membrane is negatively charged in water – salt solutions with the isoelectric point at 0.001 mol/L at pH 3.8, but there are no iso-electric points at 0.01 and 0.1 mol/L. This may be to adsorption of  $\text{Cl}^-$  ions onto the surface of the membrane. The membrane is designed for solvent systems so passing a voltage across the membrane in EKA measurements may have changed the surface chemistry of the membrane, allowing the adsorption. As the manufacturer stipulates in the instruction manual that the operating pH for this membrane is 7, this suggests that subjecting Duramem membranes to acid/alkali conditions will change the performance of the membrane, which is evident from the results show in Figure 4.29.

In summary, while the Duramem 150 does appear to have slightly lower MWCO when compared to the Duramem 200 membrane, this is not the case in all solvents tested as each membrane has different performance in each solvent tested. While there are some systematic studies of membrane performance, more are needed to fully understand how the performance of OSN membranes changes, and how best to pick the right membrane for the separation required.

## 5. Electrokinetic characterisation of OSN membranes

---

### 5.1 Introduction

The rejection of an aqueous solute by nanofiltration membranes is governed by a mixture of steric and donnan mechanics, however, for solvent systems there is an assumption that there is no charge within the solvent system due to a lack of dissociating  $H^+$  ions, and thus the rejection of a solute in solvent systems is governed by steric mechanics only. The results in the salt rejection studies in chapter one show that the Duramem membranes carry a surface charge, and thus donnan effect may play a role in rejection for solvent systems. From observing this phenomenon, the aim of this study is to determine if the Duramem series carry a surface charge in methanol – water systems, and if so to what degree.

The electrostatic charge of a membrane, known as its zeta ( $\zeta$ ) potential, has a role in solute rejection, particularly solutes that are in a charged state, e.g. metal ions, organic acids and dyes, so measurement of membrane zeta potential is a common form of analysis, particularly for custom made and/or modified membranes (S.Deshmukh & Childress, 2001) (Ernst, et al., 2000) (Hoseinpour, et al., 2016). Despite this large catalogue of data for aqueous systems, there is no published zeta potential data available for organic solvent systems, to the best of the authors knowledge. Some authors in literature has made assumptions that OSN membranes have charge based on solute rejection but have not published data to justify the assumptions (Yao, et al., 2016).

Initial testing of the method published by Thomas, *et al* (2017) on the Duramem 200 showed that the membrane had a positive charge in methanol. This then led to a development of the method described herein for LDE testing of membrane surface charge of positively charged membrane that is accurate, and repeatable, by using particles that are the same charge as the membrane surface. Use of LDE for OSN membranes would be more practical than EKA as the measurements uses much less solvent for analysis (200 mL as opposed to 2 litres) and requires a much smaller membrane area when compared to the amount needed for EKA measurements. PTFE membranes were selected for modification as the material is chemically resistant, and the method used for modification showed a good bonding of the APTES onto the surface of the membrane, shown by the highly charged positive surface (Wang, et al., 2015).

After analysis of the data, the initial results were found to be misleading as the Aradite used to bond the membrane onto the testing equipment was found to be the substance giving the positive reading. After discovering this, double sided tape is used to bond the membrane, and the surface charge was found to be negligible and intelligible by LDE measurements, as methanol does not carry a voltage easily (low dielectric constant). While the LDE method of measuring membrane surface charge derived for the experimentation needs further work to provide accurate and repeatable results for solvent systems, the method provides a viable alternative for EKA surface charge measurements on positively charged membranes.

## 5.2 Experimental procedures

0.2 $\mu$ m PTFE membrane was obtained from Porex, (Alness UK) and modified in the method detail by Wang *et al* (2015) and in section 3.6.3. A detailed method for TSP measurements conducted on an EKA can be found in section 3.4.3. A method derived from Thomas, *et al* (2017) for use in positively and negatively charge aqueous solutions and solvent solutions can be found in section 3.4.4.

## 5.3 Experimental results

### 5.3.1 Zeta Potential measurements of PTFE membrane

TSP data obtained from the EKA shows good correlation with zeta potential data obtained from Wang, *et al* with the iso-electric point being around pH 5 (Figure 5.1). The LDE data using negatively charged particles obtained using the zetasizer also shows good correlation with data obtained using TSP measurements, which is consistent with data obtained by Thomas, *et al* and thus further illustrating that LDE measurements are a viable method for determining zeta potential of a membrane. Data obtained using positive particles on the negatively charged membrane show very poor correlation with data obtained using negatively charged particles, and the argument could be made that the charge doesn't change with data for pH 7.2 being anomalous.

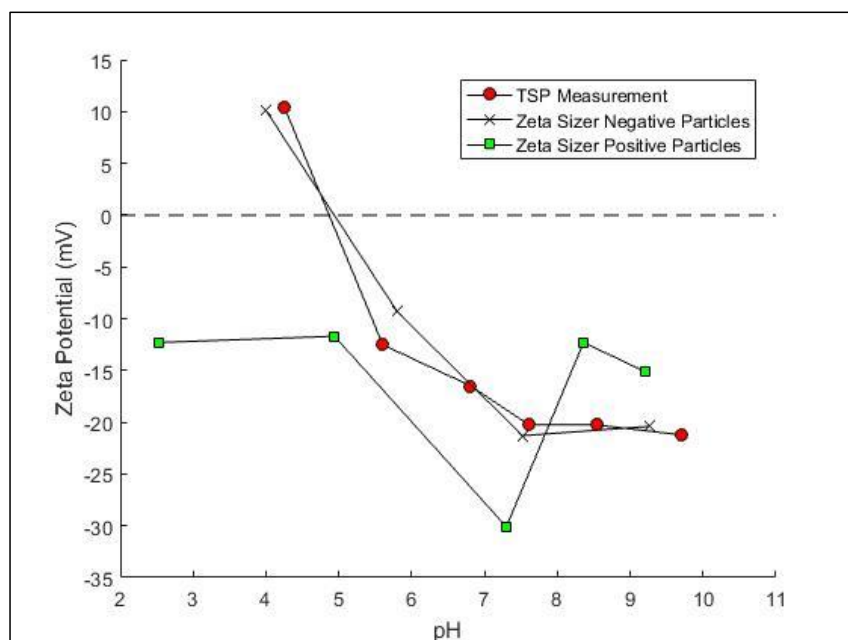


Figure 5.1 Zeta Potential of unmodified PTFE membrane using TSP and LDE methods

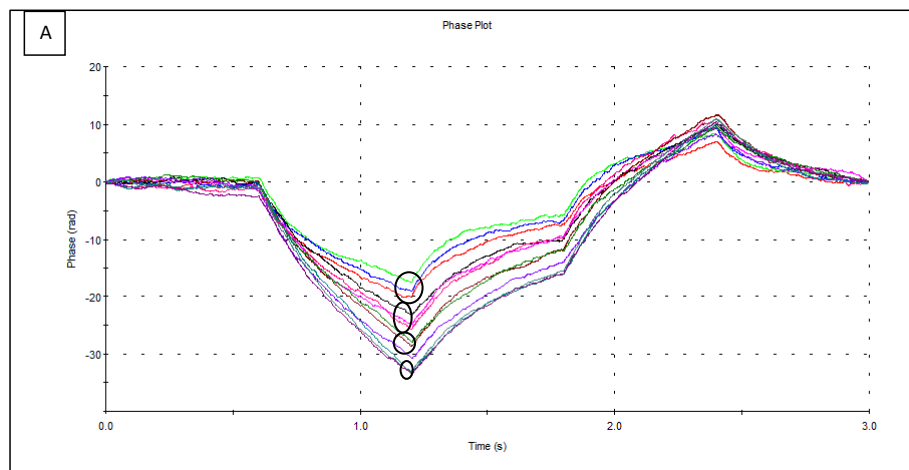
## Electrokinetic characterisation of OSN membranes

	Amidine	Carboxylate
<b>Zeta Potential (mV)</b>	12.4	-52.8
<b>Standard Deviation</b>	2.83	8.56
<b>Mobility (<math>\mu\text{mcm/Vs}</math>)</b>	0.784	-4.119
<b>Conductivity (mS/cm)</b>	0.104	0.192

**Table 5-1 Properties of charged beads used in LDE experiments**

### 5.3.1.1 Comparison of LDE measurements using charged beads

Zeta potential measurements using LDE method with negatively carboxylate beads (Figure 5.2) show good correlation with those using TSP measurements with very little error, shown in Figure 5.2B. The 3 averaged phase measurements are clear at each of the 4 displacements and are highlighted in Figure 5.2A, with the surface equivalent mobility of  $-1.411 \mu\text{mcm/Vs}$  ( $R^2 = 0.994$ ). Conversely, while the 4 bands or 3 averaged results are clearly distinct for negatively charged particles, they are not when positively charged particles are used, Figure 5.3A, with the surface equivalent mobility regression having a value of  $-2.36 \mu\text{mcm/Vs}$  and having a good fit also ( $R^2 = 0.984$ ), see Figure 5.3B. The good correlation would indicate that the data is of high quality, implying that the amidine particles are adsorbing onto the surface due to the voltage and charge of the membrane being oppositely charged to the particles.



# Electrokinetic characterisation of OSN membranes

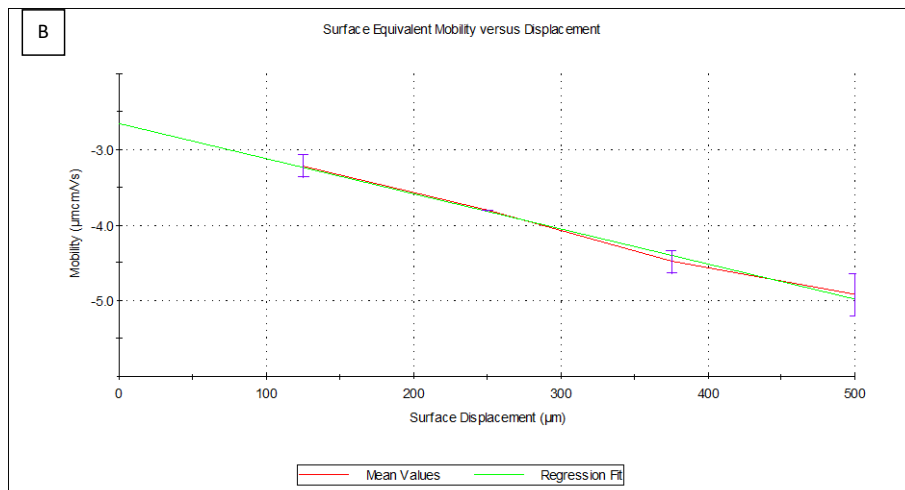
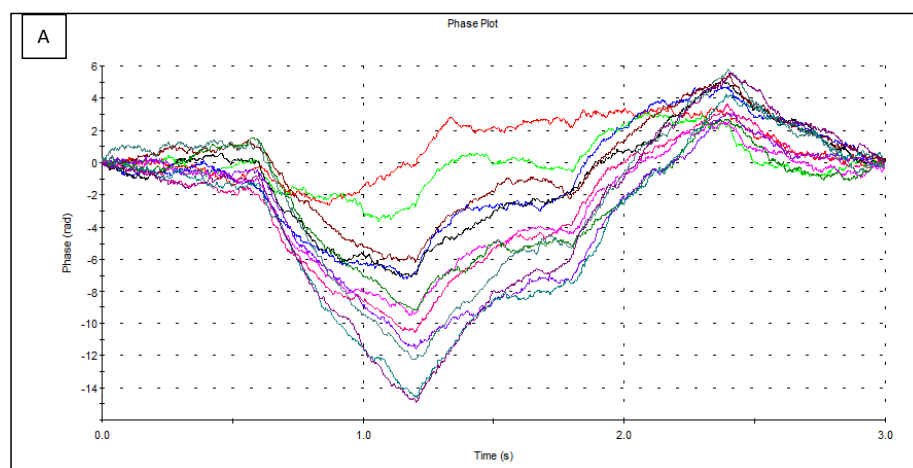
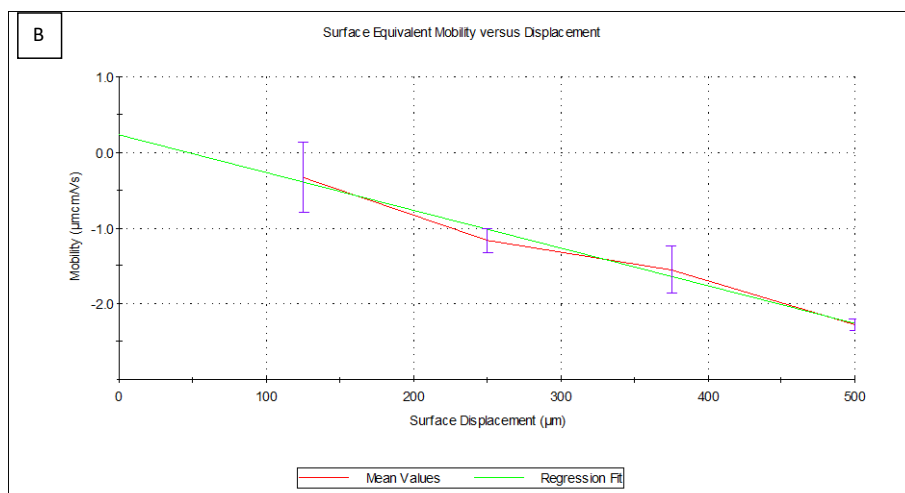


Figure 5.2 (A) Phase graph of carboxylate beads with unmodified PTFE with applied voltage (B) Particle mobility at each measurement displacement/height



## Electrokinetic characterisation of OSN membranes



**Figure 5.3 (A) Phase diagram of Amidine beads on unmodified PTFE at the applied voltage (B) Particle mobility at each membrane displacement/height**

### 5.3.2 Zeta Potential measurements of APTES-modified PTFE membrane

TSP measurements and LDE measurements using amidine particles show good correlation, while LDE measurements using negatively charge carboxylated particles for the pattern that negatively charged particles produce when undergoing zeta potential measurements, shown in Figure 5.4. The modification of PTFE with APTES gives the membrane a positive charge at neutral pH, with the membrane charge decreasing in a linear fashion as the pH becomes more basic, with the iso-electric point occurring at pH 9.



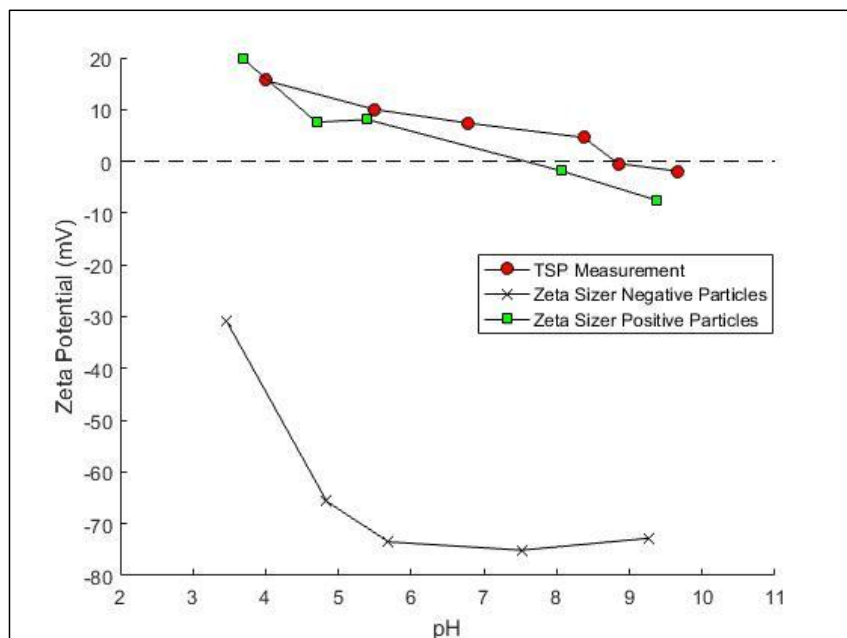
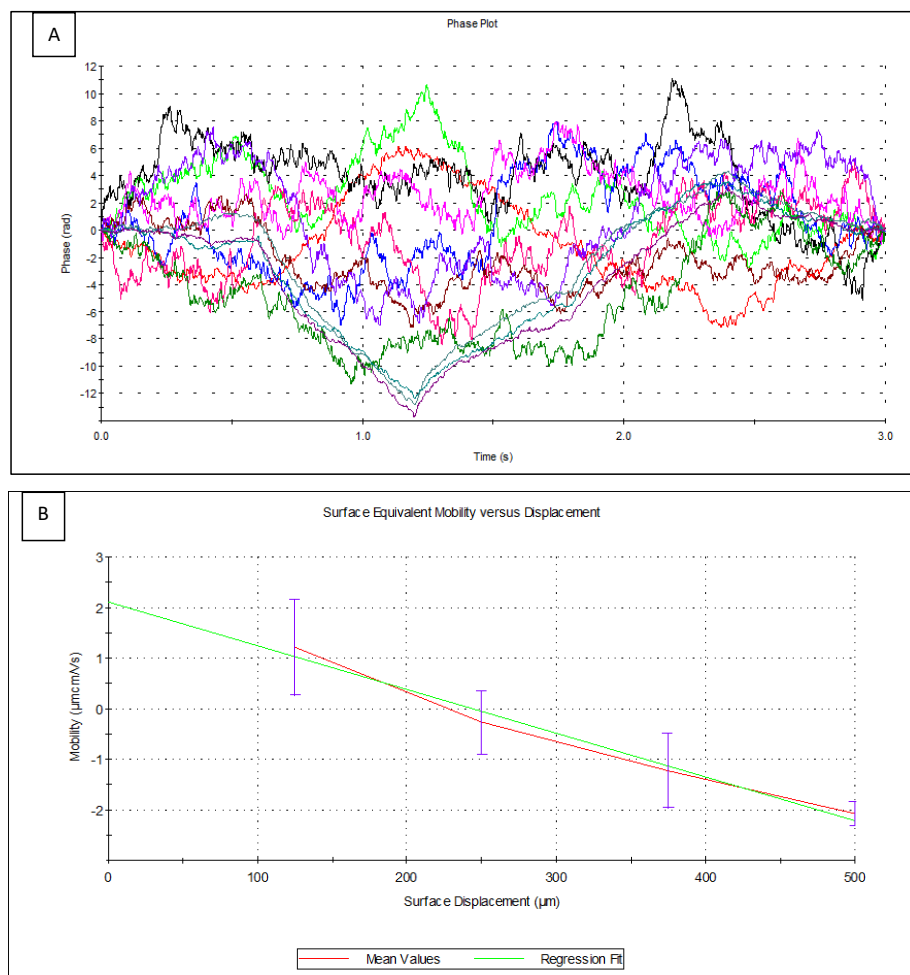


Figure 5.4 Zeta Potential measurement of APTES-modified PTFE membrane using TSP and LDE methods

#### 5.3.2.1 Comparison of LDE measurements using charged beads

The phase diagram for LDE measurements using carboxylated beads shows no distinct pattern which is likely due to the beads adsorbing onto the surface due to the charge the beads and the voltage being oppositely charged from the membrane surface, Figure 5.5A. The mobility regression shows good correlation ( $R^2 = 0.982$ ) having a mobility value of  $-7.086 \mu\text{mcm}/V_s$ , see Figure 5.5B, meaning that the beads are adsorbing onto the positively charged surface of the membrane. Conversely, use of amidine beads with APTES modified PTFE membranes show good correlation with results from TSP measurement with the phase diagram observing the same pattern as show in Figure 5.2A, but without the 4 band of 3 averaged results. This information can be used in conjunction with the mobility backward regression showing a good fit ( $R^2 = 0.977$ ), giving a mobility value of  $0.632 \mu\text{mcm}/V_s$ , see Figure 5.6B.

# Electrokinetic characterisation of OSN membranes



**Figure 5.5 (A) Phase diagram of carboxylate beads on APTES-modified PTFE at the applied voltage (B) Particle mobility at each membrane displacement/height**

## Electrokinetic characterisation of OSN membranes

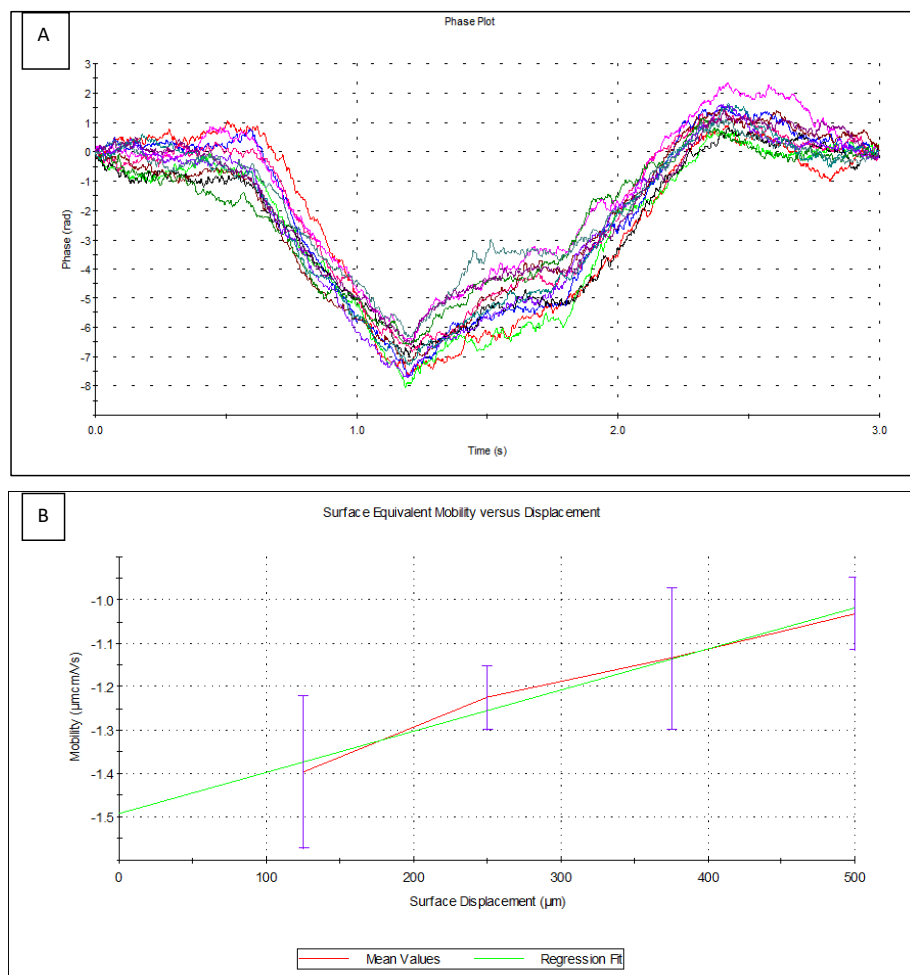


**Figure 5.6 (A) Phase diagram on Amidine beads on APTES-modified PTFE at the applied voltage (B) Particle mobility at each membrane displacement/height**

### 5.3.3 TSP measurements of Duramem 200 in methanol-water systems

The addition of methanol to the system alters the zeta potential profile of the Duramem 200 membrane from observing a negative profile to having a linear profile, as displayed in Figure 5.7. A mixture of 75% water/methanol has little change on the profile of the membrane, while a 67% mixture has a large change of ZP ( $\approx 20\text{mV}$ ) between pH 6 to 7.5 and the isoelectric point moving to pH 6 as opposed to pH 4. The membrane moves from a polynomial profile to a linear profile with increasing methanol content, as shown

### Electrokinetic characterisation of OSN membranes

for 50, 40 and 25% water, the zeta potential profile has little change. A hypothesis can be made that the membrane has 3 behavioural states:

1. 100-75% water – methanol content has little to no effect on the zeta potential on the membrane.
2. 67% water – there is a transitional phase where there is a drastic change in zeta potential around the iso-electric point.
3. 50 – 25% water – zeta potential changes in a linear fashion with the iso-electric point gradually moving from pH 5.4 to pH 7.25 – indicating that at 100% methanol (pH 7) there is little to no surface charge.

The change in the ZP profile of this membrane with increasing methanol content may be down to changes in hydrogen dissociation potential of the solvent, the self-protonation constant  $pK_w$  extrapolated from literature and the constant behaviour is shown in Figure 5.8 (Farajtabar, et al., 2013). While the change in  $pK_w$  is minimal, the effect of the addition of protons or hydroxyl groups seems to have a significant effect on  $pK_w$  of the system. With increasing methanol content, the hydronium ion ( $H_3O^+$ ) increases, see Figure 5.8, as well as the surface charge of the Duramem 200 membrane, suggesting that the methanol is acting as a weak base, forming  $MeOH_3^{++}$  and may be adsorbing onto the surface of the membrane.

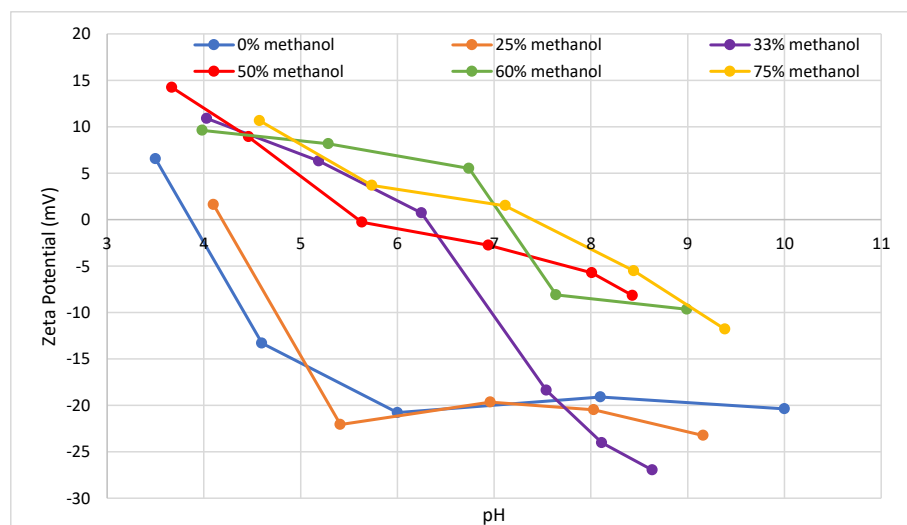
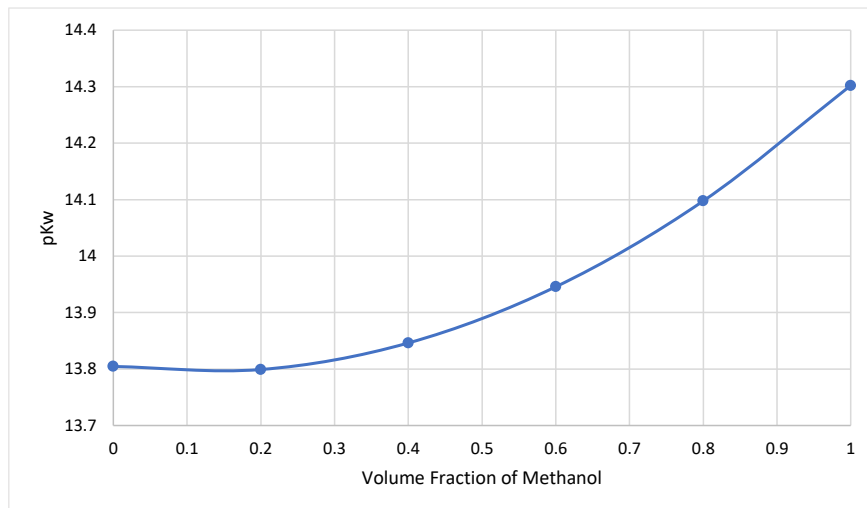


Figure 5.7 Zeta potential of Duramem 200 membrane using 1mmol/L NaCl in different methanol - water systems

#### Electrokinetic characterisation of OSN membranes



**Figure 5.8 Extrapolated  $pK_w$  as a function on methanol in water-methanol-NaCl tertiary systems**

#### 5.3.4 Zetasizer Measurements on Duramem 200

##### 5.3.4.1 Water Measurements

The Duramem 200 membrane was subjected to LDE experiments using both positively charged particles and negatively charged particles, see Figure 5.9. The results show that the LDE method of measuring zeta potential show good correlation with TSP measurements with both negatively and positively charged particles, suggesting that the positively charged particles are adsorbing onto the surface of the membrane when a voltage is passed across the face of the membrane. For this reason, when positively charged membranes are to be analysed using LDE measurements, the applied voltage should be low to minimise the adsorption of particles.

#### Electrokinetic characterisation of OSN membranes

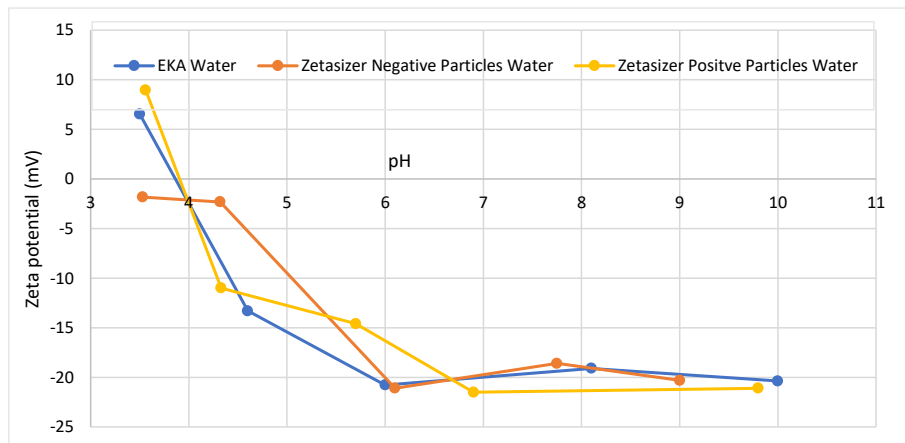


**Figure 5.9 Zeta potential of Duramen 200 in 1mmol/L NaCl (aq) by TSP and LDE measurements**

#### 5.3.4.2 Methanol – water measurements

When using LDE experiments to determine the zeta potential of the Duramen 200 membrane in methanol – water solutions, the LDE results gave inconsistent results, shown in Table 5-2, which shows the results of sequential LDE experiments. The phase vs time graphs give are little more than noise, and the originally positively charged particles are negatively charged in the presence of an organic solvent. From the results shown in Table 5-2, the method for using LDE measurements for analysis of membranes in organic solvents needs further development.

Run Number	Surface Zeta Potential (mV)	Tracer Zeta Potential (mV)	Tracer Mobility
1	0.699	-9.44	-0.3371
2	18.2	-6.78	-0.2421
3	-4.09	-11	-0.3925
4	-2.88	-10.9	-0.3882
5	7.3	-5.37	-0.1920

**Table 5-2 Zetasizer results of Duramen 200 in methanol - water solutions (3-1) using positive particles and 10mMol NaCl**

## 5.4 Conclusions

Application of LDE measurements for positively charged particles was successfully developed. The use of positively charged amidine particles for LDE experiments to determine the zeta potential of positively charged membranes which show good correlation to zeta potential measurements conducted through TSP

measurements. All measurements using LDE show good mobility backward regression ( $R^2 > 0.97$ ), while highlighting the limitations of LDE as a tool for measurement of membrane surface charge. Such limitations of using positively charged membranes are 1) the positively charged particles will adsorb onto the surface when a voltage is applied for measurements 2) when a lower voltage is used to accommodate the use of positively charged particles, the zetasizer loses resolution meaning that there can be more error in the LDE measurements. Based on the results, best practice for testing surface charge for unknown membranes is to use positively charged particles at neutral charge initially, as the particles will either be repelled by the membrane, if the membrane is positive, or adsorb onto the surface and give a negative result, if the membrane is negative. After this initial result, a judgement can then be made as to which charge of particles is needed to conduct successful LDE measurements.

Application for LDE measurements in organic solvents on an OSN membrane were unsuccessful, which could be due to several factors, such as the solvent dielectric constant, conductivity. The zeta sizer uses the solvents dielectric constant when interpreting the data, so the lower dielectric constant of methanol (34 at 20°C) will give a much weaker result as opposed to when water is the solvent (with a dielectric constant of 80 at 20°C (Toolbox, 2008)). Further testing of different organic solvents is needed to determine if the method is viable for zeta potential measurements of membranes in organic solvents. Analysis of initial LDE measurements of the Duramem 200 membrane suggest that the positive charge of the membrane appears to have been given by the aradite used to fix the membrane onto the instrument, so care is needed when selecting an appropriate adhesive..

TSP measurements of the Duramem 200 membrane show that the surface charge of the membrane changes with increasing solvent percentage, becoming more linear with methanol percentages of 50% and above. At 33% methanol, the membrane appears to be in transition, with a unique profile compared to the other methanol percentages tested. At methanol percentages of 25 and 0% i.e. water, the membrane is predominantly negatively charged and follows the plot follows the trend of other negatively charged membranes.

When comparing the surface zeta potential using the zetasizer, the machine shows good consistency when using water as the solvent, but not when alcohols are introduced. This is likely due to the lack of conductivity in the solution which the machine uses as to make zeta potential measurements. Further work is needed to develop a method for accurately determining the zeta potential of OSN membrane in solvents using this system, such as searching for charged particles that retain charge in organic solvents, and solvent with higher dielectric constants and/or conductivity. Testing of other commercial membranes in organic solvents should also be considered.

## 6. Investigation into of the separation mechanisms of OSN membranes

---

### 6.1 Introduction

As previously stated, there are currently 16 parameters that influence the rejection of a solute from an OSN membrane (Darvishmanesh, et al., 2010), which are stated in Table 2-2. Of these parameters, the process properties (cross-flow/dead-end filtration, operating pressure, temperature) are the only ones that can be controlled. Furthermore, some properties are interlinked such as viscosity and surface tension which are affected by the temperature. In a controlled system i.e. laboratory and pilot studies, the solute or solvent can be changed so that a greater understanding of how an OSN membrane rejects a given solute can be ascertained.

Systematic studies of OSN membrane rejection have been conducted previously analysing how the shape of a solute effects the retention/rejection (Zheng, et al., 2008), and the solute and solution properties affect retention properties (albeit in aqueous solutions) (López-Muñoz, et al., 2009). The mode of operation also effects the rejection properties as operating a dead-end filtration cell will lead to lower rejection of the solute and more fouling on the surface of the membrane, which is why correlations have been developed to account for this phenomenon (Oatley-Radcliffe, et al., 2015).

The aim of this study is to investigate the mechanisms by which an OSN membrane rejects a solute, which is to be conducted using the Duramem® 500 membrane and two dyes of near identical molecular weights (Safranin O and Methyl Orange) but are oppositely charged in both water and alcohols. The alcohols that will be used will be increasing in carbon content; methanol, ethanol, iso-propanol and butan-1-ol. The purpose of using this family of solvents is that the change in solvent properties (e.g. polarity, solubility, viscosity) tend to change with increasing carbon length, which should allow trends to be identified more easily.

### 6.2 Experimental procedure

#### 6.2.1 Dye rejection

A Sterlitech dead-end filtration cell was utilised in the manner described in section 3.4.1. The Duramem® 500 has a maximum operating pressure of 20 bar, which was utilised. The two dyes used were Safranin O and Orange II, each made up separately in the dissolved solvent at 100PPM. During operation, 100 mL of solution was emptied into the vessel, 9 mL of solution was permeated through the membrane in order to obtain flux data before 1mL of permeate was collected in a cuvette for absorbance analysis.



## 6.2.2 Zeta potential

An Electro-Kinetic Analyser (EKA) (Anton Paar GmbH, Graz, Austria) was used in the manner described in section 3.4.3. 1mM of NaCl was dissolved in water and water-methanol solutions for surface charge analysis. A solvent resistant pH probe (Jenway 924076) was used to measure the pH in alcohol – water solutions, and was calibrated in the method described by Gelsema, *et al* (1966). The buffer solution was mixed with methanol to give the desired volume %age of methanol before the probe was inserted into the container for calibration. The probe was left in the container until the voltage remained constant. This method, according to literature, is still an accurate measure of the pH in solvent systems as the theory determines that the dissociation occurs in water rather than alcohol, thus replacing the water with buffer will give an accurate reading for calibration.

## 6.3 Methanol – Water Solutions

### 6.3.1 Rejection and flux of charged dyes in methanol – water solutions

The rejection of Safranin O is 0.99 in water and decreases to 0.7 at 75% methanol, before increasing to 0.9 in 100% methanol, see Figure 6.1. The rejection of Orange II follows the same trend as Safranin O but is always lower (0.95 in water decreasing to 0.55 at 75% methanol), with the rejection increasing to 0.77 in 100% methanol. The permeate flux when Safranin O is the solute, the rejection is lower than when Orange II is the solute, except for 100% methanol, see Figure 6.2. The permeate flux of Safranin O is 100 L/m<sup>2</sup>h in water and decreases to 30 L/m<sup>2</sup>h in 50% methanol. The flux then increases to 45 L/m<sup>2</sup>h in 75% methanol before increasing drastically to 220 L/m<sup>2</sup>h in 100% methanol. The permeate flux of Orange II is 150 L/m<sup>2</sup>h in water and decreases to 48 L/m<sup>2</sup>h in 50% methanol. At 75% methanol, the flux increases to 145 L/m<sup>2</sup>h before increasing slightly again to 148 L/m<sup>2</sup>h in 100% methanol.

# Investigation into of the separation mechanisms of OSN membranes

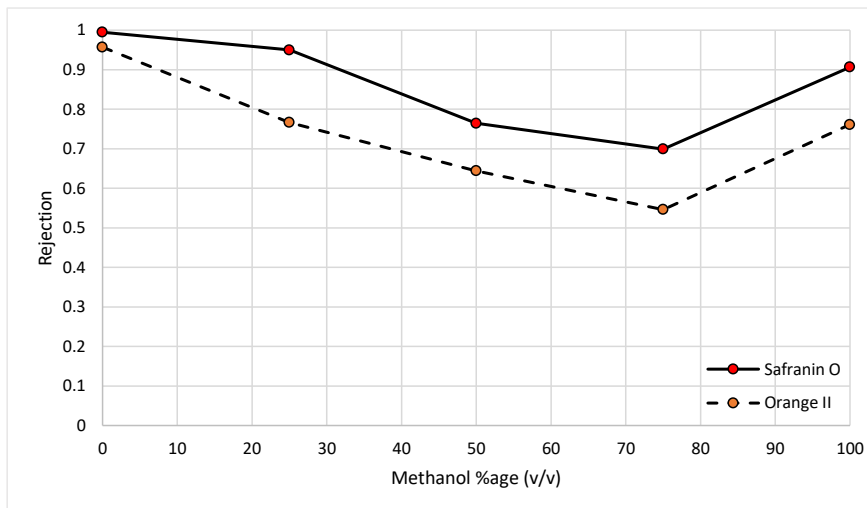


**Figure 6.1 Rejection of 100 PPM Safranin O and Orange II using the Duramem 500 membrane as a function of methanol content in solution**

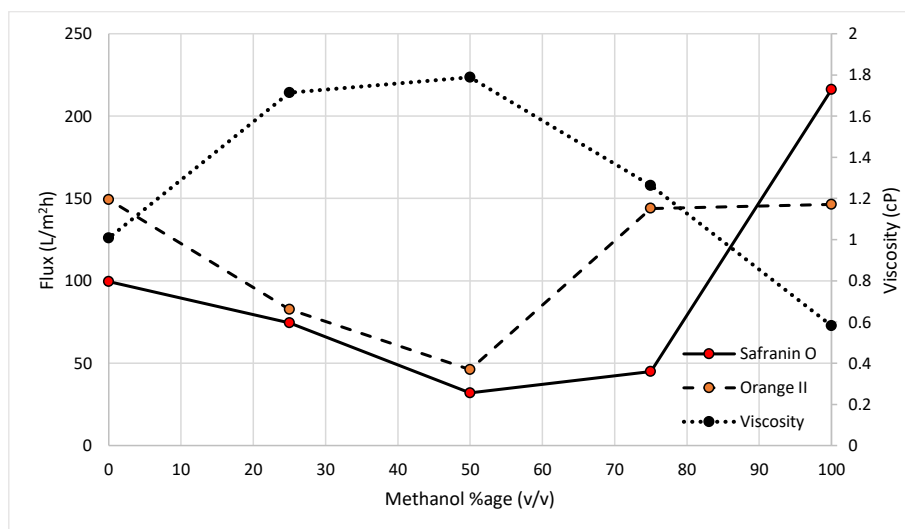


**Figure 6.2 Flux of 100 PPM Safranin O and Orange II using the Duramem 500 membrane as a function of methanol content in solution**

The rejection data of both dyes is shown in Figure 6.1 and is in good agreement with literature (Yao, et al., 2016) with higher rejection of Safranin O when compared to Orange II. While Yao, *et al* attributes this to the positively charged membranes, to some extent is true for their study (the higher rejection of Safranin O compared to Orange II), the solubility of the dyes (amongst other properties of the solvents) must be

considered. Safranin O is a solvent soluble dye while Orange II is a pH indicator for acidic aqueous conditions and becomes more difficult to dissolve as the methanol percentage increases, which would help to explain the lower rejection of Orange II when compared to Safranin O. The permeate flux of both dye solutions appear to be inversely proportional the viscosity of methanol – water mixtures, with the exception of Orange II in 100% methanol.

What is clear at this stage, is that while the 16 parameters defined by Darvishmanesh, *et al* (2010) all contribute to the membrane performance, some parameters (such as viscosity) have greater effects on flux rather than solute rejection and *vice versa*. Other parameters which may effect the flux and rejection performance of the Duramem 500, which are not taken into account by Darvishmanesh, *et al* (2010) such as membrane swelling are commonly reported to decrease the permeate flux, but are not recorded in this data set.

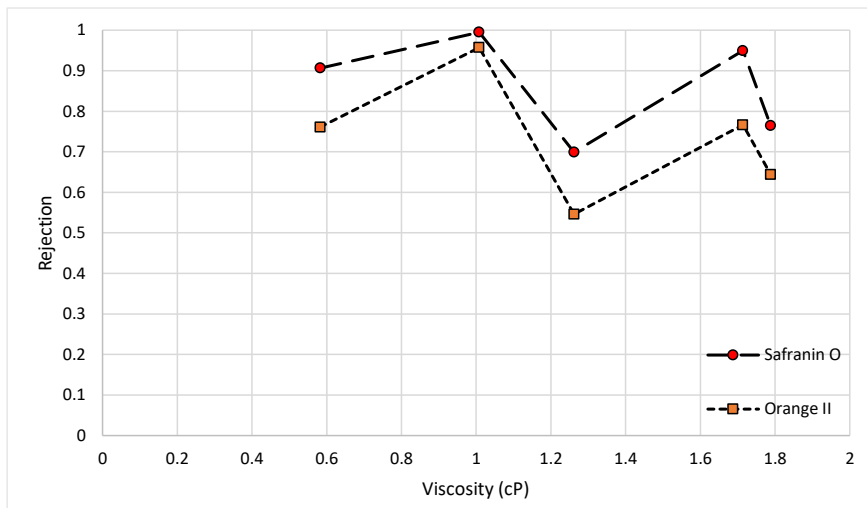
### 6.3.2 The role of viscosity of methanol – water solutions in membrane performance

The rejection of the dyes generally decrease with increasing solvent viscosity, with the rejection of Safranin O decreasing from 0.9 at 0.59 cP to 0.76 at 1.79cP and the rejection of Orange II decreases from 0.76 at 0.59 cP to 0.64 at 1.79 cP, see Figure 6.3. However, the rejection is not linear for either of the dyes tested indicating that the rejection is not directly proportional to the viscosity. The viscosity does appear to be proportional to the permeate flux, see Figure 6.4, where the permeate flux of Orange II decreases from 149 L/m<sup>2</sup>h at 0.59 cP to 49 L/m<sup>2</sup>h at 1.79 cP in a polynomial fashion, with the permeate flux of Safranin O decreasing from 216 L/m<sup>2</sup>h to 49 L/m<sup>2</sup>h at 1.26 cP before further decreasing to 46 L/m<sup>2</sup>h.

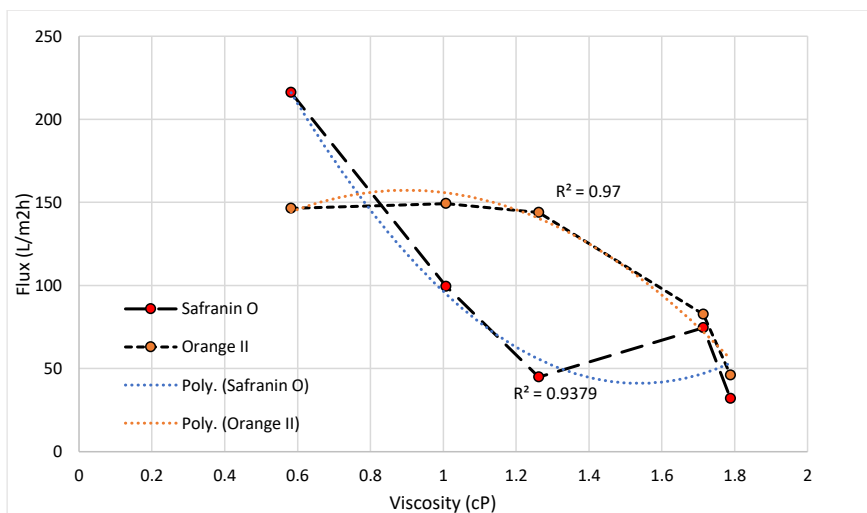
Methanol %age (v/v)	Viscosity (cP)
0	1.0079
25	1.71395
50	1.7884
75	1.26205
100	0.58224

Table 6-1 Viscosity of Methanol - Water Solutions (Mikhail & Kimel, 1961)

#### Investigation into of the separation mechanisms of OSN membranes



**Figure 6.3 Rejection of Safranin O and Orange II as a function of solution viscosity**



**Figure 6.4 Permeate flux of Safranin O and Orange II as a function of solution viscosity**

The fluctuation in the dye rejection suggests that viscosity has an effect on the rejection of the dye but other solvent parameters, still to be investigated, may have more effect the rejection. The viscosity appears to play a direct role in the permeate flux of the membrane, which is further reinforced by the general membrane equation. Interestingly, the two dyes have different permeate trends, with Orange II plateauing

to 1.26 cP before decreasing, with Safranin O decreasing to 1.26 cP before plateauing, suggesting that the permeate flux in solvent is not dictated by viscosity alone.

### 6.3.3 The role of Zeta Potential on membrane performance

The surface charge of the Duramem 500 membrane decreases with decreasing methanol content, see Figure 6.5, where the zeta potential of the Duramem 500 membrane decreases from -12mV in 99% methanol to -30.5mV in 100% water in a linear fashion. Coupling this with the data shown in Figure 6.1, the membrane becomes more positive (in this case, less negative) with increasing methanol content thus leading to the increased rejection of Safranin O when compared to the negatively charged Orange II dye.

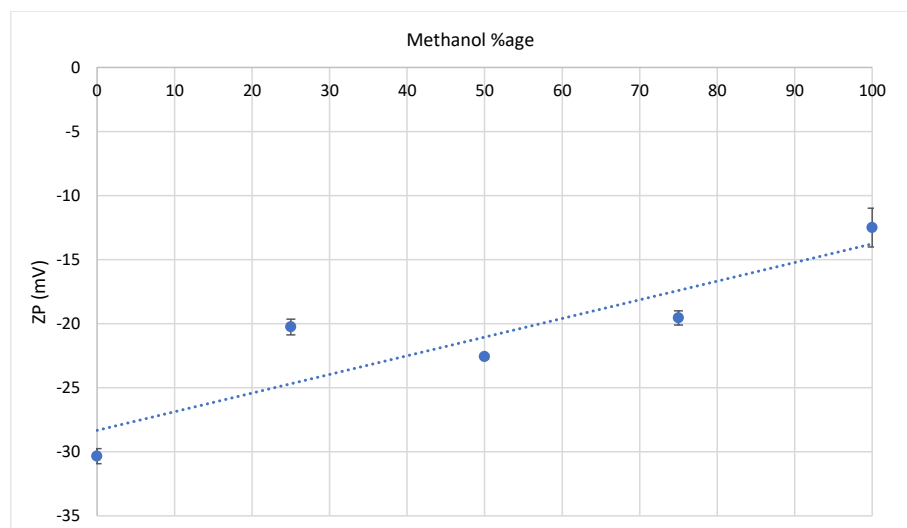


Figure 6.5 Duramem 500 surface zeta potential in 1mmol/L NaCl at neutral pH

The zeta potential of membranes in solvent systems has not been measured (to the best of the authors knowledge) which is normally attributed to the assumption that there is a lack of dissociation in solvents, which is why the zeta potential experiment is carried out in 99% methanol and not 100% methanol as calibration of the equipment would've been conducted using carboxylic acids.

The rejection of Safranin O decreases as the zeta potential becomes more positive, decreasing from 0.99 at -30.78 mV to 0.9 at -12 mV, with the lowest point occurring at -19.5 mV with a rejection of 0.7, see Figure 6.6. Orange II follows the same trend, decreasing from 0.96 at -30.78 mV to 0.76 at -12 mV, with the lowest rejection also occurring at -19.5 with a rejection of 0.55. The permeate flux of Safranin O increases in a polynomial fashion from 100 L/m<sup>2</sup>h at -30.78 mV to 216 L/m<sup>2</sup>h at -12.5 mV, see Figure 6.8. The permeate

# Investigation into of the separation mechanisms of OSN membranes

flux of Orange II is similar at zeta potentials of -30.78 and -12.5 mV with permeate fluxes of 149 and 146 L/m<sup>2</sup>h respectively, with the lowest flux occurring at -22.59 mV with a permeate flux of 46 L/m<sup>2</sup>h.

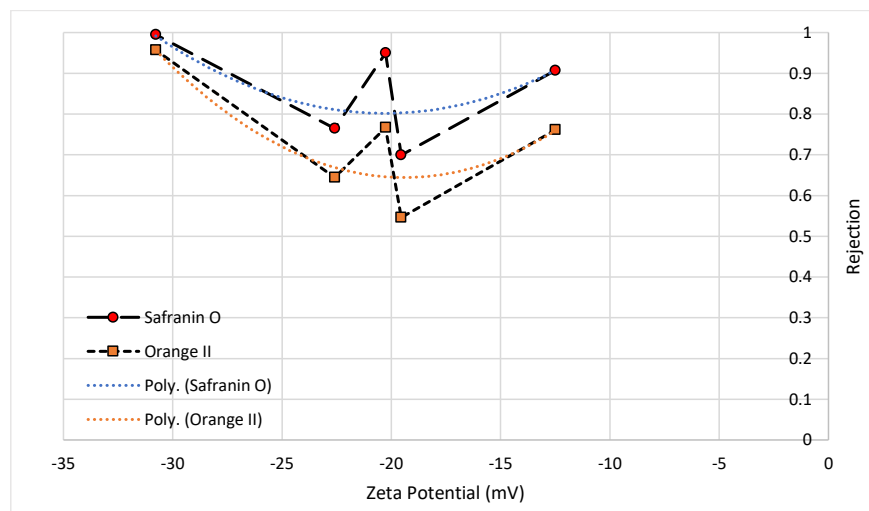


**Figure 6.6 Rejection of 100 PPM Safranin O and Orange II as a function of Zeta Potential**

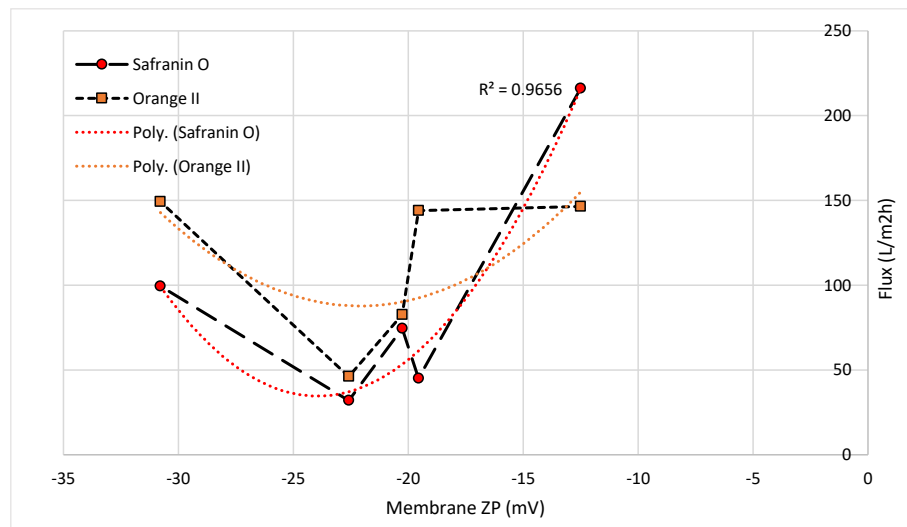


**Figure 6.7 100 PPM Safranin O and Orange II permeate flux as a function of ZP**

Both the permeate fluxes and rejections of both dye solutions follow polynomial trends, with the lowest values for both occurring at different values (-20.5mV for rejection and -22.59 mV for permeate flux), showing that donnan effects in OSN systems are minimal, resulting in the rejection mechanisms being due to steric effects.

#### 6.3.4 The role of surface tension on membrane performance

The rejection pattern of both dyes follow the same pattern with increasing surface tension, see Figure 6.8, where the rejection of Safranin O and Orange II is 0.9 and 0.76 at a surface tension of 22.95 mN/m (100% methanol) respectfully. The rejection then decreases to 0.7 and 0.55 in 75% methanol respectfully, before increasing with increasing surface tension with rejections of Safranin O and Orange II of 0.99 and 0.97 at a surface tension of 72.75 mN/m (100% water) respectfully.

The permeate flux of Safranin O is initially high at 216 L/m<sup>2</sup>h at a surface tension of 22.95 mN/m, see Figure 6.9, before decreasing to 32 L/m<sup>2</sup>h at 33.37 mN/m before increasing again to 99 L/m<sup>2</sup>h at 72.75 mN/m. Orange II follows a similar pattern with the permeate flux at 22.95 of 146 L/m<sup>2</sup>h before decreasing to 46 L/m<sup>2</sup>h at 33.37 mN/m. The permeate flux then increases to 82.6 and 150 L/m<sup>2</sup>h at surface tensions of 44.38 and 72.75 mN/m respectfully.

Methanol %age (v/v)	Surface tension (mN/m)
100	22.95
75	25.05
50	33.37
25	44.38
0	72.75

Table 6-2 Surface tension of methanol - water solutions (Vazquez, et al., 1995)

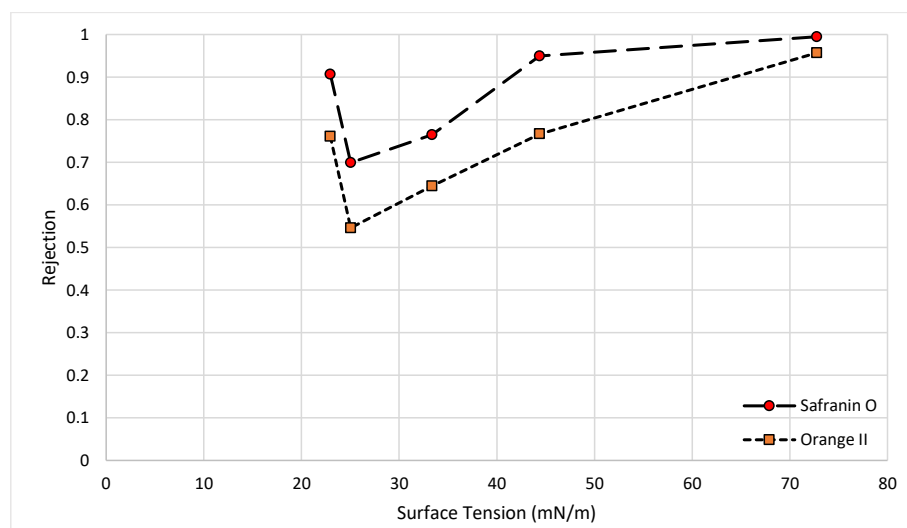
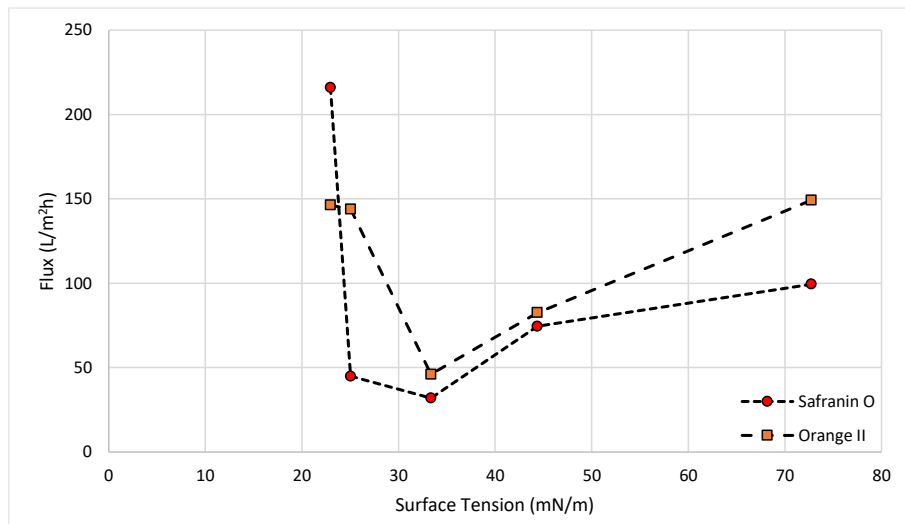


Figure 6.8 Rejection of Safranin O and Orange II as a function of solution surface tension



**Figure 6.9** Permeate flux of Safranin O and Orange II as a function of surface tension

The surface tension does not appear to play a direct impact on the flux or rejection of solutes in a solution, however, the dead-end vessel is being continuously stirred so this may play a part in the results. The low speed (300 RPM) and low height of the stirrer gives a laminar Reynolds number so it can be assumed that stirring plays a negligible effect.

Analysing the data for dye rejection in methanol – water solutions, we find that some solvent properties don't have a large enough impact to suggest that a given property dictates the rejection or flux of a membrane. The main determining factor, for methanol – water systems, appears to be viscosity, while the surface charge of the membrane does affect the rejection, however, this is not a new concept and is more applicable to aqueous systems due to the assumed lack of disassociation occurring in the system (Bellona & Drewes, 2005).

## 6.4 Single solvent systems

### 6.4.1 Rejection and flux of charged dyes in alcohols

The rejection and permeate flux of Safranin O decreases with increasing carbon length, see Figure 6.10 and Figure 6.11. The rejection of Safranin O decreases linearly with increasing carbon content, decreasing from 0.9 in methanol to 0.52 in pentanol. Orange II exhibits an unusual rejection behaviour where the rejection of this dye is lowest in ethanol (0.41) compared to 0.61 in isopropanol, 0.66 in butanol and 0.91 in pentanol. Interestingly, not all the Orange II dye dissolved in isopropanol or butanol despite being mixed for over 1 hour and the flask being sonicated, which would help confirm that solubility is a governing factor in solute rejection, however, all of the dye dissolved in pentanol.



#### Investigation into of the separation mechanisms of OSN membranes

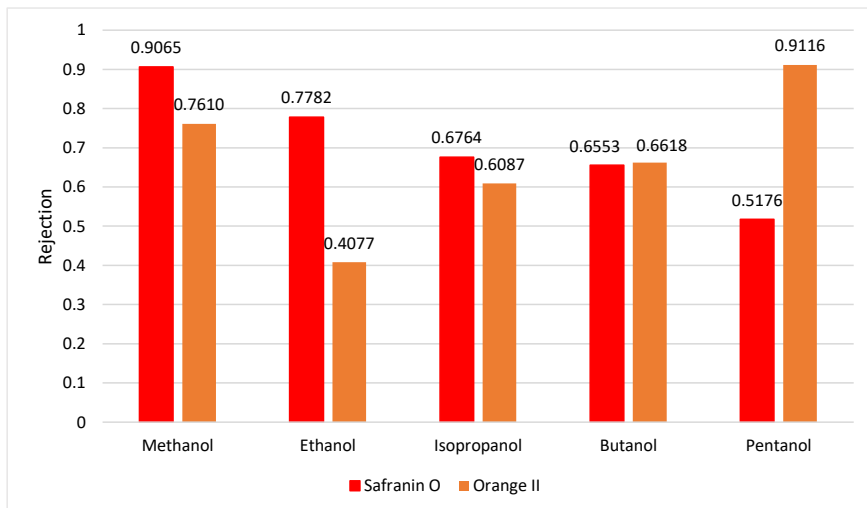


**Figure 6.10 Rejection of Safranin O and Orange II in alcohols of increasing carbons**

The permeate flux decreases drastically with increasing carbon content for both dyes, suggesting that the membrane is hydrophilic (Hosseinabadi, et al., 2014). The permeate flux of Safranin O in methanol is 216 L/m<sup>2</sup>h then decreases to 44 L/m<sup>2</sup>h in ethanol, see Figure 6.11. The permeate flux then begins to plateau with the flux in isopropanol, butanol and pentanol being 7.78, 5.76 and 1.9 L/m<sup>2</sup>h respectively. The permeate flux of Orange II halves from 146 in methanol to 77 L/m<sup>2</sup>h ethanol. The permeate flux then plateaus between isopropanol and butanol with permeate fluxes of 8.4 and 9.6 respectively, before decreasing further to 1.1 L/m<sup>2</sup>h in pentanol.

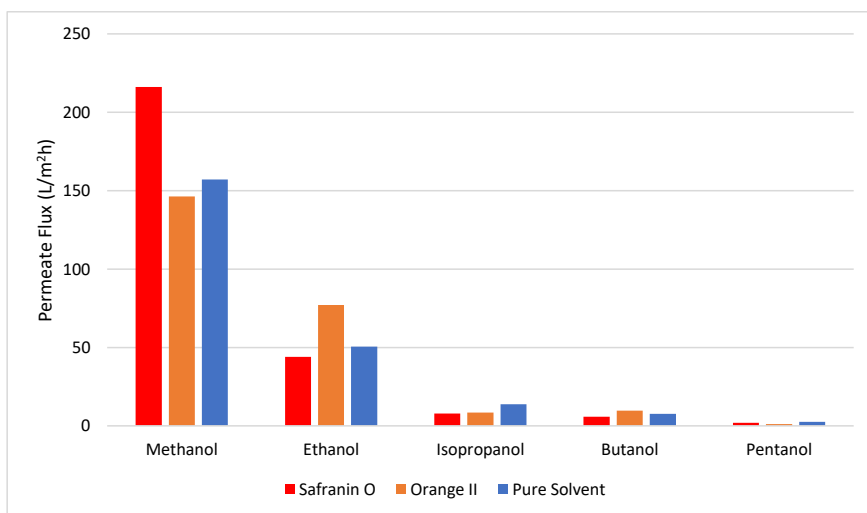


**Figure 6.11 Permeate flux of Safranin O and Orange II in alcohols and pure alcohols of increasing carbons**

Comparing the clean solvent permeate fluxes of methanol and ethanol with data published by Shi, *et al* (2019), see Figure 6.12, the lab data from this study shows significantly higher values when compared to the data published by Shi, *et al*, which may be due to the higher stirrer speed that was used in that study (1000 RPM) compared to the 300 RPM used in this study.

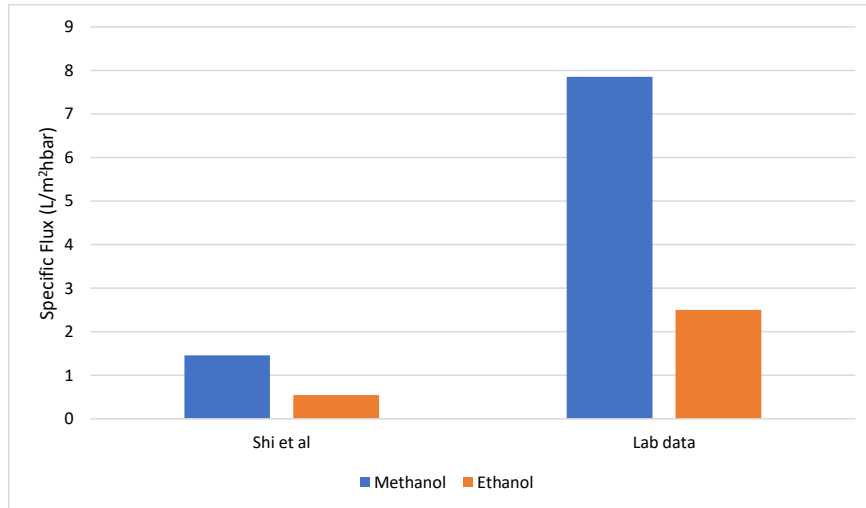


Figure 6.12 Comparison of clean solvent fluxes using the Duramem 500 membrane

#### 6.4.2 The role of solvent solubility on membrane performance

The solubility values used for this study are calculated using the Hansen Solubility Parameter software, with the values calculated shown in Table 6-3 and Table 6-4. The solubility value of the alcohols used decreases with increasing carbon chain length, shown with decreasing polarity energy ( $\delta P$ ) and hydrogen bonding energy ( $\delta H$ ).

Where:

$$\delta D = \frac{\text{Dispersive Cohesive Energy}}{\text{Molar Volume (Mvol)}}$$

$$\delta P = \frac{\text{Polarity Cohesive Energy}}{\text{Molar Volume (Mvol)}}$$

$$\delta H = \frac{\text{Hydrogen Bonding Cohesive Energy}}{\text{Molar Volume (Mvol)}}$$

$$HSP = \sqrt{\delta D^2 + \delta P^2 + \delta H^2}$$

$$Ra^2 = 4(\delta D_1 - \delta D_2)^2 + (\delta P_1 - \delta P_2)^2 + (\delta H_1 - \delta H_2)^2$$

$$RED = \frac{Ra}{Ro}$$

Where RED is calculated using the Hansen Solubility Parameter software based on how easily the dye dissolves in a solvent, as shown by the score (1 is easily dissolve and 4 is barely dissolves).

	$\delta D$	$\delta P$	$\delta H$	Mvol	HSP	Score	RED
	MPa <sup>0.5</sup>	MPa <sup>0.5</sup>	MPa <sup>0.5</sup>	Cm <sup>3</sup>	MPa <sup>0.5</sup>		
Safranin O	20.1	4.2	7.2				
Methanol	14.7	12.3	22.3	40.6	29.41	1	0.994
Ethanol	15.8	8.8	19.4	58.6	26.52	2	0.338
Isopropanol	15.8	6.1	16.4	76.9	23.58	2	0.98
Butanol	16	5.7	15.8	92	23.2	3	1.16
Pentanol	15.9	5.9	13.9	108.6	21.93	4	1.448

**Table 6-3 Hansen Solubility Parameters of Safranin O and Alcohols**

	$\delta D$	$\delta P$	$\delta H$	Mvol	HSP	Score	RED
	MPa <sup>0.5</sup>	MPa <sup>0.5</sup>	MPa <sup>0.5</sup>	Cm <sup>3</sup>	MPa <sup>0.5</sup>		
Orange II	21.9	10.5	16.3				
Methanol	14.7	12.3	22.3	40.6	29.41	1	0.735
Ethanol	15.8	8.8	19.4	58.6	26.52	2	0.99
Isopropanol	15.8	6.1	16.4	76.9	23.58	3	1.299
Butanol	16	5.7	15.8	92	23.2	3	1.358
Pentanol	15.9	5.9	13.9	108.6	21.93	4	1.497

**Table 6-4 Hansen Solubility Parameters of Orange II and Alcohols**

The rejection of Safranin O increases linearly with increasing solvent solubility, see Figure 6.13, increasing from 0.52 to 0.91 at solubility range of 21.93 to 29.41 MPa<sup>0.5</sup> respectfully. The rejection of Orange II decreases from 0.91 to 0.4 at a solubility range of 21.93 to 26.52 MPa<sup>0.5</sup> before increasing again to 0.76 at 21.93 MPa<sup>0.5</sup>. The permeate flux of Safranin O increases exponentially from 1.9 L/m<sup>2</sup>h at 21.93 MPa<sup>0.5</sup> to 216 L/m<sup>2</sup>h at 29.41 MPa<sup>0.5</sup>. The permeate flux of Orange II increases slightly from 1.1 to 8.4 L/m<sup>2</sup>h between 21.93 to 23.58 MPa<sup>0.5</sup> respectfully, then the permeate flux then increases linearly to 146 L/m<sup>2</sup>h at 29.41 MPa<sup>0.5</sup>.

#### Investigation into of the separation mechanisms of OSN membranes

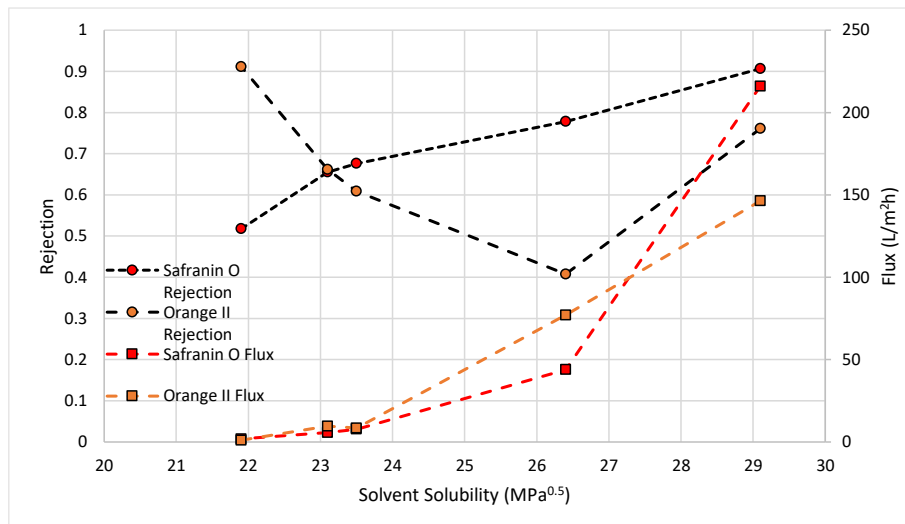


**Figure 6.13 Rejection and permeate flux of 100 PPM charged dyes as a function of solvent solubility**

Solubility has been used as a metric for rejection by Darvishmanesh, *et al* (2011) looking at dye rejection in methanol and ethanol using the Duramem 150, NF-270 and the DK membranes. The authors had mixed results depending on the solubility calculations used, meaning that when considering models for OSN systems, care is needed to determine that the right parameters are being used.

#### 6.4.3 The role of solvent polarity on membrane performance

As the carbon chain increases the polarity value of the solvent decreases, see Table 6-5, which is also reflected in the Hansen Solubility Parameters, see Table 6-3 and Table 6-4 ( $\delta_P$ ). As the carbon chain becomes longer, and the hydroxyl group moves further down the carbon train, the solvent becomes more oil like in its properties, where the electronegativity from the oxygen molecule is further away from the opposite end, effectively creating polar and non-polar ends (Reichardt & Welton, 2010).

Solvent	Polarity (kcal/mol)
Methanol	55.4
Ethanol	51.9
Isopropanol	48.4
Butanol	49.7
Pentanol	49.1

**Table 6-5 Polarity of solvents studied (Reichardt & Welton, 2010)**

### Investigation into of the separation mechanisms of OSN membranes

The rejection of Safranin O is generally linear, increasing from 0.68 at 48.4 kcal/mol to 0.9 at 55.4 kcal/mol. Orange II shows mixed rejection values, fluctuating between 0.91 at 49.1 kcal/mol and 0.75 at 55.4 kcal/mol. The permeate flux of Safranin O and Orange II both increase in a polynomial fashion from 1.9 and 1.1 L/m<sup>2</sup>h at 48.4 kcal/mol to 216 and 146 L/m<sup>2</sup>h at 55.4 kcal/mol respectively.

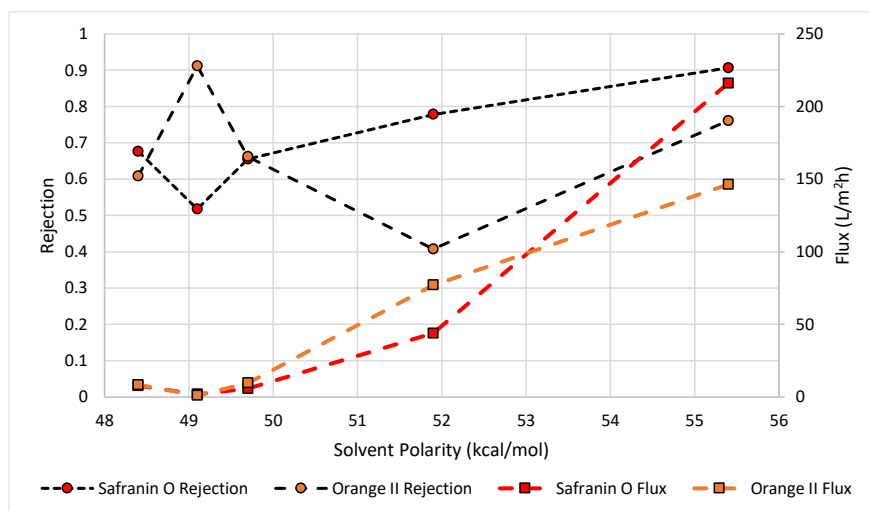


**Figure 6.14 100 PPM charged dye flux and rejection as a function of solvent polarity**

The inconsistent rejection of Orange II and linear profile of Safranin O suggests that the polarity of the dye, in the form of dipole moment, rather than the polarity of the solvent is a factor in the rejection of a dye, a phenomenon also illustrated by Darvishmanesh, *et al* (2011). The authors suggest that the longer chain solvents allow the solute to align inline to the solvent molecule due to the decreased polarity, which allows for easier passage through the membrane, shown in Figure 6.14.

There is a direct correlation between the solvent's solubility and the polarity of the solvent, this then is likely due to the hydroxyl group moving further down the carbon chain, creating one polar end and one non-polar end (Reichardt & Welton, 2010).

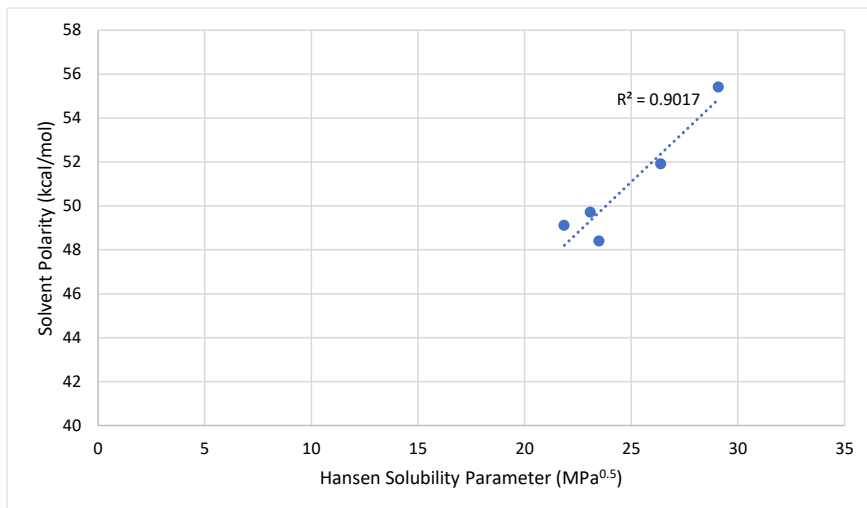


Figure 6.15 Solvent Solubility as a function of solvent polarity

#### 6.4.4 The role of solvent molar volume on membrane performance

The molar volume (the volume that 1 mole of solvent occupies) increases with increasing molecular weight, which corresponds to the decreasing permeate flux of both dyes. As with other comparisons the permeate flux decreases in a power law fashion for both Safranin O and Orange II, decreasing from 216 and 149 L/m<sup>2</sup>h at 42.5 cm<sup>3</sup> to 1.9 and 1.1 L/m<sup>2</sup>h at 108.5 cm<sup>3</sup>, see Figure 6.16. The rejection of Safranin O decreases in a linear fashion from 0.91 at 42.5 cm<sup>3</sup> to 0.52 at 108.5 cm<sup>3</sup>, while the rejection of Orange II decreases from 0.76 to 0.41 at molar volumes of 42.5 to 59 cm<sup>3</sup> respectively, then the rejection then increases 0.91 at 108.5 cm<sup>3</sup>. This phenomenon is likely a combination of all a solvent's parameters playing a part, but the effect is more prevalent when data is plotted against molar volume and solvation energy, section 6.4.5. Referring to a study by Thiermeyera, *et al* (2018), the authors found that the hydrogen bonding capacity of the solvent influences the rejection of a given solute, along with the solute properties also, eluded to in Figure 6.15.

Solvent	Molar Volume cm <sup>3</sup>
Methanol	42.5
Ethanol	59
Isopropanol	75.9
Butanol	92
Pentanol	108.5

Table 6-6 Solvent molar volume from Marvin Sketch program

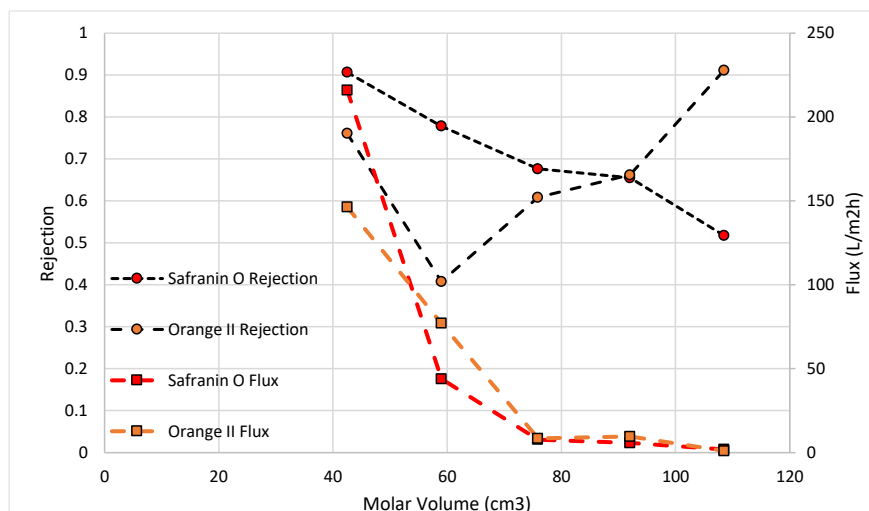


Figure 6.16 100 PPM charged dye flux and rejection as a function of solvent molar volume

#### 6.4.5 The role of solvent solvation energy on membrane performance

The rejection of Safranin O decreases linearly with increasing solvation energy, see Table 6-7 and Figure 6.17, where the rejection decreases from 0.91 at -5.05 kJ/mol to 0.52 at 12.79 kJ/mol. The rejection of Orange II decreases from 0.76 at -5.05 kJ/mol to 0.4 at -0.42 kJ/mol before increasing to 0.91 at 12.79 kJ/mol. The permeate flux of Safranin O decreases in a power law fashion from 246 L/m²h at -5.05 to 1.9 L/m²h at 12.79 kJ/mol. The permeate flux of Orange II decreases from 146 L/m²h at -5.05 kJ/mol to 1.1 L/m²h at 12.79 kJ/mol

The role of solvation energy appears to give an indication for the precipitation issues of Orange II in the larger solvents. As Orange II has an oxygen-sodium ion which dissociate in solution creating a polar  $O^-$  side and a  $Na^+$  ion. As the solvent length becomes longer, there is less polarity due to less dissociation which leads to increased electro-stability across the molecule. This leads to the increase in solvation energy of the solvent (Table 6-7) and means that there is less charge for dipole attraction leading to the precipitation. This seems to be evident with the decreased rejection of the dye in ethanol, with a possible different solute transport method for IPA and BtOH, as hypothesised in section 6.4.4. With regards to Safranin O, the dye is constructed of carbon-carbon bonds and carbon-nitrogen bonds, meaning that dye is dissolved and dispersed by solvation as opposed to hydrogen bonding as seen with Orange II.

#### Investigation into of the separation mechanisms of OSN membranes

Solvent	Solvation Energy kJ/mol
Methanol	-5.05
Ethanol	-0.42
Isopropanol	3.64
Butanol	6.02
Pentanol	12.79

Table 6-7 Solvation energy of solvents provided by Marvin Sketch

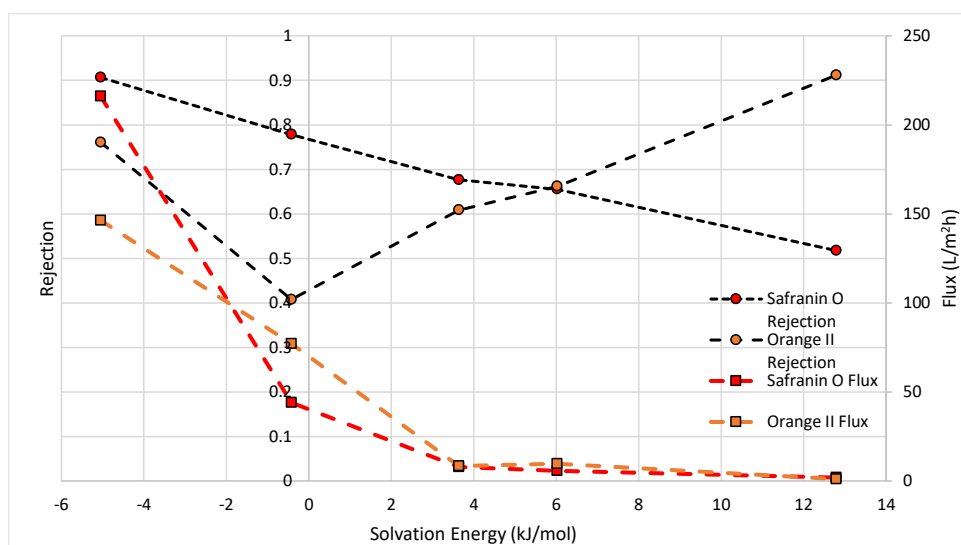


Figure 6.17 100 PPM charged dye flux and rejection as a function of solvent solvation energy

#### 6.4.6 The role of solvent viscosity and its effect on membrane performance

The rejection of Safranin O decreases linearly with increasing viscosity, see Figure 6.18, decreasing from 0.91 to 0.52 over a viscosity range of 0.6 to 3.8 cP. The rejection of Orange II decreases from 0.76 to 0.41 over a viscosity range of 0.6 to 1.25 cP, before increasing to 0.91 at 3.8 cP. The permeate flux of Safranin O decreases exponentially from 216 to 1.9 L/m²h over the viscosity range of 0.6 to 3.8 cP. Similarly, the permeate flux of Orange II decreases from 149 to 1.1 L/m²h over the same viscosity range.



#### Investigation into of the separation mechanisms of OSN membranes

Solvent	Viscosity (cP)
Methanol	0.60565
Ethanol	1.25425
Isopropanol	2.319351
Butanol	3.020696
Pentanol	3.8278

**Table 6-8 Solvent viscosity at experiment temperature**

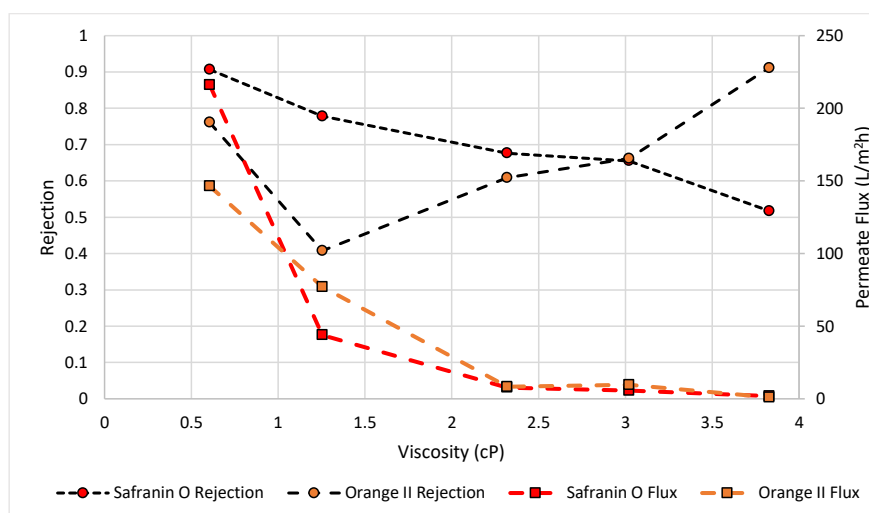


**Figure 6.18 100 PPM charged dye flux and rejections as a function of solvent viscosity**

The viscosity of the solvents decreases with increasing carbon length, see Table 6-8, with the solvent length effecting other properties e.g. polarity (see Table 6-5). The increase in viscosity leads to rapidly declining viscosity, which is shown in the general membrane equation. To the best of the authors knowledge, the study of a solvent's viscosity and membrane performance in solvent systems has been conducted in no other studies aside from Darvishmanesh, *et al* (2010).

#### 6.4.7 The role of membrane swelling and its effect on membrane performance

The swelling factor generally increases with increasing carbon length, see Table 6-9, and subsequently the solvent volume fraction inside the membrane, decreasing from 0.283 to 0.359 in methanol to pentanol respectfully after a 24 - hour period of submersion, however, ethanol demonstrates the lowest mount of swelling with a solvent volume fraction of 0.447.

# Investigation into of the separation mechanisms of OSN membranes

Solvent	Swelling Factor	Swelling Degree	Solvent Volume Fraction
Methanol	1.395	0.395	0.283
Ethanol	1.807	0.807	0.447
Isopropanol	1.391	0.391	0.281
Butanol	1.510	0.510	0.338
Pentanol	1.561	0.561	0.359

**Table 6-9 Swelling properties of Duramem 500 in alcohols**

Where:

$$\text{Swelling Degree} = \text{Swelling Factor} - 1 = \frac{\text{mass}_{\text{swollen}}}{\text{mass}_{\text{dry}}} - 1$$

$$\text{Solvent Volume Fraction} = 1 - \frac{1}{\text{Solvent Factor}} \quad (\text{Kappert, et al., 2019})$$

The rejection of Safranin O show no tangible pattern with respect to solvent volume fraction, see Figure 6.19, with the rejection of the dye at a solvent volume fraction of 0.281 being 0.68, and a rejection of 0.78 at a solvent volume fraction of 0.447. A similar pattern can be observed in Orange II, where the rejection increases from 0.6 to 0.91 over a solvent volume fraction range of 0.281 to 0.36 respectively, before decreasing to 0.41 at a solvent volume fraction of 0.447. The permeate flux of Safranin O shows little consistency with regards to solvent volume fraction, increasing from 7.78 to 216 L/m<sup>2</sup>h over a solvent volume range of 0.281 to 0.283, then decreasing to 5.76 L/m<sup>2</sup>h at a solvent volume fraction of 0.33 respectively. Orange II also shows a similar pattern with the permeate flux increasing from 8.4 to 146 L/m<sup>2</sup>h over a solvent volume fraction range of 0.281 to 0.283 then decreasing to 9.64 L/m<sup>2</sup>h at a solvent volume fraction of 0.33 respectively.

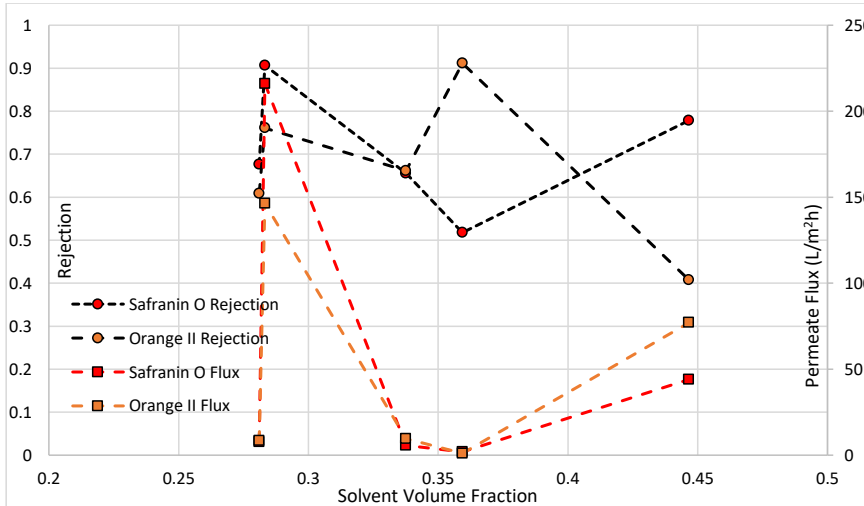


**Figure 6.19 100 PPM charged dye rejection and permeate flux as a function of free volume fraction**

## Investigation into of the separation mechanisms of OSN membranes

The free volume fraction decreases with increasing carbon chain length, which in turn leads to decreasing polarity. As the membrane appears to be hydrophilic in nature, the membrane is less likely to absorb the solvents as the polarity decreases. Membrane swelling is commonly investigated in solvent systems, where the proportion of swelling can be used as an indicator of solvent compatibility (Yang, et al., 2001). The Duramem 500 appears to show little swelling in alcohols, and the lack of consistency regarding the rejection and permeate flux with respect to the solvent free volume suggests that the membrane performance is not dependent on the swelling of the membrane, in this case.

### 6.4.8 The role of solvation and its effect on solute size and membrane performance

Using a free program called MarvinSketch, the radius of the solvents and Safranin O used were calculated, see Table 6-10. The radius of Safranin O dissolved in each solvent is also calculated at both the minimum and maximum projection radii respectively. Safranin O is calculated solely as Orange II dissolves more sparingly with increasing carbon length, while Safranin O dissolved easily in all of the alcohols tested. The rejection of Safranin O is plotted against the solute projection radius and is shown in Figure 6.20. Generally the rejection of the dye increases with increasing solute radius, increasing from 0.51 to 0.91 over a solute radius range of 136.12 to 370.08 respectively. The rejection is plotted against the maximum solute radius in Figure 6.21 where the rejection shows a good linear trend with solute radius.

Solvent	Solvent Radius (Å)		Solute Radius (Å)		Rejection
	Min	Max	Min	Max	
Dry	-	-	6.41	6.9	-
Methanol	2.16	2.62	436.48	370.08	0.9065
Ethanol	2.37	3.23	406.28	286.77	0.7782
Isopropanol	2.95	3.36	323.81	270.48	0.6764
Butanol	2.62	4.52	370.08	162.68	0.6552
Pentanol	2.62	5.17	370.08	136.12	0.5179

**Table 6-10 Solvent and solute atomic radii calculated by MarvinSketch program**

### Investigation into of the separation mechanisms of OSN membranes

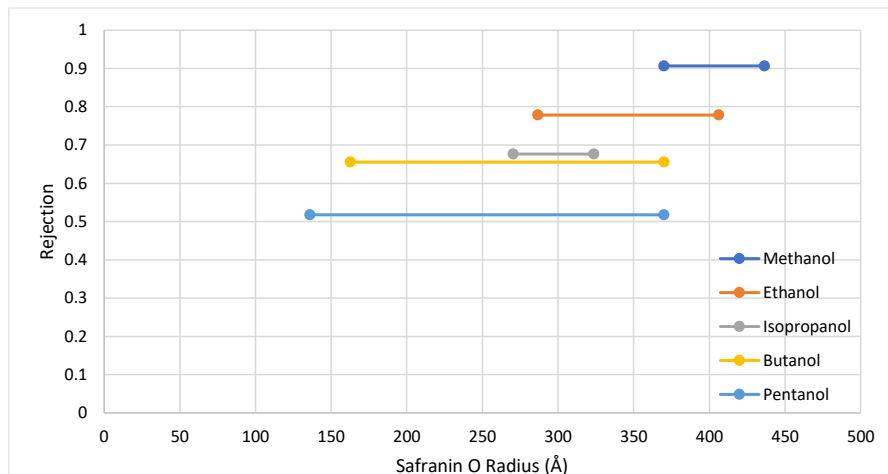


**Figure 6.20 Safranin O rejection as a function of solute solvation radius**

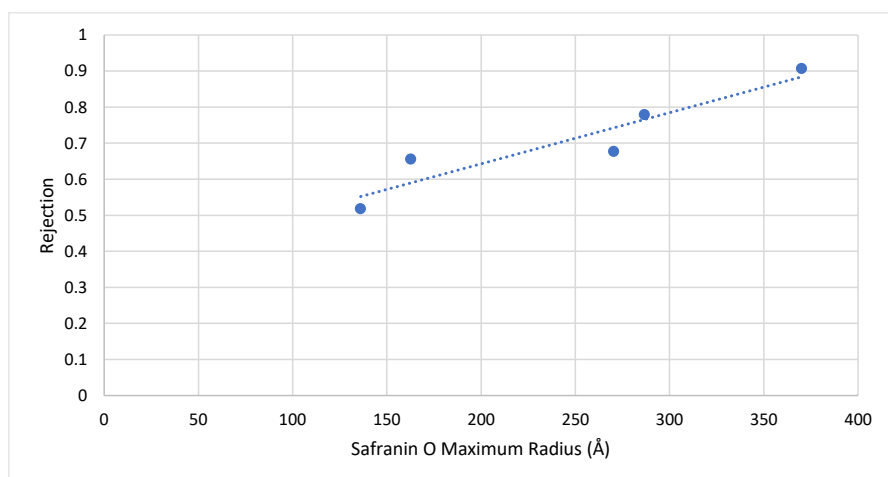


**Figure 6.21 Safranin O rejection as a function of the maximum solvation radius**

The increased size of Safranin O due to solvation highlights the importance of membrane – solvent – solute selection. Using the Marvin Sketch software, the solvation of a solute in a solvent can be calculated quickly, suggesting how the solute will reject in the solvent of choice. The program does not take into account a solute's solubility in a solvent so solubility and filtration experiments are required, thus the programme can be used a tool for prediction and analysis only.

#### 6.4.9 Dimensionless correlations of data

Comparing dye rejection and permeate flux rates with dimensionless correlations, which have been calculated in Table 6-11, shows that the Reynold's number of the system has more of an effect on the permeate flux than the rejection, as the permeate flux increases linearly with increasing Reynold's number, see Figure 6.22. The permeate flux of Safranin O increases from 1.9 to 216 L/m<sup>2</sup>h when the Reynold's number increases from 1.088 to 6.651 respectively, with the permeate flux of Orange II increasing from 1.1 to 146 L/m<sup>2</sup>h over the same range. This trend is to be expected as in the general membrane equation, the flux is a function of the reciprocal of the viscosity ( $J = A/\mu$ ) so the Reynold's number should be effected in the same fashion. The Reynold's number of each solvent system is laminar, and there is great difficulty in increasing the turbulence in the system while preventing vortexing from occurring in the cell.

The rejection of Safranin O shows a logarithmic trend with increasing Reynolds number in the system, Figure 6.22. As the Reynolds number is a function of the viscosity, there is no surprise that there is a similar trends of rejection and flux data in Figure 6.18 and Figure 6.22, with permeate flux being governed by a power law. The rejection of orange II show little observable trend, with the exception of similar rejection values between Reynolds number of 1-2. The rejection of safranin o is decreasing with increasing Schmidt number, Figure 6.23, indicating that the rejection of the dye is more reliant on viscous forces rather than diffusive forces, with the plateauing of the flux with increasing Schmidt number, which is in agreement with Figure 6.22. The opposite is true for Orange II, with the rejection increasing, after a Schmidt value of 3, with increasing Schmidt number. As this dye was less soluble in alcohols of carbons >3 (giving a higher RED value (**Error! Reference source not found.**)), the diffusivity of the solution decreases, which then leads to increasing rejection (Figure 6.23). The low Sherwood number of each solution (Figure 6.24) is indicative of low porosity of the membranes and suggests that rejection is based on diffusion rates of the dyes. However, the swelling of the membrane is increasing with increasing Sherwood number, as the channel length is increasing with membrane swelling, which leads to the increase in Sherwood Number.

Solvent	Reynolds Number (Re)	Diffusivity (di) m <sup>2</sup> /sec	Schmidt Number (Sc)	Péclet Number (Pe)	Mass Transfer Coefficient (k) (m/s)	Sherwood Number (Sh)
Methanol	6.651	0.000971	0.793	5.273	0.038781	0.134176
Ethanol	3.193	0.000559	2.87	9.164	0.029209	0.082577
Isopropanol	1.719	0.000311	9.571	16.457	0.02163	0.050615
Butanol	1.337	0.00023	16.676	22.289	0.018513	0.039705
Pentanol	1.088	0.000202	23.296	25.35	0.01733	0.035267

Table 6-11 Dimensionless correlations of dye rejections in alcohol

Where;

$$Re = \frac{\rho \cdot n \cdot d^2}{\mu}$$

Equation 6.1

$$Sc = \frac{\mu \cdot di}{\rho}$$

Equation 6.2

$$Pe = Re * Sc$$

Equation 6.3

$$Sh = \frac{k \cdot r}{D_i}$$

Equation 6.4

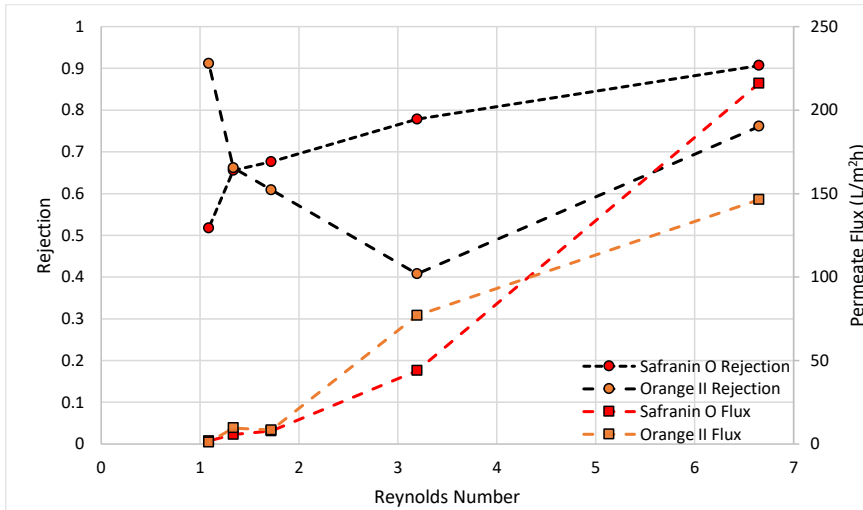
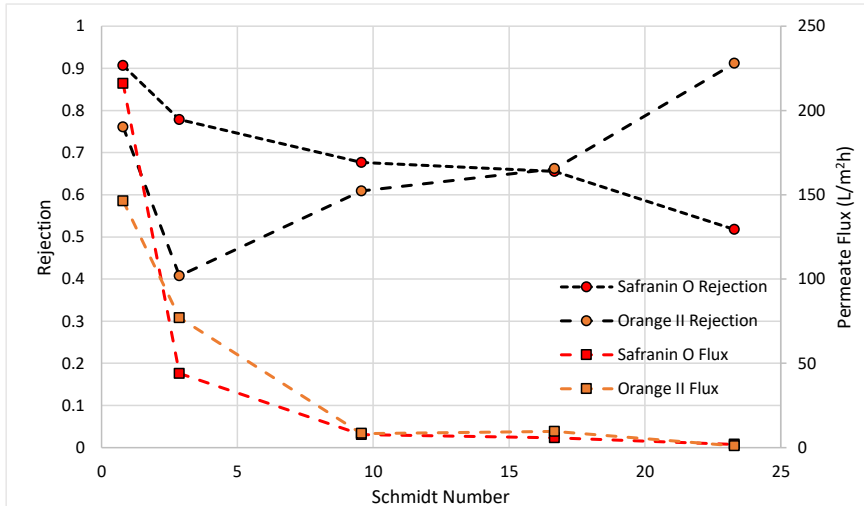


Figure 6.22 Dye rejection and permeate flux as a function of Reynolds number of the experimental system

The rejection of Safranin O decreases with increasing Schmidt number, see Figure 6.23, decreasing from 0.91 to 0.52 over a Schmidt Number range of 0.793 to 23.296 respectively. The rejection of Orange II increases with increasing Schmidt Number, increasing from 0.78 to 0.91 over a range of 0.793 to 23.296 respectively. The decreasing rejection of Safranin O with increasing Schmidt Number suggests that the rejection is more dependent on viscous forces rather than diffusive forces, while the rejection of Orange II is the opposite.



**Figure 6.23 Dye rejection and permeate flux as a function of Schmidt number of the experimental system**

The rejection of Safranin O increases with increasing Sherwood Number from 0.51 to 0.91 over a Sherwood Number range of 0.05 to 0.13. The rejection of Orange II decreases from 0.91 to 0.41 over a range 0.05 to 0.083, before increasing to 0.9 at 0.136 respectively. The increasing rejection of Safranin O with increasing Sherwood Number, suggesting that the rejection becomes dependant on convection mechanisms rather than diffusion mechanisms, which coincides with the data shown in Figure 6.20. The increasing permeate flux with increasing Sherwood Number also coincides with this, as the Sherwood Number typically decreases with increasing carbon length.

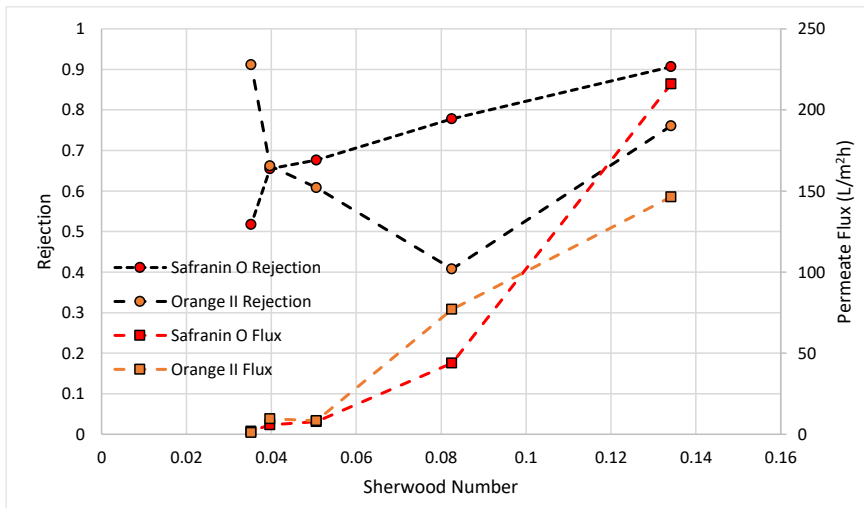


**Figure 6.24 Dye rejection and permeate flux as a function of Sherwood number of the experimental system**

## 6.5 Conclusions

The effect of changing solvent conditions on membrane performance was investigated. When considering methanol – water systems, the rejection of both dyes decreases with increasing methanol content but with higher rejection in methanol. The permeate flux of safranin O solution is lower than orange II solution is consistently lower in for aqueous and methanol – aqueous systems but safranin O flux was significantly higher than orange II in methanol. Based on Figure 6.2, the membrane flux appears to be directly related to the viscosity of the solution. The solute rejection appears to be related to several factors such as solubility, surface tension and zeta potential.

The zeta potential of the membrane in methanol – water appears to generally decrease with increasing water content, which to most likely due to the hydrogen dissociation occurring more readily in water molecules than methanol molecules. With increasing magnitude of charge, there is a trend for increasing rejection but the not much correlation with regards to flux.

For single solvent systems, the viscosity of the systems plays a part in the permeate flux of the system, but other factors must be taken into consideration such as solute solubility, solvent polarity and solvent molar volume. With regards to solute rejection, the solute solubility which is in turn linked the polarity, appears to be the main contributing factor along with molecule molar volume. The solute solvation based on the solvent used must be taken into account as this will affect the rejection of the solute along with membrane swelling. Furthermore, free software is available to predict the behaviour of the solute in solvent which can be used for modelling of a system and predict the average pore size of the membrane.



## 7. Modification of polyethersulfone (PES) membranes for improved OSN performance

---

### 7.1 Introduction

When considering OSN as a means of filtration, the chemical compatibility of the polymer and any modification chemicals used for the membrane must be considered. While most polymers used for aqueous systems will operate in solvent systems, the solvent may cause swelling or damage to the membrane (Tarleton, et al., 2006) (Kappert, et al., 2019). To minimise degree of swelling or damage, more robust polymers are being used for OSN such as modified Polyimide (PI) e.g. P84 Lenzig®, PDMS and PES. These polymers typically have little branching and have an inorganic substance within the polymer to help with them become more robust e.g. silicon in PDMS and sulphur in PES. The use of PES membranes for filtration of acids and hazardous materials has been well documented, and manufacturers of commercially available PES NF membranes (Mircodyn Nadir®) have claimed an operational pH of 0-14 (Sterlitech, 2018) (Torkabad, et al., 2017) (Werner, et al., 2018). While there is scope then to expand PES membranes into OSN membranes, there is little in the way of publications for this use, however, there are were publications into methods of modifying PES membranes (Ahmad, et al., 2013).

There are multiple ways to modify a polymeric membrane, such as plasma grafting, crosslinking and SIM modification to name a few (Volkova, et al., 2015) (Vanherck, et al., 2010). For this study, the method of modification are standard crosslinking (submerged in crosslinking bath for pre-set amount of time), additive crosslinking (addition of crosslinking agent, additive or co-polymer in in dope solution), SIM modification (crosslinking agent in the water bath during phase inversion) and flux crosslinking (crosslinking agent permeated through the membrane until permeate flux is stable) (Holda & Vankelecom, 2014) (Holda & Vankelecom, 2014) (Reddy, et al., 2003) (Vanherck, et al., 2010). The use of additive modification for polysulfone membranes have been conducted by Holda & Vankelecom (2014) using a wide range of small and large additives blended with the polysulfone, each influencing the flux and rejection of Rose Bengal dye. Due to the chemical robustness of PES as a membrane, additive modification appears to be a suitable method for modification. Similarly with SIM modification method, where the crosslinking agent is dissolved in the water bath used for phase inversion of the membrane. While the SIM method has only been published for polyimide at present, there is then scope for this method to be used successfully for PES membranes. In principal, the flux and 'POST' (as dubbed by Vanherck, *et al* (2010)) modification methods are identical, with the only exception being that the crosslinking agent is forced through the pores of the membrane, ensuring that all of the surface area and pores are modified, whereas during the normal crosslinking ('POST') there may be some air bubbles or hydrostatic forces which could prevent some crosslinking.

## Modification of polyethersulfone (PES) membranes for improved OSN performance

There is a wide range of molecules available on the commercial market which can be used as crosslinking of polymeric membranes, which typically have non-carbon group (e.g. hydroxyl or amine) at either end to allow for crosslinking to occur, but this is not always the case (Vanherck, et al., 2010) (Holda & Vankelecom, 2014) (Wang, et al., 2015). For the crosslinking to occur, a charge may need to be induced on the membrane, typically through submersion into an acid or base, depending on the inherent surface charge of the membrane but this is not always necessary. The chemical composition of the crosslinking agent will affect the surface charge of the membrane with crosslinking occurring on an hydroxyl group producing a negative charge, while crosslink bonding occurring on a amine or sulphur bond yielding a positive charge (Wang, et al., 2015) (Yao, et al., 2016).

## 7.2 Experimental Methods

Experimental methods are detailed in section 3.6

### 7.2.1 Dye Rejection

Dye rejection methodology is detail in section 3.4.1, where the solute used in this study is Rose Bengal dye (Sigma Aldrich, UK) dissolved in isopropanol (Honeywell, UK) was used for dye rejection at a concentration of 50  $\mu\text{Mol/L}$ . A pressure of 20 bar was used for experiments with the additive modification membranes and 40 bar was used for surface/ SIM/ Flux modification membranes. Membranes were conditioned by permeating 50 mL of isopropanol at the operating pressure before rejection experiments took place. Analysis of the dye feed and permeate was carried out on a Shimadzu UVmini-1240 UV-VIS Spectrophotometer at a wavelength of 520.5nm. Each rejection experiment was conducted twice, and the average result is shown.

### 7.2.2 Zeta Potential

Zeta potential measurements are carried out using the method described in section 3.4.3 using NaCl (aq) at a concentration of 1mMol/L.

### 7.2.3 Fourier Transform Infra-Red Spectroscopy (FTIR)

FTIR measurements were conducted using a Perkin-Elmer Spectrum Two FT-IR Spectrometer (Seer Green, UK). Membrane samples were cut into 1cm<sup>2</sup> squares and air dried for 24 hours. Samples were then placed into the machine and held onto the lens using a pressure of  $\approx$  120 PSI.

## 7.3 Results

### 7.3.1 Additive Modification

#### 7.3.1.1 Methanol

When methanol is used as an additive, the dye rejection initially decreases from 0.81 to 0.6 at no modification and 5% additive respectively, see Figure 7.1, before increasing and plateauing at 0.78 at 10, 15 and 20% additive. The permeate flux increases from 3.78 to 77.09 L/m<sup>2</sup>h over the range of 0 – 15% additive respectively, before decreasing to 27.7 L/m<sup>2</sup>h at 20% additive.

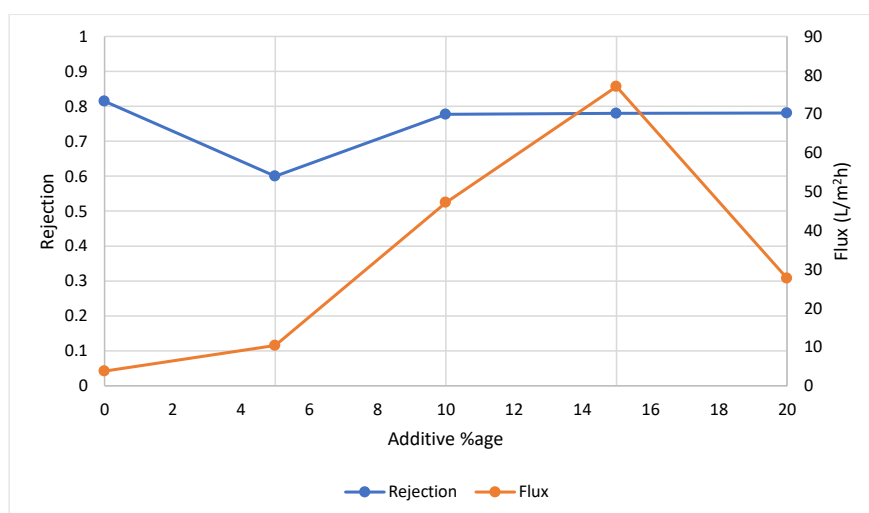


**Figure 7.1 Effect of methanol as an additive on membrane performance**

Using methanol as an additive significantly increases the permeate flux while giving yielding comparable levels of rejection of Rose Bengal dye. 5% methanol decreases the rejection of the dye, suggesting that additive hinders the crosslinking during phase inversion. There is also a significant decrease in permeate flux between 15 and 20% additive with no change to dye rejection, this indicates that the flux may still increase with additive percentage between 15 and 20%, and that at 20% additive, there is an indication that there is more crosslinking inside the membrane hindering the permeate flux. The consistent dye rejection suggests that the additive does not affect the surface pore size of the membrane but does affect the crosslinking within the membrane. These results suggest that the addition of methanol into the dope solution between 5 and 15 wt% will yield increased permeate flux while yielding similar results to unmodified PES membrane.

## 7.3.1.2 Ethanol

The use of ethanol as an additive show mixed results with regards to both dye rejection and permeate flux, see Figure 7.2, where the dye rejection decreases from 0.81 to 0.52 between 0 and 5% additive before increasing to 0.86 at 10% additive and decreasing to 0.7 and returning to 0.8 at 15 and 20% additive respectively. The permeate flux increases from 3.78 to 121 L/m<sup>2</sup>h over a range of 0 to 10% additive respectively. The permeate flux then decreases to 83 L/m<sup>2</sup>h at 15% additive and then increases to 103 L/m<sup>2</sup>h at 20% additive.

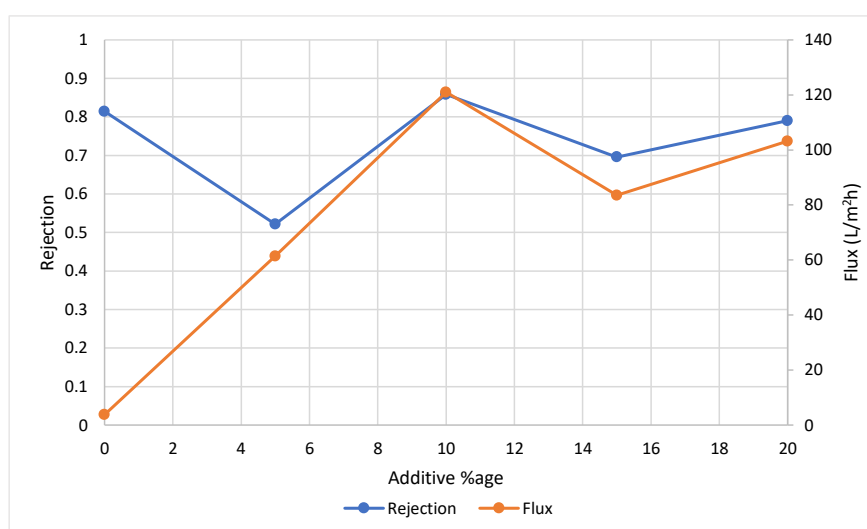


**Figure 7.2 Effect of ethanol as an additive on membrane performance**

The permeate flux increases with the addition of ethanol as an additive, yielding higher permeate flux rates than methanol with comparable dye rejection, see Figure 7.1. Similarly to methanol, the dye rejection decreases at 5% additive while the permeate flux increases, suggesting that at 5 wt% the additive hinders crosslinking during phase inversion. While the dye rejection between 10 and 20% ethanol as an additive is not constant when compared to methanol, the rejection fluctuates around  $0.78 \pm 0.07$  which means that the results are comparable. The results shown in Figure 7.2 suggests that using between 5 and 20 wt% ethanol as an additive will yield further increased permeate flux rates while yielding comparable rejection data to unmodified PES membranes and methanol doped PES membranes.

### 7.3.1.3 Isopropanol

The addition of isopropanol as an additive initially decreases the rejection of Rose Bengal from 0.81 to 0.66 over an additive percentage range of 0 – 5% respectively, see Figure 7.3. The dye rejection then increases to 0.81 over the range of 5 – 20% additive respectively. The permeate flux increases from 3.78 L/m<sup>2</sup>h at no additive to 11.47 L/m<sup>2</sup>h at 5% additive, before further increasing to 93 L/m<sup>2</sup>h at 10 wt% additive. The permeate flux then decreases to 69 L/m<sup>2</sup>h at 15% additive before increasing to 98 L/m<sup>2</sup>h at 20% additive.

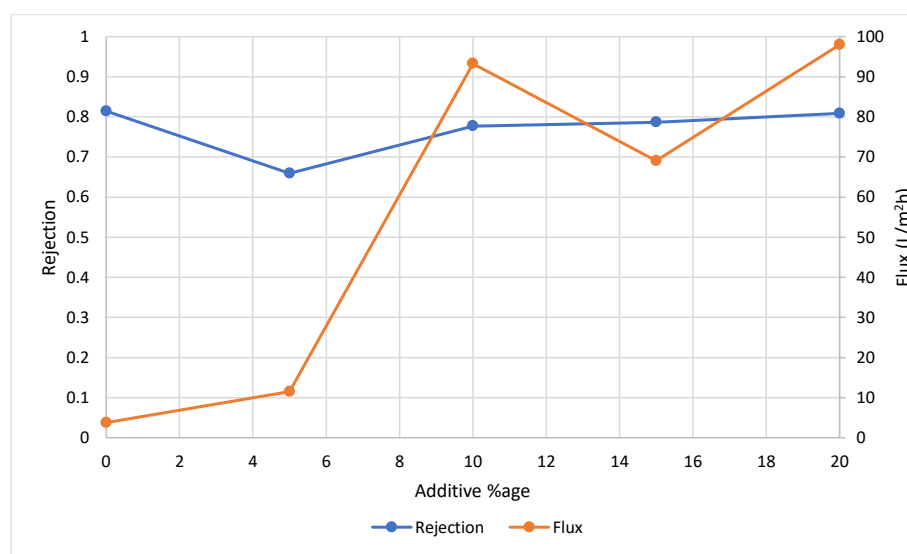


**Figure 7.3 Effect of isopropanol as an additive on membrane performance**

Isopropanol as an additive appears to show more consistency with regards to dye rejection compared to ethanol as an additive. This may be due to mixing in the dope solution, no all air being removed during degassing or casting conditions rather than PES solubility. Never the less, isopropanol addition shows consistent levels of rejection when compared to methanol and ethanol addition, but with lower permeate flux when compared to ethanol, at but higher permeate flux than methanol addition.

### 7.3.1.4 N-butanol

The rejection of Rose Bengal dye initially decreases with the addition of 5% butanol, decreasing from 0.81 to 0.72, see Figure 7.4. The dye rejection then increases to 0.74 at 10% butanol then at 0.74 at 15% butanol, before further increasing to 0.89 at 20% butanol. The permeate flux increases from 3.78 L/m<sup>2</sup>h at no additive to 54 and 66 L/m<sup>2</sup>h at 5 and 10% butanol respectively. The permeate flux then decreases 44 L/m<sup>2</sup>h at 15% before significantly increasing to 142 L/m<sup>2</sup>h at 20% additive.

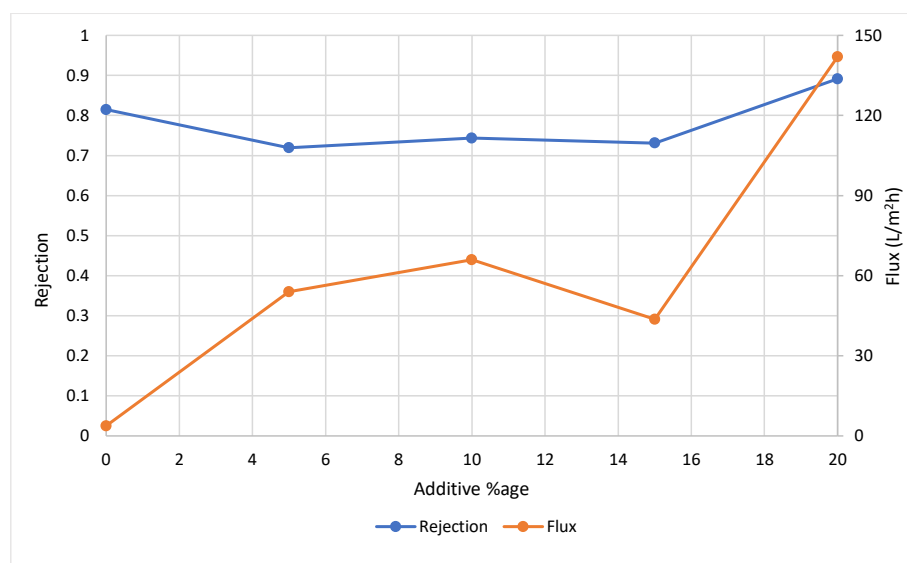


**Figure 7.4 Effect of n-butanol as an additive on membrane performance**

Butanol as an additive appears to be not as effective for improving the membrane properties with regards to rejection between the ranges of 5 – 15% when compared to the other alcohols tested in this study. This maybe due to the increased size of the butanol molecule allowing for larger pores and channels in the membrane. At 20% the permeate flux significantly increases to 142 L/m<sup>2</sup>h suggesting that this percentage of butanol drastically hinders the crosslinking process. 25% butanol was tested but the PES powder would not dissolve in the NMP – butanol solution, forming a spherical shape, couple this with the results at 20% butanol, a suggestion can be made that the PES powder is close to the solubility limit at 20%, hence the larger permeate flux.

### 7.3.2 Surface Modification

#### 7.3.2.1 HDA Crosslinking

Using Hexane Diamine (HDA) as a crosslinking agent shows a slight decline in rejection of Rose Bengal, decreasing from 0.63 to 0.52 over a crosslinking range of 0 – 5% respectively, see Figure 7.5. The dye rejection then increases to 0.58 and 0.6 over the range of 5 – 10% crosslinking agent respectively. The permeate flux decreases from 30.4 L/m<sup>2</sup>h at no crosslinking agent to 10 L/m<sup>2</sup>h at 2.5% crosslinking agent. The permeate flux then increases to 16 L/m<sup>2</sup>h before decreasing slightly to 13.35 L/m<sup>2</sup>h over a range of 5 – 10 % crosslinking agent.

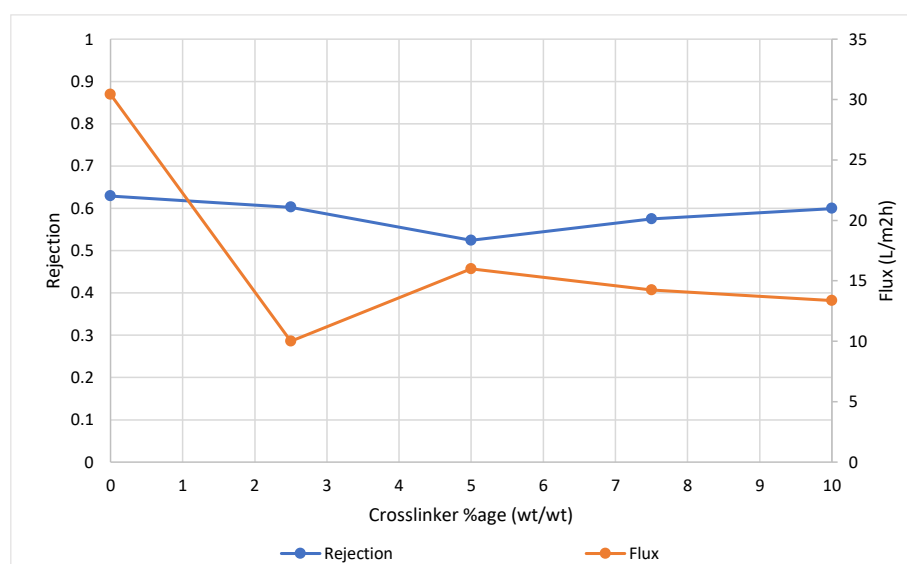


**Figure 7.5 Flux and rejection of RB in IPA as a function of HDA percentage**

The use of HDA as a crosslinking agent decreases the rejection of Rose Bengal and the permeate flux. This would then suggest that there is little steric rejection of this dye through this membrane. The decrease in permeate flux would suggest that the crosslinking agent is in fact decreasing the pore size on the surface of the membrane, which leads to the suggestion that there is little steric rejection of the dye. Hexane diamine modification is likely to make the PES membrane positively charged, due to the NH crosslinking bonds (which is to be explored later in this study if this hypothesis is correct). If the HDA crosslinked is shown to be positively charged, this would then explain the decreased rejection of Rose Bengal of crosslinked and uncross linked membranes.

### 7.3.2.2 PEG 200 Crosslinking

Using PEG 200 as a crosslinking agent slightly decreases the rejection of Rose Bengal from 0.63 to 0.62 at 2.5% crosslinking agent, see Figure 7.6. The rejection then increases from 0.62 to 0.82 over a crosslinking percentage range of 2.5 to 10% respectively. The increase in solute rejection, leads to decreased permeate flux, decreasing from 30.4 L/m<sup>2</sup>h to 15.8 L/m<sup>2</sup>h at 2.5% crosslinking agent. The permeate flux then generally plateaus and fluctuates between 13 and 16 L/m<sup>2</sup>h over a crosslinking percentage range of 2.5 – 10%.

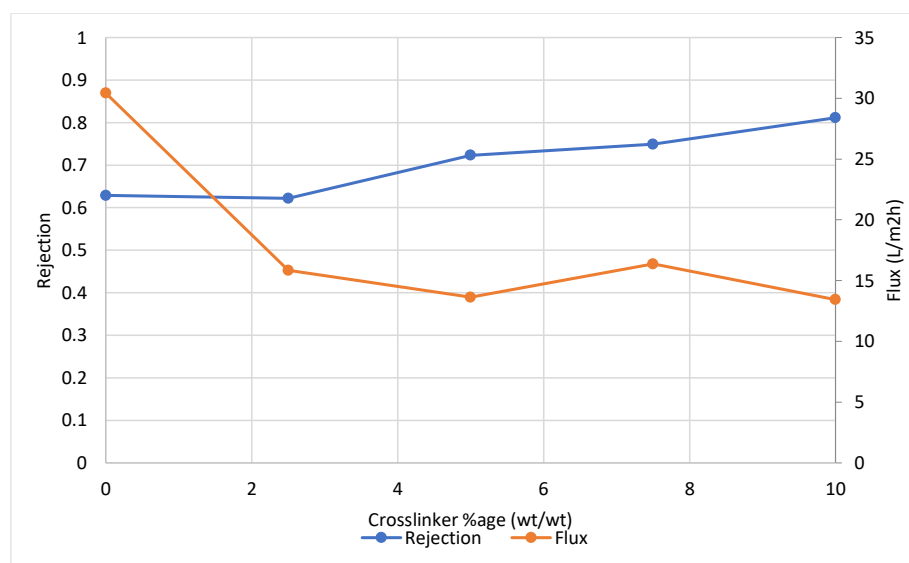


**Figure 7.6 Flux and rejection of RB in IPA as a function of PEG 200 percentage**

The use of PEG 200 as a crosslinking shows a significant improvement in permeate rejection when compared to HDA (Figure 7.5), where the dye rejection does not improve with increasing crosslinking concentration. The permeate flux of both crosslinking agents are comparable, thus suggesting that the rejection of the dye by the crosslinking agent is not by size exclusion. As Rose Bengal dye is negatively charged, the surface charge of the membrane may be affecting the rejection of the dye, thus this should be investigated.



### 7.3.3 Zeta Potential

The surface charge of PES is negative between pH 9.4, where the zeta potential is -13.6 mV, before becoming increasing in positivity slightly to -5.3 mV at pH 8, see Figure 7.7. The surface charge then generally remains the same (within experimental error) to pH 4.8 (zeta potential = -8.3 mV) before becoming positively charge at pH 3 with a zeta potential of 8.63 mV, with the isoelectric point occurring around pH 3.9. The zeta potential of HDA modified PES membrane is positively charged between the pH range of 3.4 to pH 6.85, decreasing from a surface charge of 30.42 mV to 12.67 mV respectfully. The membrane then becomes negatively charged with a zeta potential of -22.46 mV at pH 8.6, with the isoelectric point occurring around pH 7.5. PEG 200 modification has the opposite effect on the surface charge of PES membranes, where the membrane is negatively charged with a zeta potential measurement of -226.4 to -29.5 mV over a pH range of 4.9 to 8.3 respectfully. The membrane is then slightly positively charge at pH 3.3 with a zeta potential measurement of 0.71, with the isoelectric range occurring at pH 3.5.

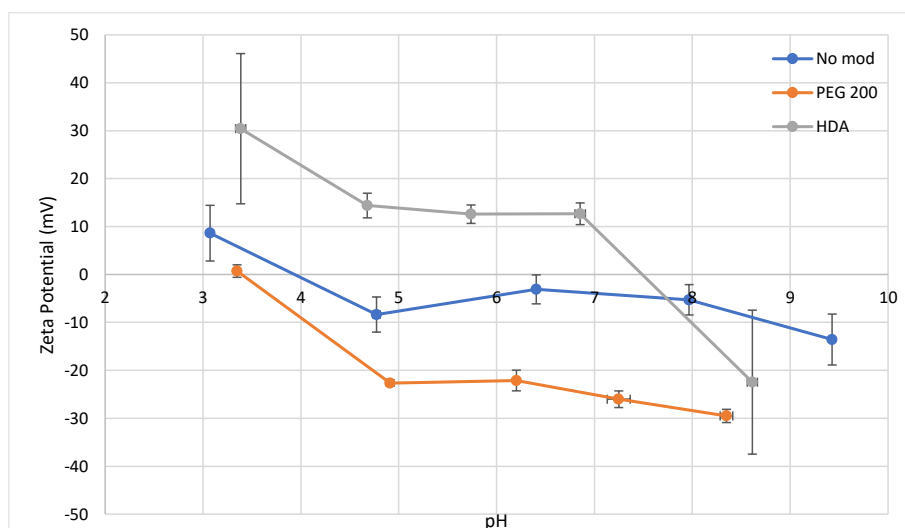


**Figure 7.7 Zeta potential of modified and unmodified PES membrane as a function of pH using 10 wt% crosslinking agents**

The two crosslinking agents used alter the surface charge of PES membranes in opposite ways, which can go some way into difference in rejection properties. The rejection of the negatively charged Rose Bengal is higher in PEG 200 modified PES membranes when compared to HDA modified membranes, which suggests that the same electromagnetic charge of both the solute and membrane is leading to the increased rejection when compared to unmodified membrane. There is further evidence of this when comparing the permeate flux rates of the two crosslinking agents, where the permeate flux of both are comparable with significantly differing rejection profiles.

### 7.3.4 FTIR

Peaks between  $3000\text{--}2800\text{ cm}^{-1}$  indicate N-H stretching, with the peak height increasing with HDA concentration, with the peaks of 10% being lower than the others, Figure 7.8. the peaks between  $3000\text{--}2800\text{ cm}^{-1}$  are missing on the unmodified membrane. The small peak between  $2175\text{--}2140\text{ cm}^{-1}$  is indicative of S-C≡N bond stretching. Also, there is an absorbance between  $1300\text{--}1350\text{ cm}^{-1}$  which is indicative of S=O bond, suggesting that the crosslinking agent is attaching to the benzene ring as opposed to the oxygen.

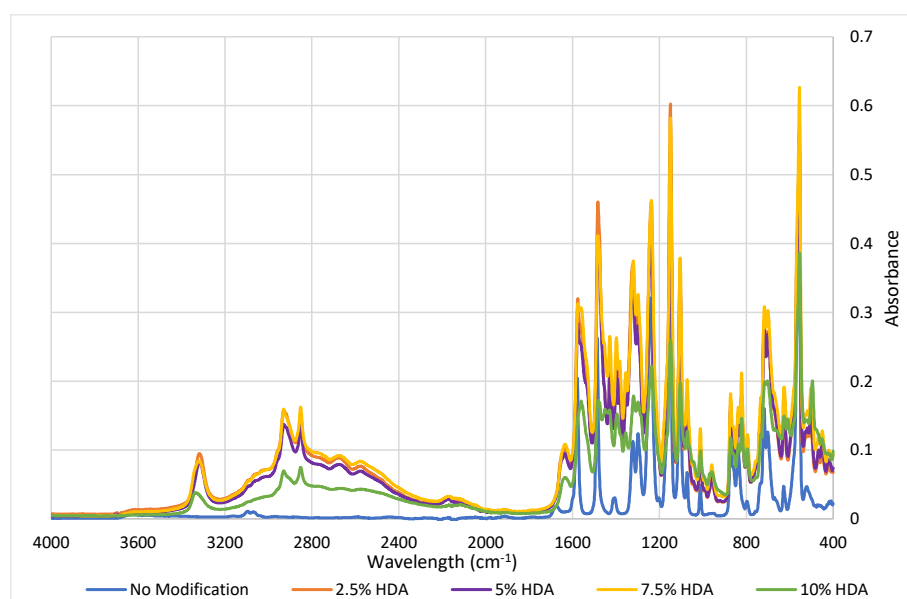


**Figure 7.8 FTIR of PES membranes using HDA as a crosslinker at increasing weight percentages**

The broad peak between  $2700\text{--}3000\text{ cm}^{-1}$  is indicative of stretching of O-H alcohol bonds, which suggests that the PEGs have attached to the membrane, Figure 7.9. furthermore, the peak between  $1050\text{--}1080\text{ cm}^{-1}$  is also indicative of an O-H alcohol bond. The unmodified membrane has a larger peak at  $1120\text{--}1165\text{ cm}^{-1}$  which is a S=O sulfone bond, which would suggest that the PEG is attaching to the oxygen group during modification as opposed to the cyclic ring which the HDA appears to bind to. Furthermore, there is a peak between  $1372\text{--}1355\text{ cm}^{-1}$  on the PEG modified membrane (which is absent on the unmodified) which is usually for sulfonate bonding, also indicating that the PEG is bonding on the S=O after NaOH modification.

### Modification of polyethersulfone (PES) membranes for improved OSN performance

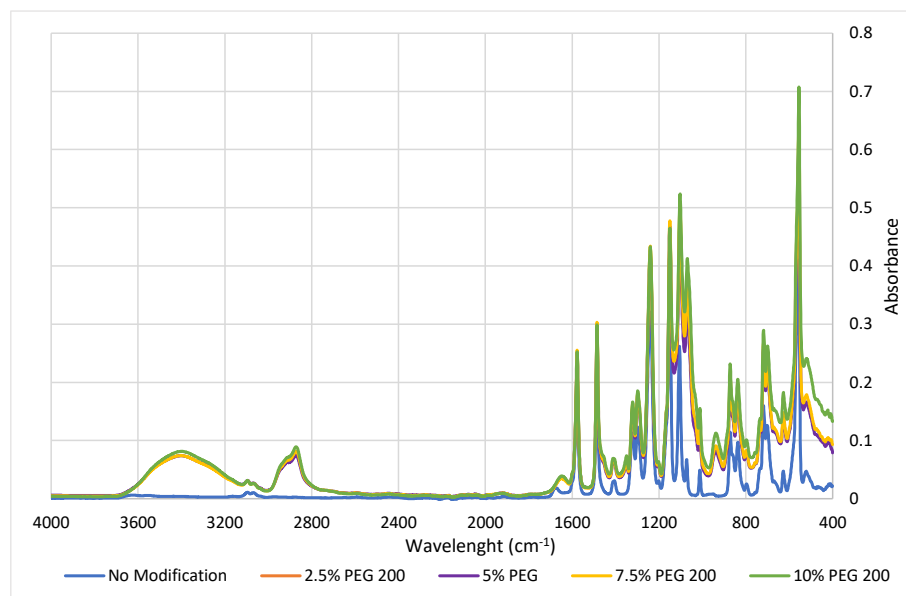


**Figure 7.9 FTIR of PES membranes crosslinked using PEG 200 at increasing weight percentages**

### 7.3.5 Comparison of modification methods

#### 7.3.5.1 Flux and Rejection

Of all 3 modification methods tested, the flux methodology using PEG 200 rejects RB the most but has significantly lower permeate flux than the other two methods used, see Figure 7.10. As is usually seen in membrane studies, higher solute rejection typically means lower permeate flow rates, this is illustrated by using PEG as the crosslinking agent. The SIM method of modification gives the lowest flow rate of the three methods tested, with RB rejection similar to unmodified PES membrane but with worse permeate flux.

HDA modified PES membrane have lower permeate flux rates than those modified using PEG 200 and have lower rejection rate of RB when compared to PEG 200 also, with the exception of SIM modified membranes where the two are comparable. The lower flow rates could be attributed to fouling on the surface of the membrane blocking pores due to the magnetic attraction of the negatively charged dye and positively charged membrane, or due to the HDA molecule being of one size and the PEG 200 having a range of molecules in the standard thus creating some channels larger than others.

### Modification of polyethersulfone (PES) membranes for improved OSN performance

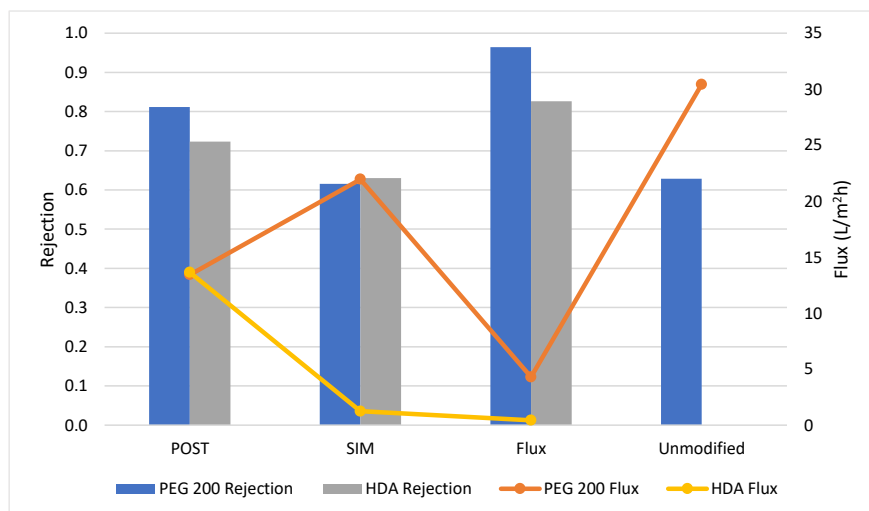


**Figure 7.10 Comparison of flux and rejection of PES membranes using different methods of crosslinking using 10 wt% PEG 200 and 5wt% HDA**

#### 7.3.5.2 FTIR

The N-H stretching peak between  $3550\text{--}3200\text{ cm}^{-1}$  is clearly visible for flux and POST modification while the peak for SIM modification is significantly larger, also incorporating the  $3000\text{--}3800\text{ cm}^{-1}$  N-H stretching peak combined with O-H stretching peak. Furthermore, there is a higher amount of absorbance around  $700\text{ cm}^{-1}$  for SIM modification than the other two, coupling this with the higher  $3550\text{--}3200\text{ cm}^{-1}$ , and flux data from Figure 7.11, we can infer that there is a higher degree of crosslinking when membranes are modified using the SIM method, however, the rejection data does not correlate due to the charge of the dye.

#### Modification of polyethersulfone (PES) membranes for improved OSN performance

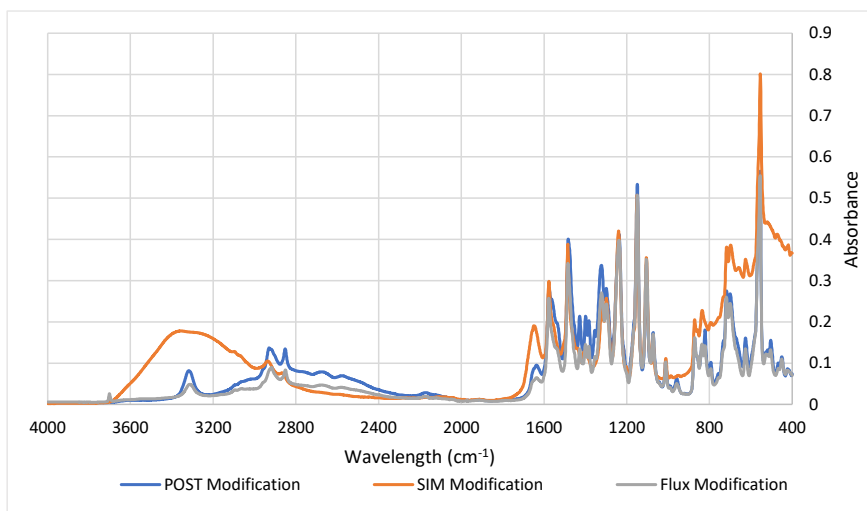


**Figure 7.11 Comparison of FTIR results of the 3 different crosslinking methods tested using 5 wt% HDA as the crosslinking agent**

The overall pattern of shapes and peaks of the FTIR of the 3 modification methods using PEG 200 are identical in Figure 7.12, with minor fluctuations in peaks at various points. Notably, the flux modification has the least absorbance than the other 2 methods over the entire range.

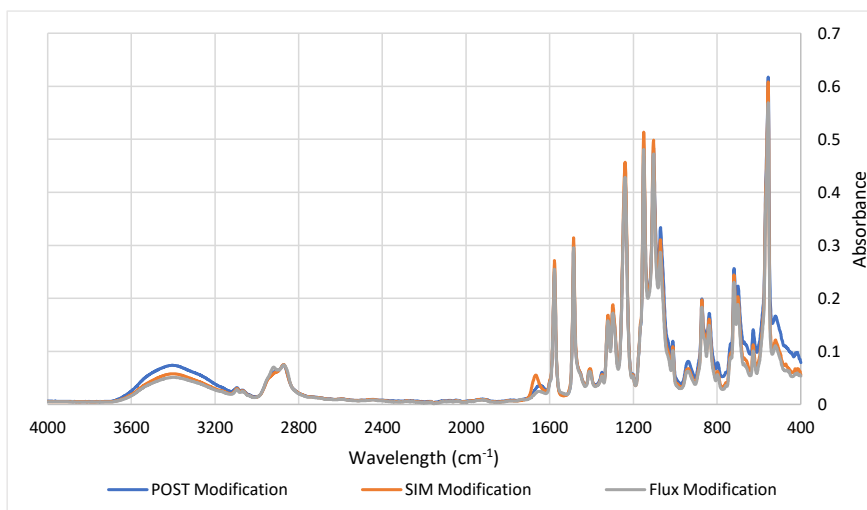


**Figure 7.12 Comparison of modification methods of PES membranes using PEG 200 as a crosslinking agent**

## 7.4 Conclusions

Use of PES membranes has successfully been used for OSN. Use of solvents as additives has had mixed results in terms of permeate flux but the rejection of RB dye is generally consistent for all additive percentages with the odd exception. For all additives used, 2.5% additive always gives lower dye rejection when compared to the others. This lower rejection and higher permeate flux indicate that the small addition an additive inhibits the crosslinking of the PES polymer when in the solvent exchange bath. None of the additives reject over 90% of the RB concentration in the feed, thus cannot be considered as NF membranes.

Use of two different crosslinking agents attached via the POST modification method give varying results, which appears to be dependent on the surface charge of the membrane. For PEG 200, the rejection increases with increasing crosslinker percentage, with the permeate flux rate remaining generally consistent. For HDA, the permeate flux and dye rejection stay fairly consistent no matter what concentration of crosslinking agent is used. The FTIR results show that there is crosslinking agent on the surface of the membrane, which suggests that the surface charge plays a role on the rejection of the dye.

When comparing the 3 methods of crosslinking the flux method of crosslinking has the highest rejection properties consistently when compared to the other methods. Interestingly, the rejection of the dye of all 3 methods for both dyes are comparable to each other with the permeate flux being the determining factor. The permeate flux of modification via the flux method is the lowest of the 3, which is generally the trend when a membrane has high rejection properties. The SIM method proved to have the worst rejection properties of the 3 methods, with both crosslinking agents having near identical permeate flux rates but HDA having a substantially lower permeate flux rate than the PEG 200. This again may be due to surface charge, or due to the fact that the HDA is a single molecule in solution but the PEG 200 in a range of molecules from a range of PEG 100 – 350, thus suggesting that some pores are larger than others during the crosslinking process.

## 8. Application of OSN for Counter Current Chromatography Solvent Recycling

### 8.1 Introduction

When working with solutes of a pharmaceutical or biological nature, non-thermal processes are typically preferred to minimise denaturing of biological products and to prevent two phase flow which would require an increase in pressure, with an increased cost burden, as well as possibly requiring a change in equipment design. As a potential remedy to this, Counter Current Chromatography (CCC) can be deployed as a mean of product concentration. CCC is a non-thermal process that uses a bi-phasic mixture and solute retention in solvents to extract solutes based on the solute's retention time (Hu & Pan, 2012). Ito (2005) gives a good account of how the separation in CCC occurs, whereby the biphasic mixture is forced to mix in a mixing tube due to the centrifugal forces being exerted onto it by rotation. The solutes then pass through the various chambers at different speeds based on their retention in each particular chamber (based on each chambers' solvent composition) leading to an efficient separation process where the desired product will pass through the CCC at a specific "fraction". A schematic of a CCC device is shown in Figure 8.1. CCC can be used to separate multicomponent systems

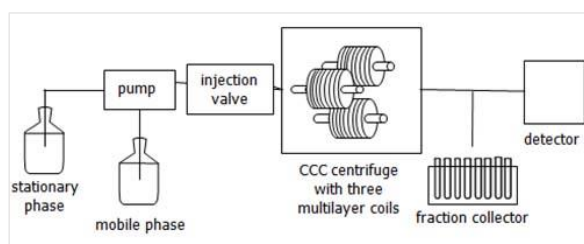


**Figure 8.1 Basic schematic of how a Counter Current Chromatography (CCC) device operates**

CCC as a separation method has some draw backs which are; CCC uses a large amount of solvents for each separation, and at the end of each batch, the user is left with several different compositions of solvent mixtures and solute concentrations based on the number of solutes that are to be separated, which is where membrane separations can be used in conjunction with CCC.

The use of OSN as a form of filtration is still a relatively new method, after first being used commercially by Burgal, *et al* (2015), and since there has been a large amount of developments into the application as a non-thermal means of solid-liquid and liquid-liquid separation in solvent systems (Schmidt, *et al.*, 2014) (Schmidt, *et al.*, 2013) (Geens, *et al.*, 2005). To date, there has only been one published study of OSN being used in conjunction with CCC, where the authors found that the efficiency of CCC can be improved by integration of OSN into the system, where the authors used an API for their study, and recycled the

concentrate back into the CCC as fresh liquid stage (Rundquist, et al., 2012). As the authors have shown that OSN can be a viable method of improving CCC efficiency, there is scope to expand the use of CCC from pharmaceutical products to enrich large protein or bacteria yield via CCC and recycling of solvents (Yang, et al., 2018) (Ma & Ito, 2015).

#### 8.1.1 Proposed uses of filtration with CCC

Nano or ultrafiltration can be used in conjunction with CCC by either concentrating the initial feedstock, concentrating the fractions that are produced by CCC or a combination of both. By using filtration to concentrate the feedstock before being subjected to CCC, there will be less solvents which will result in less being needed for CCC which will result in reduction of operational expenditure. This can work if the solutes aren't concentrated enough to go above the solubility limit of the solute in the given solvent. This may be circumvented as the solute will be in a mixture of two solvents but testing should be carried out first to ensure that the solute doesn't crash out of the solvent mixture.

By concentrating the resultant fractions through filtration, this will allow for greater recovery of product from fractions which would normally be discarded, furthermore, use of OSN can remove 1 or 2 of the solvents in the resulting fraction, allowing for potential recycling of the solvents, further reducing operational expenditure.

### 8.2 Experimental Procedure

#### 8.2.1 Membrane screening by dead-end filtration

A Sterlitech dead-end filtration cell was utilised in the manner described in section 3.3.1. A range of membranes were initially screened using an operating pressure of 40 bar. The samples of both "late minors" and "early minors" were both concentrated using the method described in section 3.4.1. The samples have unknown ratios of solvent (methanol, ethyl acetate, hexane and water) but it is known that the both samples have different ratios of the solvent. Several NF membranes were tested to ascertain their viability to be used for solvent recycling, information from the manufacturer's datasheets are shown in Table 8-1;



#### Application of OSN for Counter Current Chromatography Solvent Recycling

	GE Osmonics			Dow Filmtec		Evonik MET
	DK	HL	DL	NF-90	NF-270	Duramem 200
MWCO (Da) (manufacturer)	~150-300	~150-300	~150-300	~200-400	~200-400	200
Water Specific Flux (GFD/psi) (manufacturer)	5-20	0.39	0.127	0.55-0.75	0.35-0.46	1.18 (this work)
Water Specific Flux (L/m <sup>2</sup> hbar) (manufacturer)	5.42	9.60	3.13	13.54-18.47	8.62-11.33	2.00 (this work)
Maximum Operating Temperature (°C)	50	50	50	45	45	50
Maximum Operating Pressure (bar)	41.37	41.4	41.37	41	41	60
pH range	3-9	3-9	3-9	2-11	2-11	7
Reference	(Lenntech, 2018)	(Lenntech, 2018)	(Lenntech, 2018)	(Dow, 2018)	(Dow, 2018)	(Sterlitech, 2018)

**Table 8-1 Properties of membranes used in CCC recycling screening experiments**

Membranes were first compressed by permeating 200mL of water of ultra-pure water at 40 bar, then clean water flux experiments were conducted. The specific flux experiments were then conducted at pressures 10-40 bar, before concentration experiments were conducted (see section 3.4.1). The two samples, provided by Bioextractions Wales, are denoted as 'early minors' and 'late minors'. The early minor sample is a mixture of mostly Spinosyn J (70%) with some Spinosyn L (30%) with a ratio methanol, water, ethyl acetate and hexane. The late minors sample is only Spinosyn L with a different ratio of methanol, water, ethyl acetate and hexane to that of early minors. They are denoted as such as early minors is the fraction before the desired product fraction passes through the CCC, and the late minors is the fraction after the desired product fraction. The membrane is then cleaned, and specific water flux experiments were carried out again to monitor any change in permeate flux. The membrane is then removed from the cell and stored in a sample of the feed in a solvent cupboard for 28 days. After the saturation time, the membrane is removed from the sample and cleaned using water. The membrane then undergoes specific flux experiments again, then a sample concentration experiment is conducted to monitor if there is any change in the membrane flux and rejection. The permeate samples are analysed using a HPLC (method described in section 3.5.5).

#### 8.2.2 Solvent Recycling using OSN

The Duramem 200 membrane was conditioned and cleaned by permeating 75mL of methanol through the membrane at the operating pressure (40 bar), this acts to remove the protective layer on the membrane and compress the membrane to allow for optimal separation. In the sterlitech cell, 300mL of mixed solvent (1:1:1:0.01) of methanol, water, ethyl acetate and hexane pressurised to the operating pressure at room temperature with a stirring bar operating at 300 RPM. Initially, 5 mL was permeated through as waste then

#### Application of OSN for Counter Current Chromatography Solvent Recycling

the following 10mL was taken as sample. The cell was then left for 24 hours and another 10mL of sample was collected. This experiment was conducted to a) understand what the membrane will reject, b) possibly understand how the membrane allows solvent to pass through (pore flow or diffusion). Samples were analysed using a headspace analyser which fed into a GC/MS system (section 3.5.4.3).

#### 8.2.3 Crossflow ultrafiltration

The UF filtration was set up in the manner described in section 3.3.2. The membrane used was a GE Osmonics JW (MWCO 25-50 kDa). A collagen sample was donated by ProColl Ltd (Swansea, UK) of a bovine collagen of MW 105,000 g/mol. The sample for pre CCC concentration was made up to 1000 mg/L in a mixed solvent system of methanol, water, ethyl acetate and hexane (each 33% (vol/vol) except for hexane which was 1% (vol/vol)). The feed solution was concentrated by removal 20% of the feed, using an applied pressure of 5 bar(g) with a TMP of 0.625 bar. As this is a single pump system, the velocity of the pump cannot be manually controlled, the crossflow velocity at 5 bar was 0.5 m/s. Retentate concentration was measured by dry mass analysis, and solvent analysis on the feed, permeate and retentate was analysed via headspace GC/MS.

Post CCC feed was of the concentration of 4500 mg/L and was found to have a solvent ratio of methanol, water, ethyl acetate and hexane of 37.5%, 37.5%, 25% and 1% respectively. The UF settings, method and membrane were the same as the pre CCC concentration.

The yield of the diafiltration is calculated by drying 10 mL of sample in an oven for 60 minutes at 120°C, and is defined by:

$$Yield = \frac{Retentate\ Dry\ Mass}{Feed\ Dry\ Mass} * 100\% \quad \text{Equation 8.1}$$

### 8.3 Results

#### 8.3.1 Membrane Screening by dead-end filtration

The concentration of the desired product varies depending on the membrane used, along with the permeate flux through the membrane, Table 8-2 and Table 8-3 and visualised in Figure 8.2, Figure 8.3 and Figure 8.4.

	GE Osmonics			Dow Filmtech		Evonik MET
	DK	HL	DL	NF-90	NF-270	Duramem 200
Water Specific Flux (pre-concentration) (L/m <sup>2</sup> hbar) [1]	3.27	6.46	4.17	8.74	9.24	2.00
Early Minors Specific Flux (L/m <sup>2</sup> hbar)	0.32	1.85	0.56	0.86	0.88	0.21
Water Specific Flux (post concentration) (L/m <sup>2</sup> hbar) [2]	1.59	7.86	2.26	3.79	4.41	0.59
Solute Rejection (%)	96.87	62.50	82.17	78.39	79.93	82.9
Clean Water Flux After Saturation (L/m <sup>2</sup> hbar) [3]	2.16	6.76	2.98	3.89	4.01	0.74
Early Minors Specific Flux After Saturation (L/m <sup>2</sup> hbar)	0.43	1.41	0.64	0.98	0.94	0.13
Solute Rejection (%)	94.66	71.17	80.74	64.65	66.07	93.51
Change in Water Specific Flux [2/1] (%)	-51.38	21.67	-45.80	-56.64	-52.27	-70.5
Change in Water flux post saturation from fouled flux [3/2] (%)	35.85	-13.99	31.86	2.64	-9.07	25.42
Change in water specific flux post saturation from initial [3/1] (%)	-33.94	4.64	-28.54	-55.49	-56.60	-63.00
Change in Early Minors Specific Flux (%)	34.38	-23.78	14.29	13.95	6.82	-38.1
Rejection change (%)	-2.34	12.18	-1.78	-21.26	-20.98	11.34

**Table 8-2 Data from dead-end concentration of early minors in several membranes**

# Application of OSN for Counter Current Chromatography Solvent Recycling

	Dow Osmonics			Dow Filmtech		Evonik MET
	DL	HL	DK	NF-90	NF-270	Duramem 200
Water Specific Flux (pre-concentration) (L/m <sup>2</sup> hbar) [1]	3.27	6.46	4.17	8.74	9.24	2.00
Late Minors Specific Flux (L/m <sup>2</sup> hbar)	0.37	2.10	0.50	0.72	0.64	0.11
Water Specific Flux (post concentration) (L/m <sup>2</sup> hbar) [2]	1.69	6.98	2.35	3.79	4.41	0.14
Solute Rejection (%)	80.96	22.07	88.53	52.78	75.09	97.66
Water Specific Flux after saturation (L/m <sup>2</sup> hbar) [3]	2.25	7.07	3.17	5.37	6.06	0.12
Late Minors Specific Flux after Saturation (L/m <sup>2</sup> hbar)	0.46	1.89	0.65	0.98	1.46	0.04
Rejection (%)	72.81	35.45	81.59	63.44	44.35	100.00
Change in Water Specific Flux [2/1] (%)	-48.15	8.15	-43.68	-56.64	-52.26	-92.9
Change in Water Specific Flux post Saturation [3/2] (%)	33.14	1.29	34.89	41.69	37.41	-14.29
Change in Specific Water Flux post saturation from initial [3/1] (%)	-31.19	9.44	-23.98	-38.59	-34.42	-14.29
Change in Late Minors Specific Flux (%)	24.32	-10.00	30.00	36.11	128.13	-63.64
Rejection Change (%)	-10.07	60.63	-7.84	20.2	-40.94	2.4

**Table 8-3 Data from dead-end concentration of late minors in several membranes**

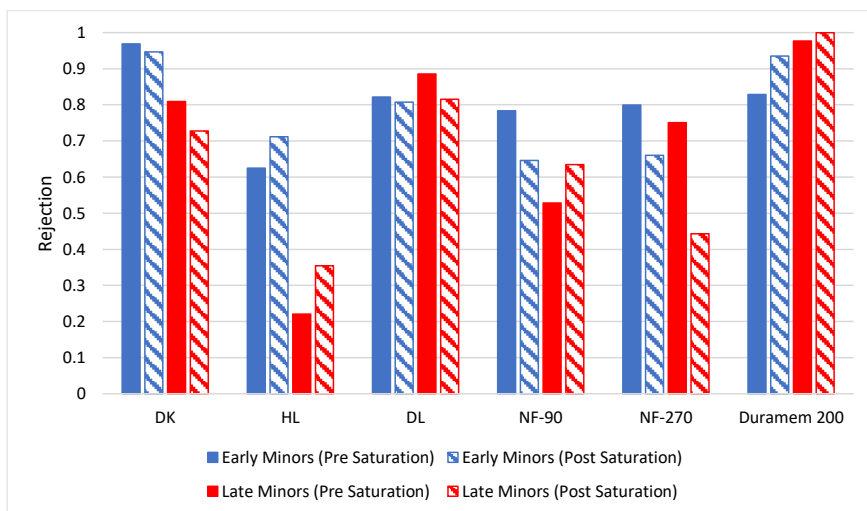


**Figure 8.2 Rejection of Early and Late Minors in several membranes before and after 4 week saturation**

#### Application of OSN for Counter Current Chromatography Solvent Recycling

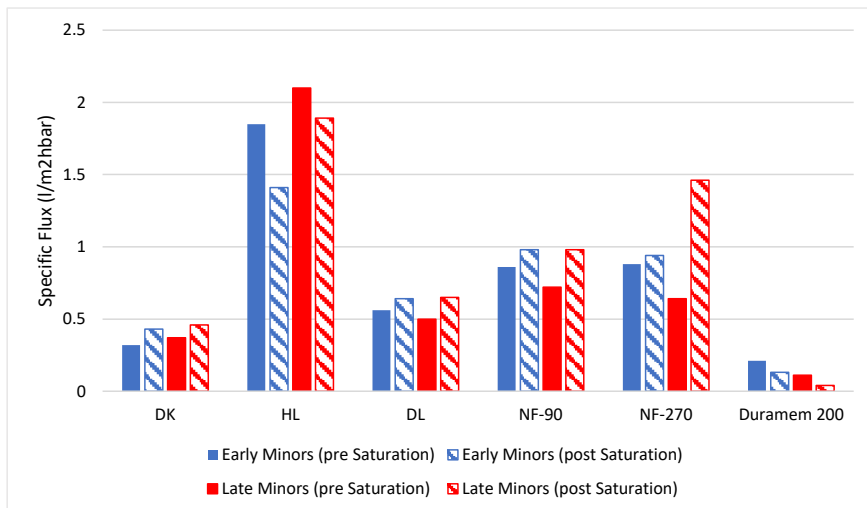


**Figure 8.3 Specific Flux of Early and Late Minors in several membranes before and after 4 week saturation**

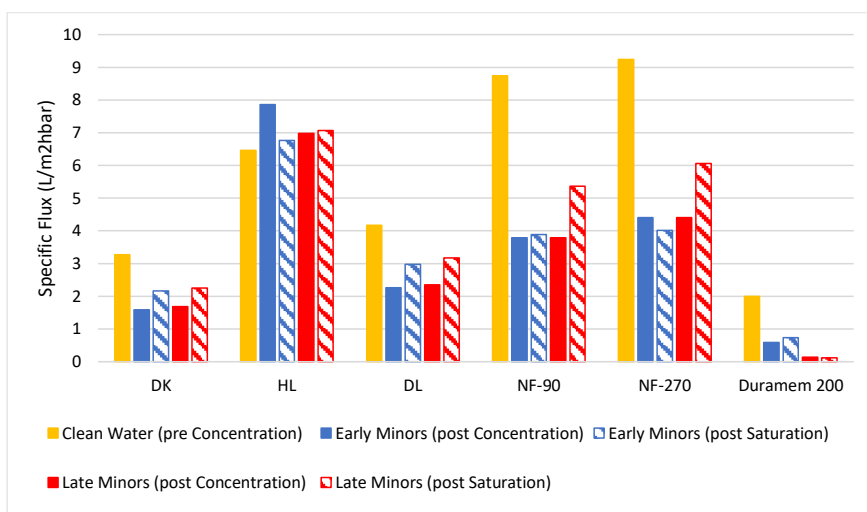


**Figure 8.4 Water Specific Flux of several membranes before and after Early and Late Minors concentration and 4 week saturation**

The rejection of the desired product typically decreases in all membranes after saturation in the feed solvent mixture for 4 weeks, with the exception of the HL and Duramem membranes, see Figure 8.2. The high rejection of a solute with MW>700 is to be expected of the Duramem as this is a dedicated OSN membrane, constructed from more robust polymers which are more stable in chemical solutions. The decrease in rejection and the subsequent increase in specific flux after 4 week saturation, see Figure 8.3,

are indicators that the pores are opening in the presence of solvent, whereas the membrane is swelling where the flux is decreasing, and the rejection increases (HL and Duramem membranes). The significant drop in water flux through the membranes (except for HL) would suggest that the structure of the membrane has altered due to the presence of solvents, see Figure 8.4, most likely attributed to ethyl acetate due to its harsh chemical nature (ethyl acetate can dissolve many plastics). To that end, the suggested choice of membrane will be the DL membrane as the change in rejection and specific flux is the most consistent of all the membranes tested, with the Duramem 200 being the second choice with regards to consistency with the drawback of a low permeate flux. The clean water flux of the membranes tested declines for all of the membranes after concentration in either the early or late minors samples, with the exception of the HL membrane, see Figure 8.4. The clean water flux increases in all the membranes after saturation in both early and late minors samples, with the exception of the HL membrane in early minors and the NF270 membrane also in early minors. This change in behaviour may be due to the crosslinkers used for the formation of these membranes. Unfortunately, a crossflow NF system was not completed in this project to progress this study, thus an ultrafiltration study was constructed in its place. A crossflow NF system was not constructed for further testing due to a) a suitable gear/piston pump that can produce the system pressure required to facilitate NF systems was not found until the last 6 months of the project, and with delays to the construction of the pump, there was only a few weeks left to test and use the pump. b) the pump was faulty, i.e. the pump was very loud when the technical documents supplied with accompanying the pump suggest that the pump should be quiet. This may be that the pump had custom made ports to allow for a 0.5" fitting. Furthermore, the pump did not have a 100% duty cycle and would overheat after 5 minutes. Lastly, c) finances for the project would not allow for the purchase of another or a more expensive pump and given the delayed delivery, there was not enough time to find a suitable replacement.

### 8.3.2 Ultrafiltration of collagen

A batch of collagen was dissolved in the feed solution as described in section 8.2.3, and the permeate flux of solutions before and after CCC concentration are shown in Figure 8.5. The pre-CCC flux is more than double the flux of CCC concentrated solution but the flux decreases at a significant rate up to 40 minutes (129 to 93 L/m<sup>2</sup>h) before stabilising, which may be due to fouling due to the nature of the concentration. The CCC concentrate has a significantly lower permeate flux but is also more stable than the pre-CCC feed solution, this lower flux may be due to fouling on the membrane (same membrane disc used from initial concentration), or it may be due to the higher concentration of the solute in the solution. As the flux is not decreasing at a significant rate, when compared to the pre-CCC flux, the lower flux rate can be attributed to the higher concentration of solutes in the system.

The membrane performed consistently with a pre-CCC yield of 187.5% and a post-CCC yield of 160%, see Table 8-4, the decrease in yield is expected at higher concentrations is expected due to the performance of

## Application of OSN for Counter Current Chromatography Solvent Recycling

membranes decreasing with increasing solute concentration. The decrease may also be due to the change in the solvent ratio, see section 8.2.3, as membranes tend to behave differently in the presence of different ratios of solvents (Rundquist, et al., 2012).

	Pre CCC	Post CCC
<b>Feed Concentration (mg/L)</b>	0.8	4.5
<b>Concentrate Concentration (mg/L)</b>	1.5	7.2
<b>Yield (%)</b>	187.5	160

Table 8-4 Gelatin concentrations in Pre CCC and Posts CCC ultrafiltrations

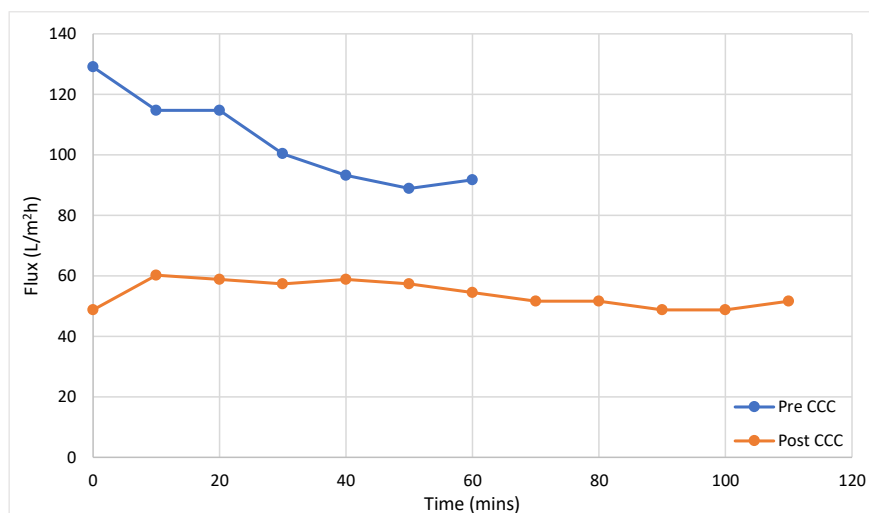


Figure 8.5 Flux of collagen solutions before and after CCC concentration

### 8.3.3 Solvent exchange during filtration

#### 8.3.3.1 Nanofiltration

The dead-end nanofiltration yield very little change in the solvent make up when using the Duramem 200, see Table 8-5, this is likely due to a) the solvents used are of a lower molecular weight than the cut-off, with the largest being ethyl acetate with a MW of 89 g/mol, b) there is only one route for the solvent to move dead-end filtration so chemical interactions between the solvent and the membrane cannot occur. Interestingly, hexane is rejected during the filtration (99.77%) which could be due to a) the small amount in comparison to the other solvents present, b) the non-polarity of hexane is easily rejected by the hydrophilic membrane.

#### Application of OSN for Counter Current Chromatography Solvent Recycling

Solvent	Solvent Area		Rejection
	Feed	Permeate	%
Methanol	6836367	7280628	-6.5
Water	1642477	1573913	4.17
Ethyl Acetate	2721550	2847391	-4.62
Hexane	2930850	6870	99.77

**Table 8-5 Solvent analysis of Late Minors before and after filtration using the Duramem 200**

#### 8.3.3.2 Ultrafiltration

As a result of the pre-CCC concentration, the difference in the concentration of methanol between the permeate and retentate is negligible, see Table 8-6, changing by approximately 0.4% according to the mass balance conducted on the analysis. The water concentration appears to be retained rather than permeate through the membrane, which is to be expected as the membrane is quoted to be hydrophobic (Agana, et al., 2013). The permeate samples shows a significant concentration of ethyl acetate compared to the retentate and the feed, which may be due to the compatibility between water and ethyl acetate, thus as the water is retained by the membrane, the ethyl acetate passes through the membrane due to its hydrophobicity. The membrane shows a 40% rejection of hexane which is high considering the 25-50 kDA cut-off of the membrane. The reason for this can be speculated as hexane permeating through the membrane due to its immiscibility with both water and methanol, thus even at a mid-UF range, solvent solubility still plays a large role in the rejection of a solute.

Solvent	Percentage in sample (%)		
	Feed	Permeate	Retentate
Methanol	33	32.59	33.41
Water	33	28.10	37.90
Ethyl Acetate	33	40.05	25.95
Hexane	1	0.6	1.4
Total	100	101.34	98.66

**Table 8-6 Solvent percentages in feed, permeate and retentate of pre-CCC concentration**

Similar to the pre-CCC concentrations, methanol shows little difference in change of concentration with respect the feed, see Table 8-7. There is much less deviation in the water concentration between the permeate and retentate samples when compared to the pre-CCC filtration, a difference of  $\pm 1\%$  with respect to the amount of water in the feed concentration, compared to  $\pm 5\%$  of the pre-CCC filtration. Ethyl acetate again has the largest exchange, but not to the extent to that of pre-CCC, of  $\pm 3\%$  when compared to the levels in the feed stock. The membrane shows a rejection of -33% of hexane in this ratio of solvents, which when observing ethyl acetate being more readily retained, is again explained by the solubility of hexane in ethyl acetate rather than size exclusion which is typical in UF systems.



#### Application of OSN for Counter Current Chromatography Solvent Recycling

Solvent	Percent in sample (%)		
	Feed	Permeate	Retentate
Methanol	37.5	37.14	37.86
Water	37.5	36.78	38.22
Ethyl Acetate	24	20.69	27.31
Hexane	1	1.33	0.67
Total	100	95.94	104.06

**Table 8-7 Solvent percentages in feed, permeate and retentate of post-CCC concentration**

## 8.4 Conclusions

The dead-end filtration of the pesticides spinosyn J (early minors) and L (late minors) showed mixed results depending on the choice of membrane used for the filtration. The GE osmonics DL membrane performed the most consistently before and after 4-week exposure to the solvent mixture and with a reasonable permeate flux rate of each pesticide solution. The Duramem 200 has the highest rejection of all the membranes tested, but the permeate flux of each solution through this membrane is significantly slower than the others tested. This may be due to the thickness of the membrane compared to the thin-film composites of the other membranes tested, which is justified by the harsh chemical environments that the Duramem 200 is designed to be exposed to. The dead-end filtration shows little change in solvent composition between the permeate and the retentate with the exception of hexane, which is being rejected due to its alkane nature. The ultrafiltration of collagen shows that CCC can be a viable method of concentration via non-thermal means at a faster rate than evaporative techniques which would denature and destroy the biological product. The pre-CCC concentration of collagen had a higher yield when compared to the post-CCC concentration, with a higher permeate flux rate also. The composition of the solvent mixture of the permeate and concentrate will shift depending on the initial feed composition, which can be related to each solvents solubility towards each other, while some testing has been done on binary and tertiary mixtures, more study is need on solvent-membrane interactions in mixed solvent systems.

## 9. Conclusions

---

With the increasing usage of OSN as a non-thermal separation process, industry requires an understanding of how the technology works, what are its limitations etc, particularly the pharmaceutical industry where material and running costs are an order of magnitude higher due to materials and conditions used in this industry. The main theme for this thesis is to thoroughly examine one brand of OSN membranes, attempt to determine what parameters effect the separation mechanisms, and apply this information to a separation to see how the membrane performs. In doing so, a new method of determining the surface charge of positively charged membranes was discovered, which is of use for membranes being developed and used in both aqueous and non-aqueous systems. Furthermore, 2 crosslinking agents were applied to polyethersulfone membranes in different ways to determine their effectiveness and determine which method is best used for crosslinking membranes in the future.

### 42Characterisation of the Duramem OSN membranes

When testing both the Duramem 150 and 200 in salt solutions, the membranes have similar separation properties to membranes designed for aqueous systems, but with significantly slower flux rates. This is likely due to the dense layer of membrane required to be stable in harsh solvent environments compared to the thin film composites of other aqueous membranes. Rejection and permeate flux data show that the Duramem series of membranes are hydrophilic in nature and carry a negatively charge surface.

Both the Duramem 150 and 200 membranes are stable in methanol, ethanol and acetonitrile with differing permeate fluxes and solute rejection. Ethanol displays the lowest permeate flux of the three solvents tested in both membranes. The usual method of plotting the rejection of a membrane i.e. using the molecular weight of the solute, as a way to determine the MWCO of a membrane, is not applicable for small solutes as the introduction of halogens (Cl) can inflate molecular weight of a solute while not increasing the physical size of the solute. The measurement of Van der Waals radius in the chosen solute is the best way to determine rejection of a solute as the radius will change in size depending on the solvent(s) to which it is dissolved.

### Electrokinetic characterisation of OSN membranes

Use of LDE as a method of determining surface zeta potential of positively charged membranes was successfully demonstrated, reinforcing that this method is a viable option for surface zeta charge measurements of membranes that are small in size and are not yet suitable to a larger size of manufacture e.g. if the use of expensive chemicals in the dope solution is used. However, for this method to be useful for positive membranes, the user must know which magnetic charge the membrane is initially or there will be adsorption of the particles onto the membrane and giving a false reading. Alternatively, (and if available)

## Conclusions

experiments using one set of charged particles should be done first then repeated using the oppositely charged particles and fresh membrane. If both results come back as negatively charged, then the membrane is positive.

When applied to solvent systems, the LDE method is not suitable for analysis due to the nature by in which the measurement is taken. The lack of conductivity in solvents, even in solvent-water systems, gives poor resolution in the phase diagram with no distinct shape to the graphs, despite experiments with increased salt concentration. In principal, LDE can be applied for solvent system but a method for increasing the resolution of the results is needed.

## Investigation into of the separation mechanisms of OSN membranes

Of all the properties examined when looking that the rejection and flux of the Duramem 500, the solubility of the dye in the alcohol used appears to be the most directly relatable. When examining the flux and rejection in methanol – water of both dyes, the flux appears to be inversely proportional to the viscosity of the solution with the rejection of the dyes being governed by other properties. The surface charge of the membrane and charge of the dyes appears to have little effect when solvents are introduced.

When examining single solvent systems, again the viscosity of the solvent is the dominant property for permeate flux with the molar volume of the solvent also attributing, with the solubility of the dye being the dominant property for the rejection of the dye. Other properties examined such as the surface tension of the solution and the swelling degree appear to not have any impact on the rejection and flux properties of the membrane.

The solvation of the dye on each alcohol appears to be directly linked to the rejection of the dye, particularly Safranin O, which can easily be calculated using the free software Marvin Sketch. When the size of the solute in each solvent is plotted against the performance of the membrane, a linear trend can be seen.

## Modification of polyethersulfone (PES) membranes for improved OSN performance

Use of alcohols in the dope solution for casting membranes appears to yield no real change in the rejection of the Rose Bengal dye but with some significant changes to the permeate flux. Generally, the use of volatile alcohols increases the permeate flux through the membrane when compared to unmodified PES membranes. Interestingly, the rejection of the dye decreases at 5% alcohol for all alcohols tested, suggesting that that there is a chemical interaction happening.

The success of the crosslinking agent depends to appear on the charge of the agent used. The rejection of the dye increases with increasing PEG 200 concentration, whereas the rejection appears to be unchanged

## Conclusions

when HDA is used, when crosslinking agents are applied via submersion. The SIM method of modification yields similar rejection properties for both crosslinking agents used despite the change in surface charge of the membrane. The best method for crosslinking to increasing rejection is the flux method, yielding the highest rejection values of the 3 methods tested.

FTIR analysis shows that PEG200 appears to bond with the polymer no matter which concentration or method is used, but HDA has a maximum saturation of 7.5% when applied via submersion, and shows most crosslinking when applied via the SIM modification method.

This study also shows that surface charge of a membrane plays a role even in solvent systems, where the general consensus is that there is no charge due to the lack of hydrogen dissociation. To this end, greater care in membrane selection for OSN systems is needed as this can impact the rejection of a given solute by the membrane chosen.

## Application of OSN for Counter Current Chromatography Solvent Recycling

Dead – end filtration studies show that rejection of the pesticide in mixed solvent solutions can vary in different membranes of roughly equal MWCO. This is due to the different chemical make-up of each membrane reacting and swelling differently in the mixed solvent feed. Interestingly, the dedicated OSN membrane, Duramem 200, did not perform as the DK and similarly to the rest membranes tested, but with significantly slower permeate flux rates. There is little to no change in the solvent make-up which is due to the dead-end filtration method, where any chemical interactions are negated by the high pressure used in the study.

Due to the cross-flow set-up, the system was only capable to provide 5 bars of pressure through a single pump, thus the pressure and flow rate could not be independently controlled. The gelatin concentration study shows that the desired product can be concentrated before CCC concentration and post CCC for further concentration. Even using a 25k Da membrane, there is rejection of hexane when examining the solvents before and after concentration, with the amount of ethyl acetate in the permeate being determined by the amount in the feed.

## 10. Future Work

---

From the results shown in this series of studies, there are clear gaps in knowledge for OSN. The majority of publications surrounding the topic are for one specific use i.e. concentration of a certain compound. There is very little studies completed surrounding performance, while the ones that exist tend to be for modelling for a single or a multicomponent system. For accurate models to be determined, one core thing is needed: data. Simply put, the model the performance of OSN systems more data is needed using different solvents and solutes to measure the performance of the chosen membrane. Only once multiple studies have been completed can accurate models constructed.

The choice of solute is also important, as solvent – solute interactions are largely determined by the solubility of solute in the given solvent. While there are predictive tools available e.g. Hansen Solubility Parameter software, the software also requires dissolution experiments to determine the compatibility, thus more data is required to be collected and shared.

While some of a solute's parameters are mapped against membrane performance in this study, many more solute parameters that can be examined and compared against each other to better understand how membrane function in an organic solvent environment. One method of examining solvent – membrane interactions is Atomic Force Microscopy (AFM) which can be used to probe the surface of the membrane that is submerged in solvent. A study of the surface of membranes in solvent would show any if a membrane's pore will swell or constrict in a solvent as a method to ascertain the compatibility of a solvent with a membrane.

With regards to modification of PES membranes and their use in OSN systems, very little research has been completed. PES has been regarded for it's used filtration of hazardous chemicals e.g. uranium and is known to be robust, but very little has been published in way of modification of PES compared to other polymers. There are many more crosslinking agents commercially available and methods of implementing into the membrane, which can be tested for their viability for compatibility with PES and OSN systems.

CCC can be a powerful tool for separating solutes from a multicomponent system and coupled with OSN the process can be made more cost effective. The major downside for use of OSN with this is finding a pump that can deliver the required pressure while being ATEX rated. There are some pumps commercially available which were too beyond the budget of this project but utilisation of OSN with CCC is feasible with the correct equipment. Different ratios of solvents and mixtures of solvents can be examined; indeed this study has two ratios but the study by Rundquist *et al* (2012) uses different solvents for CCC and has different results for OSN depending on the ratios and solvent used. In short, the area of study that is OSN is very broad in size and current research has barely scratched the surface of topic. More data is required to answer the near endless amount of questions that can be answered.

## 11. References

---

- Adi, V. S. et al., 2016. Optimization of OSN Membrane Cascades for Separating Organic Mixtures. *Computer Aided Chemical Engineering*, Volume 38, pp. 379-384.
- Agana, B. A., Reeve, D. & Orbell, J. D., 2013. Industrial water reclamation using polymeric membranes – case studies involving a car manufacturer and a beverage producer. *Journal of Water Reuse and Desalination*, 17 July, 3(4), pp. 357-372.
- Agenson, K. O. & Urase, T., 2007. Change in membrane performance due to organic fouling in nanofiltration (NF)/reverse osmosis (RO) applications. *Separation and Purification Technology*, 15 June, 55(2), pp. 147-156.
- Ahmad, A., Abdulkarim, A., Ooi, B. & S.Ismail, 2013. Recent development in additives modifications of polyethersulfone membrane for flux enhancement. *Chemical Engineering Journal*, 1 May, Volume 223, pp. 246-267.
- Almazán, J. E., Romero-Dondiz, E. M., Rajal, V. B. & Castro-Vidaurre, E. F., 2015. Nanofiltration of glucose: Analysis of parameters and membrane characterization. *Chemical Engineering Research and Design*, February, Volume 94, pp. 485-493.
- Arkell, A., Krawczyk, H., Thuvander, J. & Jönsson, A., 2013. Evaluation of membrane performance and cost estimates during recovery of sodium hydroxide in a hemicellulose extraction process by nanofiltration. *Separation and Purification Technology*, 30 October, Volume 118, pp. 387-393.
- Baker, R. W., 2012. Chapter 2 Membrane Transport Theory. In: *Membrane Technology Application*. 3 ed. s.l.:John Wiley & Sons, Inc, pp. 15-96.
- Baker, R. W., 2012. Overview of Membrane Science and Technology. In: *Membrane Technology and Applications*. 3 ed. s.l.:John Wiley and Sons Inc., pp. 1-14.
- Bastin, M., Hendrix, K. & Vankelecom, I., 2017. Solvent resistant nanofiltration for acetonitrile based feeds: A membrane screening. *Journal of Membrane Science*, 15 August, Volume 536, pp. 176-185.
- Behnke, S. & Ulbricht, M., 2015. Thin-film composite membranes for organophilic nanofiltration based on photo-cross-linkable polyimide. *Reactive and Functional Polymers*, January, Volume 86, pp. 233-242.
- Bellona, C. & Drewes, J. E., 2005. The role of membrane surface charge and solute physico-chemical properties in the rejection of organic acids by NF membranes. *Journal of Membrane Science*, 1 March, 249(1-2), pp. 227-234.
- Bhattacharya, S. & Hwang, S.-T., 1997. Concentration polarization, separation factor, and Peclet number in membrane processes. *Journal of Membrane Science*, 20 August, 132(1), pp. 73-90.
- Bowen, W. R., Cassey, B., Jones, P. & Oatley, D. L., 2004. Modelling the performance of membrane nanofiltration—application to an industrially relevant separation. *Journal of Membrane Science*, 15 October, 242(1-2), pp. 211-220.
- Burgal, J. d. S., Peeva, L. & Livingston, A., 2017. Negligible ageing in poly(ether-ether-ketone) membrane widnes application range for solvent processing. *Journal of Membrane Science*, Volume 525, pp. 48-56.
- Burgal, J. d. S., Peeva, L., Marchetti, P. & Livingston, A., 2015. Controlling molecular weight cut-off of PEEK nanofiltration membranes using a drying method. *Journal of Membrane Science*, 1 November, Volume 493, pp. 524-538.
- Butler, E., Petit, C. & Livingston, A. G., 2019. Poly(piperazine trimesamide) thin film nanocomposite membrane formation based on MIL-101: Filler aggregation and interfacial polymerization dynamics. *Journal of Membrane Science*, 24 September.

## References

- Cao, X.-L., Yan, Y.-N., Zhou, F.-Y. & Sun, S.-P., 2020. Tailoring nanofiltration membranes for effective removing dye intermediates in complex dye-wastewater. *Journal of Membrane Science*, 1 February, Volume 595.
- Chau, J. et al., 2018. Performance of a composite membrane of a perfluorodioxole copolymer in organic solvent nanofiltration. *Separation and Purification Technology*, 30 June, Volume 199, pp. 233-241.
- Conidi, C., Cassano, A., Caiazzo, F. & Drioli, E., 2017. Separation and purification of phenolic compounds from pomegranate juice by ultrafiltration and nanofiltration membranes. *Journal of Food Engineering*, February, Volume 195, pp. 1-13.
- Cook, M., Gaffney, P. R., Peeva, L. G. & Livingston, A. G., 2018. Roll-to-roll dip coating of three different PIMs for Organic Solvent Nanofiltration. *Journal of Membrane Science*, 15 July, Volume 558, pp. 52-63.
- Darvishmanesh, S., Degreè, J. & Bruggen, B. v. d., 2010. Mechanisms of solute rejection in solvent resistant nanofiltration: the effect of solvent on solute rejection. *Physical Chemistry Chemical Physics*, 12(40), pp. 13333-13342.
- Darvishmanesh, S. et al., 2011. Performance of solvent resistant nanofiltration membranes for purification of residual solvent in the pharmaceutical industry: experiments and simulation. *Green Chemistry*, 1 December, Volume 12, pp. 3476-3483.
- Darvishmanesh, S. et al., 2011. Physicochemical Characterization of Solute Retention in Solvent Resistant Nanofiltration: the Effect of Solute Size, Polarity, Dipole Moment, and Solubility Parameter. *The Journal of Physical Chemistry B*, 15 December, 115(49), pp. 14507-14517.
- Davey, C. J., Low, Z.-X., Wirawen, R. H. & Patterson, D. A., 2017. Molecular weight cut-off determination of organic solvent nanofiltration membranes using poly(propylene glycol). *Journal of Membrane Science*, 15 March, Volume 526, pp. 221-228.
- Dohmen, M. P. J. et al., 2008. Hydrodynamic Radii of Polyethylene Glycols in Different Solvents Determined from Viscosity Measurements. *Journal of Chemical Engineering Data*, January, 53(1), pp. 63-65.
- Donnan, F. G., 1995. Theory of membrane equilibria and membrane potentials in the presence of non-dialysing electrolytes. A contribution to physical-chemical physiology. *Journal of Membrane Science*, 31 March, 100(1), pp. 45-55.
- Dow, 2018. *DOW FILMTEC Nanofiltration 4" Elements*. [Online]  
Available at: <https://www.dow.com/en-us/markets-and-solutions/products/DOWFILMTECNanofiltration4Elements/DOWFILMTECNF904040>  
[Accessed 11 1 2018].
- Ernst, M., Bismarck, A., Springer, J. & Jekel, M., 2000. Zeta-potential and rejection rates of a polyethersulfone nanofiltration membrane in single salt solutions. *Journal of Membrane Science*, 1 February, 165(2), pp. 251-259.
- Farajtabar, A., Naderi, F. & Gharib, F., 2013. Autoprotolysis in water/methanol/NaCl ternary systems. *Journal of the Serbian Chemical Society*, 78(10), pp. 1561-1567.
- Garcia-Ivars, J. et al., 2017. Nanofiltration as tertiary treatment method for removing trace pharmaceutically active compounds in wastewater from wastewater treatment plants. *Water Research*, 15 November, Volume 125, pp. 360-373.
- Geens, J., Peeters, K., Van der Bruggen, B. & Vandecasteele, C., 2005. Polymeric nanofiltration of binary water-alcohol mixtures: Influence of feed composition and membrane properties on permeability and rejection. *Journal of Membrane Science*, 15 June, 255(1-2), pp. 255-264.

## References

- Gelsema, W. J., Ligny, C. L. d., Remijnse, A. G. & Blijleven, H. A., 1966. pH-Measurements in alcohol-water mixtures, using aqueous standard buffer solutions for calibration. *Recueil des Travaux Chimiques des Pays-Bas*, 85(7), pp. 647-660.
- Goebel, R., Glaser, T., Niederkleine, I. & Skiborowski, M., 2018. Towards predictive models for organic solvent nanofiltration. *Computer Aided Chemical Engineerin*, Volume 43, pp. 115-120.
- Griffiths, P. R. & Haseth, J. A. D., 2007. *Fourier Transform Infrared Spectroscopy*. 2nd ed. s.l.:John Wiley & Sons INC.
- Hermans, S. et al., 2015. Efficient synthesis of interfacially polymerized membranes for solvent resistant. *Journal of Membrane Science*, 15 February, Volume 476, pp. 356-363.
- Holda, A. K. & Vankelecom, I. F., 2014. Integrally skinned PSf-based SRNF-membranes prepared via phase inversion - Part A: Influence of high molecular weight additives. *Journal of Membrane science*, 15 January, Volume 450, pp. 512-521.
- Holda, A. K. & Vankelecom, I. F., 2014. Integrally skinned PSf-based SRNF-membranes prepared via phase inversion-Part A: Influence of high molecular weight additives. *Journal of Membrane Science*, 15 January, Volume 450, pp. 512-521.
- Holda, A. K. & Vankelecom, I. F., 2014. Integrally skinned PSf-based SRNF-membranes prepared via phase inversion—Part B: Influence of low molecular weight additives. *Journal of Membrane Science*, 15 January, Volume 450, pp. 499-511.
- Hoseinpour, H., Peyravi, M., Nozad, A. & Jahanshahi, M., 2016. Static and dynamic assessments of polysulfonamide and poly(amide-sulfonamide) acid-stable membranes. *Journal of the Taiwan Institute of Chemical Engineers*, October, Volume 67, pp. 453-466.
- Hosseiniabadi, S. R. et al., 2014. Organic solvent nanofiltration with Grignard functionalised ceramic nanofiltration membranes. *Journal of Membrane Science*, Volume 454, pp. 496-504.
- Hu, R. & Pan, Y., 2012. Recent trends in counter-current chromatography. *TrAC trends in counter-current chromatography*, November, Volume 40, pp. 15-27.
- Ito, Y., 2005. Golden rules and pitfalls in selecting optimum conditions for high-speed counter-current chromatography. *Journal of Chromatography A*, 18 February, 1065(2), pp. 145-168.
- Kappert, E. J. et al., 2019. Swelling of 9 polymers commonly employed for solvent-resistant nanofiltration membranes: A comprehensive dataset. *Journal of Membrane Science*, 1 January, Volume 569, pp. 177-199.
- Kappert, E. J. et al., 2019. Swelling of 9 polymers commonly employed for solvent-resistant nanofiltration membranes: A comprehensive dataset. *Journal of Membrane Science*, 1 January, Volume 569, pp. 177-199.
- Kim, J. H. et al., 2018. A robust thin film composite membrane incorporating thermally rearranged polymer support for organic solvent nanofiltration and pressure retarded osmosis. *Journal of Membrane Science*, 15 March, Volume 550, pp. 322-331.
- Koros, W. J., Ma, Y. H. & Shimidzu, T., 1996. Terminology for membranes and membrane processes (IUPAC Recommendations 1996). *Pure and Applied Chemistry*, 1 1, 68(7), pp. 1479-1489.
- Lenntech, 2018. *GE Membrane Elements*. [Online]  
Available at: <https://www.lenntech.com/products/membrane/ge-elements.htm#Nano>  
[Accessed 11 1 2018].



## References

- Lim, S. K., Goh, K., Bae, T.-H. & Wang, R., 2017. Polymer-based membranes for solvent-resistant nanofiltration: A review. *Chinese Journal of Chemical Engineering*, 25(11), pp. 1653-1675.
- Livingston, A., Peeva, L. & Silva, P., 2006. Organic Solvent Nanofiltration. In: S. P. Nunes & K. Peinemann, eds. *Membrane Technology in the Chemical Industry, Second, Revised and Extended Edition*. 2 ed. Weinheim: WILEY-VCH, pp. 203-229.
- Li, X. et al., 2009. Evaporative Light Scattering Detector: Towards a General Molecular Weight Cutoff Characterization of Nanofiltration Membranes. *Analytical Chemistry*, 81(5), pp. 1801-1809.
- Li, Y. et al., 2019. Tuning the porosity of asymmetric membranes via simple post-synthesis solvent-treatment for non-aqueous applications. *Separation and Purification Technology*, 15 June, Volume 217, pp. 147-153.
- Loeb, S. & Sourirajan, S., 1963. Sea Water Demineralization by Means of an Osmotic Membrane. *Advances in Chemistry*, 1 January, Volume 38, pp. 117-132.
- López-Muñoz, M. J., Sotto, A., Arsuaga, J. M. & Bruggen, B. V. d., 2009. Influence of membrane, solute and solution properties on the retention of phenolic compounds in aqueous solution by nanofiltration membranes. *Separation and Purification technology*, 7 April, 66(1), pp. 194-201.
- Marchetti, P., Butté, A. & Livingston, A. G., 2013. NF in organic solvent/water mixtures: Role of preferential solvation. *Journal of Membrane Science*, 9 May, Volume 444, pp. 101-115.
- Marchetti, P. & Livingston, A., 2015. Predictive membrane transport models for Organic Solvent Nanofiltration: How complex do we need to be?. *Journal of Membrane Science*, 15 February, Volume 476, pp. 530-553.
- Mariën, H. & Vankelecom, I. F., 2017. Transformation of cross-linked polyimide UF membranes into highly permeable SRNF membranes via solvent annealing. *Journal of Membrane Science*, 1 November, Volume 541, pp. 205-213.
- Mariën, H. & Vankelecom, I. F., 2017. Transformation of cross-linked polyimide UF membranes into highly permeable SRNF membranes via solvent annealing. *Journal of Membrane Science*, 1 November, Volume 541, pp. 205 - 213 .
- Martínez, M. B. et al., 2013. Effect of impurities in the recovery of 1-(5-bromo-fur-2-yl)-2-bromo-2-nitroethane using nanofiltration. *Chemical Engineering and Processing: Process Intensification*, Volume 70, pp. 241-249.
- Ma, X. & Ito, Y., 2015. New analytical spiral tube assembly for separation of proteins by counter-current chromatography. *Journal of Chromatography A*, 31 July, Volume 1405, pp. 193-196.
- MET, E., 2017. *Home Page*. [Online]  
Available at: <http://duramem.evonik.com/product/duramem-puramem/en/Pages/osn-membranes.aspx>  
[Accessed 12 9 2017].
- MET, E., 2018. *Download*. [Online]  
Available at: <http://duramem.evonik.com/product/duramem-puramem/en/footer-en/pages/downloads.aspx>  
[Accessed 22 1 2018].
- Mikhail, S. Z. & Kimel, W. R., 1961. Densities and Viscosities of Methanol-Water Mixtures. *Journal of Chemical & Engineering Data*, 6(4), pp. 533-537.
- Mitev, D. et al., 2018. PECVD modification of nano & ultrafiltration membranes for organic solvent nanofiltration. *Journal of Membrane Science*, 15 February, Volume 548, pp. 540-547.

## References

- Mooter, P.-R. V. d., Daems, N. & Vankelecom, I. F., 2019. Preparation of solvent resistant supports through formation of a semi-interpenetrating polysulfone/polyacrylate network using UV cross-linking – Part 1: Selection of optimal UV curing conditions. *Reactive and Functional Polymers*, March, Volume 136, pp. 189-197.
- Mooter, P.-R. V. d., Daems, N. & Vankelecom, I. F., 2020. Preparation of solvent resistant supports through formation of a semi-interpenetrating polysulfone/polyacrylate network using UV cross-linking - Part 2: Optimization of synthesis parameters for UV-LED curing. *Reactive and Functional Polymers*, January, Volume 146, p. 104403.
- Mulder, M., 1996. Chapter VI Membrane processes. In: *Basic Principles of Membrane Technology*. s.l.:Kluwer Academic Publishers, pp. 280-416.
- Mulder, M., 2012. Preparation of synthetic membranes. In: *Basic Principles of Membrane Technology*. third ed. s.l.:Kluwer Academic Publishers, pp. 71-156.
- Nightingale, E., 1959. Phenomenological Theory of Ion Solvation. Effective radii of Hydrated Ions. *The Journal of Physical Chemistry*, 1 September, 63(9), pp. 1381-1387.
- Nunes, S. P. & Peinemann, K.-V., 2006. Presently Available Membranes for Liquid Separation, Second Revised Edition. In: S. P. Nunes & K. Peinemann, eds. *Membrane Technology in the Chemical Industry*. Weinheim: WILEY-VCH, pp. 15-39.
- Oatley, D. L. et al., 2012. Review of the dielectric properties of nanofiltration membranes and verification of the single oriented layer approximation. *Advances in Colloid and Interface Science*, 15 May, Volume 173, pp. 1-11.
- Oatley-Radcliffe, D. L., Williams, S. R., Lee, C. & Williams, P. M., 2015. Characterisation of Mass Transfer in Frontal Nanofiltration Equipment and Development of a Simple Correlation. *Journal of Membrane and Separation Technology*, 4(4), pp. 149-160.
- Oatley-Radcliffe, D. L. W. M. et al., 2017. Nanofiltration membranes and processes: A review of research trends over the past decade. *Journal of Water Process Engineering*, October, Volume 19, pp. 164-171.
- Ormerod, D. et al., 2013. Demonstration of purification of a pharmaceutical intermediate via organic solvent nanofiltration in the presence of acid. *Separation and Purification Technology*, 30 August, Volume 115, pp. 158-162.
- Paar, A., 2018. *Viscosity of Methanol*. [Online]  
Available at: <https://wiki.anton-paar.com/en/methanol/>  
[Accessed 30 11 2018].
- Pan, K., Fang, P. & Cao, B., 2012. Novel composite membranes prepared by interfacial polymerization on polypropylene fiber supports pretreated by ozone-induced polymerization. *Desalination*, 15 May, Volume 294, pp. 36-43.
- Peeva, L. G. et al., 2004. Effect of concentration polarisation and osmotic pressure on flux in organic solvent nanofiltration. *Journal of Membrane Science*, 236(1-2), pp. 121-136.
- Peshev, D. et al., 2011. Application of organic solvent nanofiltration for concentration of antioxidant extracts of rosemary (*Rosmarinus officinalis* L.). *Chemical Engineering Research and Design*, March.89(3).
- Priske, M., Lazar, M., Schnitzer, C. & Baumgarten, G., 2016. Recent Applications of Organic Solvent Nanofiltration. *Chemie Ingenieur Technik*, February, 88(1-2), pp. 39-49.
- Pulido, B., Chisca, S. & Nunes, S. P., 2018. Solvent and thermal resistant ultrafiltration membranes from alkyne-functionalized high-performance polymers. *Journal of Membrane Science*, 15 October, Volume 564, pp. 361-371.

## References

- Reddy, A. et al., 2003. Surface modification of ultrafiltration membranes by preadsorption of a negatively charged polymer: I. Permeation of water soluble polymers and inorganic salt solutions and fouling resistance properties. *Journal of Membrane Science*, 1 April, 214(2), pp. 211-221.
- Reichardt, C. & Welton, T., 2010. Empirical Parameters of Solvent Polarity. In: *Solvents and Solvent Effects in Organic Chemistry, Fourth Edition*. s.l.:s.n., pp. 425-508.
- Reynolds, O., 1886. IV. On the theory of lubrication and its application to Mr. Beauchamp tower's experiments, including the experimental determination of the viscosity of olive oil. *Philosophical Transactions The Royal Society*, Volume 177, p. 157.
- Rezzadori, K. et al., 2015. Evaluation of reverse osmosis and nanofiltration membranes performance in the permeation of organic solvents. *Journal of Membrane Science*, 16 June, Volume 492, pp. 478-489.
- Richardson, J., Harker, J. & Backhurst, J., 2002. Membrane Separation Processes. In: *Coulson & Richardson's Chemical Engineering Volume 2 Particle Technology & Separation Processes*. s.l.:Elsevier, pp. 437-474.
- Rohani, R., Hyland, M. & Patterson, D., 2011. A refined one-filtration method for aqueous based nanofiltration and ultrafiltration membrane molecular weight cut-off determination using polyethylene glycols. *Journal of Membrane Science*, 15 October, 382(1-2), pp. 278-290.
- Rohani, R., Hyland, M. & Patterson, D., 2011. A refined one-filtration method for aqueous based nanofiltration and ultrafiltration membrane molecular weight cut-off determination using polyethylene glycols. *Journal of Membrane Science*, 15 October, 382(1-2), pp. 278-290.
- Rundquist, E., Pink, C., Vilminot, E. & Livingston, A., 2012. Facilitating the use of counter-current chromatography in pharmaceutical purification through use of organic solvent nanofiltration. *Journal of Chromatography A*, 18 January, Volume 1229, pp. 156-163.
- Rundquist, E., Pink, C., Vilminot, E. & Livingston, A., 2012. Facilitating the use of counter-current chromatography in pharmaceutical purification through use of organic solvent nanofiltration. *Journal of Chromatography A*, 16 March, Volume 1229, pp. 156-163.
- Ryzhkov, I. I. & Minakov, A. V., 2016. Theoretical study of electrolyte transport in nanofiltration membranes with constant surface potential/charge density. *Journal of Membrane Science*, 15 December, Volume 520, pp. 515-528.
- S.Deshmukh, S. & Childress, A. E., 2001. Zeta potential of commercial RO membranes: influence of source water type and chemistry. *Desalination*, 20 October, 140(1), pp. 87-95.
- Saiz, C. A., Darvishmanesh, S., Buekenhoudt, A. & Bruggen, B. V. d., 2018. Shortcut applications of the Hansen Solubility Parameter for Organic Solvent Nanofiltration. *Journal of Membrane Science*, 15 January, Volume 546, pp. 120-127.
- Santos, B., G.Crespo, J., Santos, M. A. & Velizarov, S., 2016. Oil refinery hazardous effluents minimization by membrane filtration: An on-site pilot plant study. *Journal of Environmental Management*, 1 October, Volume 181, pp. 762-769.
- Satyawali, Y. et al., 2017. Asymmetric synthesis of chiral amine in organic solvent and in-situ product recovery for process intensification: A case study. *Biochemical Engineering Journal*, 15 January, 117(Part B), pp. 97-104.
- Schäfer, A. et al., 2004. Fouling in Nanofiltration. In: *Nanofiltration – Principles and Applications*. s.l.:s.n., pp. 169-239.

## References

- Schmidt, P., Bednarz, E. L. & Lutze, P. G. A., 2014. Characterisation of Organic Solvent Nanofiltration membranes in multi-component mixtures: Process design workflow for utilising targeted solvent modifications. *Chemical Engineering Science*, 1 August, Volume 115, pp. 115-126.
- Schmidt, P., Bednarz, E. L., Lutze, P. & Górak, A., 2014. Characterisation of Organic Solvent Nanofiltration membranes in multi-component mixtures: Process design workflow for utilising targeted solvent modification. *Chemical Engineering Science*, 8 April, Volume 115, pp. 115-126.
- Schmidt, P., Köse, T. & Lutze, P., 2013. Characterisation of organic solvent nanofiltration membranes in multi-component mixtures: Membrane rejection maps and membrane selectivity maps for conceptual process design. *Journal of Membrane Science*, 15 February, Volume 429, pp. 103-120.
- See-Toh, Y. H., Silva, M. & Livingston, A., 2008. Controlling molecular weight cut-off curves for highly solvent stable organic solvent nanofiltration (OSN) membranes. *Journal of Membrane Science*, 17 July, 324(1-2), pp. 220-230.
- Sereewatthanawut, I. et al., 2011. Nanofiltration process for the nutritional enrichment and refining of rice bran oil. *Journal of Food Engineering*, January, 102(1), pp. 16-24.
- Shaaban, A. M. F. et al., 2016. Process engineering optimization of nanofiltration unit for the treatment of textile plant effluent in view of solution diffusion model. *Egyptian Journal of Petroleum*, March, 25(1), pp. 79-90.
- Shi, G. M. et al., 2019. Separation of vegetable oil compounds and solvent recovery using commercial organic solvent nanofiltration membranes. *Journal of Membrane Science*, 15 October, Volume 588, pp. 117-202.
- Silva, P., Peeva, L. & Livingston, A., 2008. Nanofiltration in Organic Solvents. In: *Advanced Membrane Technology*. New Jersey: John Wiley & Sons Inc., pp. 451-487.
- Singh, N., M.Husson, S., Zdyrko, B. & Luzinov, I., 2005. Surface modification of microporous PVDF membranes by ATRP. *Journal of Membrane Science*, 1 October, 262(1-2), pp. 81-90.
- Smith, B. C., 2011. *Fundamentals of Fourier Transform Infrared Spectroscopy*. 2nd ed. Boca Raton: CRC Press.
- Soltane, H. B., Roizard, D. & Laboratoire, E. F., 2016. Study of the rejection of various solutes in OSN by a composite polydimethylsiloxane membrane: Investigation of the role of solute affinity. *Separation and Purification Technology*, 25 January, Volume 161, pp. 193-201.
- Sotto, A., Arsuaga, J. M. & Bruggen, B. d., 2013. Sorption of phenolic compounds on NF/RO membrane surfaces: Influence on membrane performance. *Desalination*, 15 January, Volume 309, pp. 64-73.
- Sourirajan, S., 1964. *Separation of Hydrocarbon Liquids by Flow Under Pressure Through Porous Membranes*, s.l.: s.n.
- Sterlitech, 2018. *Chemically Resistant Membranes*. [Online]  
Available at: <https://www.sterlitech.com/chemically-resistant-membranes.html?designation=Duramem%20200>  
[Accessed 11 1 2018].
- Sterlitech, 2018. *Flat Sheet Membranes*. [Online]  
Available at: <https://www.sterlitech.com/flat-sheet-membranes.html#>  
[Accessed 25 9 2018].
- Székely, G. et al., 2011. Organic solvent nanofiltration: A platform for removal of genotoxins from active pharmaceutical ingredients. *Journal of Membrane Science*, 30 September.381(1-2).

## References

- Tarleton, E., Robinson, J. & Salman, M., 2006. Solvent-induced swelling of membranes — Measurements and influence in nanofiltration. *Journal of Membrane Science*, 1 September, 280(1-2), pp. 442-451.
- Tarleton, E., Robinson, J., Smith, S. & Na, J., 2005. New experimental measurements of solvent induced swelling in nanofiltration membranes. *Journal of Membrane Science*, 22 April, 1-2(261), pp. 129-135.
- Thiermeyera, Y., Blumenschein, S. & Skiborowski, M., 2018. Solvent dependent membrane-solute sensitivity of OSN membranes Yvonne. *Journa of Membrane Science*, 1 December, Volume 567, pp. 7-17.
- Thomas, T. E. et al., 2017. Laser Doppler Electrophoresis and electro-osmotic flow mapping: A novel methodology for the determination of membrane surface zeta potential. *Journal of Membrane Science*, 1 February, Volume 523, pp. 524-532.
- Toolbox, E., 2008. *Dielectric constants of common liquids*. [Online]  
Available at: [https://www.engineeringtoolbox.com/liquid-dielectric-constants-d\\_1263.html](https://www.engineeringtoolbox.com/liquid-dielectric-constants-d_1263.html)  
[Accessed 11 9 2019].
- Torkabad, M. G., Keshtkar, A. & Safdari, S., 2017. Comparison of polyethersulfone and polyamide nanofiltration membranes for uranium removal from aqueous solution. *Progress in Nuclear Energy*, January, Volume 94, pp. 93-100.
- Torkabad, M. G., Keshtkar, A. & Safdari, S., 2018. Selective concentration of uranium from bioleach liquor of low-grade uranium ore by nanofiltration process. *Hydrometallurgy*, June, Volume 178, pp. 106-115.
- Tsehay, M. T. et al., 2018. Development and characterisation of polyethersulfone-based nanofiltration membrane with stability in hydrogen peroxide. *Journal of Membrane Science*, 15 March, Volume 550, pp. 462-469.
- Tylkowski, B. et al., 2010. Extraction of biologically active compounds from propolis and concentration of extract by nanofiltration. *Journal of Membrane Science*, 15 February, 348(1-2), pp. 124-130.
- Vandezande, P., Gevers, L. E. M. & Vankelecom, I. F. J., 2008. Solvent resistant nanofiltration: separating on a molecular level. *Chemical Society Reviews*, 37(2), pp. 365-405.
- Vanherck, K. et al., 2010. A simplified diamine crosslinking method for PI nanofiltration membranes. *Journal of Membrane Science*, 1 May, 353(1-2), pp. 135-143.
- Vanherck, K. et al., 2010. A simplified diamine crosslinking method for PI nanofiltration membranes. *Journal of Membrane Science*, 1 May, 353(1-2), pp. 135-143.
- Vanherck, K., Koeckelberghs, G. & F.J.Vankelecom, I., 2013. Crosslinking polyimides for membrane applications: A review. *Progress in Polymer Sciences*, June, 38(6), pp. 874-896.
- Vankelecom, I. F. et al., 2004. Physico-chemical interpretation of the SRNF transport mechanism for solvents through dense silicone membranes. *Journal of Membrane Science*, 1 March, 231(1-2), pp. 99-108.
- Vazquez, G., Alvarez, E. & Navaza, J. M., 1995. Surface Tension of Alcohol Water + Water from 20 to 50 .degree.C. *Journal of Chemical & Engineering Data*, 40(3), pp. 611-614.
- Vieira, G. S. et al., 2018. Influence of nanofiltration membrane features on enrichment of jussara ethanolic extract (*Euterpe edulis*) in anthocyanins. *Journal of Food Engineering*, June, Volume 226, pp. 31-41.
- Volkova, A. et al., 2015. Surface modification of PTMSP membranes by plasma treatment: Asymmetry of transport in organic solvent nanofiltration. *Advances in Colloid and Interface Science*, August, Volume 222, pp. 716-727.

## References

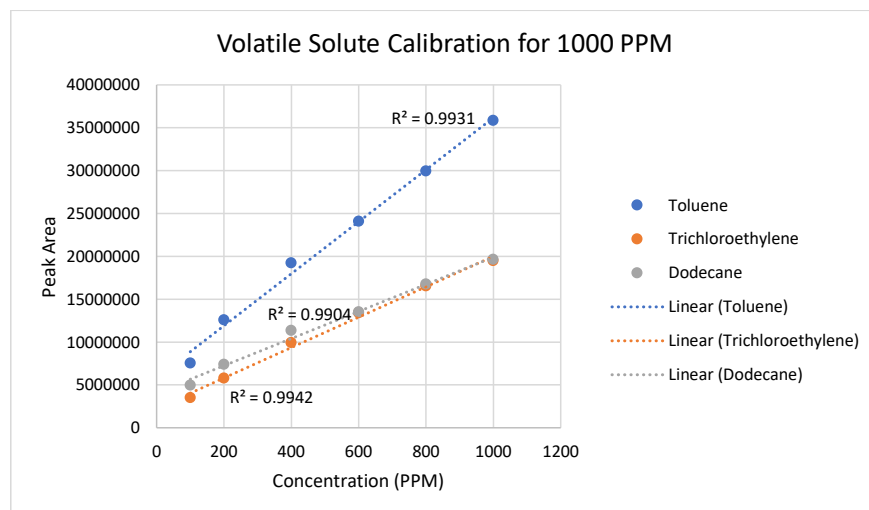
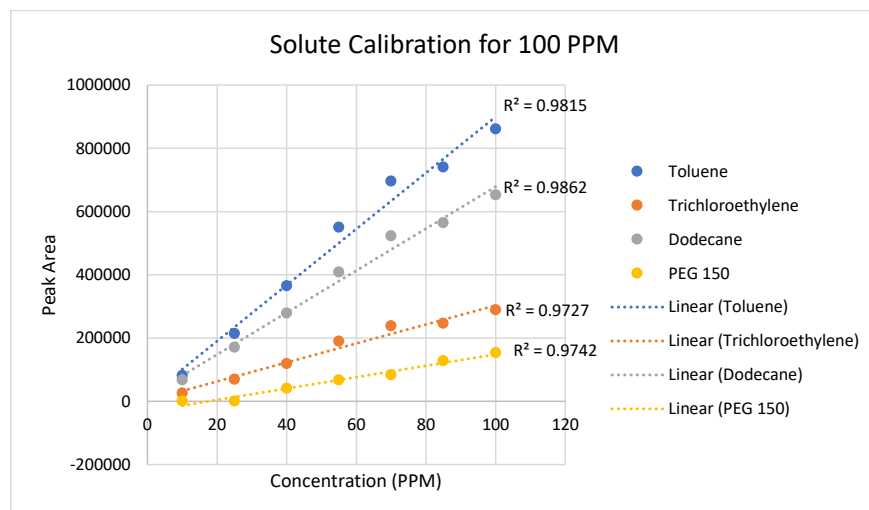
- Wang, F. et al., 2015. Effect of surface hydrophilic modification on the wettability, surface charge property and separation performance of PTFE membrane. *Journal of Water Process Engineering*, December, Volume 8, pp. 11-18.
- Wang, J., Mo, Y., Mahendra, S. & Hoek, E. M., 2014. Effects of water chemistry on structure and performance of polyamide composite membranes. *Journal of Membrane Science*, 15 February, Volume 452, pp. 415-425.
- Wang, L. et al., 2011. Preparation of Thin Film Composite Nanofiltration Membrane by Interfacial Polymerization with 3, 5-Diaminobenzoylpiperazine and Trimesoyl Chloride. *Chinese Journal of Chemical Engineering*, April, 19(2), pp. 262-266.
- Wei, G. et al., 2018. Polyethersulfone enwrapped hydrous zirconium oxide nanoparticles for efficient removal of Pb(II) from aqueous solution. *Chemical Engineering Journal*, 1 October, Volume 349, pp. 500-508.
- Wei, X.-Z. et al., 2008. New type of nanofiltration membrane based on crosslinked hyperbranched polymers. *Journal of Membrane Science*, 15 October, 323(2), pp. 278-287.
- Werner, A. et al., 2018. Nanofiltration of indium and germanium ions in aqueous solutions: Influence of pH and charge on retention and membrane flux. *Separation and Purification Technology*, 3 April, Volume 194, pp. 319-328.
- Whu, J., Baltzis, B. & K.K., S., 2000. Nanofiltration studies of larger organic microsolute in methanol solutions. *Journal of Membrane Science*, 31 May, 170(2), pp. 159-172.
- Yang, X., Livingston, A. & Santos, L. F. d., 2001. Experimental observations of nanofiltration with organic solvents. *Journal of Membrane Science*, 31 August, 190(1), pp. 45-55.
- Yang, Y. et al., 2018. Type-I counter-current chromatography with the multilayer coil for protein separation. *Journal of Chromatography B*, 15 November, Volume 1100-1101, pp. 39-42.
- Yao, Y. et al., 2016. Development of a positively charged nanofiltration membrane for use in organic solvents. *Journal of Membrane Science*, 15 December, Volume 520, pp. 832-839.
- Yuan, S. et al., 2019. Facile synthesis of Kevlar nanofibrous membranes via regeneration of hydrogen bonds for organic solvent nanofiltration. *Journal of Membrane Science*, 1 March, Volume 573, pp. 612-620.
- Yuan, S. et al., 2018. New promising polymer for organic solvent nanofiltration: Oxidized poly (arylene sulfide sulfone). *Journal of Membrane Science*, 1 March, Volume 549, pp. 438 - 445.
- Yuan, Z. et al., 2017. The performance of integrally skinned polyetherimide asymmetric nanofiltration membranes with organic solvents. *Journal of Membrane Science*, 15 December, Volume 544, pp. 119-125.
- Yun, T., Chung, J. W. & Kwak, S.-Y., 2018. Recovery of sulfuric acid aqueous solution from copper-refining sulfuric acid wastewater using nanofiltration membrane process. *Journal of Environmental Management*, 1 October, Volume 223, pp. 652-657.
- Zedel, D., Drews, A. & Kraume, M., 2016. Retention of surfactants by organic solvent nanofiltration and influences on organic solvent flux. *Separation and Purification Technology*, 28 January, Volume 158, pp. 396-408.
- Zhang, Y. et al., 2017. The performance of integrally skinned polyetherimide asymmetric nanofiltration membranes with organic solvents. *Journal of Membrane Science*, 15 December, Volume 544, pp. 119-125.
- Zhao, Y. & Yuan, Q., 2006. A comparison of nanofiltration with aqueous and organic solvents. *Journal of Membrane Science*, 28 February, 279(1-2), pp. 453-458.

## References

- Zheng, F., Li, C., Yuan, Q. & Vriesekoop, F., 2008. Influence of molecular shape on the retention of small molecules by solvent resistant nanofiltration (SRNF) membranes: A suitable molecular size parameter. *Journal of Membrane Science*, 20 June, 318(1-2), pp. 114-122.
- Zheng, F., Zhang, Z., Li, C. & Yuan, Q., 2009. A comparative study of suitability on different molecular size descriptors with the consideration of molecular geometry in nanofiltration. *Journal of Membrane Science*, 15 April, 332(1-2), pp. 13-23.
- Zhu, W.-P. et al., 2014. Dual-layer polybenzimidazole/polyethersulfone (PBI/PES) nanofiltration (NF) hollow fiber membranes for heavy metals removal from wastewater. *Journal of Membrane Science*, 15 April, Volume 456, pp. 117-127.

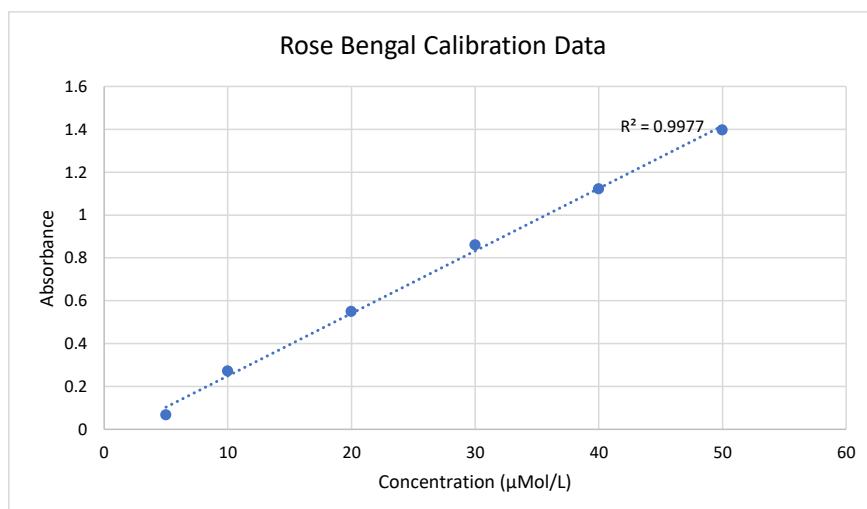
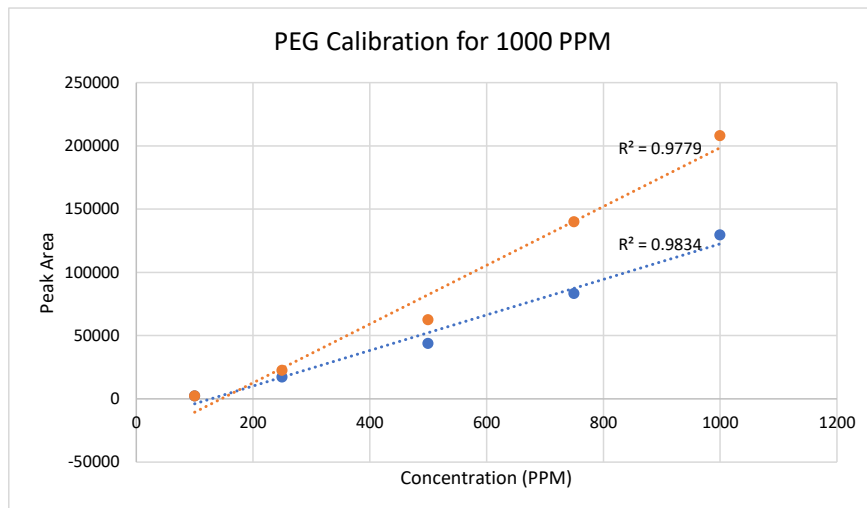
## 12. Appendix

### 12.1 Calibrations

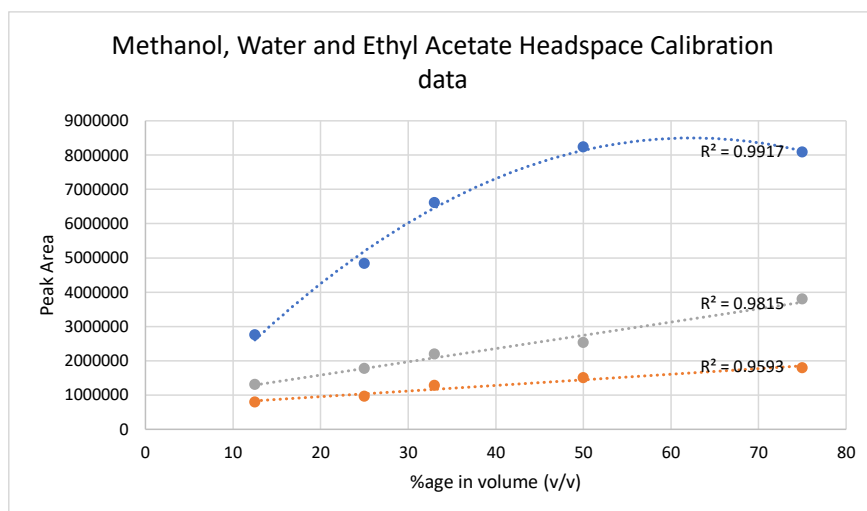
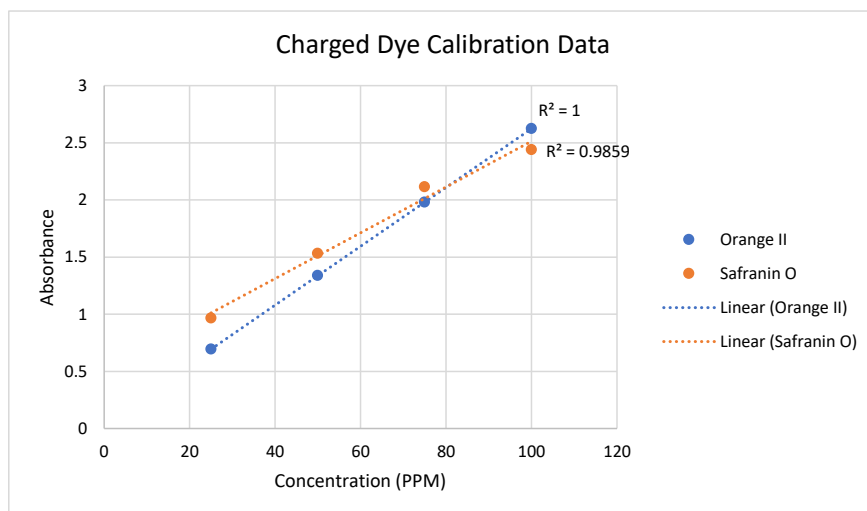




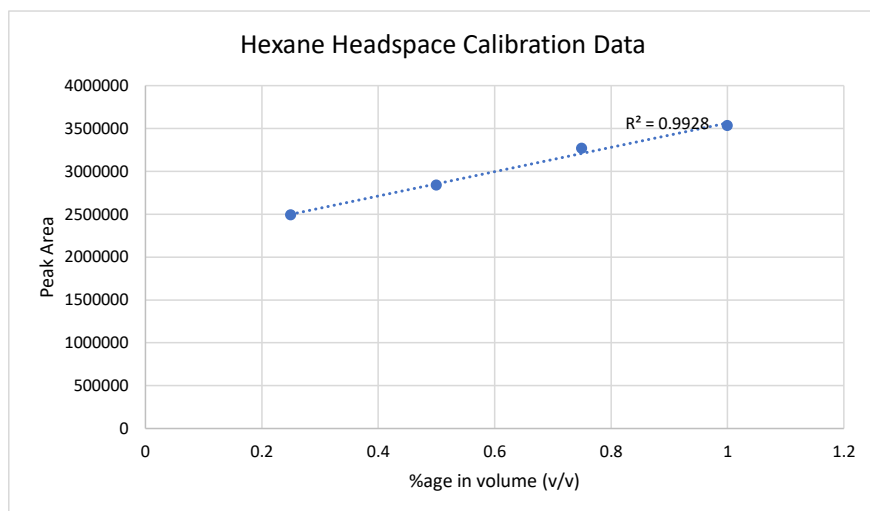
## Appendix



# Appendix



# Appendix



# Appendix

## 12.2 Studies on Duramem series by other authors

### Duramem 150

Solvent	Solute	Flux	Permeability	Rejection	MWCO	Temperature	Source
		L/m <sup>2</sup> h	L/m <sup>2</sup> hbar	%		°C	
Methanol	PPGs				300	30	(Davey, et al., 2017)
	PPG 300			90			
	Compound A	32	≈1.6	65	-	30	(Siew, Livingston, C. C. Ates, <i>et al.</i> , 2013)
	Compound A	45	≈1.5	75			
	Compound A	53	≈1.325	78			
	Compound C	32	≈1.6	100			
	Compound C	45	≈1.5	100			
	Compound C	53	≈1.325	100			
Ethanol	G-1*	-	0.16	55	296.9 (estimated)	unknown	(Martínez <i>et al.</i> , 2013)
	G-1 + pyridine		0.149	66			
	G-1 + pyridine		0.05	69			
	G-1 + pyridine		0.05	50			
Ethyl Acetate, Heptane, Methanol, Water	API	0.2	0.0067	76.1	-	Ambient (25-30)	(Rundquist <i>et al.</i> , 2012)
Ethyl Acetate	API	5	0.167	99.1			
Methanol, MIBK, Toluene	API	16	0.53	16			
THF	Dimer	2.5	0.125	98	-	Unknown	(Ormerod <i>et al.</i> , 2013)
	API			97			
THF/Water	Dimer	4.7	0.235	97			

# Appendix

	API			97			
THF/Water, HCl	Dimer	3.8	0.19	>99.8			
	API			79			

\*G-1 is 1-(5-bromo-fur-2-yl)-2-bromo-2-nitroethane

## Duramem 200

Solvent	Solute	Flux	Permeability	Rejection	MWCO	Temperature	Reference
		L/m <sup>2</sup> h	L/m <sup>2</sup> hbar	%		°C	
Methanol	PPG's	-	-		300	30	(Davey <i>et al.</i> , 2017)
	PPG 300			90		30	
	Dimer			99		unknown	(Ormerod <i>et al.</i> , 2013)
	API-intermediate			94			
	Compound A	24	2.4	75	-	30	(Siew, Livingston, C. C. Ates, <i>et al.</i> , 2013)
		42	2.1	78			
		58	1.93	81			
	Compound C	24	2.4	100			
		42	2.1	100			
		58	1.93	100			
	Ethanol	Caffeic Acid	0.77	93.9	200	25±1	(Peshev <i>et al.</i> , 2011)
		Rosmarinic Acid		99.7			
		Caffeic Acid	0.6425	96.1			
		Rosmarinic Acid		99.5			
		Flavones & flavonols	2.66	0.08867			(Tylkowski <i>et al.</i> , 2010)
			4.05	0.081			
		Flavonones & dihydroflavonols	2.66	0.08867			
			4.05	0.081			
		Phenols	2.66	0.08867			
			4.05	0.081			
Ethanol:Water (4:1)	Rosmarinic acid	-	-	99.7	-	21±0.5	(Peev <i>et al.</i> , 2011)
Ethanol:Water (1:1)				99.2			
DMF	Bengal Rose	9.5	0.95	98	-	ambient	

Appendix

	Methyl Orange	9.1	0.91	29.4			(Hendrix, Vanherck and Vankelecom, 2012)
	Dimer	-	-	100			
	API-intermediate	-	-	99			
THF	Dimer	6.3	0.315	98	-	unknown	(Ormerod <i>et al.</i> , 2013)
	API-intermediate			94			
THF: Water	Dimer	7.4	0.37	>99.8			
	API-Intermediate			98			
THF:Water (2.6 mol HCl)	Dimer	6.6	0.33	>99.8			
	API-Intermediate			78			
THF:Water (1 mol HCl)	Dimer	8.1	0.405	>99.8	-	unknown	(Ormerod <i>et al.</i> , 2013)
	API-Intermediate	8.1	0.405	98			
THF:2-Propanol (2.6 Mol HCl)	Dimer	3	0.15	98			
	API-Intermediate			96			
THF (2.6 mol HCl)	Dimer	0.6	0.03	>99.8			
	API-Intermediate			95			
Ethyl Acetate, Heptane, Methanol, Water	API	28	0.933	21.7	-	Ambient	(Rundquist <i>et al.</i> , 2012)
Ethyl Acetate	API	29	0.967	91.6			
Methanol, MIBK, Toluene	API	55	1.83	96.5			
Acetone	PPG's	-	-	-	200	30	(Davey <i>et al.</i> , 2017)
	PPG 300			92		30	

# Appendix

Duramem 300

Solvent	Solute	Flux	Permeability	Rejection	MWCO	Temperature	Source
		L/m <sup>2</sup> h	L/m <sup>2</sup> hbar	%		°C	
Ethanol	Extract	17.146	0.8573	-	-	25±1	(Tsibranska and Tylkowski, 2013)
		26	0.867				
		42.7	0.854				
	Caffeic Acid	24.4	1.22	87.8	-	25±1	(Peshev <i>et al.</i> , 2011)
	Rosmarinic Acid			94			
	Caffeic Acid	41.1	1.0275	90.7			
	Rosmarinic Acid			94.7			
Ethyl Acetate	FFA	2	0.4	-	-	30	(Sereewatthanawut <i>et al.</i> , 2011)
	γ-oryzanol			92.1			
	glycerides			78.7			
	FFA	3	0.1	70.4			
	γ-oryzanol			96.8			
	glycerides			96.7			
Hexane	FFA	17.1	3.42	14.3	-	30	(Sereewatthanawut <i>et al.</i> , 2011)
	γ-oryzanol			10.3			
	glycerides			37.4			
	FFA	49.3	1.643	41.9			
	γ-oryzanol			22.5			
	glycerides			59.9			
Methanol	Compound A	35	7	57	-	30	(Siew, Livingston, C. C. Ates, <i>et al.</i> , 2013)
		50	5	61			
		87	4.35	78			
	Compound C	35	7	95			
		50	5	97			
		87	4.35	98			
DMF	Bengal Rose	0.5	0.05	98	-	Ambient	(Hendrix, Vanherck and Vankelecom, 2012)
	Methyl Orange	14.9	1.49	35.8			

# Appendix

	Polystyrene	7.5	0.25	-	300	30	(da Silva Bural, Peeva and Livingston, 2017)
		1.5	0.05		800	85	
DCM	Polystyrene	21	0.7	-	300	30	(Siddique <i>et al.</i> , 2014)
Acetone	Dimer	125	4.167	92.5			
THF:Water (3:1)	API A	10.5	0.35	97			
	API B			47			
Ethyl Acetate: Methanol (9:1)	API	20-23	0.767	-	-	30	(Siew, Livingston, C. Ates, <i>et al.</i> , 2013)



# Appendix

Duramem 500

Solvent	Solute	Flux	Permeability	Rejection	MWCO	Temperature	Source
		L/m <sup>2</sup> h	L/m <sup>2</sup> hbar	%		°C	
Methanol	PPG's	-	-	90	700	30	(Davey <i>et al.</i> , 2017)
Acetone	PPG's	-	-				
Ethanol	Caffeic Acid	21.4	1.07	82	-	25±1	(Peshev <i>et al.</i> , 2011)
	Rosmarinic Acid			94.5			
	Caffeic Acid	31.3	0.7825	91.5			
	Rosmarinic Acid			97.4			
Ethanol:Water (2:3)	Flavan-3-ols (various)	3.2	0.4	87-98	-	40	(Syed <i>et al.</i> , 2017)
Ethyl Acetate	Vanillin	268.4	14.53	15.9	500	30	(Werhan, Farshori and Rudolf von Rohr, 2012)
	methyl vanillate			17.5			
	2-benzylphenol			11.95			
	benzyl phenyl ether			15.05			
DMF	Methyl Orange	14.9	1.49	35.8	-	Ambient	(Hendrix, Vanherck and Vankelecom, 2012)
Isopropanol	Rose Bengal	1.8	0.09	93.4	-	Ambient	(Hendrix <i>et al.</i> , 2013)

# Appendix

## Duramem 700

Solvent	Solute	Flux	Permeability	Rejection	MWCO	Temperature	Source
		L/m <sup>2</sup> h	L/m <sup>2</sup> hbar	%		°C	
Ethyl Acetate	FFA	5	1	9.1	-	30	(Sereewatthanawut <i>et al.</i> , 2011)
	$\gamma$ -oryzanol			45.4			
	glycerides			75			
	FFA	8	0.267	40.7			
	$\gamma$ -oryzanol			67			
	glycerides			82.4			
Hexane	FFA	117.9	23.58	0	-	30	(Sereewatthanawut <i>et al.</i> , 2011)
	$\gamma$ -oryzanol			12			
	glycerides			34.9			
	FFA	248.6	8.2867	48.4			
	$\gamma$ -oryzanol			37.3			
	glycerides			72.2			

## Duramem 900

Solvent	Solute	Flux	Permeance	Rejection	MWCO	Temperature	Source
		L/m <sup>2</sup> h	L/m <sup>2</sup> hbar	%		°C	
Ethyl Acetate	Vanillin	2017.3	100.75	-0.6	-	30	(Werhan, Farshori and Rudolf von Rohr, 2012)
	methyl vanillate			-0.5			
	2-benzylphenol			0.2			
	benzyl phenyl ether			-0.2			
Toluene	Unisol Blue	48.3	2.1	18	-	20	(Behnke and Ulbricht, 2015)
Hexane	Unisol Blue	23	1	82			
Isopropanol	Unisol Blue	13.8	0.6	80			
	Rose Bengal			95			
DMF	Unisol Blue	1288	5.6	40			
	Rose Bengal			62			

## 12.3 Prospective publications

### 12.3.1 Predictive computational modelling of Organic Solvent Nanofiltration (OSN) membranes in alcohols: a systematic study

The modelling and predicted behaviour of solute rejection and permeate flux in Organic Solvent Nanofiltration (OSN) are influenced by chemical interactions which occur between solute – solvent, solvent – membrane and solute – solvent – membrane interactions, which means that a general model for permeate flux or solute rejection cannot be easily made. By observing the permeate flux and rejection of Safranin O dye in alcohols of increasing carbon content (C1 to C5) by the Duramem® 500 membrane, a predictive model for rejection of a solute by size exclusion can be constructed by measuring pore size swelling due to the decreasing polarity of the alcohols with increasing carbon content. The model is constructed using a freely available software (Marvin Sketch), which shows excellent correlation between rejection and solute swelling due to the polarity of the solvent that the dye is being dissolved in.

### 12.3.2 Comparative study of membrane crosslinking methods on Polyethersulfone (PES) membranes for Organic Solvent Nanofiltration (OSN)

Polyethersulfone (PES) membranes have shown excellent rejection properties when dealing with hazardous and destructive solutes in water but to date, very little work has been conducted on using PES membranes for Organic Solvent Nanofiltration (OSN) despite their robust nature. Furthermore, due to their robust nature, this polymer is difficult to modify or enhance. Thus a methodology for crosslinking PES membrane has been developed to accommodate for creating either a positively charged negatively charged surface by crosslinking by a number of different methods. A positively charged PES OSN membrane was successfully crosslinked using hexane diamine by permeating the crosslinking agent through the membrane under pressure until the flux had stabilised.